University of Reading

Activity of Cannabidiol on Adenosine Signalling in a Chronic Model of Epilepsy

PhD Thesis

School of Pharmacy

Yuhan Hu

October 2020

Abstract

Over 50 million people worldwide have some form of epilepsy, characterised by seizures resulting from hyperexcitability of neuronal networks. Around a third of those with epilepsy are unable to control their seizures using current antiepileptic drugs or therapies, underscoring a large unmet clinical need for developing new pharmacotherapies. Cannabidiol (CBD), a nonpsychoactive component of the *Cannabis sativa* plant, has an anecdotal antiseizure history and has been gaining regulatory approval for epilepsy syndromes. However, its mechanism of action remains to be fully elucidated.

The central adenosine signalling system has been proposed as a putative target for the CBD mechanism of action. Adenosine acts as a neuromodulator within the central nervous system through activation of the inhibitory adenosine 1 receptor (A_1R), and release of adenosine is seen during seizures. This adenosine release provides an endogenous seizure termination mechanism. CBD has been shown to inhibit the bi-directional Equilibrative Nucleoside Transporter 1 (ENT1), which allows adenosine to transit cellular membranes by passive diffusion.

This thesis uses *in vitro* techniques with a rat model of chronic epilepsy to test the hypothesis that prevention of adenosine reuptake through CBD blockade at ENT1, allowing for greater activation of the inhibitory A_1R, underlies the antiepileptic efficacy of CBD. These techniques include functional electrophysiological recordings using multielectrode arrays to assess local field potentials in hippocampal slices, and enzymatic biosensors detecting adenosine concentration in the same slices. Additionally, qPCR, radioligand binding, and Western blotting were used to quantify any changes in expression of A_1R, the adenosine 2A receptor ($A_{2A}R$; which stimulates excitatory transmission), and ENT1 as a result of chronic epilepsy.

Hippocampal slices taken from epileptic rats appeared to show a decrease in the ability of endogenously released adenosine to inhibit network activity, following seizure-like stimulation. Application of CBD (10 µM) returned adenosine potency to that seen in healthy hippocampus; however, peak adenosine release as measured by biosensors was significantly lower in the presence of CBD. Through radioligand binding, a decrease in A_1R expression in epileptic hippocampus was found; a dysfunction in A_1R activation was corroborated through use of an 8-CPT, an A_1R antagonist, which potentiated field potentials significantly less in epileptic tissue than healthy. Additionally, CBD again appeared to positively modulate low concentrations of adenosine towards inhibition in epileptic hippocampal slices.

While CBD did not appear to inhibit reuptake of seizure-associated adenosine in our assays, there appears to be a modulatory role it may play at adenosine receptors. Adenosine dysfunction in chronic epilepsy is indicated, but further experiments are required to characterise the contribution of the receptors, the transporter, and the interaction with CBD.

Declaration

I confirm that this is my own work and the use of all material from other sources has been properly and fully acknowledged.

Yuhan Hu

Acknowledgements

I would like to start by profoundly thanking my academic supervisors, Dr Angela Bithell and Dr Mark Dallas for their stalwart support and guidance throughout. Also, thank you to my ex-supervisor and ex-Professor Ben Whalley for giving me the opportunity to undertake this PhD, and my industrial supervisor Dr Michael Bazelot for the guidance and training in directing this project. Thank you to my industrial sponsor, GW Pharmaceuticals, for providing funding and materials for this research project.

Huge thanks to all the PhD students, technicians and post-docs who have come through this lab the past few years, without whom the herculean task of running unending inductions down in the BRU basement would have been impossible. Also, huge thanks to many of the same people for the wine and cheese nights, which helped us all regain some collective sanity after long days/weeks/months in the lab or animal house…!

A special shout out to the entire Medical Writing team at Premier Research, who have been phenomenally supportive this past year, allowing me to juggle full-time work on clinical documents while finishing off this preclinical thesis in my spare time. I couldn't have asked for a better job or team to start my post-academia career with.

To Rix and Zoe…we've all known each other since we were fresh-faced 11-year-olds, which is frighteningly long ago now! Being able to share and vent about how the academic pressures of our teenage years have shaped and moulded the way we've dealt with our respective PhD lives has been illuminating and affirming. Our weekly chats were invaluable for getting me over the finish line, and I hope for both of you too – smash them PhDs!

My long-suffering family who have seen it all; words can't fully encompass what it's meant that you've been here for me over the years. Anyway, we're not soppy people; you know that I appreciate you.

While the years since starting this PhD have been full of ups and downs, I can never regret any of it for the experiences I've had and the people I've met. Chris, we were brought together because we both started PhDs at Reading in 2015. While both of us finishing and writing up at the same time wasn't ideal for our collective stress levels (or our finances!), it's led us to where we are now, which means more than anything. Thank you for putting up with me, reminding me to eat, hydrate, sleep, and wake up at the right times, looking after me when the thesis brain fog descends, and dealing with the chaos around this zombie version of me. We've built a wonderful life together and I wouldn't trade any of it for the world.

To my beautiful kittens, my fluffy little fireflies River and Inara, I love both of you with the entirety of my heart, soul, and existence. Please stop clawing me awake at 5am.

Table of Contents

List of Figures

List of Tables

List of Abbreviations

ABBREVIATION	DEFINITION/EXPLANATION
5-HT	5-hydroxytryptamine (serotonin)
A_1R	adenosine 1 receptor
$A_{2A}R$	adenosine 2a receptor
AAT	adenosine augmentation therapy
ADO	adenosine
AE	adverse event
aCSF	artificial cerebrospinal fluid
ADA	adenosine deaminase
ADK	adenosine kinase
AEDs	antiepileptic drugs
AMPA	α-amino-3-hydroxy-5-methyl-4-isoxazolepropionic acid receptor
ANOVA	analysis of variance
ASPA	Animals Scientific Procedures Act
ATP	adenosine triphosphate
BK	Maxi Calcium-Activated Potassium channel
B_{MAX}	maximum binding (total number of receptors in a tissue)
BSA	bovine serum albumin
CA1	cornu ammonis 1
CA3	cornu ammonis 3
CBD	cannabidiol
CBDV	cannabidivarin
cDNA	complementary DNA
CI	confidence interval
CNS	central nervous system
cpm	counts per minute
CRO	contract research organisation
$^{\Delta 9}$-THC	Δ9-tetrahydrocannabinol

ABBREVIATION	DEFINITION/EXPLANATION
DEG	diethylene glycol
ddH_2O	double distilled water
DMSO	dimethyl sulfoxide
DNA	deoxyribonucleic acid
DNMT	DNA methyltransferase
DPM	disintegrations per minute
DS	Dravet syndrome
EDTA	ethylenediaminetetraacetic acid
EEG	electroencephalography
ENT1	equilibrative nucleoside transporter 1
etOH	ethanol
FDA	Food and Drug Administration
FSCV	fast-scan cyclic voltammetry
GABA	gamma-aminobutyric acid
GAPDH	glyceraldehyde 3-phosphate dehydrogenase
gDNA	genomic DNA
GFAP	glial fibrillary acidic protein
GPCR	G-protein coupled receptor
H_2O_2	hydrogen peroxide
HRP	horseradish peroxidase
ILAE	International League Against Epilepsy
i.p.	intraperitoneal
IODO	5-iodotubericidin
KA	kainic acid
KCl	potassium chloride
KO	knockout
LFP	local field potential
LGS	Lennox-Gastaut Syndrome

ABBREVIATION	DEFINITION/EXPLANATION
LiCl	lithium chloride
MEA	multielectrode array
MES	maximal electrical shock
NMDA	N-methyl-D-aspartate
PCR	polymerase chain reaction
PEI	polyethylenimine
PP	paired pulse
PPF	paired pulse depression
PPF	paired pulse facilitation
PPI	paired pulse interval
PPP	paired pulse profile
PPR	paired pulse ratio
PSBB	post-seizure behavioural battery tests
PTZ	pentylenetetrazole
qPCR	quantitative polymerase chain reaction
RCF	revolutions per minute
RISE	reduced-intensity status epilepticus
RISE-SRS	reduced-intensity status epilepticus - spontaneous recurrent seizures
RNA	ribonucleic acid
RPM	revolutions per minute
RT	room temperature
RT-qPCR	reverse-transcriptase quantitative polymerase chain reaction
s.c.	subcutaneous
SAH	S-adenosyl-L-homocysteine
SAM	S-adenosyl-L-methionine
SDS	sodium dodecyl sulfate
SE	status epilepticus
SEM	standard error of the mean

ABBREVIATION	DEFINITION/EXPLANATION
SRS	spontaneous recurrent seizures
SWD	spike-wave discharge
TAE	tris base, acetic acid, and EDTA buffer
TBS	tris-buffered saline
TEMED	tetramethylethylenediamine
TLE	temporal lobe epilepsy
UV	ultraviolet
WT	wildtype

1. General Introduction

1.1. Introduction to Epilepsy

Epilepsy describes a broad category of neurological syndromes, conceptually defined by the International League Against Epilepsy (ILAE) to be "a disease of the brain characterised by an enduring predisposition to generate epileptic seizures, and by the neurobiological, cognitive, psychological, and social consequences of the condition." Epileptic seizures themselves are defined as "a transient occurrence of signs and/or symptoms due to abnormal excessive or synchronous neuronal activity in the brain." (Fisher et al., 2005; Fisher et al., 2014). Broadly speaking, epilepsy is characterised by recurrent seizures, resulting from a neuronal imbalance between excitatory and inhibitory activity, resulting in hyperexcitability of neuronal networks. This hyperexcitability can occur at different locations within the brain, with seizure symptoms dependent on the origin or spread of the activity (Engel, 2013).

According to the World Health Organisation, approximately 50 million people globally have some form of epilepsy, making it one the most common neurological diseases. The percentage of the global population with active epilepsy, pharmacologically controlled or otherwise, is estimated to be between 0.4 and 1%, with around 80% of people with epilepsy living in low- and middle-income countries (WHO, 2015). Epilepsy and seizures are most likely to occur in the elderly population at greater than 75 years of age, and also have a high incidence in the first year of life (Hauser et al., 1996).

1.1.1. Organisation and classification of seizures and epilepsy

An increasing body of knowledge of epilepsy from over the past decade, mainly due to a greater understanding of the genetic causes as well as improvements in techniques and methods for studying brain function and seizure development, led to a need for updating the methods of classifying and diagnosing epilepsy. A taskforce was commissioned from 2011 by the ILAE to revise the concepts, terminology, and approaches for classifying seizures and types of epilepsy, with ongoing feedback from the epilepsy community allowing the development of a new operational classification both for patient diagnosis and epilepsy research.

1.1.1.1. Seizure types

Seizure nomenclature is complicated, with a myriad of different seizure presentations and various onsets and patterns associated with different epilepsies. Clear classification of seizure type is necessary to enable the correct management and prognosis once diagnosed. The newest nomenclature by which seizures are described was presented in 2017, with all seizures initially divided into onset of seizure activity: focal, indicating seizures originating in one hemisphere or anatomical region; generalised, indicating seizures rapidly spreading across bilateral networks; or unknown onset. Within these general

categories, subcategories describe the seizure presentation (motor or non-motor) as well as an awareness categorisation (knowledge of self and environment during a seizure) within focal seizures (Figure 1-1). Focal seizures can generally be diagnosed based upon imaging techniques, such as electroencephalography (EEG) or MRI, or clear bilateral motor seizures on one side.

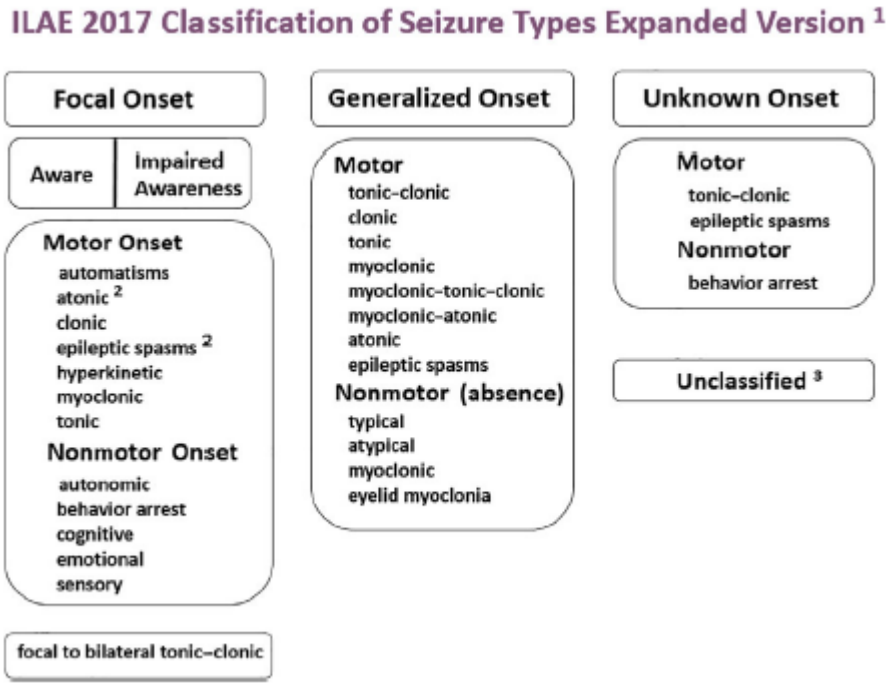

Figure 1-1: Expanded ILAE operational classification of seizure types, taken from Fisher et al. (2017). 1- Detailed descriptions are provided by the ILAE glossary of terms. 2- Focal onset atonic or epileptic spasms seizures usually do not specify awareness. 3- Unclassified refers to when inadequate information is provided or seizures cannot be otherwise classified.

Motor seizures encompass involvement of musculature of any form, including an increase or decrease of muscle contraction producing movement. Briefly, tonic seizures involve a sustained contraction of muscle, lasting between seconds to minutes, while atonic seizures refer to a loss of muscle tone. Clonic seizures are repetitive regular muscular jerks involving the same muscle groups, while myoclonic seizures are sudden and brief (<100 ms) muscle contractions, which are less regular, repetitive and sustained than clonic seizures. Tonic-clonic seizures, historically described as grand mal seizures, refer to a sequence of bilateral stiffening (tonus) followed by shaking (clonus).

Generalised non-motor seizures include absence seizures, previously described as petit mal seizures. These are typically a few seconds to half a minute long, are sudden onset and interrupt ongoing activity but do not involve any change in muscular tone; they can be identified with an EEG showing generalised

epileptiform activity. Atypical absence seizures can involve more pronounced changes in tone, with a slower onset/cessation. Non-motor focal seizure subtypes include emotional seizures, in which the seizure is accompanied by presentation of a strong emotion, cognitive seizures, referring to functions such as language, spatial perception or memory, autonomic seizures in which the autonomic system is altered, sensory seizures in which a hallucinatory perception is experienced, or behaviour arrest seizures in which activities are paused or frozen.

Focal to bilateral tonic-clonic describes what was previously known as secondary generalised seizures, as a more descriptive term for a focal onset seizure evolving to a generalised tonic-clonic seizure.

Normally, seizures are self-limiting, lasting up to 2-3 minutes depending on the seizure type (Jenssen et al., 2006), at which point endogenous seizure termination mechanisms are able to return neuronal network activity to its non-seizing state. These mechanisms are believed to occur at a variety of levels, including that of single neuron, such as activation of potassium currents and reduced ATP levels, as well as within a local neuronal network, including glutamate depletion and glial buffering, an increase in GABAergic inhibition, and inhibitory actions mediated by neuromodulators such as adenosine, which will be described in more detail below. In addition to more local mechanisms, seizure termination can also be mediated through the more remote contribution of brain nuclei (Lado and Moshe, 2008).

Following seizures, which can be described as ictus, patients can experience a postictal state, described as a transient central nervous system (CNS) dysfunction beginning when the ictus has ended (Blume et al., 2001). Symptoms tend to include tiredness, confusion, nausea and a low mood, and postictal periods can last from a few hours through to several days depending on seizure type. However, it has been identified that there is ambiguity in distinguishing the start of the postictal period from the ictal event, and the end of the postictal period from the interictal state between seizures, with patient recollection and behaviour not necessarily corresponding with concurrent EEG recordings (Fisher and Engel, 2010).

1.1.1.1.1. Status Epilepticus

The most extreme form of seizure, known as status epilepticus (SE), is a condition due to either the failure of seizure termination mechanisms or other mechanisms leading to abnormally prolonged seizures. It is generally accepted that after 30 minutes of SE, long-term consequences such as neuronal death or alteration of neuronal networks can take place. Although generalised SE with tonic-clonic seizures are most common and dangerous, SE can occur with any form of focal or generalised seizure. Increasing levels of understanding of the pathophysiology of seizures over the last few decades has steadily shortened the limit to about 5 minutes before a prolonged seizure is treated as a medical emergency (Trinka et al., 2015). As seizure activity progresses beyond 5 minutes, it becomes less likely to self-terminate and also more difficult to pharmacologically control with anticonvulsant drugs. In

addition, the hyperexcitation of neuronal networks induces a greater degree of cellular damage as the seizure continues. Over half of the patients who present with SE have had no prior history of epilepsy or seizures, with potential causes varying from CNS infections, alcohol intoxication and possible genetic factors, to anticonvulsant withdrawal for patients with pre-existing epilepsy. SE carries with it a high degree of risk for complications and morbidities, as well as up to 50% mortality (Cherian and Thomas, 2009).

1.1.1.2. Epilepsies

The epileptic condition is diagnosed following repeated seizure incidences, following the epilepsy definition as being "an enduring predisposition to generate epileptic seizures" (Fisher et al., 2005). Along with the wide range of seizures that exist, the classifications of epilepsy are similarly multiple and varied. The newest framework for classification of epilepsies describes three levels of diagnosis – firstly, seizure type, as previously described, followed by epilepsy type (focal, generalised, combined generalised and focal, or unknown) based on seizures as well as EEG readings, and finally, if possible, diagnosis of a specific Epileptic Syndrome (Scheffer et al., 2017). At all stages, the aetiology of the epilepsy is considered, and individuals may fall into more than one aetiology. The category 'genetic' replaced the old term 'idiopathic', which meant that the epilepsy had no identifiable cause and was therefore presumed to be genetic. This category includes several syndromes now known to be due to genetic defects, whether inherited or *de novo*. The 'Structural', 'Metabolic', 'Infectious' and 'Immune' categories are an expansion upon what was previously described as symptomatic, when there was a known cause for a patient's epilepsy such as a physical trauma or inflammation. The final category of 'Unknown' replaces the historical category 'cryptogenic', used when a cause was not known (Berg et al., 2010).

A structural aetiology is associated with a physical neural abnormality, and can be associated with trauma, stroke, infection or malformations such as tubers associated with Tuberous Sclerosis – which can be classified as both structural and genetic. Other genetic aetiologies include Dravet syndrome (DS), in which an *SCN1A* mutation results in heightened glutamatergic network activity, as well as a GLUT1 deficiency, which also is classified as a metabolic aetiology. Most metabolic causes of epilepsy are also likely to have a genetic component. Immune epilepsies, such as anti-NMDA receptor encephalitis, result from an immune disorder, and diagnoses are increasing due to greater access to antibody testing. Finally, an infectious aetiology is one of the most common worldwide, with epilepsy resulting from a known infection causing seizures. Examples include tuberculosis, HIV, cerebral malaria and congenital infections such as Zika (Scheffer et al., 2017).

1.1.1.2.1. Temporal Lobe Epilepsy

One of the most commonly reported epileptic syndromes is the focal onset temporal lobe epilepsy (TLE). This is an epilepsy with seizures that have a focal onset on the temporal lobe region, including subcortical structures such as the amygdala, hippocampus, and limbic system.

Incidence of TLE varies by reporting study, depending upon the definition of TLE at the time, and location from which the study recruited - specialist epilepsy centres are likeliest to be treating patients with higher intractability, while general practitioners recruit wider patients from the community (Tellez-Zenteno and Hernandez-Ronquillo, 2012). TLE, particularly medial TLE (mTLE) is one of the most common focal epilepsies, with studies varying from TLE accounting for between 21% to 66% of focal epilepsies, or 9% to 24% of all epilepsies (Manford et al., 1992; Semah et al., 1998). TLE can, however, be described as one of the most intractable epilepsies, with an increased incidence of reporting and referral to further treatment centres, with many patients unable to pharmacologically control their seizures.

TLE with hippocampal sclerosis is understood to have a structural aetiology, for instance due to traumatic brain injury, SE, or due to infection or potentially febrile seizures. Adult-onset TLE is generally seen following a childhood brain insult, with a potentially decades-long latent period before seizure manifestation. These temporal lobe seizures can be particularly resistant to medication, particularly when a clear hippocampal lesion can be identified (Spooner et al., 2006).

1.1.2. Current antiepileptic drugs and management of epilepsy

Approximately 70% of people with epilepsy respond to current pharmacological antiepileptic treatment, which means almost a third are treatment-resistant, many of which include patients with TLE and hippocampal sclerosis. Treatment resistance in the epileptic population has led to development of many new antiepileptic drugs (AEDs) in recent decades, resulting in a large range of anticonvulsant drugs currently licensed to treat epilepsy, all of which offer a method of controlling the seizures of epileptic patients rather than targeting the pathological 'source'. In addition, as seizures themselves can stimulate the progression of epilepsy, if AEDs are unable to fully control the seizures or patients do not fully comply with their drug regime, breakthrough seizures may occur which are likely to exacerbate disease condition.

AEDs tend to be a variety of different classes of drugs, generally demonstrated throughout history to have anticonvulsant effects. These include channel blockers, barbiturates, benzodiazepines and fatty acids. For most AEDs, the mechanism of action is not fully understood; generally, they reduce excessive neuronal activity by inhibiting excitatory neuronal systems, for instance acting on voltage-gated sodium or calcium channels, or augmenting the inhibitory neuronal systems by binding to GABA receptors or

preventing GABA reuptake. The greater research and understanding in recent decades into the actions of established anticonvulsant drugs, as well as the pathophysiology of seizures and specific epilepsies, has allowed for the rational development of newer drugs. These have come about either through designing drugs to act at novel targets, such as pregablin and gabapentin, derived as GABA analogues although in fact acting by blocking the α2β subunit of voltage-gated calcium channels, or a refinement of older drugs. However, a study carried out between 1984 and 1997 at a Glaswegian epilepsy unit showed that there was no significant difference between the efficacy newer or older drugs with regards to patients becoming seizure-free (Kwan and Brodie, 2000). This study included over 400 patients on single drug therapy, with approximately 70% on the older drugs (carbamazepine, sodium valproate, phenytoin and ethosuximide) and 30% on next generation drugs (lamotrigine, gabapentin, oxcarbazepine, tiagabine, topiramate, vigabatrin). Despite next generation AEDs not appearing to improve upon the efficacy of the older drugs, they do offer variety for combination therapy as well as improving side effect profiles for patients (Lee, 2014).

Currently, the type of AEDs prescribed as first-line therapy depend upon the type of seizures/epilepsy, and the demography of the patient. NICE guidelines in the UK advise prescribing a single drug (monotherapy) in the first instance to control newly developed seizures, and moving onto adjunctive treatment if necessary. There are many options which can be taken as monotherapy or combination therapies; for instance, for focal seizures, first-line treatment involves carbamazepine, lamotrigine, levetiracetam, or oxcarbazepine, with additional optional adjunctive treatments if monotherapy with the first-line therapies were ineffective. For generalised seizures, treatment is less straightforward; sodium valproate is still offered as first-line treatment for boys, men, and women not of childbearing potential. Lamotrigine is the next option if sodium valproate is unsuitable; however lamotrigine may exacerbate myoclonic seizures. Carbamazepine and oxcarbazepine can be considered, but can also exacerbate myoclonic or absence seizures.

AEDs are associated with a variety of side effects, with some of these effects severe enough to lead to patient non-adherence. For example, in the Glaswegian study mentioned above, 15-25% of patients discontinued their treatment due to intolerability of side effects, even if anticonvulsant treatment had succeeded in rendering the patient seizure-free (Kwan and Brodie, 2000). Intolerability of adverse effects can also prevent administration of the optimum dose for seizure control. Adverse effects vary between different AEDs and include sedation, cognitive dysfunction, motor and coordination effects, mood-related and psychiatric effects, appetite and weight variation, increased cardiovascular risks and teratogenic effects in pregnancy (Perucca et al., 2009; Perucca and Gilliam, 2012). The adverse effects of AEDs on cognition, particularly by topiramate, a broad-spectrum AED, have been shown in a longitudinal study involving fMRI scans of patients with epilepsy. Use of topiramate corresponded to

atypical language network activation as compared to patients taking other AEDs, with verbal disruption and impairment also seen in healthy controls taking a single dose of topiramate (Beltramini et al., 2015). This highlights the difficulty for patients with epilepsy to balance drug efficacy in controlling seizures with the potentially severe adverse effects associated with treatment.

1.1.3. Preclinical epilepsy research

The development of novel AEDs, driven by the inadequacy of current drugs in 30% of cases, hinges upon testing efficacy of the drugs in preclinical models of seizures and epilepsy, both behaviourally *in vivo* and through *in vitro* brain slices (Jefferys, 2003). However, the development of these models, depending upon the particular epileptic syndrome, generally requires an understanding of the development of the neuropathophysiology. Genetic epilepsies are now able to be modelled via a direct genetic modification which allows the study of the pathophysiology in greater detail. However, epilepsies with an external aetiology, such as TLE, can be more difficult to understand and model.

1.1.3.1. Epilepsy and the hippocampus

The hippocampus, a horn-like structure which lies deep within the medial temporal lobe in humans (Figure 1-2A) has been heavily implicated in epilepsy, particularly TLE which has a structural aetiology that can include hippocampal sclerosis (Thom, 2014). In addition to observations that patients with epilepsy also suffered from hippocampal damage, resection of the temporal lobe (including the hippocampus) is a surgical treatment for seizures, implying a strong relationship between the hippocampus and seizure manifestation (Schwartzkroin, 1994). The hippocampus is generally believed to be involved with memory consolidation and retrieval processes, as well as spatial memory. In addition to epilepsy, the hippocampus is also associated with dementia, hypoxia, and encephalitis, which are characterised by memory loss and disorientation.

The hippocampus forms connections throughout the brain, including with the prefrontal cortex, septal nuclei, thalamus, and hypothalamus. The primary input to the hippocampus is from the entorhinal cortex, with which it forms the trisynaptic pathway (Figure 1-2C). Signals from layer 2 of the entorhinal cortex enter the hippocampus at the dentate gyrus via the perforant pathway, synapsing onto the granule cells of the dentate gyrus. From there, mossy fibres project onto pyramidal cells of the CA3, forming the second synapse, and axons from CA3 form the Schaffer collaterals to synapse onto CA1 pyramidal neurons as the third synapse. The circuit with the entorhinal cortex is completed by axons from CA1 returning to layers 5 and 6 of the entorhinal cortex via the subiculum. Additionally to the trisynaptic circuit, the temporoammonic pathway inputs directly from layer 3 of the entorhinal cortex onto CA1 neurons, bypassing the dentate gyrus and CA3. In addition to glutamatergic signalling, GABAergic

interneurons for approximately 10-15% of the neuronal population of the hippocampus, allowing for refinement and regulation of almost all hippocampal processes (Pelkey et al., 2017).

The hippocampus has been extensively studied with regards to its association with epilepsy. Many pathological changes are observed, particularly in the dentate gyrus; these include mossy fibre sprouting and granule cell dispersion, as well as neuronal cell loss and gliosis throughout hippocampal regions (Thom, 2014). Electrophysiology studies performed using hippocampal tissue resected from human patients with epilepsy indicated that a much lower afferent stimulation "threshold" for hippocampal pyramidal cells with discharge prolonged responses in bursts of activity. Other experiments suggested a decrease in GABAergic activity, or upregulation in glutamate receptors in the human epileptic hippocampus (Huberfeld et al., 2015). However, it remains unclear whether the hippocampus is the source of ictal events, or whether the high degree of connectivity and interconnectivity of the hippocampus allows for the amplification and spread of previously initiated hyperexcitability. It is possible that rather than being causative, the degradation of the hippocampus and dentate gyrus in particular is due to cytotoxicity from high levels of input entering the trisynaptic pathway. Regardless, the hippocampus remains a significant area for focus in research, with increased levels of CA1 output in chronic epilepsy (El-Hassar et al., 2007) and the previously described temporal lobe resections having strong therapeutic efficacy in patients demonstrating the value of the hippocampus in epilepsy research.

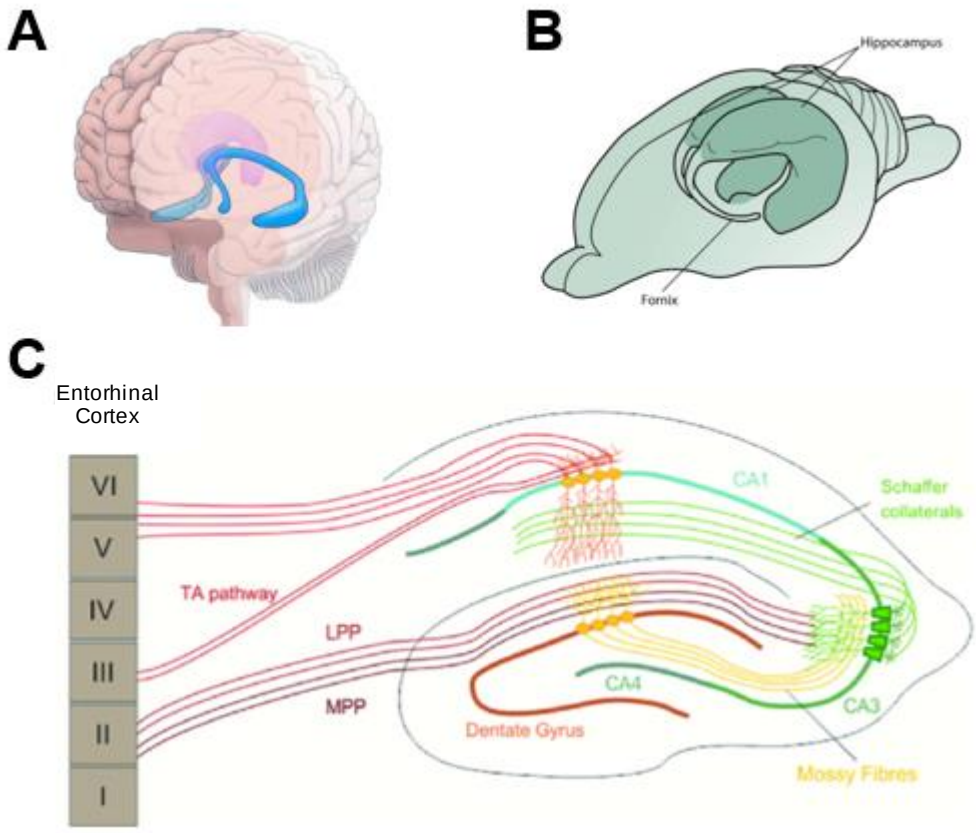

Figure 1-2: Schematic diagrams of the anatomy and circuitry of the hippocampus. A: Location of the hippocampus in the human brain. **B:** Location of the hippocampus in the rat brain. **C:** Representation of the trisynaptic pathway of the hippocampus in a transverse cross-section. Input from the entorhinal cortex (layer 2) enters the dentate gyrus of the hippocampus through the perforant pathway. Signals then travel through mossy fibres to synapse upon the pyramidal cells of CA3, which then sends axons to CA1, forming the Schaffer collaterals. Hippocampal output from CA1 is projected to layers 5 and 6 of the entorhinal cortex. ***Image sources****: A: (Psypost, 2017); B: (Hammond, 2015); C: (Pinar et al., 2017).*

1.1.3.2. Progression of epilepsy: epileptogenesis and seizures

Epileptogenesis refers to the process by which the brain develops chronic epilepsy, such as during the 'latent period' prior to manifestation of TLE following an early insult. The latent period can be years, as exemplified in adult-onset TLE through the development of seizures in the second decade of life due to a childhood insult. Epileptogenic processes are generally understood to increase the hyperexcitability of neuronal networks, aggravating the imbalance between inhibition and excitation. It is likely that synapses are strengthened and new synapses created through synaptic plasticity, increasing the likelihood of co-activation and seizure activity (Ben-Ari et al., 2008). In addition, the dentate gyrus is one of the few regions within the CNS which displays neurogenesis, with neural stem cells beneath the cell body layer differentiating into granule cells which then integrate into existing circuitry. This

neurogenesis is sensitive to physiological and pathological stimuli, and studies have suggested that after an initiating event for TLE, neurogenesis within the dentate gyrus is affected; abnormal or excessive neurogenesis may be seen immediately following the insult for a period of time, while neurogenesis may be significantly decreased in chronic epilepsy (Kuruba et al., 2009). The process is complex, with many observations seen in the development and progression of epilepsy which may or may not be related to seizure activity; for instance, mossy fibres sprouting from hippocampal granule cells observed in the dentate gyrus in TLE patients were thought to be establishing a positive feedback circuit, although it was unclear whether this was a consequence or a cause of seizures. However, blocking mossy fibre sprouting in mice following SE did not appear to have antiseizure effects, suggesting that mossy fibre sprouting is not associated with or responsible for seizure activity (Heng et al., 2013).

In addition to an initial insult or seizure that progresses to chronic epilepsy, there has long been the idea that seizures over the course of epilepsy progressively worsen the disease – that "seizures beget seizures" (Gowers, 1881). Despite this, there are many types of epilepsy that do not show progression or decline with seizure activity, such as occipital, absence or juvenile myoclonic epilepsies. For TLE, there is a clearer link between seizure activity and hippocampal sclerosis, potentially due to seizure-induced excitotoxicity. Epileptic encephalopathies show cognitive decline following onset in a young age, but it is difficult to determine whether this is due to the aetiology of the disease or if the seizure activity actively worsens disease progression. A synaptic homeostasis hypothesis suggests that during sleep, essential homeostatic downscaling of synaptic strengths gained during waking hours takes place to regulate total neuronal synaptic strength (Tononi and Cirelli, 2006). It has been postulated that this regulation of synaptic strength taking place during slow wave sleep is interrupted by focal epileptic activity in children with epileptic encephalopathies, which may lead to the cognitive worsening of their condition (Bolsterli et al., 2011; Avanzini et al., 2013).

1.1.3.3. Models of epilepsy and seizures

Epilepsy benefits from the previously described increasing body of knowledge regarding its cause and development, as compared to psychiatric disorders such as depression or neuropathic pain which struggle to precisely determine translational validity of behaviours in animal models (Belzung and Lemoine, 2011). As such, there are several animal models representative of acute seizures and the more prolonged recurrent seizures of chronic epilepsy (Loscher, 2011). Uncovering genetic variants underlying clinical epileptic syndromes allows for animal models to be created carrying the same genetic mutation, known as genetically valid models. Seizure activity can also be induced in wildtype animals through drug application or electrical stimulation (Figure 1-3). Historically, maximal electroshock seizures (MES), 6Hz auditory-induced seizures, or injection of the convulsant drug pentylenetetrazole (PTZ), have been used to induce acute generalised seizures in animal models, allowing for testing the acute anticonvulsant

efficacy of novel drugs in preventing seizures. Repeatedly inducing these seizures over a number of days is known as kindling and considered to be a model of chronic epilepsy such as TLE. Although the kindling model is less replicative of the underlying aetiology of epilepsy, it has been shown to be accurate in predicting clinical efficacy of AEDs (Loscher, 2011). Other chronic models offer a closer imitation of the progression of TLE by inducing an extended period of SE in young animals, generally around weaning age, through electrical or chemical stimulation, after which they enter a latent phase and later develop spontaneous recurrent seizures. An example is described below in section 1.1.3.3.1.

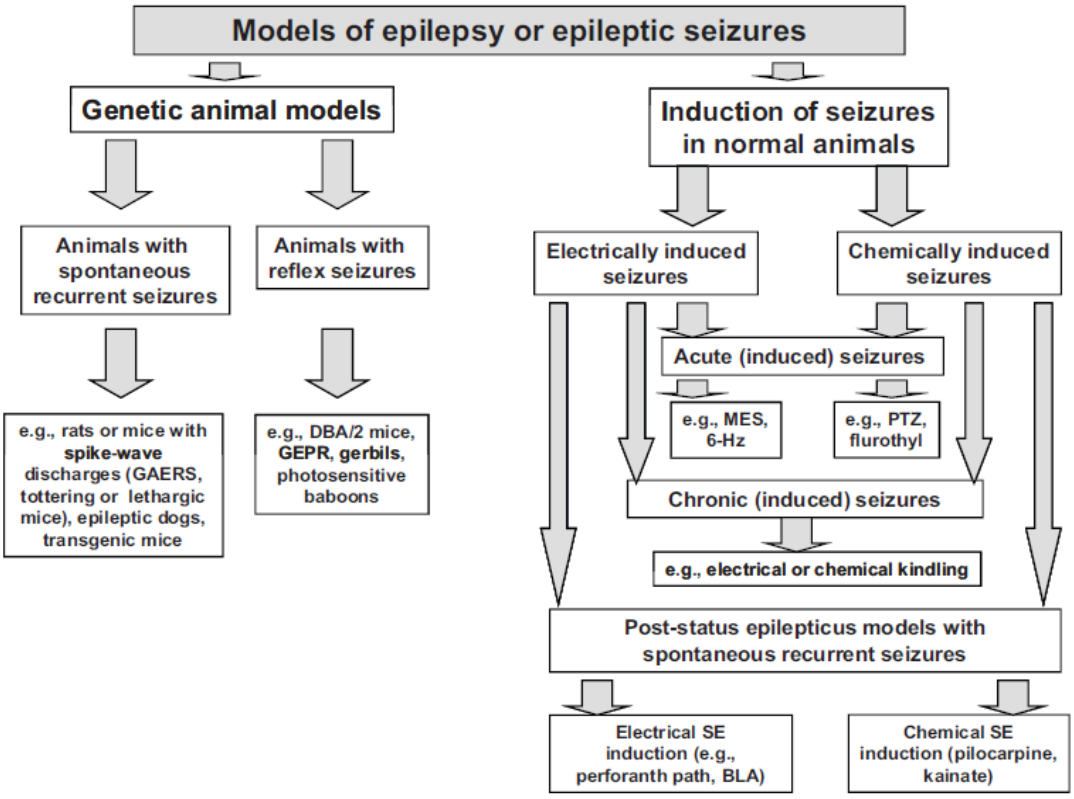

Figure 1-3: A brief overview of different types of animal models which mimic human epilepsy or epileptic seizures, taken from Loscher (2011).

These models allow for screening and testing of compounds for anticonvulsant and antiepileptic efficacy, and underlie the development and introduction of many novel AEDs over the past few decades (Kwan and Brodie, 2000). However, as the efficacy of general AED treatment has remained at approximately 70% of all epilepsy patients, concerns have been raised as to the validity of using the same animal models to develop novel drugs for treatment-resistant patients (Loscher, 2011). Additionally, many methods of rapidly screening anticonvulsant drugs rely on acute seizure models, whether in brain slices *in vitro* or in acutely induced seizures in animal models, generally with a prophylactic application of the putative anticonvulsant. While these allow development of drugs that can prevent an oncoming seizure, there are

far fewer studies that use chronic models, thus targeting post-epileptogenic systems such as those in treatment-resistant TLE.

1.1.3.3.1. The pilocarpine *in vivo* model of chronic epilepsy and epileptogenesis

Of the chemical TLE models, injection of the convulsant drug pilocarpine produces SE more rapidly than kainic acid, produces more clinically valid symptoms such as hippocampal sclerosis, and appears to be predictive of the human TLE presentation (Curia et al., 2008). While injection of pilocarpine (in the range of 300 – 400 mg/kg) typically produces SE and a clinically valid pilocarpine-TLE model in 60% of injected rats (Cavalheiro et al., 1991), mortality rates would be seen at 30% to 40%, or higher (summarised by Curia et al. (2008)). Refinements included sensitising rats with a prior injection of lithium chloride, which would decrease the dose of pilocarpine needed to induce SE by ~90% to the 30 – 50 mg/kg range, using repeated injections of lower doses of pilocarpine, and terminating SE after 30 – 90 min using diazepam. An analysis by Curia et al. (2008) was able to show that overall mortality increases with amount of time spent in SE, with 180 min in unterminated SE resulting in >60% mortality. A study by Glien et al. (2001) demonstrated that a single injection of 30 mg/kg pilocarpine in lithium-sensitised animals resulted in a 45% mortality rate, while 10 mg/kg doses in 30 min intervals decreased mortality to below 10%. In all cases, around 70% of rats developed SE, and almost all rats who experienced at least 60 min of SE developed SRS. The success rate of rats developing SRS following pilocarpine-induced SE remained similar through all iterations of the model.

A low mortality, high morbidity reduced-intensity version of the pilocarpine-induced SE with subsequent SRS was developed partly at the University of Reading, and included lithium sensitisation, low but increasing doses of pilocarpine at 30-min intervals, and SE termination at 60 min (Modebadze et al., 2016). This model also includes a behavioural test, validated using video recording, with stringent criteria favouring false negatives over false positives for detecting appearance of SRS (the behavioural test as used in this thesis is further described in section 2.1.2). Electrophysiological recordings of hippocampal slices from this model were able to show a latent, epileptogenetic period of between 4 to 8 weeks following pilocarpine induction, with CA3 activity displaying a fast oscillatory profile comparable to that shown by human hippocampal tissue from a patient with intractable seizures (Modebadze et al., 2016).

This reduced-intensity SE (RISE) model provides a valid model for studying behavioural, motor, and clinical outcomes of TLE, as well as the neuronal and molecular basis of epileptogenesis (Jones et al., 2010; Hill et al., 2012; Jones et al., 2012; Patra et al., 2019). A relatively short but intense investment of researcher time during and immediately after pilocarpine induction helps ensure a very low mortality rate, while the stringent behavioural tests allow for rapid diagnosis of SRS and experimental use in this

chronic model of epilepsy. Further details on the model used in this thesis are provided in section 2.1 and Appendix 8.1.

1.1.3.3.2. Methods of *in vitro* seizure and epilepsy modelling – multielectrode arrays

Hippocampal brain slices are a well-validated method of investigating neuronal circuitry, and a frequently-used *in vitro* model for investigating cellular and molecular mechanisms of epilepsy. The basis of *in vitro* brain slices is to remove the brain from the skull and preserve in ice-cold, isotonic solution while creating 300 – 400 µm thick slices in a transverse plane, allowing hippocampal fibres to remain intact and therefore retain signalling circuitry. Different methods of investigating the electrophysiological properties of these neuronal networks include single-cell methods, such as patch clamping, in which a glass electrode directly connects with the cell membrane of a neuron and allows manipulation to the current or voltage across the membrane; or network-based methods, where field potentials are induced and recorded using electrodes inserted into the hippocampal slice from the top. A less invasive method involves the use of multielectrode arrays, in which a slice is placed upon a pre-set pattern of electrodes, and stimulation and recording can happen from below the slice, with no damage done due to insertion of electrodes. Another advantage of multielectrode arrays is the ability to monitor activity across different locations of the hippocampus, whether due to spontaneous activity or the propagation of a stimulation across known fibre pathways.

1.1.3.4. Outlook for antiepileptic therapeutic research

Research into antiepileptic therapy continues despite the above-described difficulties. The continual search for new AEDs, preferentially with higher efficacy and fewer side effects, has developed towards investigating novel systems and mechanisms, rather than the ones known or thought to be targeted by traditional AEDs.

1.2. Cannabidiol (CBD) and Epilepsy

The *Cannabis* genus of plants has been used for millennia, both as a recreational and medicinal drug, and for manufacturing processes as hemp fibre. Among its uses as an analgesic, anti-inflammatory, anxiolytic and antiemetic drug throughout history, it has been reported to be efficacious in epilepsy as an anticonvulsant (reviewed extensively by Devinsky et al. (2014)). Cannabis plants express over 500 compounds, with over 70 being terpenophenolic compounds unique to cannabis plants known as phytocannabinoids (Elsohly and Slade, 2005; Radwan et al., 2009). The most abundant compounds, of varying concentration depending on strains of *Cannabis sativa* or *Cannabis indica*, are cannabidiol (CBD) and $^{\Delta 9}$-tetrahydrocannabinol ($^{\Delta 9}$-THC), the latter of which is responsible for the psychoactive "high" (Rosenberg et al., 2015). Following isolation of cannabinoid compounds in the early 20th century, by the 1990s, two G-protein coupled receptors, cannabinoid receptors 1 and 2 (CB_1R and CB_2R), had

been identified, with CB_1R being the most densely expressed in the CNS and mediating the psychoactive effects of cannabis through activation by $^{\Delta 9}$-THC. These receptors, together with the endogenous compounds that activate them, were labelled as the endocannabinoid system (Matsuda et al., 1990; Howlett et al., 2002).

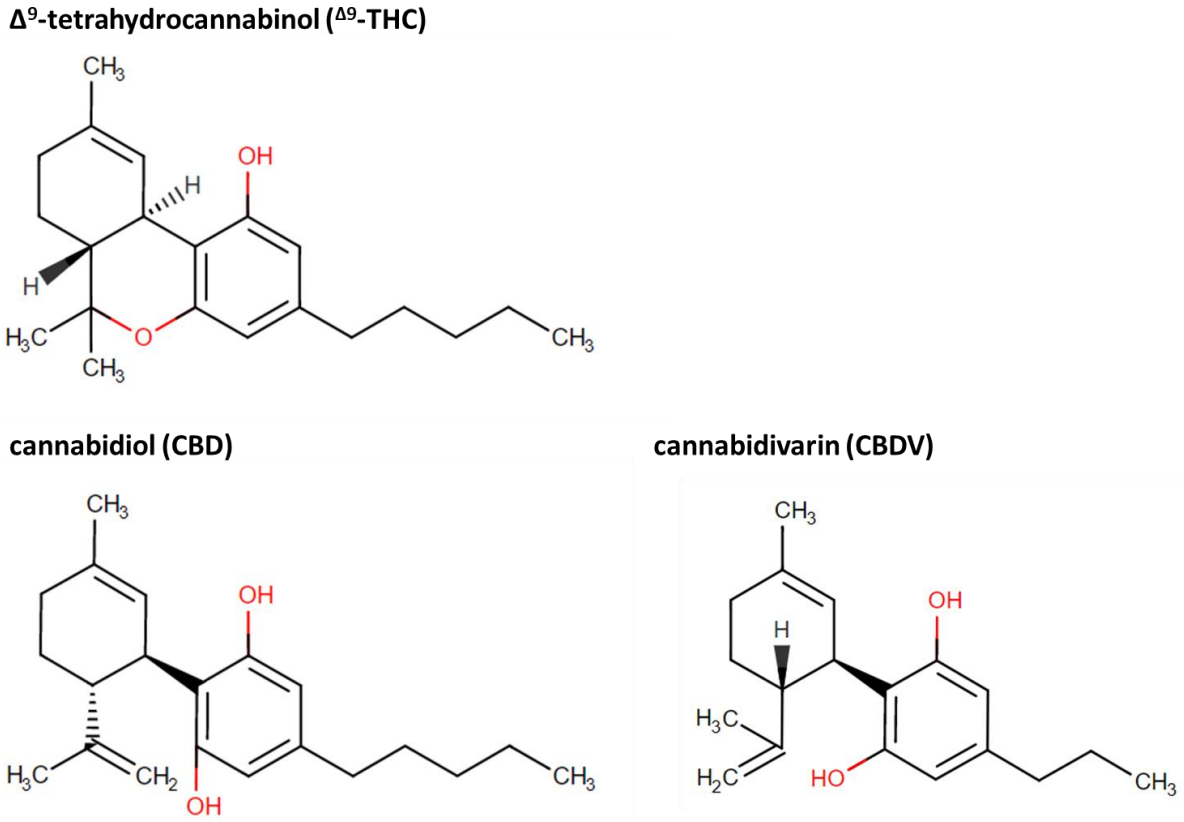

Figure 1-4: Chemical structures of the phytocannabinoids $^{\Delta 9}$-tetrahydrocannabinol ($^{\Delta 9}$-THC), cannabidiol (CBD), and cannabidivarin (CBDV). Structural images from Drugbank (2020).

Studies have shown that along with a rise in endogenous cannabinoids during seizures, activation of the endogenous cannabinoid system through CB_1Rs appears to provide anticonvulsant and neuroprotective effects (Marsicano et al., 2003; Karanian et al., 2005). However, $^{\Delta 9}$-THC acts via CB_1R to produce the psychoactive effect, and has also been reported to show proconvulsant effects in some models (Rosenberg et al., 2015). Cannabidiol alone, however, has very low affinity for cannabinoid receptors, with displacement values generally reported to be in the micromolar range (Pertwee, 2008). Interestingly, some studies have reported varying CBD actions on cannabinoid receptors, including being a potent antagonist at CB_2Rs (Thomas et al., 2007) or acting as a negative allosteric modulator at CB_1Rs (Laprairie et al., 2015). However, CBD has not been shown to be psychoactive while potentially having anticonvulsant effects (Thomas et al., 1998; Wallace et al., 2001). Therefore, the therapeutic

potential of CBD in treating epilepsy without activating the endocannabinoid psychoactive 'high' has led to a focus in the study of CBD, both as cannabis strains with high endogenous CBD, or as purified isolated CBD.

1.2.1. Early patient studies, anecdotes and surveys

For decades there have been case studies of patients presenting with seizures associated with cannabis use, which have reported either proconvulsant or anticonvulsant effects, although in some cases cannabis use had no effect on seizures (Rosenberg et al., 2015). A small clinical study at the end of the 1970s administered CBD to healthy volunteers and epileptic patients over a few months, and in addition to 7 of the 8 epileptic patients showing a decrease in seizures with 4 becoming seizure-free, in all participants CBD appeared to be well tolerated without signs of toxicity or serious side effects (Cunha et al., 1980). The tolerance and withdrawal effects seen in chronic cannabis use are understood to occur due to $^{\Delta 9}$-THC stimulation causing alteration of the endocannabinoid system and receptor expression (Oviedo et al., 1993), and studies have shown that CBD therapy does not appear to cause significant intoxication, tolerance or withdrawal (Robson, 2011).

Some of the recent public interest in cannabinoids as a therapy for epilepsy is based upon high-profile cases of children with intractable epilepsy who have been successfully treated with CBD-rich cannabis extracts. In one widely-reported case, a young patient with DS with a confirmed SCN1A mutation had attempted therapy with several AEDs with little effect. Following administration of an extract of cannabis with a high CBD:$^{\Delta 9}$-THC ratio, she then underwent a drastic reduction in seizure frequency, decreasing from over 50 seizures a day to around 2 – 3 nocturnal seizures per month. After transitioning to taking only the CBD-rich extract, and no other AEDs to control her seizures, any attempt at lowering the dosage immediately led to an increase of seizure frequency (Maa and Figi, 2014). Other researchers have surveyed parents who had attempted using CBD products to treat children suffering from a variety of childhood epileptic syndromes, and across the two reported online surveys, spanning in total 136 responses, parents reported 84 – 85% of the children showing a decrease in seizure frequency after being treated with CBD and 11 – 14% becoming seizure-free (Porter and Jacobson, 2013; Hussain et al., 2015). It is worth noting that these surveys also described other beneficial effects, including improvements in alertness, appetite and mood, along with decreases in adverse effects seen in other AEDs. However, both these surveys are evidently open to bias, with parents recruited through online social media groups advocating CBD use and no level of control regarding the answers given by parents. In addition, in all cases it is unknown the exact amount of CBD and $^{\Delta 9}$-THC administered; although parents were able to give an estimate of the composition ratio, in general the patients were being given crude extracts of cannabis.

1.2.2. Preclinical studies

The anticonvulsant efficacy of pure CBD has been demonstrated in a variety of preclinical models, both *in vivo* and *in vitro*. Following the initial isolation of phytocannabinoids, research using mice MES models demonstrated their anticonvulsive effect, including that of CBD (Karler et al., 1973). More recent investigations have used a variety of acute and chronic models to show CBD efficacy. Application of 1 – 100 µM CBD to acute rat hippocampal slices reduced both the seizing activity induced by Mg^{2+} removal from the aCSF perfusate, and also through addition of 4-AP (Jones et al., 2010). Acute *in vivo* models have also shown that CBD (in various doses and routes, e.g., ~100 mg/kg i.p., 10 mg/kg single IV, or ~200 mg/kg oral) protects against acute seizures induced by intraperitoneal PTZ injection, pilocarpine-induced SE, partial seizures induced by unilateral infusion of penicillin into the lateral ventricle, as well as MES, 6-Hz psychomotor seizures, and corneal kindling (Jones et al., 2010; Jones et al., 2012; Patra et al., 2019). Pharmacokinetic analyses in rat have shown that oral or intraperitoneal administration of 120 mg/kg CBD can reach a C_{max} in the brain of 5.2 – 12.6 µg/mL, corresponding to ~14.9 – 40 µM (Deiana et al., 2012). To assess whether the antiepileptic effect of CBD was due to muscular sedation, analyses of motor function on CBD-treated rats found very little effect of the drug on motor function (movement, balance and coordination), and no effect on grip strength and muscle tone (Jones et al., 2012).

In chronic *in vivo* models, a PTZ model of chronic epilepsy showed that rats treated with CBD prior to each PTZ injection exhibited a dose-dependent decrease in seizure severity and protection from developing chronic epilepsy following the 28-day PTZ kindling. The same study found that CBD decreased hippocampal cell loss and astrogliosis (Mao et al., 2015). A more chronic model of TLE in rats using pilocarpine-induced SE which later developed spontaneous recurrent seizures (SRS) also found that orally administered CBD over 8 weeks following appearance of SRS was able to attenuate seizure burden compared to vehicle (Patra et al., 2019). This model also demonstrated a decrease in motor comorbidities, as well as an apparent reversal of epilepsy-induced cognitive defects. This final study is significant, as it demonstrates efficacy of CBD not as a prophylactic against acute seizures, but as a treatment following SRS and therefore the most clinically valid model of treatment for TLE.

Another phytocannabinoid that has come under investigation for anticonvulsant properties is cannabidivarin (CBDV), the propyl analogue of CBD, which was isolated in 1969 (Vollner et al., 1969). CBDV has also been shown to exhibit anticonvulsant properties in several *in vivo* and *in vitro* models. Seizure activity induced in rat hippocampal slices with 4-AP was reduced upon application of CBDV, and in the Mg^{2+}-free model, while local field potential (LFP) frequency was increased, CBDV application reduced amplitude and duration of LFPs (Hill et al., 2012). The protective action of CBDV has also been shown in several *in vivo* models, including audiogenic and MES seizures in mice and also

in acute PTZ-induced seizures in rats. CBDV alone had no significant effect in pilocarpine-induced SE, but when co-administered with currently used AEDs sodium valproate or phenobarbital, CBDV significantly increased the anticonvulsant action when compared with the AED alone (Hill et al., 2012). CBDV has also been shown to reduce seizure severity in the pilocarpine model when co-administered with CBD, or as impure CBDV- and CBD-rich cannabis plant extracts, which also contain $^{\Delta 9}$-THC and $^{\Delta 9}$-THCV (Hill et al., 2013). Comparisons of the anticonvulsant effect of these extracts with and without $^{\Delta 9}$-THC and $^{\Delta 9}$-THCV removed have shown that there was no difference in strength of decrease in seizure severity. Complementary radioligand binding analysis showed that $^{\Delta 9}$-THC and $^{\Delta 9}$-THCV content improved affinity for CB1Rs, indicating that the anticonvulsant action of the cannabis extracts was mediated through CB1R-independent actions (Hill et al., 2013).

CBDV administration showed no deficits in motor coordination or grip strength, except in one case of CBDV rich extract; animals were more likely to fail the static beam test when given extracts containing $^{\Delta 9}$-THC/$^{\Delta 9}$-THCV, or high doses of extracts without $^{\Delta 9}$-THC/$^{\Delta 9}$-THCV. This suggests that cannabinoid receptor activation through $^{\Delta 9}$-THC and/or $^{\Delta 9}$-THCV or other plant constituents modulates motor effects, as pure CBDV had no effects on motor task performance (Hill et al., 2012; Hill et al., 2013).

1.2.3. Large-scale clinical trials (Epidiolex®)

Although there had been many reports and patient anecdotes regarding the therapeutic efficacy and tolerability of uncontrolled CBD administration, there had been few controlled, robust clinical investigations into the safety, mechanisms and efficacy of CBD until the last few years.

Following the publication of two previously described *in vitro* and *in vivo* studies showing the antiepileptic therapeutic potential of CBD (Jones et al., 2012), the parents of a child with intractable childhood epilepsy directly sought out GW Pharmaceuticals, the sponsor of the two published studies. The patient had been treated with multiple different epilepsy therapies but was still suffering up to 60 seizures per day. Working with GW Pharmaceuticals, this California family travelled to London in December 2012 to become the first patient to try Epidiolex®, a pure CBD preparation. After 3 days of treatment, the child was down to one seizure a day. This led to the family being permitted by the Food and Drug Administration (FDA) to use Epidiolex® under a compassionate use programme in California, the success of which led to GW Pharmaceuticals pursuing wider trials across more epilepsy centres.

Orphan Drug Designation was given by the FDA to Epidiolex® (CBD) for two Orphan Disease indications between November 2013 and February 2014 – these were DS and Lennox-Gastaut Syndrome (LGS), which represent two of the most difficult to treat genetic childhood epilepsy syndromes. Both syndromes occur in children, can persist throughout a lifetime, and are associated with a high mortality rate. DS is a severe, rare genetic disorder characterised by febrile seizures in the first year of life, and

caused in 70 – 90% of cases by a mutation in the *SCN1A* gene (Dravet and Oguni, 2013). This mutation is thought to result in a dysfunction of voltage-gated sodium channels ($Na_{v1.1}$) expressed in GABA-ergic interneurons in the hippocampus, likely to cause a reduction in sodium current activity and reduced firing (Schutte et al., 2014). It is thought that DS affects approximately 1 in every 20 000 – 40 000 births, and management of the syndrome relies upon controlling the seizures with a variety of anticonvulsant drugs (Incorpora, 2009). LGS has an unknown cause and forms 2 – 5% of childhood epilepsies, presenting with a variety of different types of seizures. LGS patients tend to be resistant to anticonvulsant drugs, making treatment and management of the condition difficult (Arzimanoglou et al., 2009).

From 2014, GW initiated an open-label trial in patients with treatment-resistant epilepsy (214 patients, 11 sites across US), as well as four international phase 2/3 randomised controlled trials specifically in DS and LGS (2 trials for each syndrome, with a total of 715 patients across the four studies). Each of these clinical studies recruited patients aged 2 – 55 years, generally with a history of at least 2 previous AEDs and displaying at least 2 uncontrolled seizures weekly during a 4-week pretreatment baseline. During the 14-week treatment period, patients were treated with placebo or Epidiolex® (20 mg/kg in all studies, and an additional 10 mg/kg arm in two studies) in conjunction with their ongoing treatment, with a primary endpoint of percentage change in monthly seizures. Across the studies, treatment groups displayed around 20 percentage points difference between treatment and placebo medians, indicating a significant decrease in seizures due to treatment (Devinsky et al., 2017; Devinsky et al., 2018; Thiele et al., 2018). Adverse events (AEs) were generally mild to moderate in severity, and included somnolence, sedation, decreased appetite, and diarrhoea. Some serious AEs included transaminase elevations in the liver, indicating drug-induced liver toxicity – however no serious liver failure events were recorded, and all transaminase elevations were resolved, including some during continued CBD treatment.

After filing a New Drug Application for Epidiolex® in the treatment of DS and LGS at the end of 2017, the FDA approved this application in June 2018, making Epidiolex® the first FDA-approved drug derived from cannabis, as well as the first FDA approval of a drug specifically for the treatment of DS. Following FDA approval, the Drug Enforcement Agency (DEA) rescheduled Epidiolex® from the highest restriction Schedule I to the lowest restriction Schedule V, assigned for drugs with a proven medical use and low potential for abuse. Epidiolex® became available for prescription in the US on 1st Nov 2018, and in the first 5 months following its market availability, net sales of Epidiolex® exceeded $37M (Gwpharma, 2019).

Although ultimately approved by the FDA, the Center for Drug Evaluation and Research review of the application highlighted that although the toxicity and safety of Epidiolex® had been adequately tested, there remained a question in the activity of the 7-COOH-CBD metabolite which had not been sufficiently investigated (Brown, 2018). However, approval was recommended due to the benefit-risk assessment of

the clinical need for treatment in the debilitating childhood epilepsies as well as the safety data from clinical programmes. This demonstrates that although CBD has been shown to have clinical efficacy, there are still mechanisms of action of the drug and its metabolites which preclinical studies have not yet been able to fully elucidate.

The 7-COOH-CBD metabolite identified by the FDA as an unknown is the most abundant metabolite of CBD, however there are many possible chemical compounds which can be formed following treatment with CBD. Recent years have seen more studies investigating these metabolites, however due to the extensive metabolism opportunities for CBD and its complex pharmacokinetics, the contribution of these metabolites to any effects caused by CBD, or their interaction with CYP liver enzymes, remains broadly unanswered (Ujváry and Hanuš, 2016).

1.2.4. Potential targets of CBD

Some investigation has been done into the targets of CBD and, to a lesser extent, CBDV. A review of the literature identified over 60 different potential molecular targets of CBD spanning receptors, transporters, ion channels and enzymes (Ibeas Bih et al., 2015). This wide range of potential mechanisms of action has made it difficult to specify the precise antiepileptic action of CBD, particularly with the possibility that this involves the synergistic action of multiple targets. Regardless, studies so far have focused on singular systems at which CBD has molecular activity to assess the antiepileptic potential.

Comparisons between CBD and cannabigerol (CBG), a similarly structured phytocannabinoid, showed that while both CBD (10 µM) and CBG (10 µM) block voltage-gated sodium (Na_v) channels *in vivo*, CBG does not display anticonvulsant effects in PTZ-induced seizures in rats, while CBD does. This suggests that the anticonvulsant action of CBD is unlikely to be completely mediated through inhibition of Na_v channel *in vivo* (Hill et al., 2014), although a recent study has suggested that CBD (1 µM) may attenuate resurgent sodium currents in a $Na_v1.6$ mutation-associated epileptiform increase in neuronal excitability (Patel et al., 2016). Another study examined the interaction between CBD administration and blockade of Maxi Calcium-Activated Potassium (BK) channels, and found that BK channel blockade attenuated the protective action of CBD (between 0.2 to 200 ng/mouse via intracranial perfusion) in PTZ mice models of acute seizures, suggesting that CBD anticonvulsive action may be mediated via BK channels (Shirazi-Zand et al., 2013). However, in mice undergoing MES, inhibition of BK channels itself was anticonvulsant, suggesting an interaction between CBD action and cytoplasmic calcium levels.

Potential targets of CBDV have been less explored. A gene expression study in rat cortex and hippocampus found that PTZ-induced seizures upregulated expression of several genes previously implicated in epilepsy, including *Fos, Egr1, Arc, Ccl4 and Bdnf*. CBDV treatment led to correlated

decreases in seizure severity with decreases in mRNA expression of these genes (Amada et al., 2013), suggesting that CBDV treatment could mitigate an anti-epileptogenic effect.

To conclude, while it is evident that CBD and potentially CBDV are efficacious in treating patients with epilepsy, the mechanism(s) by which they exert this anticonvulsant action is still unclear. Further investigation in this area, identifying the targets by which CBD and CBDV are anticonvulsant, allows for rational development of drug design to increase treatment efficacy, as well as furthering the knowledge of pathophysiology of a treatment-resistant disease. To this end, a potential target of CBD which may be involved in control of seizure activity has been identified as modulation of the central adenosine signalling system (Carrier et al., 2006; Ibeas Bih et al., 2015). As will be described below, adenosine is a powerful broad neuroregulatory molecule, and while CBD has been shown to interact with the system, this has not previously been investigated in depth.

1.3. Adenosine Signalling in Epilepsy

Adenosine is a purine ribonucleoside, ubiquitous in all living molecular systems as the backbone of ATP and cAMP. As an individual molecule, it also functions as a vasodilator, an anti-inflammatory agent and a powerful neuromodulator, through its binding to its four known GPCRs: the adenosine receptor subtypes A_1, A_{2A}, A_{2B}, and A_3. Adenosine binds with the highest affinity to A_1 and A_{2A} receptors (A_1R and $A_{2A}R$). A_1 and A_3 receptors are $G_{i/o}$-coupled, with activation inhibiting adenyl cyclase, while A_{2A} and A_{2B} receptors are G_s-coupled, stimulating adenyl cyclase. A_1R and $A_{2A}R$, as well as A_3R, are expressed centrally, and therefore act as the mechanisms through which adenosine exerts its neuromodulatory effects, for instance in the sleep-wake cycle and pain pathways (Sosnowski et al., 1989; Basheer et al., 2004). A_1Rs are widely expressed in the brain and the receptor is one of the most abundant neuronal metabotropic receptors. They are located both pre- and postsynaptically, and decrease excitation through inhibition of transmitter release as well as postsynaptic modulation of glutamatergic receptors and membrane potential (Cunha, 2005). $A_{2A}Rs$ are less abundant in the brain, although they are particularly highly expressed in the striatum and basal ganglia where expression is mostly postsynaptic. However they are also found in limbic and cortical regions with primarily presynaptic localisation (Cunha, 2005). $A_{2B}R$ are primarily expressed peripherally, while A_3R may act with A_1R and $A_{2A}R$ to modulate glutamatergic transmission via hippocampal AMPA receptors (Fredholm et al., 2001; Eltzschig, 2009; Layland et al., 2014; Sheth et al., 2014; Di Angelantonio et al., 2015).

1.3.1. Endogenous acute neuroprotective role of adenosine

Adenosine was first demonstrated to have anticonvulsant properties *in vivo* when given intraperitoneally to mice undergoing audiogenic seizures (Maitre et al., 1974). *In vitro*, adenosine exhibits tonic inhibitory properties on induced ictal events in hippocampal slices, and was therefore proposed to be an

endogenous neuroregulator (Dunwiddie, 1980). Microdialysis experiments in human TLE patients have shown that adenosine levels increase in the hippocampus during seizure activity and remain elevated in the postictal period, suggesting that adenosine is likely to play a role in endogenous seizure termination and preventing refractory seizures (During and Spencer, 1992). As A_1R are among the most abundant metabotropic receptors in the brain, with highly synaptic localisation on neurons throughout the cortex, hippocampus and cerebellum, as well as presence on glial cells, it is generally understood that the inhibitory role of seizure-induced adenosine is mediated via the $G_{i/o}$-bound A_1R. This seizure-induced rise in adenosine has also been shown in a large animal model of epilepsy, using faster and more accurate electrochemical adenosine-measuring techniques than the slower microdialysis. Following subcortical penicillin injection-induced epileptiform activity in pigs, adenosine biosensors implanted in the cortex were able to measure an increase in adenosine levels, beginning just prior to termination of electrocortical epileptiform activity and peaking postictally (Van Gompel et al., 2014). This corroborates the model of adenosine acting as retaliatory neuroprotector during seizures.

To examine the therapeutic potential of augmenting endogenous anticonvulsant seizure-induced adenosine release, several studies applied exogenous adenosine in *in vivo* models of acute and chronic (1 – 2 months) seizures, in studies known as adenosine augmentation therapy (AAT) (Boison, 2012a). Models include electrical kindling and hippocampal or amygdala injections of kainic acid or bicuculline, adenosine-releasing implants including stem cell grafts, or silk or polymer scaffolds shown to steadily release adenosine over 1 – 2 weeks, with AAT studies generally showing an anticonvulsant effect on measured seizure parameters (Huber et al., 2001; Anschel et al., 2004; Guttinger et al., 2005; Li et al., 2007b; Wilz et al., 2008; Li et al., 2009; Szybala et al., 2009; Boison, 2012a).

1.3.2. Sources and uptake of endogenous neural adenosine

The adenosine signalling molecule is generally sourced from the metabolic cycle of ATP, with adenosine produced from the dephosphorylation of ATP by intracellular nucleotidases, or extracellular ecto-nucleotidases. For the neuromodulatory effects of adenosine signalling at the synaptic level, the most important methods of adenosine uptake and release involve equilibrative nucleoside transporters (ENTs), which facilitate passive diffusion of adenosine across cellular membranes, as well as the astrocyte-based enzyme adenosine kinase (ADK) and nucleotidases, both intracellular and extracellular (schematically represented in Figure 1-5 below) (Boison, 2012b).

1.3.2.1. Adenosine metabolism

Following adenosine release into the extracellular space, the metabolism of endogenous extracellular synaptic adenosine has been found to be regulated by surrounding astrocytes (Etherington et al., 2009). Sources of adenosine clearance are the enzymes adenosine deaminase (ADA), which converts adenosine

to inosine, and ADK, which phosphorylates adenosine to produce AMP. ADA, while distributed throughout the CNS, is known to show the lowest detectable activity within the hippocampus (Geiger and Nagy, 1986) Experiments with rat hippocampal slices have shown that blocking ADA had little effect on excitability, while inhibition of ADK with iodotubercidin (IODO) heavily decreased the excitability of pyramidal cells, indicating a rise in tonic inhibitory adenosine. Use of adenosine biosensors were also able to directly show that addition of IODO to hippocampal slices caused a rise in the purinergic tone of adenosine and inosine (Pak et al., 1994; Etherington et al., 2009). Therefore, ADK is presumed to be the primary "sink" of extracellular adenosine, while ADA is less involved in clearance. Further evidence can be found *in vivo*, as mice overexpressing ADK can undergo spontaneous non-convulsive seizures at a similar rate to mice lacking A_1Rs, as well as having a greater susceptibility to induced seizures (Li et al., 2007a). This shows that overexpression of ADK leads to a decrease in protective adenosine tone.

Cellular localisation of the developing mouse brain has shown that although immediately after birth, ADK distribution is most prominent in neurons, particularly in the cerebral cortex and hippocampus, by post-natal day 14 ADK expression had shifted almost exclusively to astrocytes with only a few neurons retaining ADK until adulthood (Studer et al., 2006). ADK expression has also been shown co-localised with glial fibrillary acidic protein (GFAP)-containing astrocytes in CA1 of the hippocampus in adult rats (Etherington et al., 2009).

As adenosine travels through astrocytic membranes through equilibrative nucleoside transporters (ENT1 and ENT2), the extracellular clearance powered by intracellular ADK clearance is facilitated by the influx of adenosine through ENT1, with inhibition of ENT1 having been shown to be effective in attenuating seizures in rats (Xu et al., 2015).

1.3.2.2. Source of adenosine release

The source of neural adenosine release has been the topic of several studies, assessing both astrocytes and neurons. These studies have shown that the basal adenosine tone is regulated by vesicular release of ATP from astrocytes, thereby forming an astrocyte-based adenosine cycle. This was demonstrated in hippocampal slices taken from transgenic mice blocking astrocytic vesicular release of ATP (Pascual et al., 2005). Field potential excitability was similar to wildtype slices with A_1R inhibition, suggesting that the tonic inhibitory adenosine tone had been removed (Pascual et al., 2005). In the same mouse hippocampal slices, the addition of exogenous ATP was able to recreate A_1R-mediated inhibition, suggesting that this exogenously applied extracellular ATP is dephosphorylated by surface-anchored nucleotidases into adenosine (Zimmermann and Braun, 1996). In adult zebrafish, blocking ecto-5'nucleotidase, which produces adenosine from extracellular AMP, has been shown to decrease the

latency of PTZ-induced seizures (Siebel et al., 2015). This vesicular release of ATP followed by extracellular breakdown, schematically represented in Figure 1-5, has been shown to be the most likely source of the majority of basal adenosine, as blocking of ENTs did not decrease adenosine tone (Pascual et al., 2005; Etherington et al., 2009).

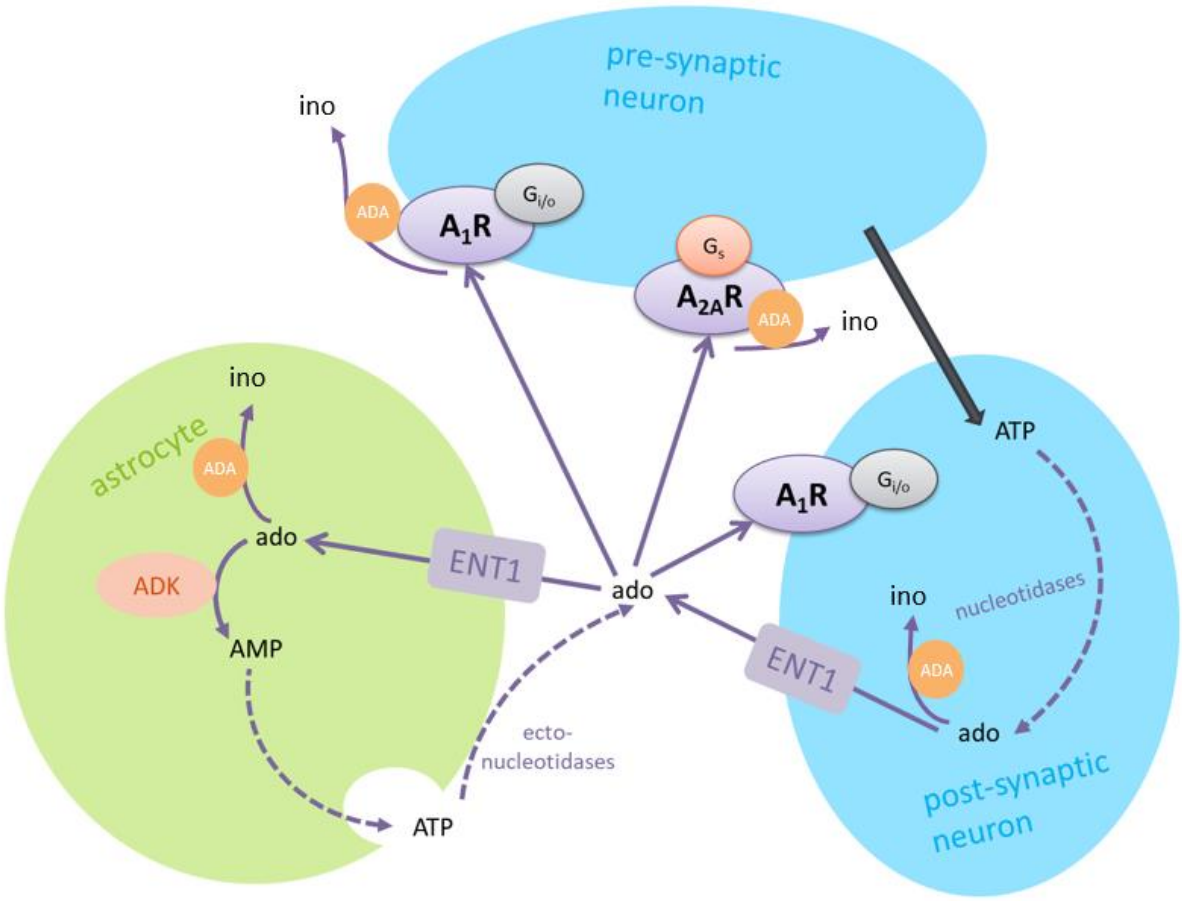

Figure 1-5: Schematic of the putative sources and metabolism of synaptic adenosine. ADA: adenosine deaminase; ado: adenosine; AMP: adenosine monophosphate; ATP: adenosine triphosphate; ENT1: equilibrative nucleoside transporter 1; ino: inosine. Solid arrows indicate direction of movement or conversion via displayed enzyme; dotted arrows indicate enzymatic cascade via enzymes not fully shown. ATP breakdown to adenosine is facilitated by intracellular nucleotidases, or extracellular membrane-bound ecto-nucleotidases. Adenosine travels through cellular membranes through the passive diffusion transporter ENT1; ATP is released from astrocytes by vesicles. ADA facilitates breakdown of adenosine to inosine; distribution is primarily cytosolic, although studies suggest ecto-ADA activity through anchoring on membrane proteins such as adenosine receptors (Latini and Pedata, 2001; Moreno et al., 2018).

However, some studies have also demonstrated that the seizure-associated rise in adenosine arises from a separate mechanism than the above-described astrocytic cycle of tonic, basal adenosine. Lovatt et al.

(2012) demonstrated in induced cortical seizures that although ATP is released from astrocytes and broken down to adenosine by ectonucleotidase enzymes in the extracellular space, ATP levels may not be sufficient to induce the A_1R-mediated synaptic depression immediately seen following seizure activity (Lovatt et al., 2012). It was established that inducing high-frequency activity in a single spiking CA1 neuron, with no recruitment of astrocytes, was sufficient to reduce synaptic transmission through A_1R activation. This relies upon postsynaptic metabolic activity leading to dephosphorylation of ATP, resulting in an intracellular accumulation of adenosine in the postsynaptic neuron, which is then released into the extracellular space via ENT1 transporters due to an increased concentration gradient (represented in Figure 1-5). Prevention of specific postsynaptic neuronal adenosine efflux, through intracellular injection of inosine, an adenosine metabolite which competes with adenosine for ENT cross-membrane transport, completely blocked the A_1R-mediated synaptic depression from stimulation of the same postsynaptic neuron (Lovatt et al., 2012).

This decrease of adenosine release due to ENT1 inhibition has also been recorded when quantifying adenosine release using enzymatic biosensors in CA1. This has been shown following a stimulation train, whereupon the adenosine release waveform was significantly decreased upon application of the ENT inhibitors, NBTI and dipyridamole (Wall and Dale, 2013), as well as in a Ca^{2+}-free model of spontaneous hippocampal activity (Diez et al., 2017). The direct adenosine quantification following electrical stimulation additionally demonstrated that astrocytic ATP release and extracellular breakdown still forms a part of the overall adenosine release following hippocampal stimulation, therefore the combination of the studies suggests that although the extracellular adenosine increased following a seizure may have both a neuronal and astrocytic source, the immediate suppression of synaptic transmission is likely to be dependent upon direct neuronal release (Lovatt et al., 2012; Wall and Dale, 2013; Diez et al., 2017). This suggests there may be a temporal and spatial dynamic to adenosine release and function, perhaps relating to the specific localisation of adenosine release and the diffusion distance to target receptors and/or transporters, either neuronal or astrocytic.

1.3.3. Adenosine and chronic epilepsy

Although a wealth of data supports the acute anticonvulsive property of adenosine, the role of adenosine in the longer-term epileptogenic processes or chronic epileptic state is less clear. The adenosine system is implicated in epileptogenic processes in multiple aspects as will be discussed below, including in adenosine metabolism, receptor balance, and even potential disruption of receptor-independent DNA methylation pathways.

It is important to initially emphasise the difference between acute seizures, which can form the epileptogenic trigger and are the basis of the majority of preclinical seizure models, and the post-

epileptogenic chronic state of epilepsy during which SRS occur. Particularly in acute seizure models, such as PTZ, penicillin, bicuculline and MES, the initial seizure insult occurs on a cellular and molecular neuronal background which is otherwise healthy. Although chronic seizure models do exist, AAT studies in particular have not reported an antiepileptic effect of exogenous adenosine past a period of 6-8 weeks following seizure initiation, with the majority of studies showing an acute effect of adenosine in suppressing seizures (Boison, 2012a).

1.3.3.1. ADK theory of chronic epilepsy

Astrogliosis is a pathological hallmark of TLE with hippocampal sclerosis, with potential epileptogenic processes involving increased inflammatory cytokines and/or excitatory gliotransmitters released by astrocytes (Boison, 2010). Among the many dysregulated proteins that occur in astrogliosis, proliferation of astrocytes is the basis of this theory of chronic epilepsy as it also causes a drastic increase in ADK, therefore increasing intracellular adenosine metabolism and modulating extracellular levels of adenosine through increased adenosine uptake into astrocytes (Li et al., 2008). A reduction in extracellular adenosine could form the basis for a mechanism of lowered seizure threshold, as lowered basal adenosine tone would decrease the tonic activation of A_1R, thereby causing an overall decrease in tonic inhibition of glutamatergic networks (Li et al., 2008; Etherington et al., 2009; Diogenes et al., 2014).

This ADK-based theory of lowered basal adenosine tone leading to seizures has been shown in some chronic models of epilepsy. Following a unilateral hippocampal injection of kainic acid, hippocampal sclerosis was seen to occur through the latent and chronic periods over the next 4 weeks, with severe loss of cells from the CA1 and CA3 regions (Gouder et al., 2004). Astrogliosis occurred alongside a rapid rise in ADK expression in the ipsilateral hippocampus and even to a lesser degree in the contralateral non-KA-injected hippocampus, indicating that hippocampal lesioning and resulting astrogliosis causes an increase in ADK activity, reducing basal protective adenosine tone and therefore leading to the appearance of seizures. In these KA-lesioned mice, application of IODO to inhibit ADK was able to completely suppress seizure activity when in the chronic, epileptic stage (Gouder et al., 2004). In addition, a study using transgenic mice modifying ADK expression in astrocytes and neurons showed that astrogliosis itself, without upregulation of ADK, did not lead to seizures (Li et al., 2008). Lowered hippocampal adenosine tone has been shown *in vivo* in rats 90 days after pilocarpine-induced SE (Dona et al., 2016). Microdialysis adenosine samples from chronic epileptic animals were significantly lower than from control, except in the case of SRS, during which adenosine and ATP concentrations increased 3-fold (Dona et al., 2016).

Upstream regulation of adenosine tone by ADK-driven metabolism has led to ADK inhibition becoming a rational drug target for epilepsy therapy, with the advantage that ADK inhibitors appear to induce less

cardiovascular side effects than adenosine or A_1R agonists. However, potential cognitive dysfunction with ADK-based therapy, and respiratory distress seen with systemic inhibition of ADK, would still require ADK modulation to be focused to epileptogenic loci, similarly to application of adenosine or A_1R agonists (Boison, 2013a).

1.3.3.2. Epigenetic role of adenosine in epileptogenesis

It has been shown that pathophysiological changes in extracellular adenosine concentration can modulate DNA methylation by shifting a reaction equilibrium to inhibit or potentiate the DNA methyltransferase (DNMT) enzymes, causing either hypomethylated or hypermethylated DNA (Boison, 2013b; Williams-Karnesky et al., 2013). A surge in adenosine, for instance as a neuroprotective mechanism following hypoxia or SE, can push the equilibrium between adenosine and *S*-Adenosyl-l-homocysteine (SAH) towards *S*-adenosyl-l-methionine (SAM), thereby preventing its demethylation and inhibiting DNMT, reducing DNA methylation and potentially allowing for pro-epileptogenic genes to be transcribed (Boison, 2013b; Boison et al., 2013). However, a decrease in extracellular adenosine, likely due to astrogliosis-related ADK overexpression, is also likely to have the opposite effect on the DNA methylation pathway (Boison et al., 2013). A decrease in adenosine would push the formation of SAH from SAM, thereby allowing for the activity of DNMT in methylating DNA. Corroborating this theory, hypermethylated DNA has been found in human TLE samples of sclerotic hippocampi (Kobow et al., 2009; Boison, 2016b). In a KA-induced SE model of SRS, areas of hypermethylation in the hippocampus were co-localised with areas of greatest ADK increase, suggesting that the process was largely driven by the increase in ADK. This chronic phase DNA hypermethylation was able be reversed by introducing transplants which release adenosine daily for 10 days at 9 weeks post kainic acid-induced SE. Seizure incidence and hippocampal methylation were reduced to levels of healthy controls within 5 days and maintained as significantly different from untreated animals for at least 10 weeks following cessation of adenosine release (represented in Figure 1-6). This indicates that a single treatment of adenosine in an early stage of chronic epilepsy is capable of reversing and preventing the worsening of epileptogenesis (Williams-Karnesky et al., 2013).

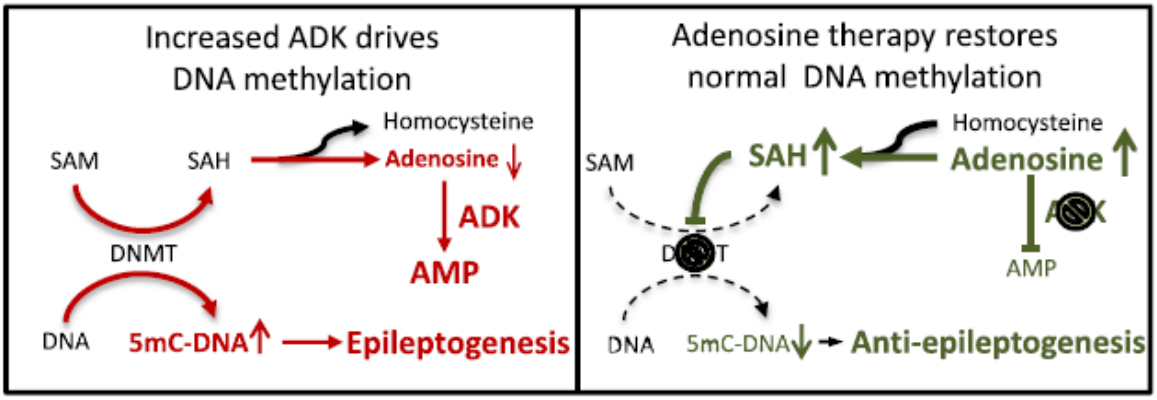

Figure 1-6: the epigenetic theory of adenosine-based epileptogenesis, taken from Boison (2016a). The hypermethylation of DNA is driven by increased ADK expression which leads to epileptogenesis. SAM: S-adenosylmethionine; SAH: S-adenosylhomocysteine; DNMT: DNA methyltransferase; 5mC: 5-methyl-cytidine.

1.3.3.3. Changes in adenosine receptor expression levels in chronic epilepsy

Along with changes in adenosine levels in chronic epilepsy, studies in human tissue and preclinical seizure and epilepsy models have shown that adenosine receptors themselves are subject to changes in density, favouring increased excitation and decreased inhibition. Decreased A_1R expression was found in resected temporal lobe tissue from human TLE patients, which showed decreased binding to [^{3}H]CHA as compared to tissue obtained from non-epileptic autopsies (Glass et al., 1996). It has also been seen in animal models immediately following SE that, although overall A_1R expression does not appear to be immediately downregulated, there is an effect of acute A_1R desensitisation (Hamil et al., 2012). These studies combined show the downregulation of expression and activity of A_1R, indicating a decrease in protective effect of adenosine very rapidly following a seizure and, crucially, in the longer-term chronic epileptic state. Decrease of A_1R may also contribute to the acceleration and spread of hippocampal cell loss, as seen in A_1R KO mice (Fedele et al., 2006).

In addition to decreased neuroprotection, studies have shown a concurrent upregulation of the excitatory G_s-coupled $A_{2A}R$ in chronic epilepsy. Although these receptors have a much lower pattern of expression in the brain compared to A_1R, radioligand binding has shown a threefold increase in $A_{2A}R$ binding in cortical membranes of rats 4 weeks after either amygdala kindling or kainate-induced seizures (Rebola 2005). Importantly, this suggests a decrease in endogenous seizure control mechanisms, while increasing neuronal excitability through $A_{2A}Rs$.

Changes and impact of adenosine receptors will be discussed further in Chapter 4.

1.3.4. Direct measurement of adenosine concentration

Several methods of detecting extracellular adenosine concentration both *in vivo* and *in vitro* exist. Most generally, adenosine levels *in vivo* can be detected through microdialysis, a technique which can be applied in both human patients (During and Spencer, 1992) and animal models (Mijangos-Moreno et al., 2014; Dona et al., 2016). However, microdialysis is a slow process, taking minutes to collect an aliquot, therefore giving an indication only of longer-term neurochemical processes and changes in substrate concentration. While this is a valuable tool, such as assessing basal levels of adenosine or when considering the longer time frame of adenosine release in relation to epileptic seizures, newer *in vitro* techniques have focused on increasing the temporal and spatial resolution of detection. These include fast-scan cyclic voltammetry (FSCV; reviewed by Nguyen and Venton (2015)), which applies a cyclic triangular potential upon a carbon fibre microelectrode and relies upon the oxidisation properties of adenosine, and enzyme-based amperometric biosensors, which will be further discussed in section 3.1. These two techniques are similar in their direct electrochemical measurement of adenosine using microelectrodes, with some small differences in temporal resolution and electrode size (FSCV uses smaller electrodes and has a faster rise time than biosensors), and the ability to measure basal adenosine currents (FSCV requires background subtraction on the adenosine signal and therefore is limited to a 90 second window, rendering the method unable to detect long-term basal shifts) (Nguyen and Venton, 2015). Both these techniques have been used in conjunction with electroencephalographic seizure recordings to detect adenosine release *in vivo* (Van Gompel et al., 2014).

1.4. CBD and Adenosine Signalling

The adenosine system has been hypothetically linked to the anticonvulsant action of CBD through action at the facilitated diffusion equilibrative nucleoside transporter, ENT1. CBD was shown to competitively bind to and inhibit ENT1-mediated uptake of adenosine into cultured macrophages and microglia (Carrier et al., 2006; Liou et al., 2008), as well as in rat striatal synaptosomes (Pandolfo et al., 2011). These studies suggest that CBD inhibits the bi-directional ENT1 transporter, potentially preventing astrocytic adenosine reuptake from the synaptic space and readdressing the ADK-mediated adenosine deficiency (Boison, 2012b). It has been shown *in vivo* that blockade of ENT1, via the inhibitor nitrobenzylthioinosine (NBTI), delays seizure onset when administered prophylactically in a pilocarpine model of epilepsy, as well as displaying inhibitory properties on slices *in vitro* (Xu et al., 2015). However, despite the general theories of CBD increasing extracellular adenosine by inhibiting ENT1, the source of seizure-associated adenosine may have a partly neuronal source and be facilitated via ENT1 as previously described in section 1.3.2.2 above. Therefore, the role that CBD would play in seizure-like situations, wherein ENT1 is potentially prevented from allowing adenosine release from neurons as well as uptake into astrocytes, remains unknown.

1.4.1.1. In vivo studies

There have been only limited *in vivo* studies of the potential interaction between CBD and adenosine metabolism and signalling. CBD-induced rise in adenosine has been shown in rats, when microinjection of CBD into the hypothalamus increased extracellular adenosine levels in microdialysis samples collected from the nucleus accumbens (Mijangos-Moreno et al., 2014). A recent study showing the anticonvulsive action of CBD in the rat PTZ kindling model of epilepsy also examined the effect of CBD treatment on hippocampal sclerosis and astrogliosis. Immunohistochemical staining showed that CBD treatment prevented loss of hippocampal pyramidal cells, and treatment also reduced the number of GFAP-positive cells as compared to untreated kindled rats, showing that administration of CBD protects CA1 and CA3 areas from astrogliosis (Mao et al., 2015). This indicates potential interaction between CBD and the epileptogenesis mechanisms of the adenosine metabolism cycle, consistent with the idea that by decreasing astrogliosis, CBD prevents ADK overexpression which decreases inhibitory adenosine tone in the hippocampus. Inhibition of hippocampal astrogliosis by CBD treatment has also been seen in adult mice with induced brain ischaemia (Schiavon et al., 2014). However, the interaction between CBD and adenosine inhibition is not a direct link, as astrogliosis forms part of the wider epileptogenic process, and the prevention of ADK overexpression by CBD is likely to be a downstream consequence of a separate anti-epileptogenic mechanism enacted by the treatment.

1.4.1.2. CBD and adenosine receptor interaction

Several studies have found links between CBD and adenosine receptor activity, generally due to the effect of CBD being ablated when antagonists are applied – for instance, the anti-inflammatory effect of CBD has been shown in several models, including rat retinal microglial cells, cultured human sebocytes, and mouse models of multiple sclerosis infection and acute lung injury (Liou et al., 2008; Ribeiro et al., 2012; Mecha et al., 2013; Olah et al., 2014). In all these cases, the anti-inflammatory effect of CBD was decreased or reversed upon application of an $A_{2A}R$ antagonist, indicating that $A_{2A}R$-activation is responsible for the anti-inflammatory effect of CBD. Although there may be a direct effect of CBD on $A_{2A}R$, the effect is likely a secondary effect of raising extracellular adenosine tone for cells which abundantly express $A_{2A}R$. Similarly, the antiarrhythmic effect of CBD in a rat model of ischaemia arrhythmia was shown to be dependent upon A_1R activation, again possibly due to a decrease in uptake increasing extracellular adenosine (Gonca and Darici, 2015).

A potential direct interaction between CBD and adenosine receptors has been suggested in zebrafish. Although CBD itself was shown to be anxiolytic, a high dose of CBD at a 10-fold increase of the anxiolytic dose appeared to impair the acquisition or consolidation of memory in an avoidance paradigm. This memory impairment effect appeared to decrease when zebrafish were pretreated with caffeine, or given specific A_1R or $A_{2A}R$ antagonists, indicating some form of memory-based adenosine effect in

response to high doses of CBD (Nazario et al., 2015). Although there have been some studies implicating receptor interactions between CB1Rs and A_{2A}Rs in striatal neurons, on both pre- and postsynaptic terminals (Ferré et al., 2010), it remains to be determined if CBD directly interact with adenosine receptors, with most studies suggesting that any observable effect of cannabinoids can be attributed to the increase of extracellular adenosine through reuptake inhibition.

1.5. Thesis aims

With TLE remaining one of the most intractable focal epilepsies, treatment with CBD presents a potential clinical pharmacotherapy. However, even for the two genetic orphan epileptic syndromes licensed for CBD treatment, the mechanism by which CBD decreases seizure activity of any seizure type or epilepsy syndrome remains not fully understood. Additionally, with some studies suggesting an interaction with the adenosine signalling system as a potential antiepileptic mechanism of action, the background of adenosine signalling in chronic epilepsy needs to be elucidated, particularly in its interaction with CBD. Therefore, the overall aim of this thesis is to assess the effect of CBD on the adenosine signalling system *in vitro*, using a rat model of chronic TLE.

The hypothesis widely described in the literature involves CBD-mediated inhibition of ENT1 causing an increase in extracellular adenosine levels and thereby conferring neuroprotection from seizures.

The aims of this thesis are:

- Firstly, to investigate the direct impact of CBD on adenosine levels in hippocampal slices *in vitro* from both healthy and epileptic rats
    - in basal conditions
    - following seizure-like stimulation, and subsequent effect on evoked LFPs
- Secondly, to investigate the adenosine signalling system in healthy and epileptic rats
    - through molecular assessment of expression of A_1R and A_{2A}R in the hippocampus
    - by using functional antagonists for adenosine receptors to investigate the effect of increasing concentrations of adenosine on evoked field potentials
- Thirdly, to assess ENT1 and its involvement in the antiepileptic action of CBD
    - to assess CBD and its metabolites for functional activity at ENT1
    - through molecular assessment of expression of ENT1 in the hippocampus

2. General Materials and Methods

This chapter describes general procedures performed for this thesis. Additional details are presented in relevant results chapters (Chapters 3 through 5), with further regulatory information on live animal procedures presented in Appendix 8.1 and details of studies performed by Contract Research Organisations (CROs) for this thesis provided in Appendix 8.3.

2.1. Lithium-pilocarpine Reduced-Intensity Status Epilepticus (RISE) model of Spontaneous Recurrent Seizures (SRS)

A model of epileptogenesis and chronic epilepsy had been developed, partly at the University of Reading (Modebadze et al., 2016), to provide a refined method of producing SRS as a model of chronic epilepsy, e.g. TLE. The model relies upon inducing an initial insult of epileptiform activity, in this case SE, prior to maturity. This is then followed by a period of latent epileptogenesis, followed by appearance of spontaneous recurrent seizures in the majority of rats. The chemical induction of SE is reduced in intensity from previous models of seizure and epilepsy, which frequently exhibited high mortality rates, through the injection of a sensitising agent (LiCl) 24 hours prior to administration of the convulsant pilocarpine, allowing a lower dose of pilocarpine to be used and substantially reducing the mortality of treated animals to less than 1%.

2.1.1. Induction of Status Epilepticus

Male Wistar rats were ordered from Harlan Envigo, UK in the STA03 (75-99 g) banding, corresponding to 4 – 5 weeks of age, and were group-housed in humidity and temperature controlled conditions under a 12 hour light/dark cycle, provided with standard food and water *ad libitum* at all times. Upon arrival, rats were habituated to their environment for at least 3 days prior to initiation of RISE-SRS induction procedure (Table 2-1).

stage	**Procedure** (all injection volumes 1 ml/kg unless stated otherwise)	**Injection time**
1	**LiCl**, 127 mg/kg s.c. (back of neck)	
2	**Methyl scopolamine**, 1 mg/kg s.c. (back of neck)	Stage 1 + 24 hour
3	**Pilocarpine**, 25 mg/kg s.c. (back of neck)	Stage 2 + 30 min
4	**Pilocarpine**, 50 mg/kg s.c. (back of neck)	Stage 3 + 30 min if R5 not reached
5	**Pilocarpine**, 75 mg/kg s.c. (back of neck, 1.5 mL/kg)	Stage 4 + 30 min if R5 not reached
	if R4 not reached by Stage 5 + 30 min: **schedule 1**	
6	**Xylazine**, 2.48 mg/kg i.m.	Immediately upon reaching R5
7	**STOP**, 1 mL/kg s.c. (side)	Stage 6 + 60 min
8	**STOP**, 0.5 mL/kg s.c. (side, 0.5 mL/kg)	Stage 7 + 30 min if still having seizures
9	**STOP**, 0.5 mL/kg s.c. (side, 0.5 mL/kg)	Stage 8 + 30 min if still having seizures
10	**2 mL saline/5% glucose** solution s.c. (sides)	when moving around, following stage 7

Table 2-1: RISE-SRS induction procedure

In compliance with project license protocol, rats were weighed prior to induction procedure to ensure a minimum weight of 70 g. In summary, rats were initially sensitised to pilocarpine through s.c. injection of 127 mg/kg LiCl (dissolved at 127 mg/mL in sterile saline). After 24 hours, rats were injected with the muscarinic antagonist methyl scopolamine (1 mg/kg in sterile saline), for attenuating peripheral effects of pilocarpine-induced SE. Pilocarpine injections started at 30 min following methyl scopolamine, with the first dose at 25 mg/kg s.c. From this stage, rats were continually monitored by investigators for behavioural seizure signs as described by the Racine scale (Table 2-2). As soon as a rat reached Racine scale 5 (R5), it was given an intramuscular injection of the sedative and muscle relaxant xylazine (2.48 mg/kg), helping to reduce seizure fatality. If a rat did not reach R5 within 30 min of the first pilocarpine injection (Table 2-1, Stage 3), increasing dosages of pilocarpine were injected at two 30 min intervals (Stages 4 – 5), with rats continually monitored for seizure behaviour. If a rat had not reached Racine scale 4 at 30 min following the max dose of 75 mg/kg, it was deemed to have not met the regulated procedure criteria and terminated via humane schedule 1 procedure.

Once a rat had reached R5 and was in SE, from this point it would be continually held by an investigator to protect the rat from seizure-related injuries and to prevent motor feedback during seizure. Saliva would be removed from the nose and mouth using cotton buds to prevent suffocation; cotton buds were

also used for controlling rats' mouth clonus, to prevent tongue impalement during seizure. Ocular keratitis was prevented during seizure through application of ocular ointments to the eyes.

From 60 min following xylazine injection, SE was terminated in rats using an ethanolic STOP injection s.c., consisting of 2.5 mg/kg diazepam, a positive allosteric modulator of $GABA_A$ receptors, 20 mg/kg MPEP, an mGluR5 antagonist, and 0.1 mg/kg MK-801, an NMDA receptor antagonist. If rats were still exhibiting seizures 30 min following initial STOP dose, another half dose injection was given s.c., followed by a final half dose if rats were still exhibiting seizures after an additional 30 min. The STOP solution effectively terminated seizures and sedated rats for 1 – 2 hours, and limited risk of breakthrough seizures in the following 24 hours.

Racine scale	Observations	Seizure syndrome
R1	masticatory movements	mouth clonus
R2	hind limb scratching, 'wet dog' shakes, nodding	head clonus
R3	unilateral seizure (forelimb clonus)	forelimb clonus
R4	bilateral seizure (rearing)	forelimb clonus, tonic immobility
R5	bilateral seizure, falling, loss of posture, uncontrollable jumping	tonic-clonic seizures

Table 2-2: Behavioural observations of seizure within an adapted Racine scale.

Sedated rats were continually visually monitored for breathing 2 – 4 hours following SE, and temperature was maintained at 37°C using veterinary heating pads. As rats regained awareness they were manually fed 20% glucose using plastic Pasteur pipettes, and once they were able to move around under their own volition they were given a 2 mL s.c. injection of 5% glucose in a saline solution, then returned to standard group-housed environment and closely monitored for their welfare for the following 24 hours. Liquid "mash" feed was provided in addition to usual food and water *ad libitum* for the week following induction to ensure that no rat lost more than 20% of their pre-induction body weight. During this first week, animals were monitored and weighed daily to ensure welfare and post-induction recovery weight gain.

2.1.2. Assessment of epilepsy

All rats were assessed twice a week for behavioural welfare. From the third week inclusive following induction, all rats underwent twice-weekly post-seizure behavioural battery (PSBB) tests, an assessment of aggression and excitability, and validated to confirm incidence of spontaneous seizures (Modebadze et al., 2016). Rats were deemed as 'confirmed epileptic' through two possible routes: firstly, visual observation of a spontaneous bilateral seizure (R4) by an investigator while performing welfare checks;

or through PSBB testing. PSBB scores consisted of two tests administered to rats: the touch test, in which the rat is gently prodded in the rump with a consistent blunt instrument (in this case, the blunt end of a marker pen), and the pickup test, in which the animal is picked up by gently grasping around the body. Responses were scored through an increasing scale of responsiveness as described in Table 2-3, and if the product of the two tests were equal or greater than 10 the rat was given a 'positive' PSBB score. If a rat received 'positive' PSBB scores in four consecutive testing sessions, i.e., for two consecutive weeks, the rat was deemed 'confirmed epileptic'. An example tracking spreadsheet for PSBB scores is presented in Appendix 8.1. Rats which were not confirmed as epileptic within the following 10 weeks were considered post-SE non-epileptic rats, and euthanised through humane Schedule 1 termination method.

PSBB - touch test	**Observed response**
1	Rat has no reaction
2	Rat turns toward object before being touched
3	Rat turns away from object before being touched
4	Rat freezes
5	Rat turns toward the touch
6	Rat turns away from the touch
7	Rat jumps with or without vocalisation
PSBB - pickup test	**Observed response**
1	Rat is picked up easily
2	Rat is picked up easily with vocalisations
3	Rat rears and faces the hand
4	Rat freezes
5	Rat moves away from the hand
6	Rat reacts aggressively - very difficult to pick up

Table 2-3: PSBB test responses

2.2. Electrophysiology

2.2.1. Hippocampal slices

For *in vitro* electrophysiology investigations, epileptic rats (~8 – 16 weeks following pilocarpine induction) or similarly-aged healthy rats (ordered by weight band from Harlan, UK) were dissected for acute hippocampal brain slices. In accordance with Schedule 1 methods, rats were terminally anaesthetised with isoflurane carried by medical grade oxygen (99.5% purity, BOC Gas, Reading) using

a veterinary anaesthesia machine. Once the rat no longer responded to the pinch reflex test, it underwent immediate cervical dislocation and decapitation. The skull was opened with a midline cut, and subsequently folded open from either side. The brain was gently removed using a spatula severing the external cranial nerves, then immediately immersed into an ice-cold 'slush' of high-sucrose 'cutting aCSF' (Table 2-4), which was continually carboxygenated (95% oxygen, 5% carbon dioxide, BOC Gas, Reading) throughout use.

Component (mM)	cutting aCSF	aCSF
Sucrose	75	-
NaCl	87	126
Glucose	25	10
$MgCl_2$	7	2
KCl	2.5	2.49
NaH_2PO_4	1.25	1.25
$NaHCO_3$	25	26
$CaCl_2$	0.5	2

Table 2-4: Components of artificial cerebrospinal fluid (aCSF) for acute slice electrophysiology.

Using a razor blade (Campden Instruments Ltd., Leicester, UK), the brain was gently cut down the midline, still immersed in cutting aCSF, and the cerebellum and any remaining removed for each hemisphere (Figure 2-1, red dissection lines 1&2). With each hemisphere resting along the midline, straight slices were made to remove the very dorsal and ventral sections of each hemisphere (Figure 2-1, lines 3&4), then the olfactory bulb and anterior part of the forebrain were removed with a straight slice (Figure 2-1, line 5). Both trimmed hemispheres were glued onto the slicing block of the vibratome (Leica, VT1200S), with both hemispheres resting on the flat ventral base (dissection line 3), and bathed in ice-cold, continually carboxygenated cutting aCSF surrounded by an ice tray. Transverse brain slices were cut at the level of the hippocampus at 400 µm thick, with 4 – 12 slices obtained from both hemispheres per rat brain. Slices were transferred using a wide glass pipette to sucrose-free aCSF (Table 2-4), heated to 37°C to overcome the cellular "shock" of the cutting protocol, and continually carboxygenated. Once all slices were obtained, slices were left to equilibrate in aCSF for at least 1 hour prior to experimental use. Equilibration was carried out at room temperature to slow metabolic processes and encourage longer-term viability of the slices, following protocols described in previous electrophysiological studies (Alcami et al., 2012; Mańko et al., 2012; Bazelot et al., 2015).

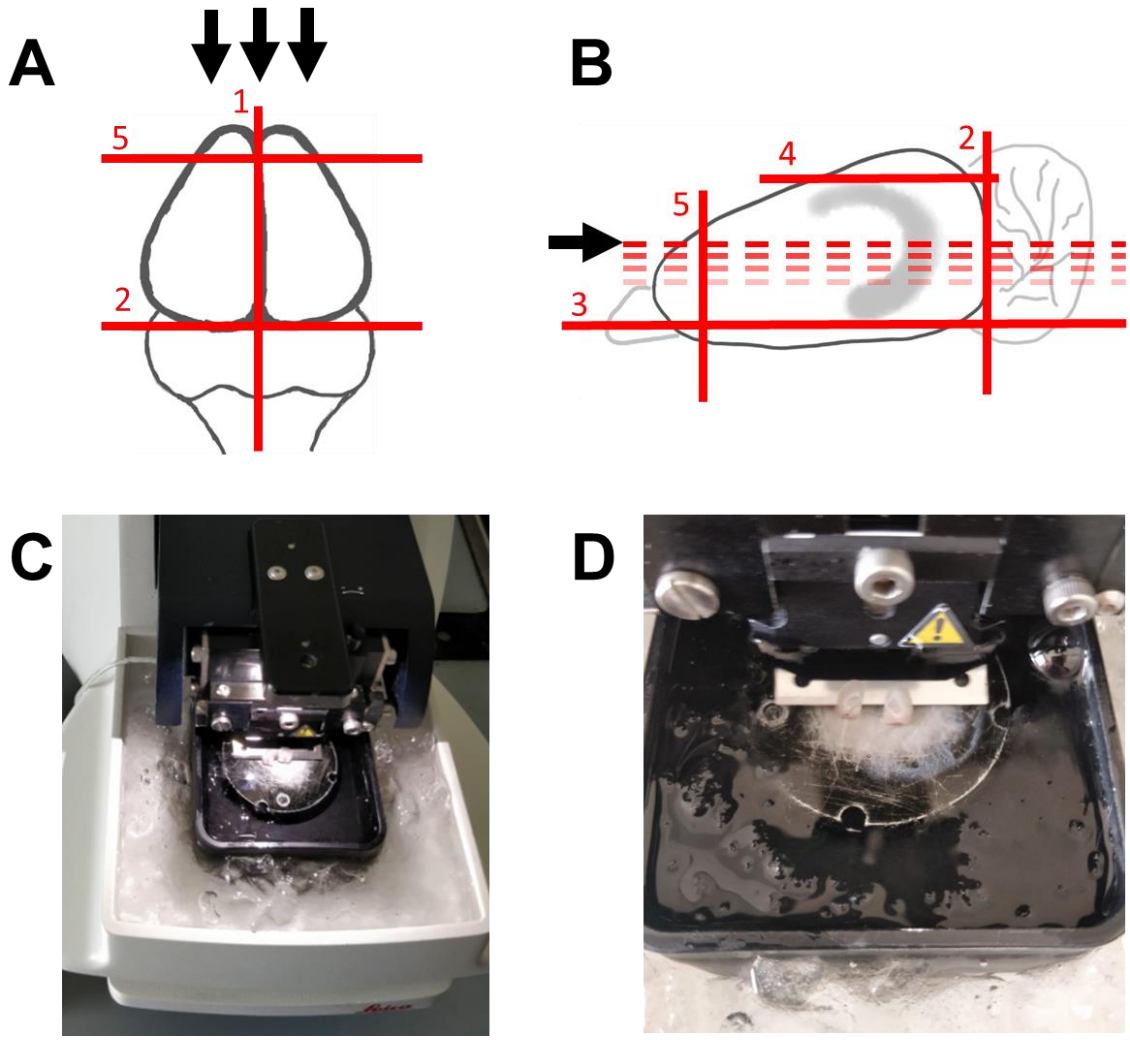

Figure 2-1: Dissection and slicing of rat brain following removal from skull. A&B: Schematic depictions showing top view (A; two hemispheres of the cerebral cortex above cerebellum with brainstem) and mid-sagittal view (B; light grey regions indicating locations of olfactory cortex [left], hippocampus [centre], and cerebellum [right]) of rat brain and manual dissections preparing brain for slicing. Solid red lines indicate dissections performed manually using a straight razor, with numbers indicating the order in which these sections were removed. Black arrows indicate the direction of movement of the mounted vibratome blade. Dotted red lines indicate transverse brain sections created by slicing (400 µm thickness). **C&D:** Representative images showing two brain hemispheres mounted on a vibratome within the cutting aCSF ice "slush", surrounded by an ice bath.

2.2.2. Multielectrode Array (MEA) electrophysiology

Recordings from slices took place in multielectrode array (MEA) chambers (Multi Channel Systems, Reutlingen, Germany). MEA chambers are centred on a 1.4 mm square of 60 electrodes in an 8 × 8 configuration, with each electrode measuring 30 µm in diameter and spaced 200 µm apart. Prior to each use, MEAs were cleaned by soaking in 5% (w/v) Terg-A-Zyme (Cole-Palmer, London, UK) dissolved in distilled water, then rinsed once in tap water and twice with distilled water. Upon being air-dried,

MEAs were cleaned with methanol using a cotton bud then under vacuum in a plasma cleaner (Harrick Plasma, New York, USA).

A slice was placed within the MEA chamber in aCSF using a wide glass Pasteur pipette, then visualised using a Leitz Diavert inverted microscope with a micro-ocular webcam. Slices were manually adjusted using a yellow pipette tip to ensure placement of the hippocampus on the array, particularly focusing on the CA1 and Schaffer collateral area covering the electrodes (Figure 2-2A). Slices were held down using a metal harp (Harvard Apparatus, Cambridge, UK) and the MEA was carefully placed in the MEA headstage (MEA1060-Inv-BC, Multi Channel Systems, Germany), maintained at 32°C, and continually perfused with constantly carboxygenated aCSF at a flow rate of 4 – 6 mL/min. At least 10 min was given for each slice to equilibrate on the MEA, allowing maximal signal contact with electrodes. Local field potentials (LFPs) were evoked by delivering a biphasic stimulation (100 µs steps, ±0.5 – 2 V amplitude) through a single electrode, selected with MEA_Select. Stimulations were delivered using an STG2004 stimulator (MultiChannel Systems GmbH, Germany), through a split output cable allowing stimulation trigger events to be recorded with electrode signals.

Signals for all 60 channels (including one reference electrode) were acquired at a sample rate of 10 kHz per channel through a 60-channel headstage amplifier (MEA60 System, MultiChannel Systems GmbH, Reutlingen, Germany), amplified at 1200× gain. Raw signals were monitored online on a PC using MC Rack software (Multi Channel Systems GmbH, Reutlingen, Germany) and processed through a 50 Hz notch filter and at a 1 kHz low pass filter.

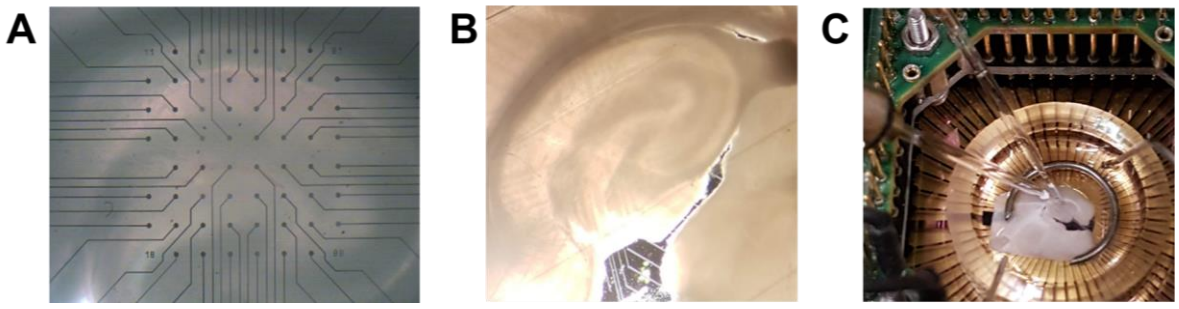

Figure 2-2: Placement of hippocampal slices on the multielectrode array, and insertion of microelectrode biosensors. A: Image showing the underside of the hippocampal slice laying on a 60-electrode (8 × 8) array, as viewed using an inverted Leitz Diavert microscope. **B:** Top view of the hippocampal slice laying on the MEA, viewed at 5× when loaded into the MEA headstage. **C:** Full view of hippocampal slice laying on an MEA loaded into the headstage with biosensors (ADO and NULL) inserted within CA1. Also visible are the metal harp holding down the slice, and the aCSF perfusion system (inflow at the 2 o'clock position, outflow at the 7 o'clock position).

2.2.2.1. Measurement of LFPs

Using the image captured of the position of the hippocampal slice on the multielectrode array (Figure 2-3A), a stimulation electrode was selected in the CA1 region of the hippocampus, which would deliver electrical pulses to induce LFPs in the Schaffer collaterals of the hippocampal slice. Online analysis was performed to monitor the slope of the field potential deflections (Figure 2-3B), and the 1100 ms window surround each stimulation trigger was recorded for all 60 electrodes.

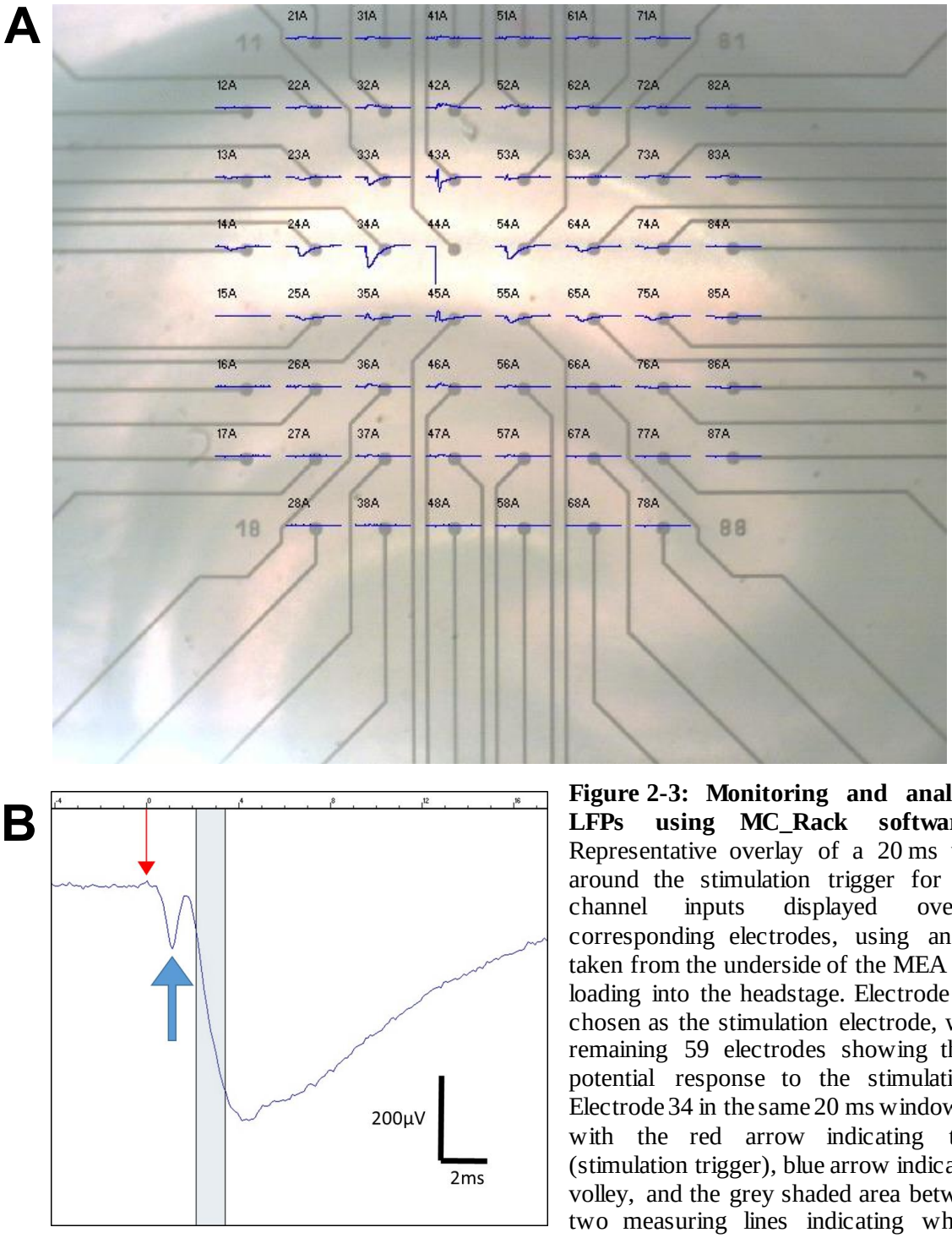

Figure 2-3: Monitoring and analysis of LFPs using MC_Rack software. A: Representative overlay of a 20 ms window around the stimulation trigger for all 60-channel inputs displayed over the corresponding electrodes, using an image taken from the underside of the MEA prior to loading into the headstage. Electrode 44 was chosen as the stimulation electrode, with the remaining 59 electrodes showing the field potential response to the stimulation. **B:** Electrode 34 in the same 20 ms window as (A), with the red arrow indicating t = 0 ms (stimulation trigger), blue arrow indicating the volley, and the grey shaded area between the two measuring lines indicating where the calculation for the field potential slope was performed.

2.2.3. Microelectrode biosensors

Enzyme-based biosensors were obtained from Sarissa Biomedical (Coventry, UK). Biosensors consist of a platinum/iridium (Pt/Ir) wire coated in an enzyme matrix layer, reducing adenosine to its metabolites through an enzymatic cascade and releasing H_2O_2. With sensors polarised to 500 mV, H_2O_2 then reacts

against the polarised Pt/Ir wire, creating a current linear to levels of detected adenosine. Sensor tips used have dimensions of 0.5 mm x 50 µm.

Two forms of sensors were used – an adenosine biosensor with a full complement of enzymes, detecting adenosine and its metabolites, and a null biosensor with no enzymes, therefore detecting no physiological change in slices but sensitive to other potentially artefact-inducing stimuli. Sensors were received in dehydrated form and stored at 4°C. Prior to use, sensors were rehydrated in buffer A (Table 2-5) for at least 1 hour before experimental use, or overnight at 4°C. Sensors were connected to an analogue dual potentiostat (Whistonbrook Technologies Ltd), with the signal digitised through a PowerLab/4SP (ADInstruments), sampled at 10 Hz and recorded through LabChart 7 software (ADInstruments). Micromanipulators were attached to probe sockets for sensors above the MEA headstage, allowing for sensors to be inserted into slices at an optimal angle (using Pythagorean trigonometry) for the 500 µm tip length to be as fully inserted as possible into the 400 µm thick hippocampal slice resting on an MEA. Care was taken to keep sensors hydrated, with sensor tips exposed to air as little as possible when moving from storage in buffer A to fitting into probe sockets and immersing immediately within aCSF being perfused through the MEA. Sensors were viewed above the slice lying on the MEA using an optical Leica microscope (Figure 2-2B), allowing for correct placement of sensors using micromanipulators (Figure 2-2C).

Sensor buffer components		**mM**
buffer A (pH 7.4)	NaPi buffer (pH 7.4)	2
	NaCl	100
	$MgCl_2$	1
	glycerol	2
100 mM NaPi buffer (pH 7.4)	$NaH_2PO_4 \cdot H_2O$	22.5
	Na_2HPO_4	76.76

Table 2-5: Components of buffer for rehydrating and storing biosensors, all made to volume in ddH_2O.

Stimulation protocols on LabChart were used for sensor polarisation. Following manufacturer's suggestions, once sensors were immersed in aCSF, a 0.05 Hz sine wave stimulation cycled sensors from -500 mV to +500 mV for 10 cycles to increase sensitivity to adenosine prior to use. Following cycling protocol, sensors were polarised to +500 mV, then using a Leica microscope to visualise sensor tips and hippocampal slice, sensors were inserted in the stratum radiatum in the CA1 area of hippocampal slices using micromanipulators.

After sensor insertion, slices were given at least 40-60 min for tissue damage-induced adenosine release to stabilise to baseline.

Following experimental protocol and sensor removal from slice, sensors were calibrated with 10 µM adenosine, in order to scale sensor current traces with the corresponding adenosine concentration, as well as 10 µM 5-HT to test the patency of the sensor screening layer. As the adenosine sensor current detects adenosine as well as its metabolites, traces once calibrated with 10 µM adenosine are described as µM', in order to reflect that rather than pure adenosine, inosine and hypoxanthine can also contribute to the signal recorded (Frenguelli et al., 2007).

2.2.4. Drugs and reagents

A summary of all drugs used for electrophysiology experiments is given in Table 2-6. Unless otherwise stated, all salts, compounds, and solvents used for buffers and solutions previously described were obtained from Fisher Scientific (UK).

Drug	Source
adenosine	Sigma, UK
5-HT	Sigma, UK
DPCPX	Tocris, UK
CBD	GW Pharmaceuticals, UK
CBDV	GW Pharmaceuticals, UK
8-CPT	Sigma, UK
SCH 58261	Tocris, UK

Table 2-6: Summary of drugs used in electrophysiology experiments.

For MEA electrophysiology experiments, a concentration of 10 µM CBD/CBDV was chosen. This was to align with previous studies showing antiseizure efficacy *in vitro* at this concentration (Jones et al., 2010; Hill et al., 2012; Jones et al., 2012), and evidence showing that orally administered CBD at clinical dosages reach a brain concentration in this range (Deiana et al., 2012). As per lab standard, due to the lipophilicity of CBD, no CBD post-wash recordings were carried out.

2.3. Molecular analysis of isolated hippocampi

2.3.1. Dissection of isolated hippocampi

For analysis of gene and protein expression in isolated hippocampi, all epileptic rats were sacrificed at 16 weeks following induction, or healthy controls age-matched at 20 weeks old. Rats were euthanised via terminal isoflurane.

The brain was extracted onto a piece of filter paper, dampened with chilled saline on a petri dish on ice. Hippocampi from both hemispheres were isolated using a spatula to gently peel the neocortex laterally from the midline outwards, revealing the hippocampus internally. This was then gently removed from surrounding tissue and flash frozen using liquid nitrogen.

For all collected samples processed in-house, hippocampi isolated from the right hemisphere were used for gene expression analysis by RT-qPCR, while left hippocampi were used for protein expression analysis.

In addition to epileptic rats and healthy controls, additional frozen isolated hippocampi were included in transcription and expression analyses. These were healthy or epileptic rats which had undergone chronic treatment of oral CBD (200 mg/kg) or vehicle (3.5% Kolliphor® HS, Sigma-Aldrich, Poole, UK) (Patra et al., 2019), and had been sacrificed at 16 weeks post-induction (20 weeks old). Briefly, 20 rats confirmed epileptic within 4 – 8 weeks following RISE-SRS induction were randomised into a CBD treatment group and a vehicle-treated group, with an additional group of 10 healthy age-matched rats also treated with vehicle as a control. Both CBD and vehicle were administered in drinking water to reduce handling-associated seizures in epileptic rats. For the CBD-treatment group, vehicle was administered for 1 week, followed by 1 week of increasing CBD dosage (starting dose 50 mg/kg with an increase of 50 mg/kg every 2 days), reaching the final dosage of 200 mg/kg which was continued for a further 8 weeks. The two vehicle groups were treated with vehicle for the entire 10-week treatment period.

2.3.2. Gene expression analysis by RT-qPCR

2.3.2.1. Primer design

Primers were designed using NCBI/Primer-BLAST, targeting the *Rattus norvegicus* (Norway Rat) organism. Optimal parameters for each gene of interest were designed following parameters listed in Table 2-7. PCR products were optimised to ~100 base pairs for efficiency, and were designed to have a melting point (Tm) of 60°C, allowing multiple primers to be run simultaneously. Where possible, primers were selected which crossed an exon-exon junction, or spanned an intron.

Parameter	min	optimum	max
Product size (base pairs)	50	**100**	150
Primer size (base pairs)	18	**20**	27
Primer Tm	57	**60**	63
Primer GC%	40	**60**	80
ΔG value	0	**>0**	-

Table 2-7: Optimal parameters for designing primer sets for RT-qPCR.

Primer sets as well as products were check for thermodynamic profiles using mfold online software (Zuker, 2003) to ensure that stable secondary structures would not form in PCR conditions during cycling, which would interfere with PCR efficiency. ΔG values were calculated at 60°C in the presence of 1.5 mM Mg^{2+} and 50 mM Na^{+}, with negative values indicating a stable structure can be formed; therefore only primer sets and products with positive ΔG values were selected. Details of primer sets are listed in Table 2-8.

Primers were ordered from Sigma, UK, and diluted to 100 µM stock in nuclease-free water, and kept at -20°C. Additional aliquots were made to 10 µM prior to usage.

		PRIMER						
Gene/ protein	**RefSeq ID/ gene length**		**Primers**	**Size**	**Tm (°C)**	**introns/exons**	**GC%**	**lowest ΔG (kcal/mol)**
Gapdh/	NM_017008.4/	+	GAAGCTCATTTCCTGGTATGACAA	24	59.06	exon boundary	42%	1.81
GAPDH	1306 bp	-	ATGTAGGCCATGAGGTCCAC	20	59.16	-	55%	1.4
Adora1/	NM_017155.2/	+	GAGCTCCATTCTGGCTCTGC	20	60.81	before intron	60%	1.02
A_1R	1079 bp	-	GCTGGGTCACCACTGTCTTG	20	60.89	after intron	60%	0.98
Adora2a/	NM_053294.5/	+	CTATCGCCATCGACCGCTAC	20	60.45	-	60%	0.97
$A_{2A}R$	2491 bp	-	AGCCATTGTACCGGAGTGGA	20	60.91	exon boundary	55%	0.32
Slc29a1/	NM_031684.2/	+	TGAAGCAGCACCACTACCTG	20	59.96	before intron	55%	1.22
ENT1	2142 bp	-	GCCTCAGCCGGTTTGACTT	19	60.6	after intron	58%	1.58

		PRODUCT			
		size	**Sequence position**	**Tm (°C)**	**lowest ΔG (kcal/mol)**
Gapdh	NM_017008.4	**69**	993-1061	42	0.93
Adora1	NM_017155.2	**89**	339-427	53.1	0.74
Adora2a	NM_053294.5	**54**	709-762	46.6	0.80
Slc29a1	NM_031684.2	**142**	1460-1601	58	0.20

Table 2-8: Properties of primers and PCR products.

2.3.2.2. RNA extraction and reverse transcription

Total RNA was extracted from frozen isolated hippocampi using an RNeasy Lipid Tissue Mini Kit (Qiagen, UK), following the manufacturer's instructions. Briefly, frozen hippocampi were immediately homogenised in 1 mL QIAzol Lysis Reagent (a phenol/guanidine thiocyanate solution) using a 2 mL glass borosilicate pestle and mortar. The homogenate was incubated at RT for 5 min, before 200 µL chloroform was added, and shaken vigorously with the sample for 15 s. This was incubated at RT for a further 3 min, before being centrifuged at 12000 RCF for 15 min at 4°C. The upper, aqueous phase following centrifugation (~400 µL) was carefully transferred to a fresh RNAase-free tube, without disturbing the lipid interphase, and one volume of 70% ethanol was added to this sample.

Samples were then spun through RNeasy Mini spin columns, following the protocol in Table 2-9, using buffers provided with the Qiagen kit. Flow-through was collected in 2 mL collection tubes and discarded following each spin, until the final spin to collect purified RNA into a fresh 1.5 mL RNAase-free tube eluted with 20 µL nuclease-free water (Ambion, Inc).

In spin column	volume	time
Sample (up to 2 spins)	max 700 µL	15 s
Buffer RW1	700 µL	15 s
Buffer RPE	500 µL	15 s
Buffer RPE	500 µL	2 min
new collection tube	n/a	1 min
Nuclease-free water	20 µL	1 min

Table 2-9: RNA extraction centrifugation protocol using RNeasy spin columns. All spins 8000 RCF at RT.

RNA concentration and purity were assessed by spectrophotometry using a NanoDrop 2000 Spectrophotometer (ThermoScientific). Nuclease-free water (1.5 µL) was used to blank the detection plates, before 1.5 µL of each sample was read for nucleic acid concentration and RNA purity. Concentration was quantified through measuring absorbance of ultraviolet (UV)-Visible light, and purity was assessed by measuring the ratio between peaks at 260 nm and 280 nm, with an ideal 'pure' RNA 260/280 ratio at ~2. Additionally, the ratio between wavelengths 260/230 provided an indication of whether the sample contained contaminants from the RNA isolation process, as phenol and other contaminants also absorb at 230 nm.

Total RNA was reverse-transcribed into cDNA using a QuantiTect Reverse Transcription Kit (Qiagen, UK). Total rat brain RNA from adult Sprague-Dawley rats was purchased from Takara Bio Europe (France) and used as a positive control.

All reagents and procedures were kept and carried out on ice. Template RNA (1 µg) was first incubated with 2 µL of the provided 'gDNA Wipeout Buffer' and diluted using nuclease-free water to a total of 14 µL. This genomic DNA elimination reaction was incubated at 42°C for 2 min using a Bio-Rad T100 Thermal Cycler. Following gDNA elimination, 6 µL of a master mix (1 µL Reverse Transcriptase, 4 µL RT buffer and 1 µL Primer mix) was added to each reaction tube for a final reaction volume of 20 µL. This reverse transcription reaction was incubated at 42°C for 15 min, then terminated by inactivating RT with a 3 min incubation at 95°C in the thermocycler. Final cDNA samples were diluted 1:5 for a final volume of 100 µL per sample and stored at -20°C ahead of real-time qPCR.

2.3.2.3. RT-qPCR assays

Real-time quantitative PCR was carried out using a QuantiNova SYBR Green PCR Kit (Qiagen, UK). Reaction components were prepared according to manufacturer's instructions (summarised in Table 2-10) using a 96-well reaction plate (Applied Biosystems). All samples were run in triplicate, including negative controls (nuclease-free water) and positive controls (adult whole rat brain RNA). Efficiency of primers was determined through construction of standard curves using a serial dilution of control RNA, described in section 2.3.2.4.

component	volume (µL)
2x SYBR Green PCR Master Mix	10
QN Rox Reference Dye	2
Forward primer (10 µM stock)	1.4
Reverse primer (10 µM stock)	1.4
Nuclease-free water	3.2
Template cDNA	2
total reaction volume	**20**

Table 2-10: RT-qPCR reaction components for individual wells.

Two-step PCR was run using StepOnePlus™ (Applied Biosystems), using the manufacturer's cycling protocol: initial heat activation at 95°C for 2 min, followed by 40 cycles consisting of denaturation at 95°C for 5 s and combined annealing/extension at 60°C for 10 s. Once 40 cycles were complete, a melting curve analysis was performed to assess PCR product specificity.

C_T values were extracted using StepOnePlus™ software, and analysed for each gene of interest using the Pfaffl method (Pfaffl, 2001).

2.3.2.4. Primer efficiency validation and efficiency-based gene expression

C_T values for RT-qPCR cycles were run using a threefold serial dilution of cDNA in triplicate. Linear regression against the log of these dilution factors generated a slope for each set of primers, from which the amplification factor (E) and primer efficiencies could be calculated using the following equations:

$$amplification\ factor\ (E) = 10^{\frac{-1}{slope}}$$

$$efficiency\ (\%) = \left(10^{\frac{-1}{slope}} - 1\right) \times 100$$

With efficiencies for primer sets calculated, the Pfaffl equation (Pfaffl, 2001) was used to compare target gene expression across experimental groups.

$$expression\ ratio = \frac{(E_{GOI})^{\Delta C_{T\,GOI}(control-sample)}}{(E_{ref})^{\Delta C_{T\,ref}(control-sample)}}$$

Here, the amplification factor (E) for each primer set is used to compare the ΔC_T values (difference between C_T values of each sample against a chosen 'control' sample), expressing the ratio in comparison to ΔC_T values of a reference gene for each sample – in this case, GAPDH.

2.3.2.5. Agarose gel electrophoresis

End-product gel electrophoresis was carried out to test primer specificity and to verify that products were the predicted size based on primer design.

A 1.5% agarose gel was cast using pure agarose and 1× TAE buffer in ddH_2O, including 1× final concentration SYBR Safe DNA gel stain (Invitrogen, Thermo Fisher Scientific). PCR loading dye (ThermoFisher) was added to end-product positive and negative control samples following PCR to a final concentration of 1× dye, and along with Fisher BioReagants ExactGENE 100bp molecular ladder (Fisher Scientific), samples were run at 70 V in 1× TAE buffer using a Bio-Rad power pack. Once fragments were separated, the agarose gel was visualised using a Syngene U:Genius3 Gel Documentation System (U:Genius software version 3.0.7.0) under UV light.

2.3.3. Protein quantification by SDS-PAGE electrophoresis and Western blotting

2.3.3.1. Sample homogenisation and lysate preparation

Frozen hippocampi were defrosted in 2 mL of ice-cold lysis buffer (Table 2-11) in a 15 mL Falcon tube, using an upright homogeniser. Each sample was homogenised for ~5 s before being placed back on ice for at least 1 min to maintain ice-cold temperature. This was repeated for 5 rounds of homogenising for each hippocampus, with the homogeniser rinsed 3 times in ice-cold clean ddH_2O and once in ice-cold clean lysis buffer between each sample. Lysates were then centrifuged at 14000 RCF at 4°C for 10 min to remove nuclei, mitochondria, and cell debris, and supernatant containing membrane and cytoplasm was stored in ~500 µL aliquots at -80°C.

Lysis buffer	
NaCl	150 mM
Triton X-100	1% (v/v)
glycerol	10% (v/v)
HEPES	30 mM
SigmaFAST protease inhibitors	1 tablet for 50 mL

Table 2-11: Lysis buffer for hippocampi homogenisation.

2.3.3.2. Determination of protein concentration

Protein lysate concentration was determined using a Pierce™ BCA Protein Assay Kit (ThermoFisher Scientific). Lysates were quantitated with a standard curve generated from serial dilution of known protein standards to calculate protein concentration in samples. Briefly, Bovine Serum Albumin (BSA) in solution (2 mg/mL, Thermofisher Scientific) was diluted in lysis buffer to make known protein concentration standards. Lysate samples were diluted 1:4 with lysis buffer, and both standards and diluted lysate samples were read in duplicate using the BCA Assay reagents. Plates were incubated at 37°C for 30 min, and optical density was read using an Emax Precision Microplate Reader (Molecular Devices) at 540 nm wavelength. Duplicates of all readings were averaged, and lysate concentrations were interpolated from linear regression of standard curve readings using a linear regression analysis on Graphpad Prism. Calculated lysate concentrations were multiplied by 4 to account for assay dilution.

2.3.3.3. Protein separation by SDS-PAGE

Samples were separated by weight using sodium dodecyl sulfate (SDS) based polyacrylamide gel electrophoresis (PAGE). Gels were made at 1.5 mm thick using Mini-PROTEAN® Tetra Handcast Systems (Bio-Rad) to a 9% acrylamide content following components described in Table 2-12.

Immediately after adding TEMED, gel mix was added between glass plates and bubbles prevented using a small volume of 100% butanol. Once resolving gel was set, butanol was removed using filter paper and stacking gel (3% acrylamide) was poured on top and a 10-well comb inserted.

Gel component	10% resolving gel mL	stacking gel mL
1.5M Tris Buffer pH 8.8	2.5	-
0.5M Tris Buffer pH 6.8	-	1.25
10% SDS	0.1	0.05
10% ammonium persulfate	0.1	0.05
Acrylamide (40%)	2.5	0.375
ddH_2O	5.8	3.275
TEMED (add last)	0.0025	0.0025

Table 2-12: Components for making one gel for SDS-PAGE.

Lysates were prepared with a total of 50 µg total protein per well, diluted to 33 µL using 3× loading buffer (Table 2-13), 5% β-mercaptoethanol and lysis buffer. Prepared samples were boiled at 95°C for 5 min using a dry hot block (Grant Prima UBD2, Grant Instruments, Cambridge) to denature protein structures.

3× sample loading buffer	
Tris-HCl (pH 6.8)	150 mM
Dithiothreitol	300 mM
SDS	6% (w/v)
bromophenol blue	0.30% (w/v)
glycerol	30% (v/v)

Table 2-13: Components of sample loading buffer for running lysates on gels.

All gels included a molecular ladder (Bio-Rad PrecisionPlus) as reference for protein size, as well as a control sample lysate to normalise across gels. Gels were immersed fully in running buffer (Table 2-14) in a Mini-PROTEAN® Tetra cell (Bio-Rad) electrophoresis tank and run using a Bio-Rad power pack at a constant current of 0.02 A per gel for ~3 hours, until samples reached the bottom of the gel.

2.3.3.4. Transfer and blotting of proteins on PVDF membranes

Separated proteins were transferred onto PVDF membrane, which had been activated by soaking in methanol for ~15 s and equilibrated in transfer buffer (Table 2-14). Gels and membranes were immersed in transfer buffer while being assembled in transfer 'sandwich' apparatus, using sponges and extra thick transfer filter paper (Bio-Rad). Transfers were run for 1 hour at a constant current of 1 A in the presence of a dry ice pack in circulating transfer buffer.

Buffer component	Running buffer	Transfer buffer
Tris Base	25 mM	25 mM
Glycine	190 mM	190 mM
SDS	0.10% (w/v)	-
methanol	-	20% (v/v)

Table 2-14: Components of running and transfer buffer for SDS-PAGE and transfer to PVDF membranes (made to volume using ddH_2O).

Following transfer, membranes were fixed by immersing in methanol for ~10 s, followed by a 5 min soak in TBS (Table 2-15), and finally blocked for 1 hour at RT in blocking solution to prevent non-specific binding. Membranes were then incubated overnight at 4°C with primary antibodies (Table 2-16), diluted in blocking solution (Table 2-15), in sealed plastic bags attached to a rotating wheel.

	TBS	TBS-T	blocking solution
10× Tris-Buffered Saline (Bio-Rad)	10%	10%	10%
Tween-20	-	1%	1%
Nonfat dry milk (Bio-Rad Blotting Grade Blocker)	-	-	5%

Table 2-15: Components of wash and block buffers for Western Blotting membranes, all made to volume using ddH_2O.

Following overnight primary incubation, membranes were washed in TBS-T (Table 2-15) 6 times, for 5 – 10 min per wash on a horizontal shaker. Membranes were then incubated with secondary antibodies (Table 2-16) for 1 hour at RT while being gently agitated on a shaker, and again washed 6 times with TBS-T.

antibodies	dilution	category number
primary		
ENT1 (rabbit)	1:2000	Proteintech Europe #11337-1-AP
GAPDH (mouse)	1:10 000	Invitrogen #MA5-15738
secondary		
Anti-Mouse IgG	1:10 000	SeraCare KPL #5450-0011
Anti-Rabbit IgG	1:10 000	SeraCare KPL #5450-0010

Table 2-16: Antibodies used for protein probing.

2.3.3.5. Membrane visualisation

Membranes were visualised through SuperSignal™ West Pico PLUS Chemiluminescent Substrate (ThermoFisher Scientific), with the two solutions mixed 1:1 and applied to membranes for at least 5 min. Chemiluminescence was detected using an ImageQuant LAS 4000 (GE Healthcare Life Sciences), with exposure for each membrane between 4 – 30 s.

Band intensity of membrane images was analysed using Image J software, allowing for manual removal of background signal. All signals on each membrane were normalised to the control lysate to control for variation in optical intensity across different membranes, and GAPDH was a loading control within each sample.

3. Results Chapter 1: Detection of Adenosine in the Hippocampus

3.1. Introduction

The main objective of this thesis was to assess the interaction of CBD with adenosine, based upon the ADK theory of chronic epilepsy. Therefore, this chapter starts by assessing concentration of adenosine within hippocampal slices, validating and utilising an amperometric method of detecting adenosine: enzyme-based biosensors. Following validation, two studies were performed, assessing both the basal concentration of adenosine as well as an induced rise of adenosine following electrical simulation.

3.1.1. Background of enzymatic biosensors

Enzyme-based biosensors were first developed by Dale (1998), and originally consisted of tubes of semi-permeable glass loaded with the enzymes adenosine deaminase, nucleoside phosphorylase and xanthine oxidase, surrounding a charged platinum wire. Upon detection of adenosine, the enzymes would enable the breakdown of adenosine to its metabolites and release hydrogen peroxide, which is then able to create a current against the charged wire. This current was shown to be a linear concentration-dependent response to applied adenosine between 10 nM and 20 µM (see Figure 3-1, bottom left (Dale et al., 2000)), a range which has remained mostly true through the developments and refinements to sensor design (sensors are currently marketed as having a linear range of 0.2 µM to 20 µM (Sarissabiomedical, 2015)). Refinements have included the development of a polymer matrix with which to trap the enzymes, rather than loading within larger microdialysis tubes, therefore coating the polarised wire with enzymes and allowing for a sensor with smaller dimensions and more rapid responses with higher degree of sensitivity (Llaudet et al., 2003; Sarissabiomedical, 2015).

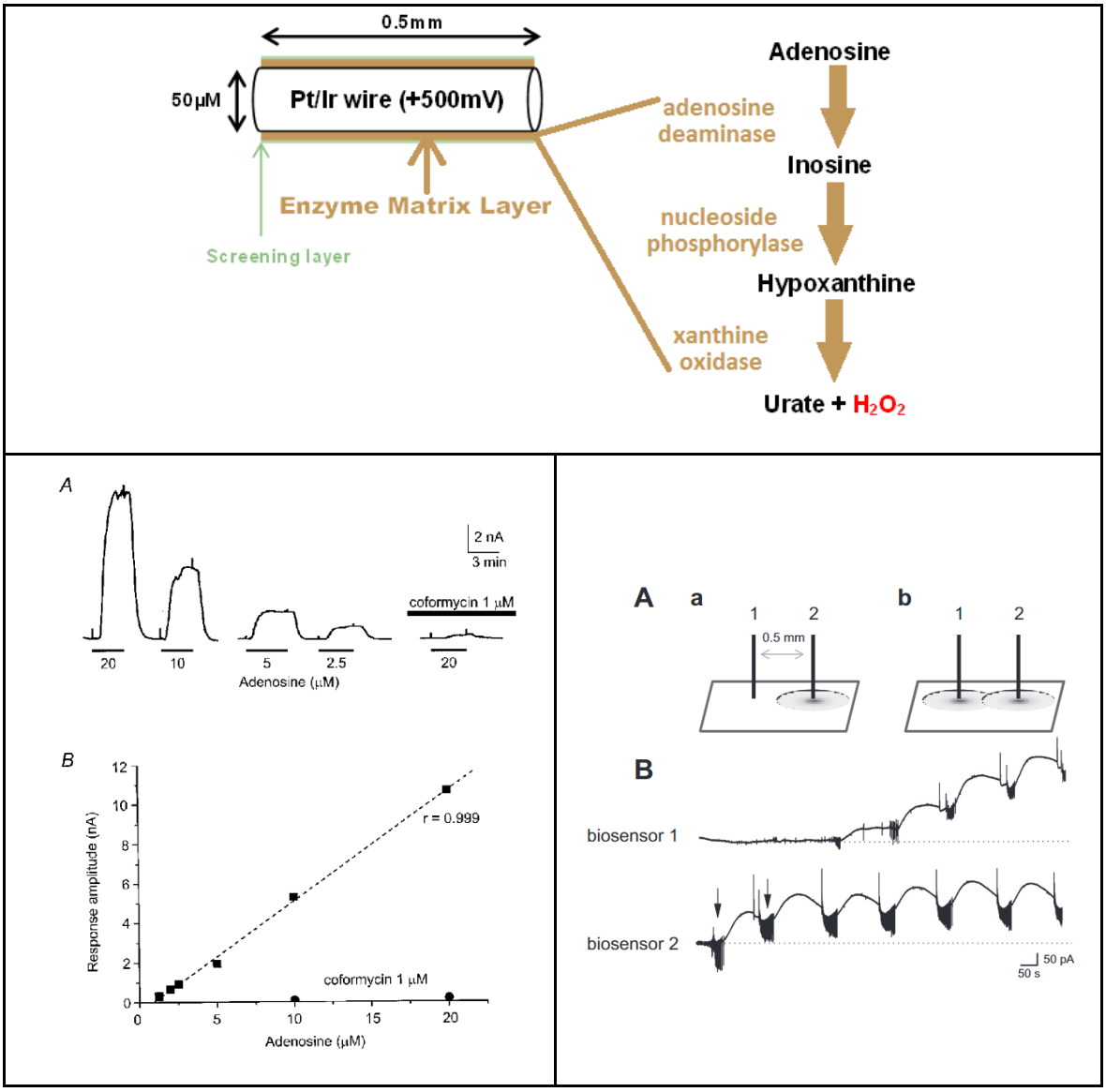

Figure 3-1: Properties and development of the adenosine biosensors used in this thesis. Top: Sensors consist of a Pt/Ir wire coated in enzymes, exploiting an enzymatic cascade to reduce adenosine to its metabolites. Production of H_2O_2 creates a current against the polarised Pt/Ir wire, and an external permselective screening layer protects against electroactive interferents, although repeated insertions into tissue are likely to damage the screening layer. **Bottom left:** Linearity of the sensor in response to 2.5 – 20 µM adenosine, as demonstrated at its first introduction (Dale et al., 2000). **Bottom right:** Demonstration of localisation of purine concentration (figure from Wall and Richardson (2015)). With two sensors placed close together in layer V of the neocortex, network activity induced by zero-Mg^{2+} aCSF would create currents on the biosensor closest to the activity, indicating localised adenosine release.

These sensors have been used in Xenopus embryos to measure adenosine release during swimming (Dale, 1998; Llaudet et al., 2003) as well as *in vitro* in hippocampal slices, for instance to measure the release of adenosine in response to hypoxia (Dale et al., 2000), hypercapnia (Dulla et al., 2005), or

pharmacological modification of the adenosine metabolism system (Etherington et al., 2009). In addition, the biosensors have been adapted for use *in vivo* in anaesthetised pigs, allowing for real-time measurement of central adenosine release during induced seizures (Van Gompel et al., 2014).

3.1.1.1. Control sensor – inosine vs NULL

Two different control sensors were used for the two studies in this chapter; the inosine sensor and the NULL sensor. Inosine sensors are almost identical to the adenosine sensor except lacking in adenosine deaminase (the first enzyme of the cascade, producing inosine from adenosine – see Figure 3-1). The advantage of an inosine sensor is its ability to detect all the metabolites of adenosine (inosine and hypoxanthine, which also contribute to the adenosine sensor recording) therefore theoretically allowing for a 'pure' adenosine concentration to be calculated from the differential between the adenosine and inosine sensors. However, as the individual sensors can have dimensions of up to 50 µm diameter and 0.5 mm length, it is impossible in practical terms for two sensors to be detecting from the exact same location, especially taking into account the highly localised nature of neuronal activity. Wall and Richardson (2015) demonstrated that two biosensors placed 0.5 mm from each other in layer V of the neocortex are only able to detect purine release from very localised neuronal activity (Figure 3-1, bottom right). Additionally, section 3.4.2 below will show that there can be a significant difference between adenosine and inosine sensors' response to 10 µM adenosine/inosine following insertion and removal from slices. This suggests a variability in loss of sensitivity between sensors which is difficult to account for in experimental recordings, as sensitivity could lost during sensor insertion, or removal, or whether it can vary between the two, which would result in a discrepancy between adenosine and inosine sensors' sensitivity during an experiment. For this reason, as well as practical difficulty in controlling the sensors' depth and angle of tissue penetration, using inosine sensors would appear to have little benefit when assessing purinergic concentration as it would be impossible to calculate a 'pure' adenosine concentration, particularly as it is also difficult to assess how much of the inosine sensor signal is due to endogenous metabolism of adenosine.

The NULL biosensor, which contains no enzymes in its polymer matrix, does not detect any form of purinergic release but will respond to non-physiological interferents in the adenosine sensor trace, for instance mechanical perfusion events or artefacts from electrical stimulation. This allows for confidence in the separation of environmental noise or artefacts from physiological activity. The null biosensor in this case acts as a physiological negative control, and the differential between the adenosine and null sensor traces, while still a reflection of the concentration of adenosine and its metabolites (therefore described as micromolar prime, or µM') rather than 'pure' adenosine, gives a much cleaner representation of adenosine concentration.

3.1.2. Chapter aims

The ADK theory of epilepsy relies upon the concept that astrogliosis in epilepsy causes increased adenosine uptake, thereby decreasing basal adenosine concentration and reducing an A_1R-mediated protective threshold. The aim in this chapter is to investigate whether lower adenosine levels can be detected using microelectrode biosensors in rat hippocampal slices taken from epileptic rats as compared to healthy rats.

Additionally, as CBD has been shown to inhibit ENT1, the CBD theory of regulating adenosine signalling involves prevention of adenosine uptake, application of CBD to slices may increase detected adenosine levels.

In addition to basal adenosine, the effect of CBD on evoked adenosine release (representing an active seizure-like environment) will be investigated.

3.2. Methods

3.2.1. Adenosine biosensors

3.2.1.1. Basal drug application protocol

As described in General Methods, adenosine sensors were polarised to 500 mV prior to insertion in the *stratum pyramidale* in the CA1 area of hippocampal slices. An inosine sensor was initially used as a control sensor for these experiments; however inosine current recordings were ultimately not used in data analysis (see section 3.1.1.1).

The experimental protocol is described schematically in Figure 3-2 below. Briefly, following 40 – 60 min to allow for damage-induced adenosine levels to stabilise, 0.01% ethanol was bath applied for 10 min as a vehicle control, followed by 30 min of 10 µM CBD or CBDV application. Following drug washout, to test the assay response (i.e. that the slice is able to release adenosine), aCSF with tenfold increased KCl concentration (24.9 mM) was bath applied for 6 min to observe adenosine release from the slice as previously described (Sims et al., 2013). Sensors were removed from the slice once a potassium-induced adenosine peak had been reached, then calibrated with 10 µM adenosine, bath applied via aCSF.

Figure 3-2: Timeline schematic of basal adenosine recordings experimental protocol.

3.2.1.1.1. Biosensor analysis

For basal drug application, adenosine current recordings were directly exported from LabChart into Microsoft Excel. For each experimental trace, comprising of all sensor recordings taken from a slice from sensor insertion until adenosine calibration, a regression equation was fitted to control for post-polarisation trace decay using the Excel 'Power' trendline formula (below), where *y* corresponds to the recorded current and *x* the timestamp.

$$y = c \times x^b$$

This regression equation was then subtracted from the entire trace recording to control for this post-polarisation decay.

The calibration measurements of 10 µM adenosine taken following each experiment were used for scaling recorded current values, with the mean of all 10 µM calibration currents used as a scaling factor to normalise. Therefore, data are presented as modified current (nA*) values, as raw nA values have undergone scaling to account for changes in sensor sensitivity between experiments (Section 3.3). For estimation of basal adenosine tone and to allow for comparison with the literature, values were also directly converted to an estimated concentration based on calibration (µM'), however it is noted that this value is likely to be an overestimation of actual adenosine concentration due to the unknown proportion of adenosine metabolites (e.g. inosine, hypoxanthine) and electroactive interferents contributing to the recorded current signal (Frenguelli et al., 2007).

To standardise the analysis a 10 min mean of sensor baseline prior to vehicle application was taken to represent basal adenosine tone in the slice, and healthy and epileptic 'tone' measurements were compared using an unpaired t-test. For drug applications, a 5 min mean of sensor trace was taken at the end of the ethanol vehicle application and compared with the 10 min mean between 20-30 min following CBD or CBDV application using a paired t-test.

3.2.1.2. Stimulation-evoked study

For these experiments, adenosine sensors were paired with NULL sensors; these are identical to adenosine sensors but lack the enzymes that allow for detection of adenosine (discussed in section 3.1.1.1).

For stimulation-evoked adenosine experiments (protocol described in section 3.2.2.2), the NULL signal was subtracted from adenosine sensor signal in LabChart (AD Instruments), thereby controlling for post-polarisation decay across recordings. Each experimental trace (ADO – NULL) was calibrated to µM', and then exported to Clampfit 10.7 (pClamp 10, Molecular Devices) for post-hoc filtering and analysis. Traces were low pass filtered at 0.25Hz prior to analysis. Post-stimulation peak amplitude was determined for the entire experimental timeline (23.5 min) following stimulation. Decay time constants (τ) were calculated for post-stimulation, post-peak waveforms by fitting the decay to a "One phase decay" nonlinear regression using GraphPad Prism.

3.2.2. MEA protocols

3.2.2.1. LFP recording through MEAs

Using an image of the hippocampus on the MEA taken prior to being placed in the MEA headstage (described in section 2.2.2), an electrode within CA1 *stratum radiatum* area was used as a stimulation electrode, evoking a LFP in surrounding electrodes. Field potentials were evoked at 15s intervals using biphasic 100 µs step pulses, at a stimulation intensity between ±0.5 – 2.0 V. A specific recording electrode was then chosen based upon LFP response, which could be visually verified to lie on Schaffer collaterals and generally adjacent to the stimulation electrode with which to analyse field potential data. Field potential slopes were monitored throughout the experiment via online analysis of the 30 – 70% of linear downward deflection on MC Rack software (Multi Channel Systems). As the objective of this study was to evoke and record field potentials, data on all live channels were only recorded 10 ms prior to each trigger and 300 ms following. Therefore, data was captured on all 59 channels for a 310 ms window around each field potential; all other live data was not recorded.

3.2.2.2. Seizure-simulating stimulation for endogenous adenosine release

Following the- 40 – 60 min stabilisation of quantified adenosine signal to baseline, as well as stabilisation of LFP slope, ten electrodes were selected to cover the CA1 Schaffer collateral area as evoking stimulation electrodes (avoiding the electrode previously chosen as the specific recording electrode). Through these ten electrodes, a 300-pulse stimulation (100 µs biphasic step pulses, ±2 V) was applied at 20 Hz, an adenosine-releasing protocol adapted from (Wall and Dale, 2013). This stimulation protocol was 15 s in length, following which the standard 15 s test stimulations were resumed. Stimulations were spaced at least 25 min apart to allow for adenosine sensor recording to return

to baseline. Following 1 – 2 stimulation trains in control conditions, 10 µM CBD was diluted in carboxygenated aCSF and washed in through the perfusion system for 30 min at 4 – 6 mL/min before 1 – 2 stimulations were again administered while perfusate was still running with CBD. Control and vehicle (0.01% ethanol) recordings were made in healthy hippocampi without concurrent sensor recordings.

3.2.2.3. Data analysis for field potential recordings

Field potential slopes were normalised to the 5 min prior to stimulation, and again where more than one stimulation was recorded in either control or CBD conditions, traces were averaged in order to obtain one field potential trace per condition per slice. Field potentials from each slice were then averaged between 8 – 13 min following stimulation and compared across conditions using a one-way ANOVA or t-test where appropriate.

3.2.3. Correlations of sensor and field potential recordings

In experiments with matching biosensor and field potential recordings, biosensor traces were averaged to obtain values for every 15 s, matching concurrent field potentials. These values were tested for correlation using Pearson's product-moment correlation. Additionally, these time-matched values were analysed using a linear regression, allowing for a gradient slope to be generated for each experiment. These slopes were analysed using a two-way ANOVA.

3.3. Validation of the RISE-SRS Model of Chronic Epilepsy

The lithium-pilocarpine model of chronic epilepsy has been well-validated, and studies using this model have been published in peer-reviewed journals (Modebadze et al., 2016; Patra et al., 2019). Details of how the animals were induced is provided in section 2.1, with further details regarding welfare monitoring and logistics provided in Appendix 8.1.

The same model was used in a concurrent *in vivo* project in the same research team, which employed video monitoring of rats following confirmation of epilepsy allowing for seizure scoring in continuous 4-day bins, before and after chronic dosing with either vehicle or CBD. (Patra et al., 2019) These rats, which were confirmed epileptic within 6 – 8 weeks following induction using the PSBB method described in section 2.1, were monitored continuously via video recording, and seizures were counted and coded. Before and after a 10-week treatment period, all rats displayed seizures, and seizure burden significantly increased in vehicle-treated rats, demonstrating the validity of the lithium-pilocarpine model in inducing chronic epilepsy in rats, as well as the PSBB method in detecting and confirming this chronic epilepsy.

During this research portion of this project, 26 inductions of this model were performed (Appendix 8.1, Table 8-1). In total, between August 2015 and December 2017, 246 rats underwent the lithium-pilocarpine induction procedure. Of these, 44 (18%) were not confirmed epileptic (either by PSBB or through visual confirmation of seizures) in the 13 weeks following induction, 1 died during induction, 11 (4%) were terminated by schedule 1 in the 48 hours following induction (not met criteria, i.e., did not develop seizures, or for welfare reasons), and 1 was terminated by schedule 1 6 weeks following induction for welfare reasons (Appendix 8.1, Table 8-1). One induction of 8 rats was terminated on induction day per Animals Scientific Procedures Act (ASPA) PPL due to a drug formulation error, resulting in a protocol violation. In total, 189 rats were confirmed epileptic in the 13 weeks following induction, resulting in a 79% success rate of the inductions this candidate attended. This is comparable to the mean 69% success rate reported in the model presentation paper (Modebadze et al., 2016). Of note, none of the 246 animals died in the initial acute SE, with only 1 death occurring following SE termination (considered to be due to excess salivation during sedation). This demonstrates the considerable improvement in mortality from previous pilocarpine-induced chronic epilepsy models, including high-dose pilocarpine and/or lithium-pretreated models with no SE termination, which have reported mean mortality rates ranging from 30% to 80% (Glien et al., 2001; Curia et al., 2008).

Experiments described in this thesis account for 65 of the confirmed epileptic rats from these inductions, with other epileptic rats used for other concurrent projects, including those described in the Patra study.

For the experiments in this thesis, rats were aged to between ~6 – 20 weeks following induction. The range in ages was due to the logistics of a group of rats being prepared in each batch of inductions, alongside the multiple projects using the rats and the uncertainty of exactly when and how many rats would be confirmed epileptic following each induction. An average age of ~16 weeks was targeted to match the age of the termination of the Patra study, as the dissected and preserved hippocampi from these treated rats were used in the microbiology studies in this thesis.

3.4. Validation of Enzymatic Biosensors

3.4.1. Assessment of the linear detection range of sensors

To establish sensor linearity, increasing concentrations of adenosine in aCSF were bath applied to sensors. Representative standard curves were created with three individual adenosine sensors, in response to application of known adenosine values (Figure 3-3). Two sensors tested a concentration range between 2.5 – 20 µM, while one sensor tested a lower concentration range from 0.01 – 5 µM. Linear regression analyses run on all three data sets yielded r^2 values greater than 0.99 (sensor 1: r^2=0.9908; sensor 2: r^2=0.9950; sensor 3: r^2=0.9996), and Runs tests did not find deviation from linearity in all three datasets ($P<0.1$). However, when isolating the lowest concentrations tested (0.01 – 0.1 µM)

current values did not have a slope which was significantly non-zero ($F(1,2) = 3.021$, $P = 0.2243$; Figure 3-3B); showing that the sensors have a limited sensitivity to adenosine concentrations below 0.1 µM.

Therefore, data showed that sensor recordings were linear between 0.1 µM and 20 µM adenosine, but the sensitivity of sensors would vary between different sensors and experiments. For this reason, sensors were calibrated with 10 µM adenosine as standard following each experimental recording.

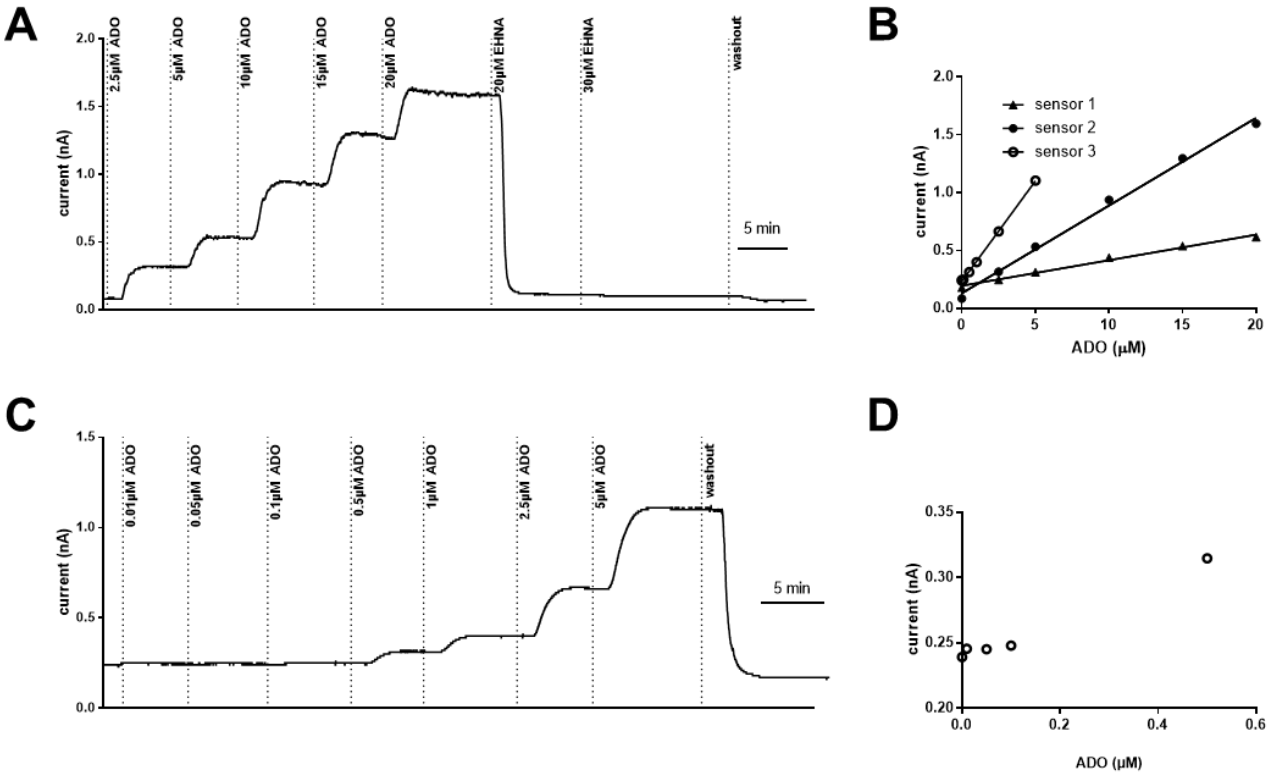

Figure 3-3: Biosensors have a linear detection range between 0.1 µM and 20 µM adenosine. A&C: Raw sensor current traces of the adenosine-detecting biosensor showing response to increasing concentrations of adenosine, with (A) testing a range of concentrations from 2.5 µM to 20 µM, and (C) testing a smaller range at lower concentrations (0.01 µM to 5 µM). Dotted lines indicate the time at which the perfusion was changed to the labelled perfusate. Note that (A) also demonstrates ADA-dependency of adenosine biosensors, with EHNA (ADA inhibitor) causing the sensor current trace to decrease down to washout levels. (C) shows the current decrease due to a direct washout from 5 µM adenosine. **B:** Three representative sensors showing linear responses to increasing concentrations of adenosine. Sensors 2 and 3 correspond to traces (A) and (C) respectively. **D:** Isolation and magnification of the 5 lowest adenosine traces of (C) between 0 – 0.5 µM show little sensitivity to adenosine below 0.1 µM.

3.4.2. Sensitivity and specificity of sensors

Due to the length of time biosensors were anticipated to be inserted in slices (previous antiseizure activity of CBD using MEAs detecting efficacy in the range of 20 – 30 min, with at least 60 min required for the adenosine released from sensor insertion to equilibrate), initial pilot experiments were performed to test the experimental set-up and explore the possibility of a loss in enzyme sensitivity over time inserted in slice.

To assess the potential loss in sensitivity, a 10 µM calibration reading was taken prior to sensors being inserted into a slice and compared with a 10 µM sensor current following sensor removal. It was also assessed whether length of time within a slice would significantly and consistently affect the sensitivity of the sensors. Therefore, adenosine and inosine sensors were left in slices for a range of times (10 – 155 min), and then calibrated following removal from the slice preparation using 10 µM adenosine and inosine.

For all time points measured, the sensor sensitivity decreased following insertion and removal from the slice preparation (Figure 3-4A). For the adenosine sensor, the response to 10 µM adenosine fell to 75.6 ± 3.01% of response prior to slice insertion (one sample t-test against 100, $P < 0.0001$), and the response to 10 µM inosine fell to 76.0 ± 3.3% of control (one sample t-test, $P = 0.0002$). A paired t-test found no difference between the two responses ($P = 0.1155$). For the inosine sensor, all pooled time points saw a decrease in sensitivity to 83.6 ± 3.0% of control inosine response ($P = 0.0009$). A paired t-test between the adenosine and inosine sensors' responses to 10 µM inosine found a significant difference between the two sensitivities ($P = 0.0263$).

Pearson's product-moment correlation coefficients used to determine if the loss in sensitivity was related to time in slice reported insignificant poor to medium correlations between the two parameters: for the adenosine sensor's response to adenosine, $r(6) = -0.64$, $P = 0.0876$, and for inosine $r(6) = -0.55$, $P = 0.1562$; for the inosine sensor's response to inosine, $r(6) = -0.27$, $P = 0.5252$. Additionally, linear regression analyses (Figure 3-4B) calculated no significant deviation from zero for all three datasets (adenosine sensors: adenosine $F(1, 6) = 4.155$, $P = 0.0876$, inosine $F(1, 6) = 2.627$, $P = 0.1562$; inosine sensor $F(1, 6) = 0.4547$, $P = 0.5252$). Therefore, no strong correlation was found between sensitivity loss and time in slice, with the regression slope not significantly non-zero.

As no linear correlation was found, this made it difficult to control for the change in sensor sensitivity throughout the duration of recordings. If a linear relationship was found, a retrograde regression could be applied for long-term experiments to account for loss of sensitivity from recordings taken earlier in the recording, to allow for accurate comparisons to traces from later in the same recording. It is unknown whether the observed loss of sensitivity occurs due to the uncontrolled mechanics of inserting the sensor,

the removal, or whether there is a time-effect which is confounded by the mechanical insertion or removal. Due to the experimental set-up, with the MEA headstage needing to be removed to insert the slice, it was not possible to calibrate sensors immediately prior to insertion without either exposing the sensors to air while removing and replacing sensors to place the MEA in the headstage, or flooding a slice with 10 µM adenosine prior to each experiment. Both these methods would be confounding factors in any experimental study following these noninterventional pilots. Therefore, as the biosensor literature calibrates sensors following removal from slice as standard (Sims et al., 2013; Diogenes et al., 2014; Frenguelli and Wall, 2016), this was also used for all biosensor studies in this thesis, with no adjustment used to account for length of time in slice.

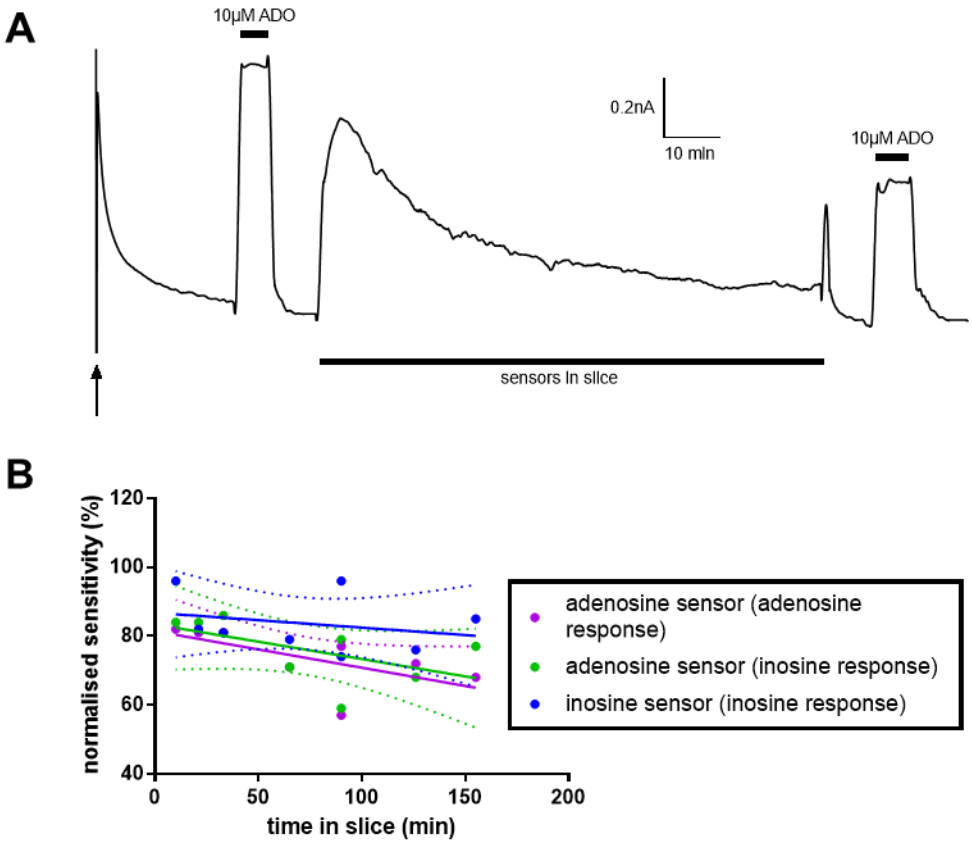

Figure 3-4: Loss in sensor sensitivity following insertion and removal from a slice could not be quantified linearly. A: Representative trace from ADO sensor showing adenosine calibration prior to sensor insertion in slice, removal of sensors after 90 min (no intervention while sensors in slice), and a second adenosine calibration. Arrow on bottom left indicates initial polarisation of sensors. **B:** Post-removal adenosine calibrations as a percentage of the initial pre-insertion across 7 time points. Values are shown for adenosine sensors (including response to 10 µM adenosine and 10 µM inosine, as well as inosine sensors' responses to 10 µM inosine.) Solid lines show linear regression, dotted lines show 95% CI.

For the two studies in this chapter using biosensors (described below in sections 3.5 and 3.6), the 10 µM adenosine calibrations taken following removal of sensors from the slice created a mean current of 1.5 ± 0.06 nA, from a total of 56 recordings. There was no significant difference between the two studies (respectively: 1.5 ± 0.07 nA, n = 30; 1.5 ± 0.14 nA, n = 26; P = 0.7565, unpaired t-test).

To ensure specificity of the biosensors, controls were utilised and pilot tests performed. After adenosine calibrations, 10 µM 5-HT was applied to test the patency of the screening layer of the biosensors (Figure 3-5A). If a 5-HT response reached above the threshold of 10% of the 10 µM adenosine calibration, or the ADO – NULL differential during 5-HT challenge was significantly non-zero, sensors were discarded and replaced with fresh sensors.

To ensure minimal possible interference with biosensor current readings, pilot tests were performed with CBD dissolved in two vehicles and two concentrations against biosensors (Figure 3-5A). CBD dissolved in 0.1% DMSO had previously been used as standard for electrophysiological slice experiments, but it was found that this vehicle created a slight deflection in the biosensor current (Figure 3-5B). Although the deflection was small, efforts were made to minimise any possible interference against biosensor current, even taking into consideration the NULL control, to ensure that as much of each sensor trace was an accurate recording of adenosine and its metabolites. As it was found that ethanol at 0.1% and 0.01% created smaller deflections than DMSO, and 10 µM CBD dissolved in a final concentration 0.01% vehicle created much smaller deflections on biosensor current compared to 0.1% for both vehicles, it was decided for all biosensor studies to use 0.01% ethanol as a vehicle to deliver 10 µM CBD.

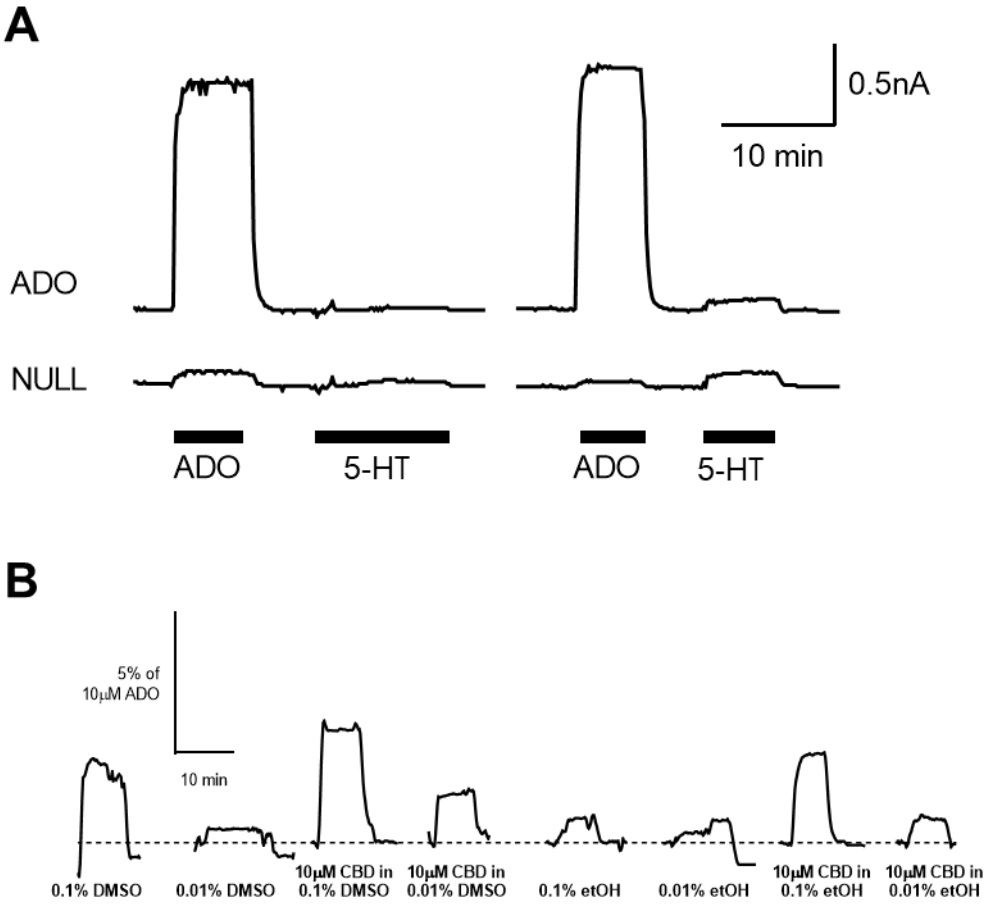

Figure 3-5: Testing and minimising sensor interference. A: Challenges with 10 µM 5-HT following calibrations with 10 µM adenosine, on the ADO and NULL sensors. Left, a sensor recording with a small 5-HT response on both sensors. Right, a sensor with a higher 5-HT response, showing on both ADO and NULL sensors. **B:** Challenging sensors with different vehicles for CBD. DMSO at 0.1% dilution created a larger response against biosensors than 0.01% dilution, and both dilutions of ethanol created smaller responses than DMSO. The target concentration of CBD (10 µM) appeared to create a large response when dissolved in 0.1% of either vehicle, but less when dissolved in 0.01% of either DMSO or ethanol. Traces are mean currents of 1 – 3 recordings for each concentration of vehicle and/or CBD, and presented as a proportion of the adenosine calibration for that sensor. Note that noise levels for these deflections are relatively high due to the small changes in current.

3.4.3. Post-polarisation trace decay

With the observation that raw sensor traces display a constant decay slope for the entirety of experimental recordings following polarisation, two methods were used to control for this decay.

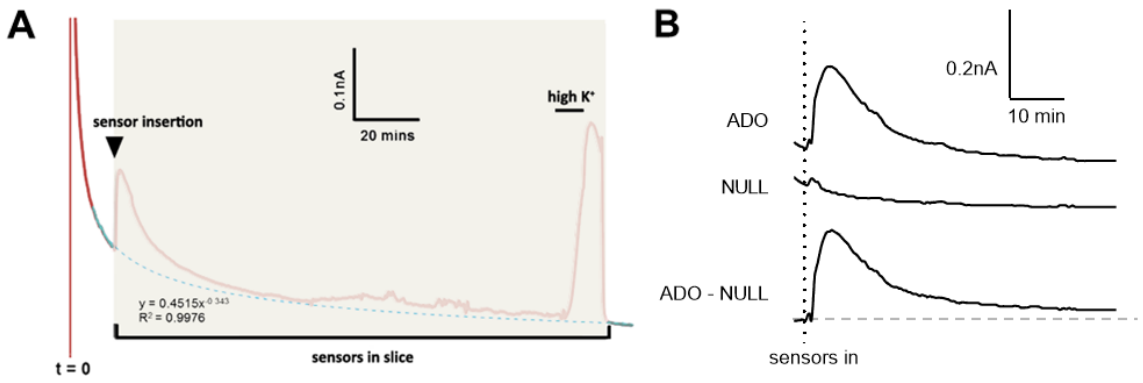

Figure 3-6: Representative raw traces from an adenosine sensor recordings showing two methods of control for post-polarisation decay. A: Regression analysis for ADO traces without corresponding NULL traces. The polarisation artefact is shown at t = 0, with subsequent trace decay continuing over several hours. Experimental recording following sensor insertion of slice are faded for figure clarity, although peaks indicating adenosine release can be seen following sensor insertion and application of high KCl (section 3.5.1). A regression equation (broken blue line) has been generated from the 5 min prior to sensor insertion and the trace baseline following sensor removal, both highlighted here in blue. **B:** Sensor insertion shown on the ADO and NULL trace recordings. For experiments performed with a NULL control, the simultaneous decay of the NULL sensor was used as a subtraction control for the ADO sensor's post-polarisation decay, and to control for electrical or mechanical interference.

For recordings performed prior to implementation of the NULL sensor, nonlinear regression analyses were performed on individual trace recordings using recorded points before and after sensor insertion into the slice preparation (Figure 3-6A). All regression equations have high fidelity for recorded current values, with r^2 values for all recordings exceeding 0.99. For recordings without a NULL sensor as control, these nonlinear regressions were used as sensor 'baselines' and subtracted from sensor recordings to provide an accurate reflection of adenosine signal.

For recordings with a NULL sensor as control, the differential between the two sensors was used to control for the post-polarisation decay (Figure 3-6B).

3.5. Interrogation of Basal Purine Levels

Basal purine levels were estimated from 10 min of stable baseline prior to vehicle application (Figure 3-7). Baseline-corrected and calibration-adjusted current recordings were 0.03 ± 0.004 nA* (healthy) and 0.02 ± 0.004 nA* (epileptic). There was no detectable difference between basal adenosine levels in rats with induced chronic epilepsy and age-matched healthy controls (unpaired t-test, P = 0.4838).

Using the adenosine calibration for each individual experiment, an approximate purine tone consisting of adenosine and its metabolites was calculated to be 0.17 ± 0.03 µM' in healthy tissue, and 0.14 ± 0.03 µM' in epileptic tissue.

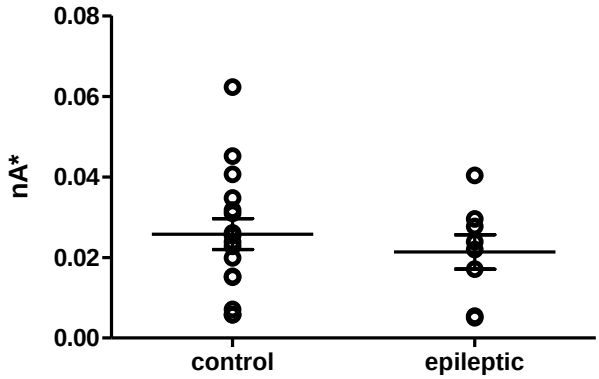

Figure 3-7: Basal purine levels recorded by adenosine biosensors were not significantly different between healthy and epileptic hippocampal slices. Adjusted current from adenosine sensor recordings taken from healthy (n = 16, 13 animals) and epileptic (n = 8, 6 animals) animals. The two conditions are not significantly different (p=0.4838, unpaired t-test). Error bars show mean ± SEM.

3.5.1. Effects of application of CBD or CBDV onto hippocampal slices

Following baseline subtraction and current scaling, mean values were taken of each experiment during the final 5 min of vehicle application, and compared with the final 10 min of a 30 min application of 10 µM CBD or CBDV (Figure 3-8A-D). In healthy slices, the mean sensor reading post CBD application was 41.6 ± 9.3 pA* compared with 34. 5 ± 8.2 pA* in the presence of vehicle (paired t-test P = 0.5695). CBDV application, in healthy slices, led to a non-significant increase in the current from vehicle measurement of 23.1 ± 6.0 pA* to 26.4 ± 6.2 A* in the presence of CDBV (P = 0.3987). For epileptic slices, CBD application changed the current from 25.4 ± 3.1 pA* at vehicle, to 21.7 ± 1.5 pA* in the presence of CBD (P = 0.2365). CBDV application on epileptic slices had no effect on the current (Vehicle: 57.1 ± 18.6 pA*; CBDV: 43.7 ± 12.2 pA*, P = 0.1569).

To serve as a positive control, aCSF with a tenfold increase in standard KCl concentration (24.9 mM, from standard 2.49 mM in regular aCSF as shown in Table 2-4) was applied to slices following washout of CBD/CBDV. Assuming an intracellular K^+ concentration of 140 mM, at the experimental temperature this rise in extracellular K^+ would increase the equilibrium potential of potassium (E_K) from the physiological equilibrium potential of -90 mV to around -45 mV, thereby decreasing the overall membrane potential to approximately -43 mV. This increased membrane potential would cause the opening of voltage-gated sodium channels in neurons, triggering widespread action potentials throughout the extent of exposure to increased extracellular potassium. Increased activity throughout the slice causes an increase in adenosine release, which has previously been measured using biosensors (Sims et al., 2013), and thus serves as assay validation for this study detecting adenosine release in slices.

As shown in Figure 3-8C-D, adenosine current increases during KCl application, then continues to rise steeply before peaking between 9 – 14 min following initial application. A two-way repeated measures ANOVA comparing peak KCl-induced adenosine release with baseline in the four groups (healthy CBD, healthy CBDV, epileptic CBD, epileptic CBDV) found a significant effect of potassium, $F(1, 10) = 34.06$, $P = 0.0002$, and no effect across the different groups, $F(3, 10) = 0.4957$, $P = 0.6933$ (Figure 3-8E). Sidak's post-hoc multiple comparisons test found no difference between the peak potassium-induced release values across the experimental groups.

The time taken for adenosine current to reach its peak value was also analysed (Figure 3-8F), as the high KCl-induced release served only as a positive control for the assay with little physiological relevance, particularly as NaCl was not concurrently reduced in order to maintain osmolarity of the solution. However, a significant difference was observed in the time for adenosine current to peak between healthy and epileptic slices – specifically, healthy slices which had previously been treated with CBDV, for which time to peak was 13.0 ± 0.7 min. This compares with healthy CBD-treated slices at 10.4 ± 0.7 min, and epileptic slices which had peak time latencies at 9.7 ± 0.4 min (CBD) and 9.9 ± 0.3 min (CBDV). A two-way ANOVA found a significant effect of epilepsy, $F(1, 10) = 12.77$, $P = 0.0051$, and also of the treatment, $F(1, 10) = 7.158$, $P = 0.0233$. The interaction was not significant, $F(1, 10) = 4.699$, $P = 0.0554$. Sidak's post-hoc multiple comparisons test found a significant difference between CBD and CBDV response specifically in epileptic tissue (adjusted $p = 0.0130$) and not in healthy (adjusted $p = 0.9225$). However, without any non-treated controls there can be no conclusions drawn from this observation with respect to the effects of CBD/CBDV application on KCl-induced adenosine spike latencies.

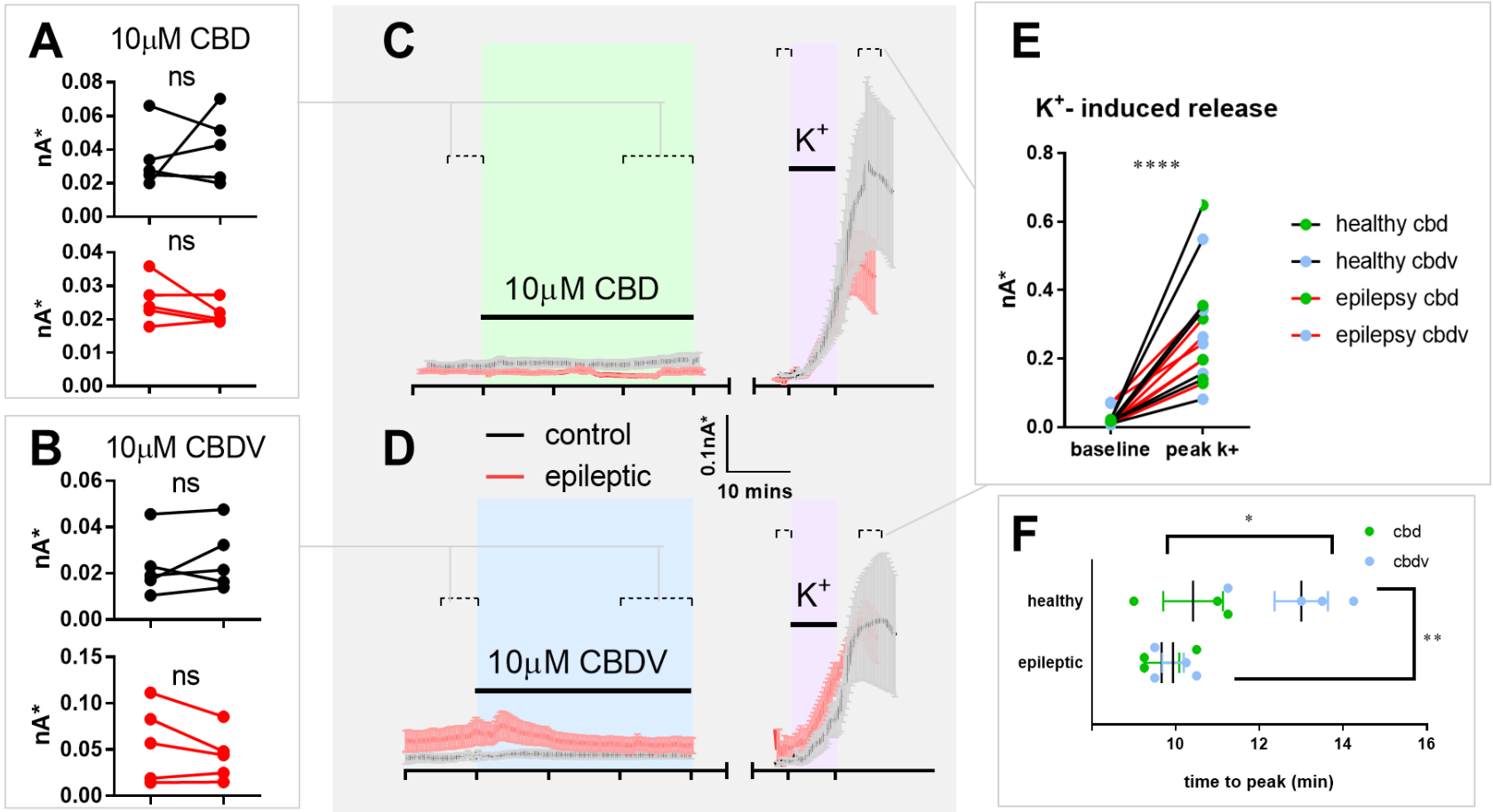

Figure 3-8: Biosensor recordings estimating adenosine concentration in healthy and epileptic hippocampi following CBD or CBDV application. A: Change in sensor recording from vehicle to 20 – 30 min following CBD application in healthy (n=5, 4 animals) and epileptic (n=5, 4 animals) hippocampal slices. **B:** Change in sensor recordings between vehicle and CBDV application from healthy (n=5, 5 animals) and epileptic (n=5, 4 animals) hippocampal slices. **C&D:** Mean ± SEM plots showing 10 min of vehicle followed by 30 min of 10 μM (A) CBD or (B) CBDV application on control and epileptic slices. Also shown for comparison

are 24.9 mM KCl-induced increases of recorded adenosine levels following CBD/CBDV washout, with broken brackets indicating baseline and peak (10-12 min following potassium application). **E:** Peak values of potassium-induced increase of adenosine current. ***:P<0.001, two-way repeated measures ANOVA. **F:** Time taken for adenosine current to peak following potassium application was significantly different between healthy and epileptic slices, due to the longer latency for CBDV treated healthy slices. *:P<0.05, **:P<0.01; two-way ANOVA with Sidak's post-hoc tests.

3.6. CBD inhibits seizure-induced adenosine release in the epileptic hippocampus

Although neither CBD nor CBDV showed any significant effect in changing biosensor-measured adenosine levels in unstimulated hippocampal slices, a further series of experiments were carried out on simulated seizure stimulations. CBD was chosen to carry into these future experiments through consideration of the literature and clinical studies (Devinsky et al., 2016; Devinsky et al., 2017; Devinsky et al., 2018; Thiele et al., 2018). There is growing evidence showing CBD's antiepileptic efficacy as well as its polypharmacology, and this therefore provides a strong rationale in assessing its potential molecular mechanisms of action.

3.6.1. Validation of adenosine release following CA1 electrical stimulation

As previously described by Wall and Dale (2013), electrical stimulation applied to hippocampal CA1 evoked signals on both adenosine and NULL biosensors. A sharp stimulation artefact was observed on both sensors from commencement of stimulation through the duration of the stimuli train, before a return to pre-stimulation baseline. Following this, the NULL sensor signal reliably remained at baseline while the adenosine sensor signal recorded a rapid increase in waveform with a slow decay (Figure 3-9A). As the adenosine signal is reliant upon enzymatic degradation of adenosine, the subtraction of ADO – NULL sensor traces allows for a more physiological representation of the extracellular concentration of adenosine and its metabolites, allowing for an estimation of adenosine concentration (Frenguelli et al., 2007). In healthy tissue, 20 Hz (300 pulse) stimulation to CA1 through 10 MEA electrodes in healthy tissue resulted in peak sensor-recorded current corresponding to 0.3 ± 0.04 µM' of peak adenosine release (Figure 3-9E, G).

3.6.2. CBD decreases stimulated adenosine release in epileptic tissue

In the presence of CBD (10 µM), peak adenosine release in healthy tissue was 0.3 ± 0.04 µM' (Figure 3-9E, G). In hippocampal slices obtained from epileptic animals, the same CA1 stimulation protocol induced a peak adenosine release of 0.37 ± 0.05 µM', comparable to that seen in healthy tissue (Figure 3-9F, H). However, application of 10 µM CBD to epileptic slices reduced peak adenosine release to 0.2 ± 0.03 µM'. A two-way repeated measures ANOVA found a significant effect of CBD, $F(1, 12) = 9.299$, $P = 0.0101$, with no effect of epilepsy, $F(1, 12) = 0.1172$, $P = 0.7380$, no significant effect of interaction, $F(1, 12) = 3.892$, $P = 0.0720$, or of matching, $F(12, 12) = 2.099$, $P = 0.1068$. Sidak's post-hoc multiple comparisons test identified a significant effect of CBD in epileptic slices (adjusted $P = 0.0047$).

Additionally, the decay waveforms of the post-stimulation adenosine release were assessed by fitting single exponential decays, and comparing the decay time constant τ (Wall and Dale, 2013; Hughes et al., 2018). Notably, while all n = 6 healthy slices were able to generate best-fit values, 3 of the n = 8

epileptic recordings were unable to return one phase decay best-fit values for either control or CBD due to inconsistent decay shapes, and therefore were excluded from the comparison, leaving n = 5 for this analysis. In healthy slices, τ was 5.8 ± 1.2 min in control conditions, and 5.5 ± 1.1 min with CBD; in epileptic slices, τ was 11.8 ± 8.6 min in control, and 10.2 ± 4.6 min in CBD. A two-way repeated measures ANOVA found no significant overall effect of epilepsy ($F(1, 9) = 1.03$, $P = 0.3367$), of CBD ($F(1, 9) = 0.07043$, $P = 0.7967$), nor of the interaction ($F(1, 9) = 0.03119$, $P = 0.8637$) or matching ($F(9, 9) = 2.231$, $P = 0.1238$) (Figure 3-9H).

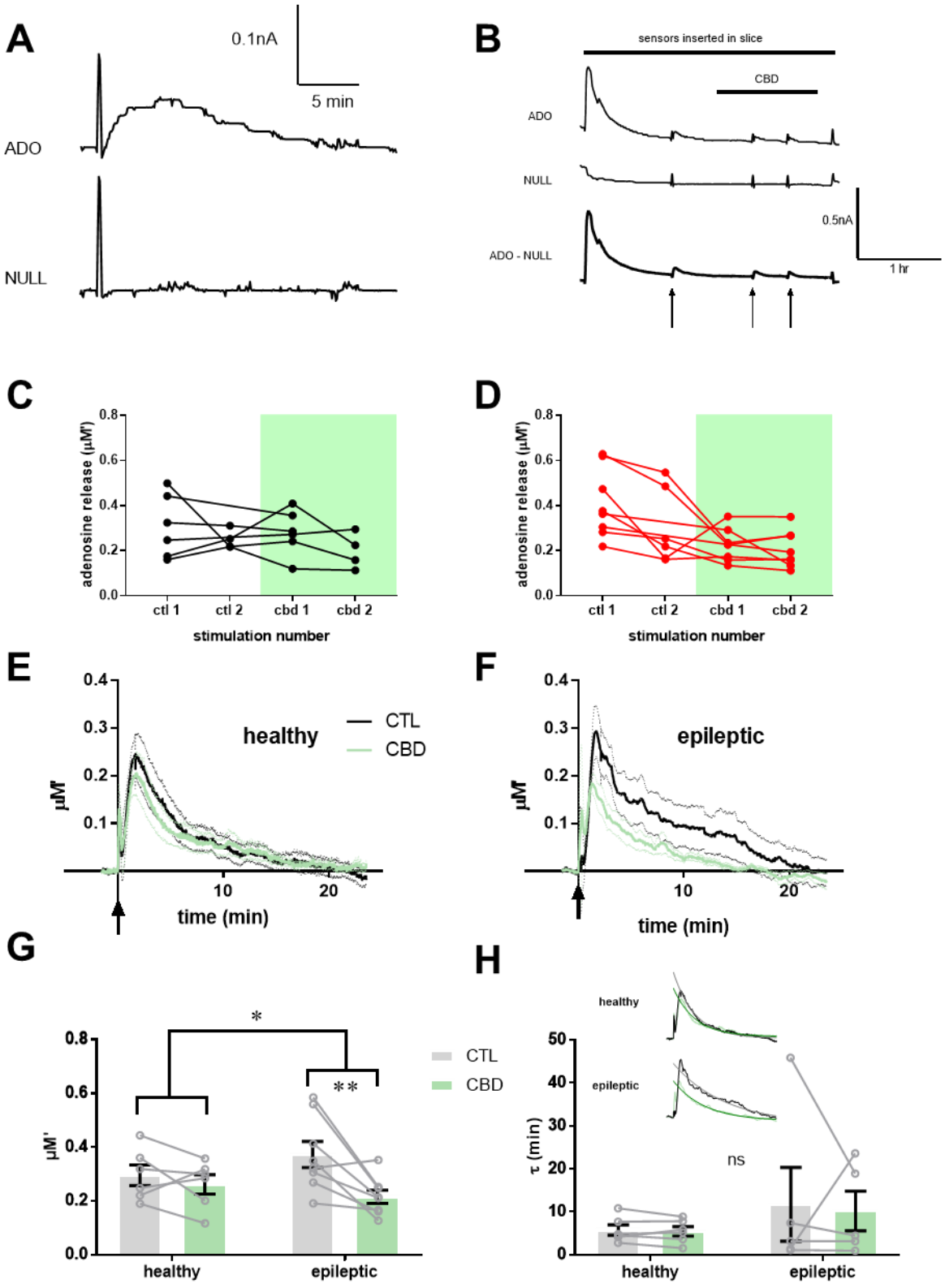

Figure 3-9: Direct quantification of stimulation-evoked adenosine release using enzymatic biosensors. A: Stimulation train causes a sharp upward deflection in both ADO and NULL sensor

current traces, but only ADO sensor detects the subsequent rapid rise and slow fall waveform. **B:** Representative ADO – NULL trace of an entire stimulation experiment, showing damage-induced sensor insertion adenosine release, and stimulation trains indicated by upward arrows. This particular experiment was performed on epileptic tissue. **C&D:** Peak amplitude detected from individual stimulations, showing lack of run-down between subsequent stimulations without external influence (i.e., CBD in epileptic slices). **E&F:** Sensor traces (mean ± SEM) from (E) healthy hippocampi (n=6, 5 animals) and (F) epileptic hippocampi (n=8, 5 animals) showing adenosine release following stimulation (indicated by arrow at time=0) in control conditions and following 30 min incubation in 10 µM CBD. Following application of CBD on epileptic hippocampi, adenosine release is reduced. **G:** Overall effect of CBD on peak adenosine amplitude across healthy and epileptic tissue (*: $P<0.05$), identified using two-way repeated measures ANOVA with post-hoc Sidak's multiple comparisons (**: $P<0.01$). **H:** No overall effect of epilepsy or CBD on decay time constant (τ) of adenosine release waveforms. Note that 3 of 8 recordings for epileptic hippocampi were unable to be fit with the nonlinear regression and so were omitted from ANOVA comparison. Inset: Mean healthy and epileptic adenosine release waveforms superimposed with exponential single phase decay regressions.

3.6.3. CBD modulates recovery of field potentials following adenosine-evoking stimulation in epileptic tissue

A probe pulse was applied to Schaffer collateral fibres on each slice using a single MEA electrode every 15 seconds throughout the duration of each experiment (except during the adenosine-evoking stimulation protocol) and the slope of the downward deflections of the probe pulse-evoked field potentials assessed as an overall estimation of network responsiveness (Figure 3-10A, B, insets). Following the adenosine-evoking stimulation protocol, field potential responses decreased for a further ~1 min, with peak inhibition of pre-stimulation baseline not significantly different across healthy or epileptic slices before and after CBD application (healthy control: 0.3 ± 0.03; CBD: 0.27 ± 0.06; epileptic control: 0.3 ± 0.09; CBD: 0.4 ± 0.07; two-way ANOVA: Epilepsy $F(1, 31) = 0.7997$, $P = 0.3781$; CBD $F(1, 31) = 1.372$, $P = 0.2504$).

Mean field potential slopes for each trace were calculated between 8 – 13 min following stimulation. A one-way ANOVA found no difference in healthy tissue between control (0.9 ± 0.07), vehicle (0.01% ethanol; 0.9 ± 0.11) or CBD (1.09 ± 0.08); $F(2, 20) = 2.079$, $P = 0.1513$. However, a two-way ANOVA of control and CBD mean 8 – 13 min values (excluding healthy vehicle due to having no epileptic comparison) found a significant effect of CBD in healthy and epileptic tissue; $F(1, 31) = 13.27$, $P = 0.0010$, with Sidak's post-hoc multiple comparisons tests identifying significance between epileptic control and epileptic CBD (adjusted $p = 0.0242$), as well as between epileptic control and healthy CBD (adjusted $p = 0.0095$; Figure 3-10C).

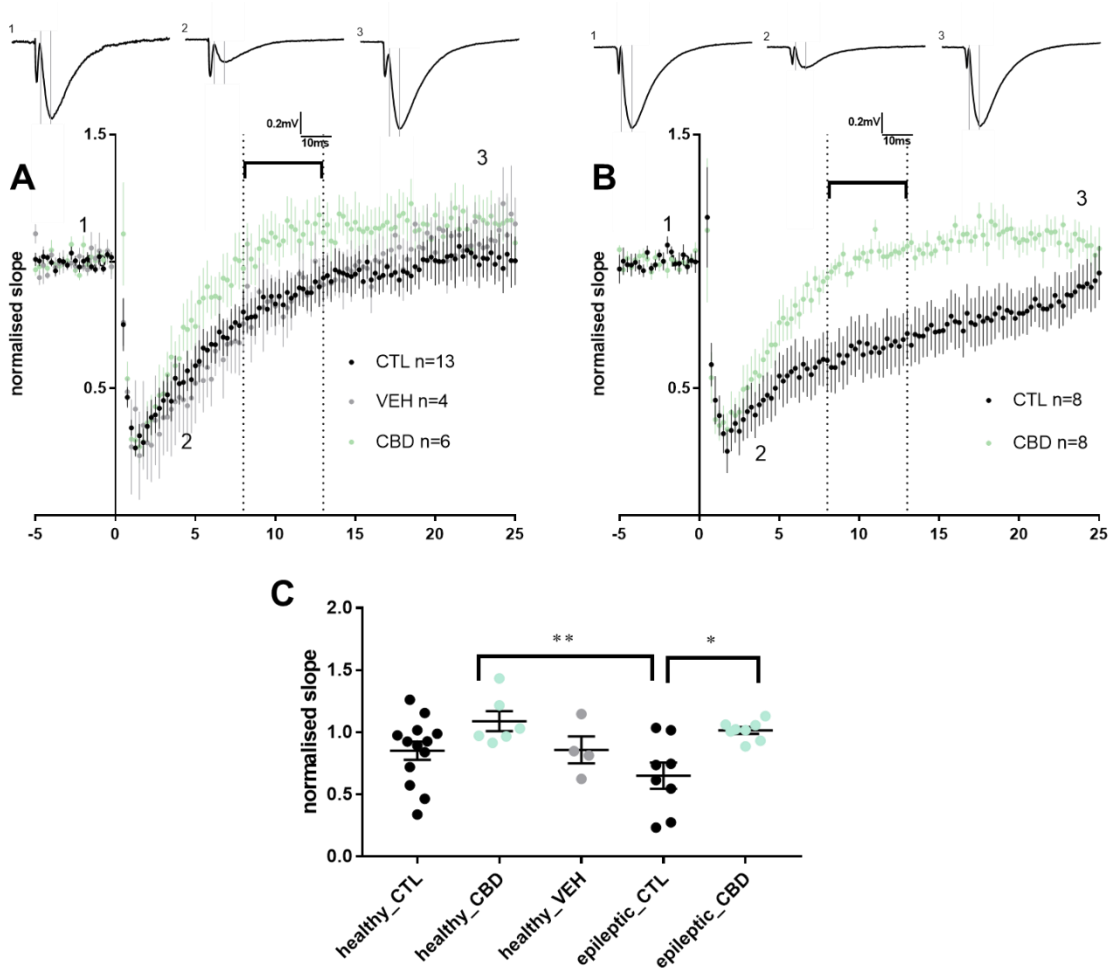

Figure 3-10: Inhibition of field potentials following adenosine-evoking stimulation protocol. A&B: Change in field potential inhibition, baselined to the 5 mins prior to stimulation, in healthy tissue (A) in control conditions (n=13, 10 animals), and following vehicle (0.01% ethanol; n=4, 3 animals) and CBD (n=6, 5 animals) application, and in epileptic tissue (B) in control (n=8, 5 animals) and CBD (n=8, 5 animals) conditions. Insets show examples of raw field potentials at 1- before stimulation, 2- at peak inhibition following stimulation, 3- following recovery. **C:** Comparisons of mean values between 8-13 min following stimulation. Two-way ANOVA (not including healthy vehicle values) found significant effect of CBD in healthy and epileptic tissue; $F(1, 31) = 13.27$, $P = 0.0010$, with Sidak's post-hoc multiple comparisons tests (*: adjusted $p<0.05$; **: adjusted $p<0.01$).

To show that the effects on field potential are due to activation of A_1R by adenosine, pilot stimulations were performed in the presence of DPCPX, an A_1R antagonist; however these were not expanded into an evaluable group of recordings. Details and initial data are provided in Appendix 8.2.1.

3.6.4. Correlation between sensor-recorded adenosine release and post-stimulation field potentials

Given that the post-stimulation sensor waveform has similar rise/decay kinetics to the post-stimulation field potentials, we assessed the relationship between the two by conducting a correlation analysis between experiments with both sets of recordings, when time-point matched following stimulation (Figure 3-11A, B).

A Pearson product-moment correlation was used to analyse these time-matched values for each individual experiment (Figure 3-11E). For each experimental group, Pearson's coefficient r values were as follows: in healthy control -0.8 ± 0.05, CBD -0.80 ± 0.04; epileptic control -0.8 ± 0.04, CBD -0.8 ± 0.06. For all correlations, df = 90, $p < 0.0001$ in all cases. A two-way ANOVA on individual correlations found no effect of either epilepsy, $F(1, 12) = 0.0437$, $P = 0.8379$, or CBD, $F(1, 12) = 0.001381$, $P = 0.9710$.

These r values indicate moderately strong linear correlation between detected adenosine concentration and concurrent normalised field potential slope, with peak adenosine concentration corresponding with maximal synaptic inhibition.

Following this correlation analysis, linear regressions were performed to assess the rates at which the measures change with respect to one another, by assessing the slopes of the linear regressions (Figure 3-11C, D, F).

Regressing the normalised field potential against the measured change in adenosine concentration in healthy (Figure 3-11C) and epileptic hippocampal slices (Figure 3-11D) demonstrated a shallower slope in epileptic tissue in comparison to healthy (healthy control: -3.2 ± 0.6; epileptic control: -1.8 ± 0.2). This suggests that there is a decrease in the rate of change of field potential inhibition in comparison to increasing measured adenosine concentration. Application of CBD increased the regression slope in epileptic hippocampal slices but not in healthy (healthy CBD: -4.9 ± 1.4, n = 6; epileptic CBD: -4.5 ± 0.6, n = 8).

A two-way repeated measures ANOVA of the individual linear regressions of each experiment found a significant variation due to CBD ($F(1, 12) = 15.54$, $P = 0.0020$) but not due to epilepsy ($F(1, 12) = 0.8933$, $P = 0.3632$). There was no significant interaction ($F(1, 12) = 0.7916$, $P = 0.3911$), but a significant effect of subject matching ($F(12, 12) = 2.754$, $P = 0.0460$). Sidak's post-hoc multiple comparisons test identified significance in the difference between control and CBD values in epileptic hippocampal slices (adjusted $p = 0.0062$). This suggests that the significant variation caused by CBD is isolated to epileptic hippocampal slices and not seen in healthy.

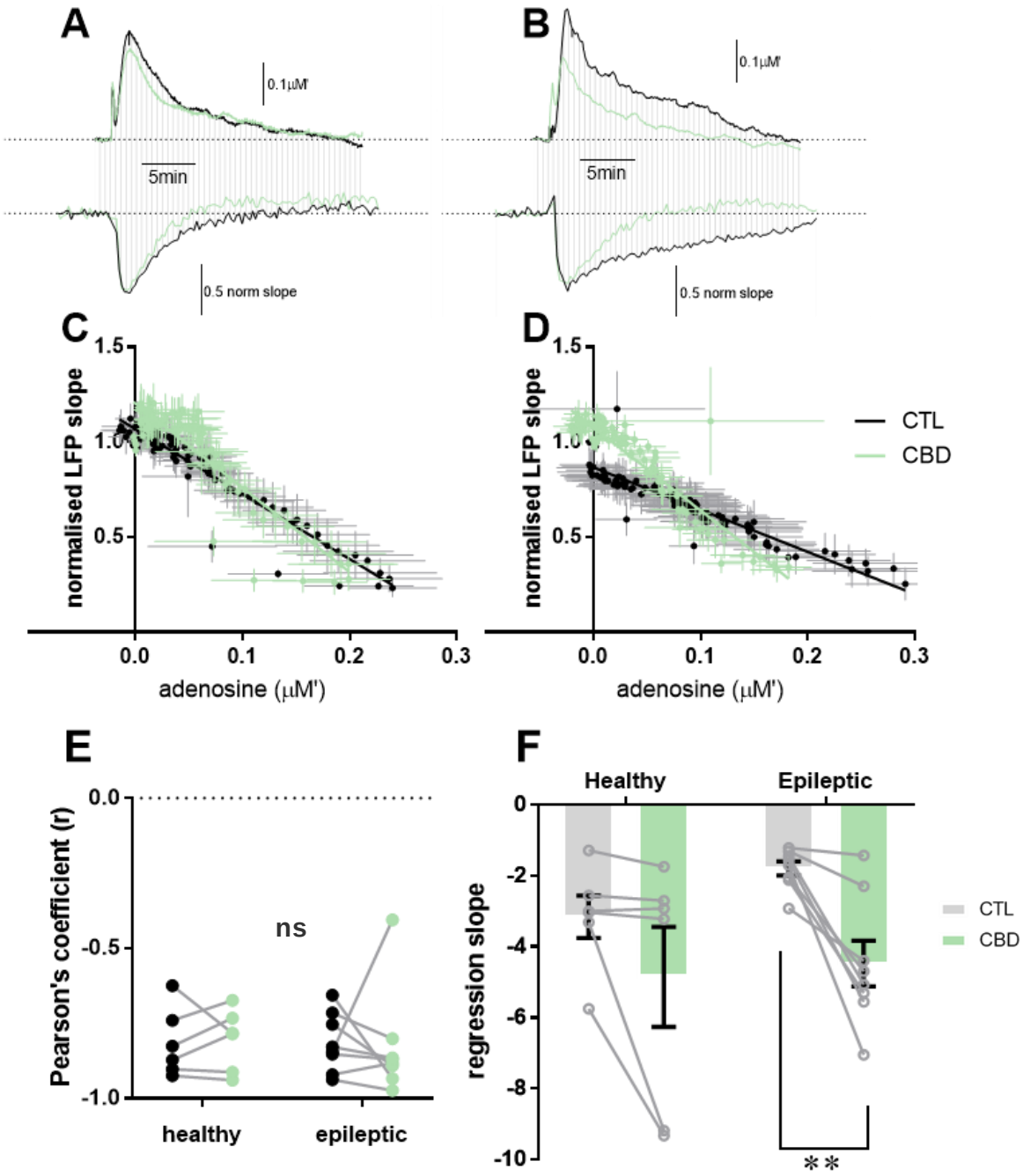

Figure 3-11: Correlating and regressing biosensor-measured adenosine concentration with field potential inhibition. A: Mean traces from sensor (top) and field potential (bottom) recordings in healthy hippocampi (n = 6, 5 animals), represented previously in Figure 3-9 and Figure 3-10. Vertical lines indicate time-matching of sensors and fields. **B:** Mean traces from sensors and field potentials in epileptic tissue (n = 8, 5 animals), demonstrating time-matching of correlations and regressions. **C:** Representative linear regression of control and CBD experiments in healthy hippocampi. Points and error bars represent mean ± SEM for original sensor and field recordings. Slope of mean overall control conditions is -3.4 and for CBD -4.4. **D:** Linear regressions of control and CBD traces in epileptic hippocampi. Slope of regression of mean traces in control conditions is -2.2 and in CBD -4.4. **E:** Pearson's product-moment correlation coefficients for each experimental recording, no significant difference (two-way ANOVA). **F:** Comparison of the slopes from regressions of individual experiments,

showing significant effect of CBD application (**: P < 0.01, two-way repeated measures ANOVA with Sidak's post-hoc tests). Error bars show mean ± SEM.

3.7. Discussion

3.7.1. Basal adenosine concentration between healthy and epileptic tissue

The estimated value in this study of basal hippocampal adenosine concentration in control animals of 0.2 ± 0.03 µM' corresponds with previous reports using similar techniques with biosensors. The first of these was a study using mice hippocampal slices that reported basal values of 0.13 ± 0.08 µM (Diogenes et al., 2014). Another study using basal forebrain slices rather than hippocampal in mice and rats reported higher but similar cross-species basal adenosine tone values (0.46 ± 0.17 µM and 0.56 ± 0.15 µM respectively) (Sims et al., 2013).

This study did not detect any difference in basal adenosine tone between control and epileptic animals, and both conditions show wide variability over a similar range of values. This is reflected in other studies using biosensors to predict tone, with Diogenes et al. (2014) observing a tendency for mice deficient in ADK to have increased basal adenosine (0.43 ± 0.16 µM') as compared to wildtype (0.17 ± 0.03 µM'), but with no significant difference due to the variability between slices. Lower levels of basal adenosine tone in the chronic epileptic hippocampus would correspond with the ADK hypothesis in decreasing basal inhibitory adenosine tone, and has been seen *in vivo* in microdialysis experiments on rats following chronic pilocarpine induction (Dona et al., 2016). However, a difference may not be detectable using our *in vitro* preparation for a number of reasons, for example: (a) factors related to the non-physiological condition necessitated by preparation of slices, which lack much of the cellular and synaptic architecture seen *in vivo*; (b) being perfused with a steady flow of aCSF, which may permit the wash of purine release to some degree; and (c) the ionic environment differs inside and outside a slice, which in this study we have been unable to control for and may affect the sensor recording (Frenguelli and Wall, 2016). Another major factor is that the low concentration of adenosine being measured lies very much on the lower end of the linear range detectable by the sensors (0.1 µM – 20 µM, shown in Figure 3-3, which therefore removes some confidence from the recorded values.

3.7.2. No effect of CBD/CBDV application on basal adenosine concentration

We applied 10 µM of CBD and CBDV for 30 min in each set of experiments, a concentration and period of time which have in previous electrophysiology experiments been shown to have significant anticonvulsant effect in decreasing epileptiform LFP burst amplitude and duration (Jones et al., 2010).

Based upon the hypothesis that CBD binds to ENT1, we would potentially expect to see a similar effect to inhibiting the transporter. Modulation of adenosine has previously been reported *in vitro*. A previous

study applied both NBTI and dipyridamole, blockers of the adenosine transporter ENT1 to a slice exhibiting spontaneous activity from nominally magnesium-free aCSF, resulting in a small rise of adenosine and creating significant enough inhibition to reduce amplitude of concurrent field potential recordings (Etherington et al., 2009) – however, these hippocampal slices were not quiescent as in this study. Despite not seeing a direct effect of CBD or CBDV upon our adenosine baseline as seen with NBTI and dipyridamole, this does not necessarily show that the cannabinoids do not bind to the ENT1 transporter, as there is likely a difference in affinity between CBD/CBDV and the specific ENT inhibitors. However, this suggests that in basal, quiescent conditions, CBD is unlikely to modulate adenosine levels within acute application windows previously shown to be therapeutic in bursting slices.

Therefore, the next step was to assess activity-related adenosine release, such as that seen in seizure situations. Rather than inducing spontaneous activity using pharmacological agents, or increasing potassium or reducing magnesium in aCSF we chose to use a model based upon electrical stimulation. An electrical stimulation train or burst protocol to the Schaffer collateral fibres as has been previously shown to induce adenosine release in a reliable manner (Wall and Dale, 2013; Diogenes et al., 2014), which would allow direct comparisons between release waveforms in each slice before and after CBD application.

It should be noted that adenosine release is consistently seen upon insertion of sensors into the slice, necessitating the up to hour-long equilibration period for the sensor current trace to return to "normal". It was chosen not the measure this release or compare between healthy and epileptic, or in the presence of CBD, for a variety of reasons. Primarily, the release of adenosine upon the damage caused by insertion of sensors is not a physiological model for epilepsy or seizures. Also, there are a variety of factors which cannot be controlled when measuring damage-induced adenosine release, such as the speed and/or force of insertion, the number of fibres damaged based upon orientation of the slice, the difference in time lapse between insertion of first and second sensor, and other mechanical variables which may influence damage-induced adenosine rise. Therefore, a more controlled method of adenosine release was sought.

3.7.3. Adenosine release following stimulation

Although previous studies using biosensors have employed concurrent field measurements, this marks the first study in our awareness using multielectrode arrays. While there are wide-ranging potential study protocols which could be employed with this experimental set-up, such as inducing spontaneous ictal activity and recording adenosine release from different compartments of the hippocampus while monitoring the movement of activity across the pathways, the objective of this study was to assess the variables of adenosine release and network excitability under controlled, timed conditions.

We adapted an adenosine-evoking stimulation protocol from Wall and Dale (2013) for detecting adenosine release using enzymatic biosensors. Key differences arise from our use of a planar multielectrode array, allowing for multiple points of stimulation or recording of field potentials without the necessity of inserting an additional stimulation electrode and the associated damage to cells and fibres. However, this planar array of much smaller electrodes, which are estimated to have a recording radius of ~1 – 200 µm, are likely to only detect electrophysiological changes in the bottom 25 – 50% of the 400 µm slice, and so it is more difficult to ensure that the biosensor tip (500 mm × 50 µm) lies within an adequate radius allowing for detection of adenosine release, especially considering the estimated distance of adenosine diffusion being undetectable by 300 µm from release source (Wall and Richardson, 2015). This necessitated the use of a more intense stimulation protocol than described by Wall & Dale (300-stimuli train as opposed to 100-stimuli train at 20 Hz), as well as the selection of multiple electrodes on the array, thereby stimulating the entirety of the hippocampal CA1 *stratum radiatum* region of Schaffer collateral fibres. This could be described as a more physiological representation of seizure activity, with activity being stimulated across the *stratum radiatum* and activating Schaffer collaterals. These changes in protocol may account for some differences in adenosine release observations between this study and the previous study of Wall and Dale, for instance our slower waveform decay (adenosine levels return to baseline within around 5 min in the previous study, compared to around 20 min in our study, and control decay time constants τ have previously been reported in WT animals in the 100 – 200 s range (Wall and Dale, 2013; Hughes et al., 2018), whereas τ in healthy rats in this study averaged at 5.8 min [approx. 350 s]).

Although no significance was found between healthy and epileptic waveform decays, partly due to the wide range in error of the epileptic recordings (as well as 3 pairs of recordings not being able to be included in the comparison), the fact of the regular, relatively small decay constants in healthy hippocampi compared to the much less regular, stochastic waveform shape of the epileptic hippocampi is indicative of dysregulation in the adenosine release and reuptake system in chronic epilepsy.

3.7.4. CBD-mediated decrease of stimulation-evoked adenosine release in epileptic hippocampus

This chapter demonstrates that application of CBD to epileptic hippocampal slices reduces adenosine peak concentration following electrical stimulation to Schaffer collateral fibres. The decrease in peak adenosine release is seen in epileptic slices but not in healthy, suggesting that the adenosine release dynamic is modified between healthy and epileptic hippocampus.

While this observed decrease in adenosine release appears to contradict the previous theory, that CBD inhibition of ENT1 mediates an increase in extracellular adenosine by inhibiting glia-based reuptake, this observed decrease is consistent with previous *in vitro* studies which have demonstrated that blockade

of ENT1 decreases adenosine release following increased neuronal activity (Lovatt et al., 2012; Wall and Dale, 2013). This suggests that the observed decrease of adenosine may in part be due to inhibition of neuronal ENT1 by CBD, as has been previously reported (Carrier et al., 2006; Liou et al., 2008; Pandolfo et al., 2011). However, further robust experiments would be required to demonstrate causality between CBD application and the decrease in adenosine, for instance through the use of ENT1 inhibitors to indicate whether the actions of CBD in this assay are consistent with ENT1 blockade. Additionally, other experiments using epileptic tissue following chronic treatment with CBD may provide further information on any longer-term effects due to chronic CBD treatment.

3.7.5. Change in adenosine relationship with field potentials

The primary finding from this chapter lies in the change in linear regression slope in epileptic slices following CBD application. Firstly, it is important to note that correlations, by their nature, do not necessarily take into account causation or even direction of dependent/independent variables. Therefore, although we do see a strong linear relationship between recorded adenosine concentration and the concurrent normalised size of field potential response with the Pearson's correlation, these are two dependent variables with we have seen move together but cannot attribute causation.

However, with linear regression slopes, we can assess the rate of change between the two measures, and whether this is affected. If we saw no change in the regression slopes, this would indicate that adenosine concentration and field potentials changed together at the same rate regardless of epilepsy or treatment – suggesting that any change in adenosine release would be reflected in field potentials changing in the same way. The fact that we do see a change in regression slopes due to both epilepsy and CBD treatment suggests that either epilepsy or CBD are changing the relationship between extracellular adenosine and field potentials, or a different mechanism is changing them both differently. The lack of change in Pearson's coefficients between the experimental groups is an indication that any effect of epilepsy or CBD on the regression slopes is not due to a 'weaker' correlation between adenosine concentration and field potential inhibition.

Following from this finding, two possibilities may underlie the change in linear regression slope. One possibility would be that the correlations seen are entirely co-incidental rather than causative. However, another possibility is that there is some degree of causation between adenosine concentration and degree of field potential inhibition. This would suggest that in epileptic tissue, the ability of adenosine to induce network inhibition is decreased – reflected in the more negative slope – and CBD modulates this to the adenosine potency seen in healthy tissue. This in turn suggests that the ability of adenosine to induce inhibition through A_1 receptors is diminished in epilepsy, potentially due to a decreased expression of inhibitory A_1 receptors, and/or an increased expression of excitatory A_{2A} receptors. Additionally, still

assuming an entirely causative relationship, CBD would be modulating adenosine potency by interacting with a cellular or molecular mechanism dysregulated in epilepsy, explaining why the decrease in adenosine potency regression slope is only seen in epileptic slices. This dysfunctional mechanism could be the same as that causing an overall decreased adenosine potency in epilepsy, e.g. potentiating under-expressed inhibitory A_1 receptors, or it could be increasing adenosine potency through a different mechanism.

The second possibility could partially explain the implications of CBD, a known anticonvulsant *in vitro*, *in vivo*, and in clinical trials, decreasing activity-related adenosine release. Although adenosine is referred to as an 'endogenous anticonvulsant', previous literature has suggested a dysregulation in the balance of inhibitory/excitatory adenosine receptors in chronic epilepsy, and therefore seizure-associated adenosine release could potentially have a less beneficial, protective effect than it would when released in an otherwise healthy brain. This putative epilepsy-related adenosine receptor dysfunction is further investigated in Chapter 4.

3.7.6. Limitations of techniques used in this chapter

The major limitation of the studies in this chapter are the lack of robust, inter-slice positive and negative controls. Within-slice controls were chosen (i.e., comparing effects prior to and following application of CBD) for economical and resource reasons; especially for epileptic rats, the principles of NC3Rs as well as time and manpower investment to run multiple inductions led us to design within-slice controls. However, a more robust experimental design would see stimulations in the presence of vehicle only, with unpaired comparisons made between recordings in vehicle only and recordings in CBD. Positive control experiments would also see the use of stimulations performed with an ENT1 antagonist, such as NBTI/dipyridamole, to compare with the activity of CBD.

Additionally, although an attempt was made at quantifying the loss of biosensor sensitivity throughout the course of an experiment, it remains unknown whether sensitivity to adenosine is changed. While this may confound some results, the finding that 10 µM CBD in 0.01% ethanol decreases evoked adenosine release in epileptic tissue remains valid due to the comparisons against healthy tissue. As noted above, vehicle-only experiments were not performed and so effect of vehicle cannot be ruled out; the concentration of vehicle used (0.01% ethanol) is consistent with a molarity of 1.7 mM. While this is lower than concentrations of ethanol used in other studies (e.g., 50 mM and 10 mM, (Hughes et al., 2018)), activity at ENT1 may be possible at this low concentration.

A future experiment to further elucidate the correlation between the adenosine release waveform and concurrent field potential inhibition would be using an A_1R inhibitor during the stimulations. While 2 initial experiments were carried out in the presence of DPCPX, these were discontinued due to doubts

about the reliability of the batches of DPCPX purchased (see Appendix 8.2.1). However, a correlation between adenosine release and concurrent field potential inhibition would prove useful to assess how much of the field potential inhibition was due to activity at A_1R, and how much was due to contribution of other short-term synaptic depression mechanisms in the hippocampus. Additionally, previous studies reporting an increase in adenosine release in the presence of 8-CPT (Etherington et al., 2009), expected correlations would be expected to be at a much shallower gradient.

We have used a method of concurrently detecting endogenous adenosine concentration released from hippocampal slices along with field potential inhibition using a planar MEA system. This has an advantage of decreasing the number of relatively large electrodes being inserted into a slice and damaging fibres (thereby release damage-associated adenosine); however this experimental set-up does introduce a vertical component. With electrodes recording and stimulating from the bottom of the slice and biosensors inserted from the top of the slice, it could be difficult to ascertain the exact distance between the electrode recording LFPs and where the sensor was recording adenosine release. This was attempted to be controlled through using Pythagorean trigonometry to ensure that the angle at which the sensor entered the slice would maximise the surface area of the sensor tip inserted within the slice, with the tip ideally penetrating the entire 400 µM depth of the slice.

Use of the planar array also introduced uncertainty in other factors; as the inverted image of the slice placement on the electrodes was taken prior to inserting the MEA into the headstage, slight movement of the hippocampus was possible. Similarly, as the sensors were inserted manually using micromanipulators, there was also the possibility that this introduced small movements of the slice on the MEA. All these potential factors influencing the placement of the hippocampus on the electrodes could decrease some confidence in the electrodes chosen for stimulation. However, this was controlled for by choosing multiple stimulation electrodes in the region of CA1 based upon image taken prior to loading in the headstage, and assessing that evoked field potentials are consistent with Schaffer collateral stimulation. Additionally, a bright light setting under the microscope was occasionally able to show that hippocampus had not shifted significantly from the initial image; some images were also taken following removal from headstage after experiments to confirm this.

3.7.7. Conclusion

In summary, this chapter has demonstrated that the theory that the antiepileptic action of CBD is due to its inhibition of adenosine reuptake does not appear to be entirely accurate or complete. While basal concentrations of adenosine might not have been detectable through the current assay, the decrease of stimulation-induced adenosine following CBD application implies that both CBD antiepileptic mechanisms of action, and the function of adenosine in chronic epileptic hippocampus, are both more

complicated than initially thought. Based upon these findings, chapter 4 will investigate the putative epilepsy-related adenosine receptor dysfunction possibly seen in this chapter, and chapter 5 will further investigate CBD activity at ENT1, including whether dysregulation of ENT1 may underlie the difference observed between healthy and epileptic slices.

4. Results Chapter 2: Characterisation of Adenosine Receptors in Epilepsy

4.1. Introduction

Adenosine is known as an endogenous anticonvulsant, however the two receptors to which adenosine binds with the highest affinity, the A_1R and $A_{2A}R$, have opposing effects upon cAMP and therefore neuronal excitability. Various studies in humans and animals have suggested an interaction between seizures and epilepsy with a pathophysiological imbalance between the inhibitory A_1R and $A_{2A}R$.

4.1.1. A_1 receptors

4.1.1.1. Inhibition and neuroprotection

Early studies with various adenosine receptor agonists showed that the anticonvulsant effect of adenosine arises from the activation of adenosine receptors (Franklin et al., 1989; Zhang et al., 1994). Further, experiments with prophylactic treatment of adenosine receptor agonists with varying degrees of affinity for A_1 and A_2 (prior to the discovery of separate A_{2A} and A_{2B} receptors) injected to the prepiriform cortex of rats concluded that A_1R-activation, rather than A_2R-activation, was responsible for the anticonvulsant effect seen in subsequent bicuculline-induced seizures (Franklin et al., 1989; Zhang et al., 1994). This has also been shown in the kainic acid (KA) mouse model of pharmacoresistant chronic epilepsy, with the intraperitoneally-given specific A_1R agonist CCPA capable of controlling seizure activity in the chronic phase as opposed to vehicle and carbamazepine treated mice (Gouder et al., 2003). The protective effect of A_1R-activation is also observed in PTZ-induced seizures in adult zebrafish (Siebel et al., 2015).

Genetic ablation of A_1Rs has also demonstrated their role in seizure neuroprotection, with both homozygous and heterozygous A_1R knockout (KO) mice exhibiting spontaneous non-convulsive CA3 seizures (Li et al., 2007a). Furthermore, A_1Rs are implicated in maintaining seizure focus, with a unilateral hippocampal KA injection in A_1R KO mice causing lethal SE with immediate contralateral hippocampal cell loss, comparable to the cell loss seen in wildtype (WT) mice several weeks post KA injection, in the chronic stage of epilepsy (Fedele et al., 2006). Severe to fatal SE was also seen in A_1R KO mice following controlled cortical impact (Kochanek et al., 2006).

In vitro experiments using rat hippocampal slices and the Mg^{2+}-free model of epileptiform activity demonstrated that antagonism of A_1Rs reduced basal inhibitory tone and increased the susceptibility and duration of seizure activity (Etherington and Frenguelli, 2004). Human tissue has also been studied *in vitro*, using neocortical slices from treatment-resistant epilepsy patients who had undergone resection surgery. These showed that potassium and bicuculline-induced seizure-like events, which displayed

resistance to high doses of the known AED carbamazepine, were completely suppressed by the specific A_1R agonist SDZ WAG 994 (Klaft et al., 2016).

4.1.1.2. Decreased expression of A_1R in epilepsy

Decreased A_1R protein expression has been seen in human chronic epilepsy; resected temporal lobe tissue from human TLE patients showed decreased binding to [3H]CHA compared to tissue obtained from non-epileptic autopsies (Glass et al., 1996), indicating that chronic TLE leads to a decreased expression of inhibitory A_1R in epileptogenic zones. It has also been seen in animal models immediately following SE that, although overall A_1R expression does not appear to be immediately downregulated, there is an effect of acute A_1R desensitisation (Hamil et al., 2012). These studies combined show the downregulation of expression and activity of A_1R due to seizures and epilepsy, indicating a decrease in protective effect of adenosine possibly immediately following a seizure and, crucially, in the longer-term chronic epileptic state. This decrease of A_1R may also contribute to the previously described acceleration and spread of hippocampal cell loss seen in A_1R KO mice (Fedele et al., 2006).

However, a study on a rare encephalitis with a pharmacoresistant focal seizure phenotype has also demonstrated an increase in neuronal A_1R expression, with the authors suggesting that overexpressed A_1Rs are responsible for preventing seizure spread and maintaining the focus (Luan et al., 2017). This indicates that A_1R overexpression may also be associated with a pathology, although whether this has a causative effect on the syndrome is unknown.

4.1.2. A_{2A} receptors

4.1.2.1. Proconvulsant activity

$A_{2A}Rs$ are less prevalent in the brain than the more widely-distributed A_1Rs with a predominantly striatal expression (Dixon et al., 1996), and their role in epilepsy is also less well defined. The literature has generally shown a proconvulsive effect of $A_{2A}R$ activation, although some studies have suggested either a protective effect or no effect – in a model of audiogenic seizures in genetically epilepsy-prone rats, $A_{2A}R$ agonism had comparable protective efficacy with A_1R agonism (Huber et al., 2002), and in adult zebrafish neither $A_{2A}R$ activation nor antagonism appeared to have any effect on PTZ-induced seizures (Siebel et al., 2015). Despite this, most seizure studies suggest that pharmacological $A_{2A}R$ blockade is protective in acute models of seizure or SE (Zeraati et al., 2006; Rosim et al., 2011). A review on the interplay between $A_{2A}R$ and Tropomyosin receptor kinase B (TrkB) receptors has suggested that epileptic neurotrophic dysfunction may underlie the discrepancy between anticonvulsive and proconvulsive effects of $A_{2A}R$-activation (Sebastiao and Ribeiro, 2009), although this has not been further investigated.

However, it has been shown that although both A_1R agonism and $A_{2A}R$ antagonism were protective against pilocarpine-induced seizures, rats treated with only the $A_{2A}R$ antagonist were liable to hippocampal and piriform cortex neurodegeneration comparable to untreated rats, whereas A_1R agonism appeared to mediate neuroprotection (Rosim et al., 2011).

The proconvulsant effects of $A_{2A}R$ activation have also been demonstrated in transgenic models. Global $A_{2A}R$ knockout mice, although not protected from electroshock seizures, are less susceptible to PTZ or pilocarpine-induced-seizures with the seizures themselves being less severe than in wildtype mice. PTZ kindling seizures were also reduced, indicating a role for $A_{2A}Rs$ in seizure generation and also development of the chronic kindling model of epilepsy (El Yacoubi et al., 2009).

In the general literature outside of epilepsy, $A_{2A}R$ activity has been implicated in a variety of seemingly opposing actions, such as inducing both neurotoxicity and activation of neurotrophic factors (Sebastiao and Ribeiro, 2009). Blockade of $A_{2A}Rs$ has been linked to neuroprotective functions in ischaemia, Alzheimer's disease, and Parkinson's disease (Chen et al., 1999; Chen et al., 2001; Matos et al., 2012a), with a body of evidence across models of different epilepsies also supporting a proconvulsant profile for $A_{2A}R$ activation. Activation of $A_{2A}Rs$ by bilateral hippocampal infusion of agonist CGS21680 prolonged the after discharge duration of piriform cortex kindled seizures, an effect reversed when an $A_{2A}R$-antagonist (ZM241385) was also prophylactically administered (Zeraati et al., 2006). The same study again found A_1R-activation to be neuroprotective (Zeraati et al., 2006). Similar findings were observed in a study using the pilocarpine model of TLE, with intraperitoneal pretreatment with an A_1R agonist or an $A_{2A}R$ antagonist decreasing the occurrence of SE and mortality immediately following intraperitoneal pilocarpine administration (Rosim et al., 2011). However, in terms of cellular neuroprotection, the same study found that rats treated only with the $A_{2A}R$ antagonist were liable to cellular neurodegeneration to the same degree found in rats treated only with pilocarpine, as opposed to the neuroprotective effect of the A_1R agonist, indicating that cellular protection is mediated primarily through A_1R action.

Use of *in vitro* rat hippocampal slices has demonstrated that antagonism of $A_{2A}Rs$, in comparison with A_1R antagonism, has no effect on basal adenosine tone, but significantly shortened the duration of epileptiform activity induced by Mg^{2+}-free aCSF (Etherington and Frenguelli, 2004). A more recent study using *in vitro* mouse hippocampal slices concluded that activation of $A_{2A}R$ in Schaffer collateral synapses in CA1 increased glutamatergic excitation, while also selectively enhancing interneuron-interneuron synaptic connections, leading to a reduction in inhibition and effectively further potentiating the CA1 pyramidal cells (Rombo et al., 2015).

4.1.2.2. Dysregulation of$_{2A}$R in epilepsy

In addition to the decrease in expression and sensitivity of A_1Rs in seizure and epilepsy, described above in section 4.1.1, several studies have shown a concurrent upregulation of A_{2A}R in chronic epilepsy (Rebola et al., 2005; Barros-Barbosa et al., 2016). Although these receptors show a reduced pattern of expression in the brain compared to A_1R, radioligand binding has shown a threefold increase in A_{2A}R binding in cortical membranes of rats, 4 weeks after either amygdala kindling or kainate-induced seizures (Rebola 2005). The same study showed a concurrent decrease in A_1R binding density. Importantly, this suggests a decrease in endogenous seizure control mechanisms while increasing neuronal excitability through A_{2A}Rs, indicating that adenosine release in a seizure may no longer be as protective in chronic epilepsy. Corroborating this radioligand binding study, it has been shown by Western blot in human hippocampal synaptosomes resected from patients with mTLE that expression of A_{2A}R is threefold higher than in hippocampal tissue from non-epileptic cadavers (Barros-Barbosa et al., 2016). This study also demonstrated that immunofluorescence-labelling with specific A_{2A}R antibodies co-localised strongly with astrocyte marker GFAP-positive cells across the hippocampus, and significantly more so in mTLE hippocampi than control. There was less overlap with neuronal markers synaptotagmin 1/2 and NF200, indicating a stronger expression of A_{2A}R on astrocytes than neurons.

A_{2A}R upregulation has also been implicated in absence epilepsy, with Wistar Albino Glaxo/Rijswijk (WAG/Rij) rats, a model of human absence epilepsy, showing lower A_{2A}R expression than control animals at presymptomatic stages, but a 3-fold increase in A_{2A}R expression density when the rats became epileptic (D'alimonte et al., 2009). It has also been suggested from the same model that while lower doses of the purine guanosine decrease incidences of 'absence seizure' spike-wave discharge (SWD), high doses of guanosine increase SWD incidence, potentially through A_{2A}R activation (Lakatos et al., 2016).

In humans, a genetic polymorphism in the A_{2A}R gene has been linked to acute encephalopathy with biphasic seizures and late reduced diffusion (AESD) in children, with up to 80% of examined patients displaying this polymorphism. It is thought that the variant leads to excessive downstream activation of A_{2A}Rs, causing excitotoxic neural damage (Shinohara et al., 2013).

Despite a degree of conflicting findings regarding how A_{2A}Rs contribute to epilepsy, in overall conclusion, it would appear that the majority of evidence currently supports the initial intuitive concept that A_{2A}R-activation has a proconvulsive action (Boison, 2016a).

4.1.3. Chapter Aims

CBD was shown to decrease seizure-induced adenosine release, possibly due to ENT1 inhibition (discussed in section 1.4). Therefore, the working hypothesis was that the reported imbalance of

adenosine receptors (described above in section 4.1) is enough that an adenosine surge in an epileptic hippocampus may no longer be protective and contributes to epilepsy pathology. In order to test this hypothesis, the change of adenosine receptor balance in hippocampus in this RISE-SRS chronic epileptic model was investigated at expressional (transcript and protein) and functional levels using qPCR, radioligand binding and MEA electrophysiology.

Chapter 3 demonstrated that CBD modulates the potency of endogenously-released adenosine following stimulation in epileptic hippocampal slices. This chapter will therefore assess whether this can be replicated with exogenously applied known concentrations of adenosine by generating concentration-response curves of adenosine concentration against LFP inhibition. This removes the variability of adenosine concentration from biosensors and assesses instead effects of known concentrations of adenosine as an independent variable. Additionally, the contribution of each adenosine receptor towards both basal network activity as well as response to exogenous adenosine will be assessed via application of specific A_1R or $A_{2A}R$ antagonists.

4.2. Methods and Data Analysis

4.2.1. Chronic CBD treatment of epileptic animals

As detailed in section 2.3.1 and (Patra et al., 2019), male Wistar rats were assigned into three groups at between 4 – 8 weeks following RISE-SRS induction if confirmed epileptic, along with healthy age-matched controls. These groups were: healthy vehicle-treated (HV), epileptic vehicle-treated (EV), and epileptic CBD-treated (ET), where vehicle was 3.5% Kolliphor in water, with CBD dissolved in vehicle and administered orally via *ad libitum* water daily over 10 weeks. At 16 weeks post-induction (20 weeks old) these rats were sacrificed and brains dissected, with hippocampal tissue frozen at -80ºC until used for molecular analysis here.

4.2.2. RT-qPCR determination of gene expression

Gene expression analysis was performed on hippocampi extracted from 5 experimental groups. These were the 3 chronically treated groups described above (4.2.1), as well as untreated age-matched healthy (H) and epileptic (E) rats dissected specifically for this study. Dissection methods are described in section 2.3.1, and PCR primers were designed as described in section 2.3.2 and summarised in Table 2-7. The primers used here were as follows:

A_1R (*Adora1*) forward GAGCTCCATTCTGGCTCTGC, reverse GCTGGGTCACCACTGTCTTG; $A_{2A}R$ (*Adora2a*) forward CTATCGCCATCGACCGCTAC, reverse AGCCATTGTACCGGAGTGGA; GAPDH (*Gapdh*) forward GAAGCTCATTTCCTGGTATGACAA,
reverse ATGTAGGCCATGAGGTCCAC.

The gene expression ratios of both receptors were calculated using the Pfaffl equation (Pfaffl, 2001), using an amplification factor calculated for each primer set to compare ΔC_T values of each sample against a control sample (equations detailed in section 2.3.2.3).

4.2.3. Radioligand binding data analysis

Raw binding data was provided by Eurofins following study completion and described in detail in Appendix 8.3, section 8.3.1. Briefly, 4 independent binding experiments were carried out using tritiated CCPA ([^{3}H]-CCPA) on either healthy or epileptic hippocampal membranes. Each experiment included 12 doses of [^{3}H]-CCPA between 0 – 7.73 nM, for a total of 35 doses spread across the range.

Non-specific binding was determined for each concentration in the presence of 10 µM CPA, with specific binding determined through subtracting non-specific signal from total counts per minute (cpm). Healthy and epileptic datasets were fit using the Graphpad Prism nonlinear regression 'Binding – Saturation, One site – Specific binding' function, from which B_{MAX} and K_D parameters (including error) were generated.

4.2.4. Adenosine-induced field potential inhibition

4.2.4.1. Multielectrode array paired pulse stimulation protocols

As previously described in sections 2.2 and 3.2.2.1, hippocampal slices were dissected from either RISE-SRS confirmed epileptic Wistar rats, or age-matched healthy controls. Following at least 1hr equilibration time following slicing, and at least 10 min after placement onto an MEA and loading into the headstage, Schaffer collateral LFPs were evoked by delivering biphasic stimulation (100 µs steps, ± 0.5–2 V amplitude) through a single electrode. Stimulation intensity was chosen for each slice based upon an initial input-output curve generated at 100 mV steps between 0–2 V, with the stimulation intensity for LFPs chosen to be approximately 50% – 60% of maximal possible LFP amplitude. This submaximal response was chosen as the stimulation software used allowed a maximum stimulation of 2 V, at which a plateau in response was rarely seen (discussed further below in section 4.4.1.2).

In this study, paired pulse LFPs were evoked every 30 s. LFPs were recorded in all 60 channels, with the LFP recording window from 100 ms prior to the stimulation trigger, until 1 s following trigger, resulting in a 1100 ms recording video around each set of paired pulse LFPs. LFP slopes were monitored online and analysed at 10 – 90% of the linear downward deflection, using the inbuilt analysis function of MC Rack (Multi Channel Systems GmbH). Paired pulses were set at a 50 ms interval throughout the duration of each protocol, except during paired pulse profiles as indicated in the experimental protocol in Table 4-3.

4.2.4.2. Paired pulse profiles

Paired pulse profiles (PPPs) were run following a 10 min baseline, following vehicle/drug application, and at every other adenosine concentration. For these PPPs, 9 sets of paired pulse stimulations were applied every 30 s, resulting in a 4 min 30 s PPP protocol. The PPIs used are described in Table 4-1 below; the log-based intervals allow for clear analysis and presentation of paired pulse ratios (PPRs) at lower time intervals (for instance as used by Booth et al. (2014)).

PP stim #	PPI (ms)
1	10
2	17
3	32
4	56
5	100
6	169
7	318
8	557
9	995

Table 4-1: Paired pulse profile stimulation intervals.

4.2.4.3. Drug application

The experimental protocol is described below in Table 4-3, with all drugs/vehicle and adenosine concentrations applied by perfusion with aCSF. Adenosine was freshly made prior to application for each slice to 10 mM in carboxygenated aCSF, and further diluted in aCSF to the concentrations described in Table 4-3 directly prior to bath application. Drugs applied were CBD, the specific A_1R-antagonist 8-CPT, and the specific A_{2A}R antagonist SCH 58261, all dissolved in DMSO and frozen in aliquots at -20°C. All drug stocks were made to allow a final concentration detailed below in Table 4-2 when applied to match the vehicle concentration of 0.01% DMSO.

Drug	Source	Final concentration
CBD	GW Pharmaceuticals	10 μM
8-CPT	Sigma, UK	1 μM (Etherington and Frenguelli, 2004)
SCH 58261	Tocris, UK	100 nM (Rombo et al., 2015)

Table 4-2: Source and final concentrations of drugs used in this chapter.

Adenosine concentrations were applied for 10 min to allow an inhibition plateau to be reached, followed by at least a 10 min washout with adenosine free aCSF (containing vehicle/drug) to allow a return to baseline.

Perfusion solution	duration (min)	additional stimulation protocol
aCSF	10	paired pulse profile
drug/veh application	30	paired pulse profile
1 μM adenosine	10	
washout (drug/veh aCSF)	10	
3 μM adenosine	10	paired pulse profile
washout (drug/veh aCSF)	10	
10 μM adenosine	10	
washout (drug/veh aCSF)	10	
30 μM adenosine	10	paired pulse profile
washout (drug/veh aCSF)	10	
100 μM adenosine	10	
washout (drug/veh aCSF)	10	
300 μM adenosine	10	paired pulse profile
washout (drug/veh aCSF)	10 (or until baseline reached)	
500 μM adenosine	10	
washout (drug/veh aCSF)	10 (or until baseline reached)	

Table 4-3: Drug application protocol for exogenously applied adenosine-induced inhibition.

4.2.5. Statistical Analysis

Field potential slopes of each first pulse were averaged between 7 – 10 min following adenosine application, after inhibition plateau was reached, and baselined to the 3-min field potential 'baseline' prior to each application of adenosine. All second pulses of paired pulse stimulations, for ongoing standard 50 ms paired pulses, as well as for PPPs, were expressed as a ratio of each paired pulse's first stimulation.

Datasets were compared using student's t-tests or ANOVA tests with post-hoc multiple comparisons, as appropriate. All data are expressed as mean ± SEM. Adenosine concentration-response curves were compared using repeated measures two-way ANOVAs, with post-hoc family-wise comparisons within each adenosine concentration using Sidak's multiple comparisons tests. These were only analysed

between 1 – 300 µM, due to some datasets missing a 500 µM data point and therefore preventing repeated measures analysis. PPPs were compared using repeated measures two-way ANOVAs. The effect of each increasing adenosine concentration was compared against the pre-adenosine baseline at each PPI in family-wise comparisons using Dunnett's post-hoc tests.

Inhibition curves were fitted for all conditions using the nonlinear regression – dose response variable slope analysis in Graphpad Prism. Outputted variables were compared through two-way ANOVA tests with Sidak's multiple comparisons tests. IC_{50} values were reported, with statistical comparisons performed on $logIC_{50}$ values due to the asymmetric design of the selected doses.

4.3. Expression Differences of Adenosine Receptors in Epilepsy

Following from the observation of a post-stimulation change in LFP association with adenosine release in epileptic tissue compared with healthy (Chapter 3), the expression of adenosine receptors was investigated in age-matched healthy and confirmed epileptic rat hippocampus, dissected at 20 weeks of age. Isolated hippocampi were assessed using radioligand saturation membrane binding as well as transcriptional expression using RT-qPCR.

4.3.1. Transcription of A_1R and $A_{2A}R$ in epilepsy

To assess the expression of A_1R and $A_{2A}R$ at the transcription level, RT-qPCR was carried out on RNA isolated from the hippocampus of age-matched healthy and epileptic rats, as well as from chronically treated rats (healthy vehicle-treated rats, and epileptic vehicle and CBD-treated rats), all dissected at the same age. No significant difference at the transcriptional level was found across any of the groups for either A_1R (*Adora1:* mean relative expression ratios: H 0.96 ± 0.06, E 0.83 ± 0.10, HV 1.15 ± 0.12, EV 0.70 ± 0.19, ET 1.03 ± 0.04; one-way ANOVA $F(4, 18) = 2.132$, $P = 0.1187$) or $A_{2A}R$ (*Adora2a:* H 0.83 ± 0.13, E 0.82 ± 0.07, HV 1.17 ± 0.13, EV 0.81 ± 0.13, ET 1.17 ± 0.14; one-way ANOVA $F(4, 17) = 2.314$, $P = 0.0993$). The expression ratio of the positive control whole-brain RNA for A_1R was 2.88 as normalised to a control experimental sample, and for $A_{2A}R$ the whole-brain expression ratio was 53.7 (Figure 4-1).

The protein expression of A_1R and $A_{2A}R$ in healthy and epileptic hippocampi were also to be investigated by using Western blotting in conjunction with transcription levels. Antibodies were purchased and multiple attempts at refining a protocol to allow for clean and specific detection of the two receptors in hippocampal tissue lysates were run; however, these did not prove to be a feasible and analysable assay. This was likely due to difficulties in isolating the membrane-bound G-protein coupled receptors in tissue lysate, despite several lysis and membrane separation protocols used. Details are given in Appendix 8.2.2.

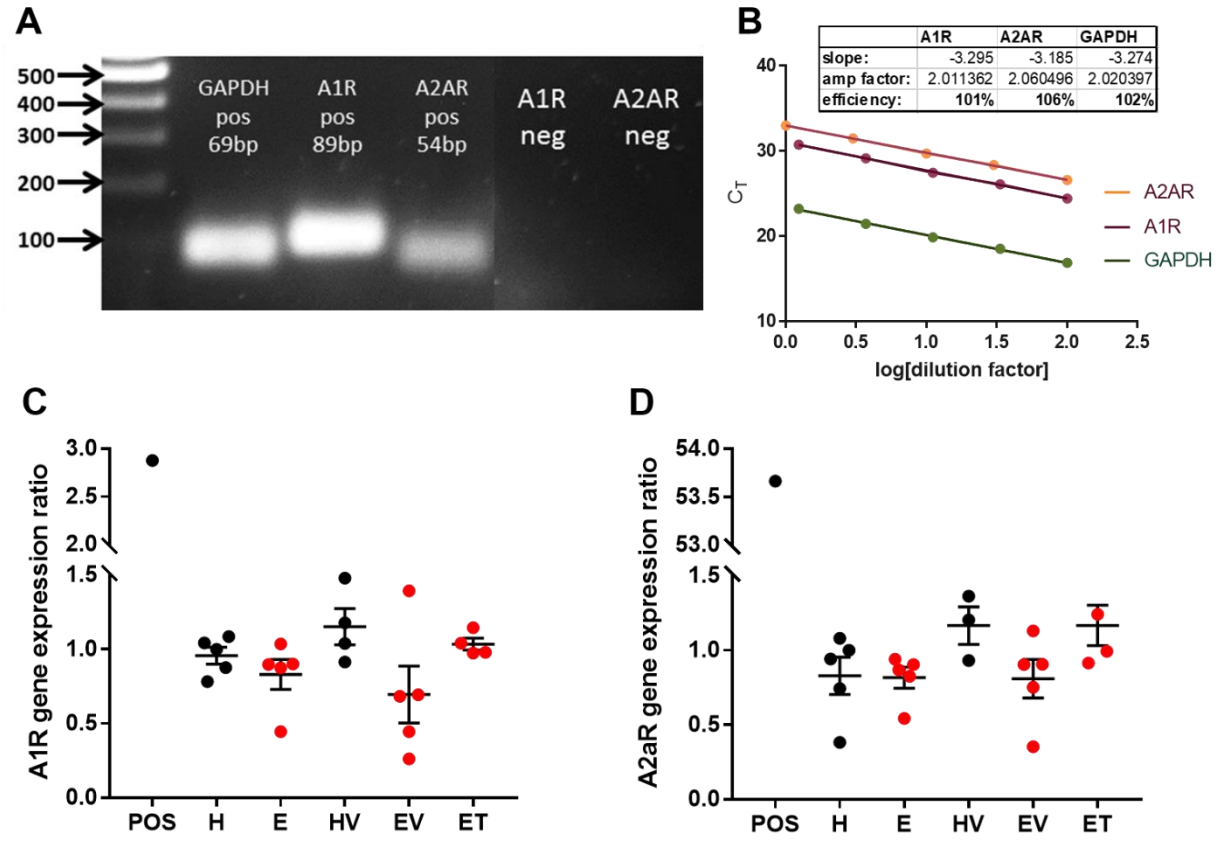

Figure 4-1: Gene expression of A_1R and $A_{2A}R$ in rat hippocampi is unchanged by epilepsy or chronic vehicle/CBD treatment. A: Representative end-product bands following RT-qPCR separated through 1.5% agarose gel electrophoresis. Positive control (pos) end products show single-band specificity corresponding to product base pair size as designed. Negative control (neg) show no amplification in water control reactions. **B:** Calculation of primer efficiency using serial dilution of cDNA. Inset: Efficiency calculations using slope from linear regression. **C:** Relative expression of A_1R in isolated hippocampi as well as commercial whole-brain RNA. No difference was found across the experimental groups. **D:** Relative expression of $A_{2A}R$ in experimental hippocampi and commercial positive control. No difference was found across the experimental groups. POS: Commercial whole-brain rat RNA; H: Healthy, untreated; E: Epileptic, untreated; HV: Healthy, vehicle-treated; EV: Epileptic, vehicle-treated; ET: Epileptic, CBD-treated. Error bars show SEM.

4.3.2. Radioligand B_{MAX} binding of A_1 receptors (Eurofins)

The A_1R-specific radiolabelled agonist [^{3}H]-CCPA was used to detect membrane-bound A_1R in isolated hippocampi. Attempted assays with [^{3}H]-SCH 58261 was not able to detect any specific binding on the same hippocampal membrane preparation. The maximum specific binding (B_{MAX}) found using saturated radioligand was significantly higher in healthy hippocampal membranes (83.8 ± 3.0 fmol/ mg) than in epileptic (73.0 ± 1.5 fmol/ mg, P = 0.0006, unpaired t-test). No difference was found in K_D (healthy

0.17 ± 0.03, epileptic 0.17 ± 0.01; P = 0.7855, unpaired t-test), indicating no change in the affinity of [^{3}H]-CCPA for the A_1 receptor between healthy and epileptic hippocampal membranes (Figure 4-2).

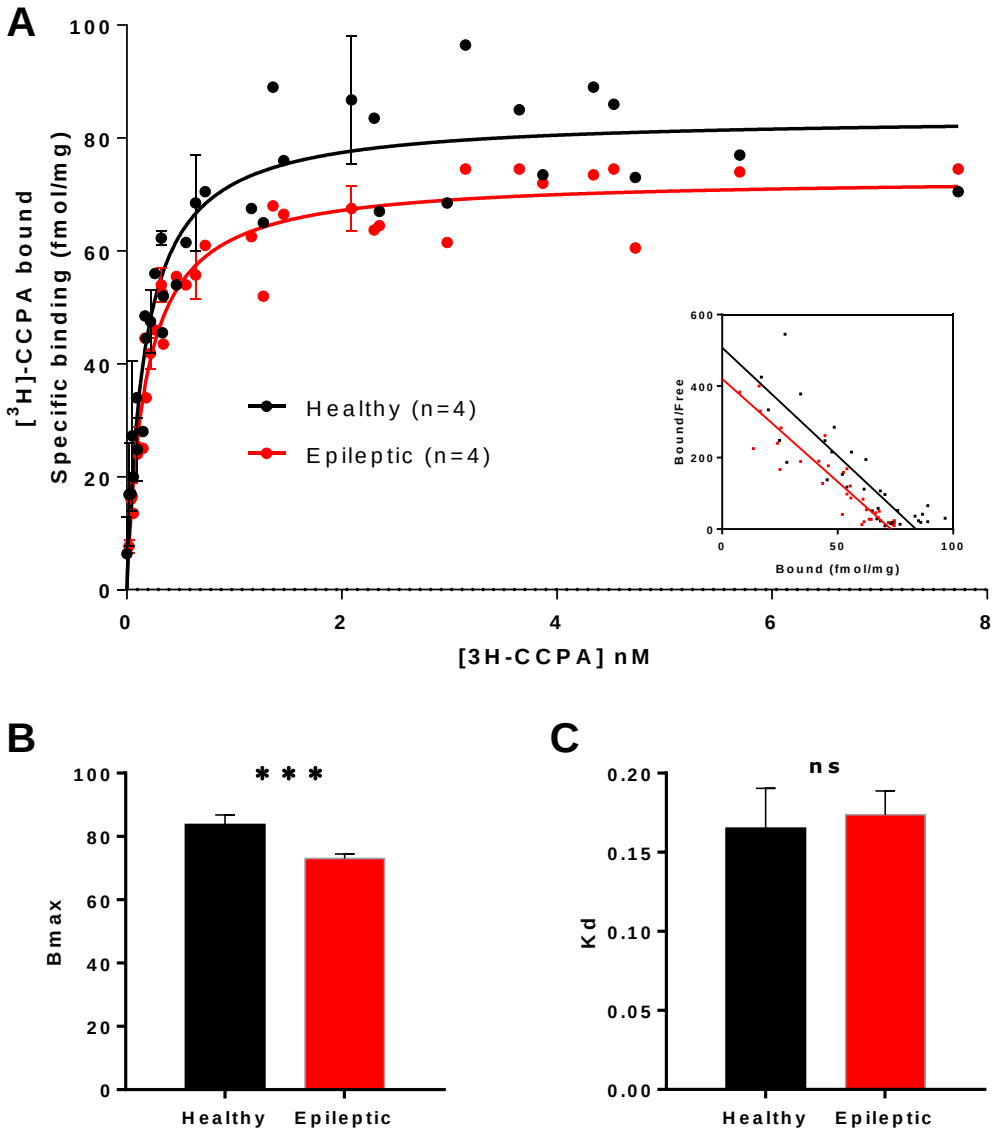

Figure 4-2: Radioligand saturation binding shows decreased A_1R binding in epileptic hippocampi as compared to healthy. A: Specific saturation binding of [^{3}H]-CCPA in healthy and epileptic hippocampal membranes shows decreased binding in epilepsy. Inset: Scatchard plot of saturation binding, indicating a decreased B_{MAX} of epileptic membranes but parallel K_D values. **B:** B_{MAX} parameter values determined by nonlinear fitting shown in (A). B_{MAX} in epileptic hippocampal membrane is significantly lower than in healthy (***: P = 0.0006, unpaired t-test). **C:** K_D parameter values from nonlinear fitting is not significantly different between healthy and epileptic membranes (ns: P = 0.7855, unpaired t-test). **NB Experimental data shown in this figure was collected from procedures performed by the CRO Eurofins (Appendix 8.3.1). Data analysis was performed following receipt of raw data from the CRO.**

4.4. Functional Contribution of A_1R and $A_{2A}R$ to Adenosine-induced Network Inhibition and Interaction with CBD

Electrophysiology was carried out with MEAs to assess the effect of exogenous adenosine on functional network activity in healthy and epileptic hippocampal slices, as well as any potential modulation with CBD. Additionally, the contribution by individual adenosine receptors on overall network response to adenosine was assessed by application of receptor antagonists.

4.4.1. Characteristics of hippocampal field potentials measured using MEAs

4.4.1.1. Distance of recording electrode from stimulation electrode

LFPs were stimulated in the CA1 of hippocampal slices using MEAs as described in section 2.2.2. Although field potential responses could be detected as far as 800 µm "downstream" from the stimulation electrode (see Figure 4-3), the most substantial response was always recorded on the adjacent electrode, 200 µm away from the stimulation electrode. Therefore, all field potential recordings described in this thesis were recorded from each recording electrode adjacent to the stimulation electrode, meaning that all field potentials show the response 200 – 283 µm downstream from the stimulation electrode (depending on angle of slice placement on MEA array). Field potentials evoked downstream from the stimulation electrode show decreased amplitude and slower waveforms, demonstrating the travelling of the evoked potential across the Schaffer collaterals. Of note, it was anecdotally observed that optimal responses were seen when a string of the "harp" slice hold-down was directly above the stimulation and/or recording electrodes, suggesting that locations where the slice was "held" down and therefore maximal contact with the electrodes allowed for optimal fibre stimulation and response recording.

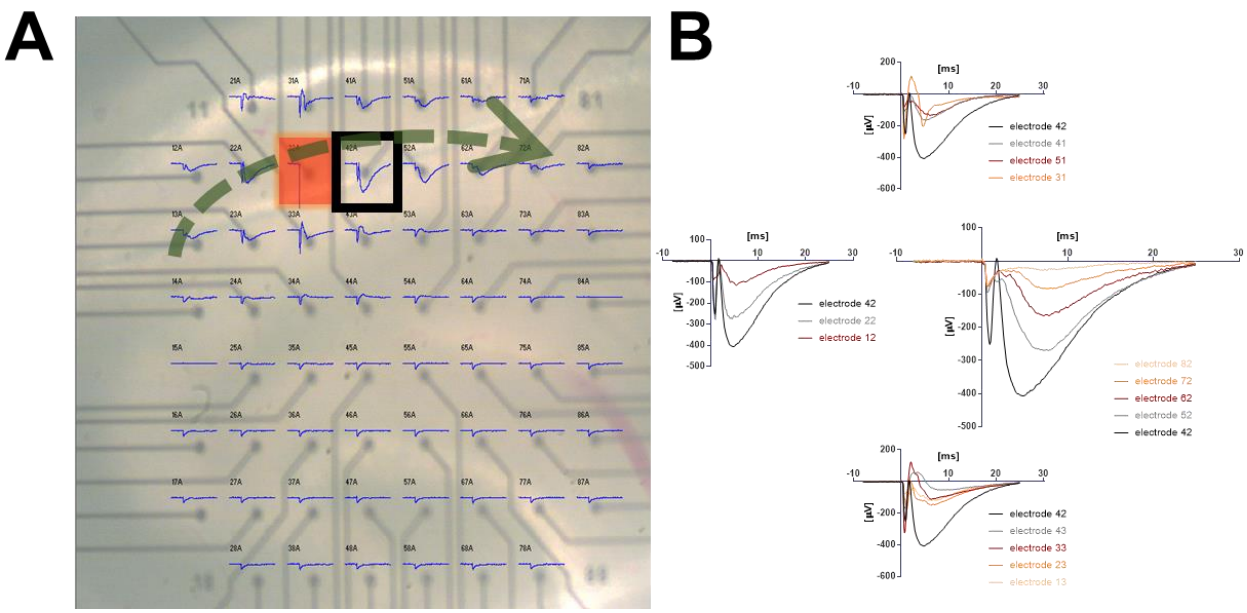

Figure 4-3: Representative example of evoked field potentials across an MEA in response to a single electrode stimulation in CA1. A: Superimposed responses to a single stimulation across the MEA on an image taken below the slice showing placement of electrodes. Electrode 32 (red box) has been selected as the stimulation electrode, and adjacent electrode 42 (black box) as the primary recording electrode. Green arrow represents the direction of Schaffer collateral fibres. Note that a thin fibre forming part of the "harp" slice hold-down can be seen directly behind the stimulation and recording electrodes (and can be seen extending past electrodes 71/81). **B:** Averaged evoked field potentials across the electrodes surrounding the stimulation electrode. Electrode 42 has been included in all graphs as a comparison. Top graph shows responses in row 1 (the row above the stimulation electrode). The centre row shows responses in the second row, with the small graph showing responses "upstream" from the stimulation electrode, and the large graph showing responses downstream. Bottom graph shows responses on row 3 (row below stimulation electrode).

4.4.1.2. Properties of evoked field potentials in healthy and epileptic slices

Prior to all recordings on healthy and epileptic slices in this chapter, the properties of each slice was tested to determine stimulation strength to be used throughout each experiment. Increasing stimulation strengths were tested (0 – 2 V, the maximum possible stimulation using the Multichannels system) and the resulting volley amplitude and field potential slope measured at each stimulation strength (see Figure 4-4). Field potential properties were comparable across healthy and epileptic slices. Of note, stimulation at the maximum strength of 2 V appeared to cause a significant increase in volley amplitude (Figure 4-4B), but not in amplitude or slope of the field potential in either healthy or epileptic slices. For this reason, submaximal response stimulation strengths resulting in LFPs in the 40% – 60% range of the size produced by the maximum 2 V stimulation were used throughout this chapter. This was to ensure that both the field potentials and volleys lay within the linear portion of the input-output curve, and to attempt for broad consistency across recordings in the size of the field potential itself.

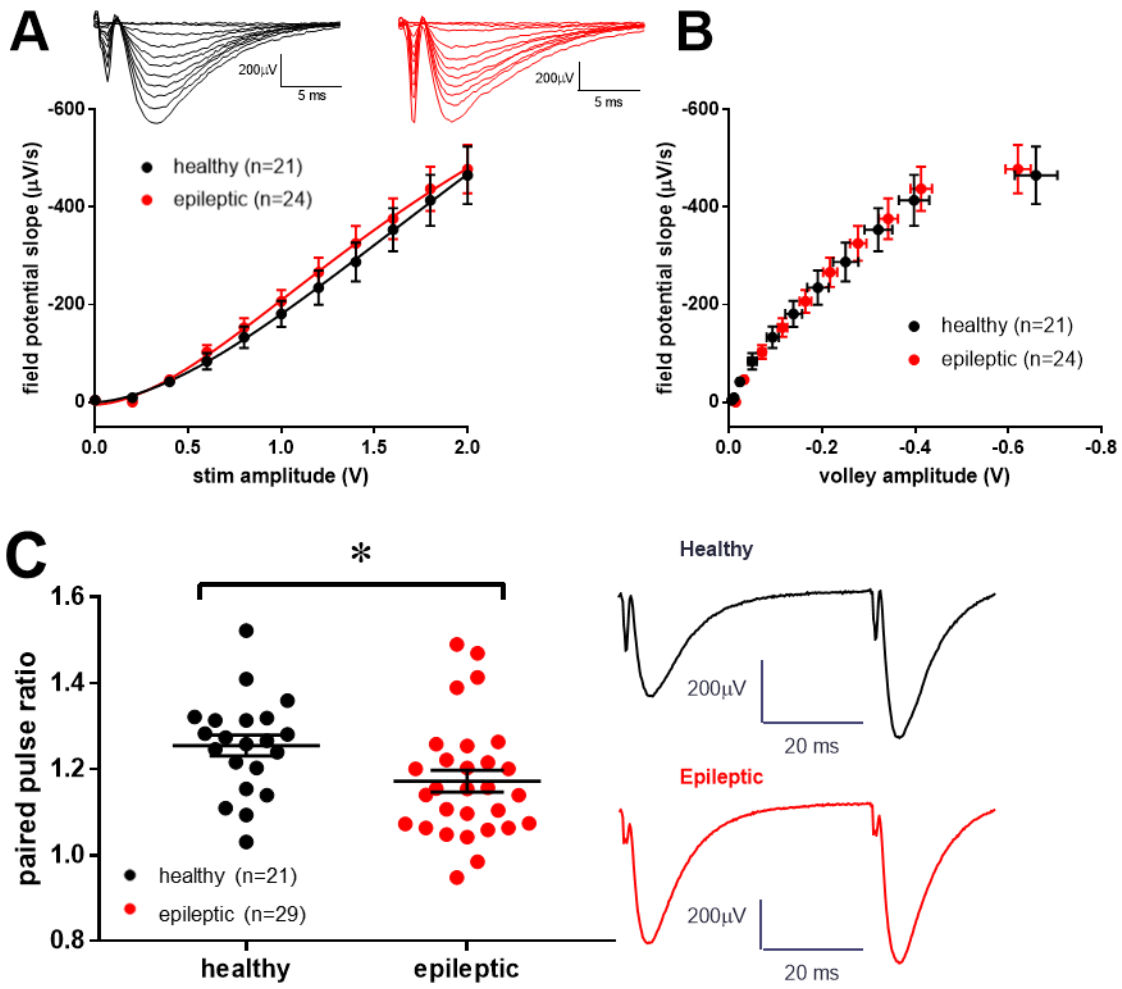

Figure 4-4: Properties of evoked field potentials in healthy and epileptic hippocampal slicesA: Input-output curve of the mean field potential slopes against stimulation intensity for all slices in this chapter. No significant difference is seen between healthy and epileptic slices regarding average slope by stimulation strength. Insets: Representative traces of healthy (black) and epileptic (red) field potentials; both are means of two sweeps at each intensity. **B:** Mean measured field potential slopes measured against mean corresponding volley amplitude; no difference is seen between healthy and epileptic recordings. **C:** Paired pulse ratios, calculated as 10-min averages at the start of each experiment during baseline, for healthy and epileptic hippocampal slices. Paired pulse facilitation was observed to be significantly lower in epileptic recordings compared to healthy hippocampal slices. Insets: Representative traces of healthy and epileptic 50-ms interval paired pulses; each trace is averaged from 10 sweeps. *: $P < 0.05$; error bars show SEM.

During the baseline at the start of experiments, with slices being perfused with regular aCSF only, 50 ms paired pulse stimulations were started through the stimulation electrode at the chosen constant stimulation strength (both described above) every 30 seconds. PPR was determined by dividing the field potential slope of the second pulse by the first, providing an indication of short-term presynaptic

facilitation. In healthy hippocampal slices, the mean ± SEM PPR was 1.3 ± 0.02, while in epileptic slices the PPR was 1.2 ± 0.03. This was found to be a significant decrease (P = 0.0264, unpaired t-test; Figure 4-4C) from healthy, suggesting pathological damage to short-term synaptic facilitation mechanisms due to chronic epilepsy. This is consistent with the literature of seizures/trauma decreasing paired pulse facilitation,

4.4.2. Characterisation of healthy and epileptic hippocampal responses in the presence of vehicle

Network activity was first observed in healthy and epileptic hippocampal slices in the presence of standard aCSF, and then following application of vehicle (0.01% DMSO). Normalised LFP slopes in both healthy and epileptic hippocampal slices were unaffected following vehicle application (healthy LFPs between 10 and 20 min following vehicle application 102.4 ± 5.15% of baseline, epileptic 103.9 ± 5.41%; P = 0.8474, unpaired t-test; Figure 4-5A-B). Ongoing 50 ms paired pulse stimulations before and after vehicle application was also not significantly different in either healthy or epileptic hippocampal slices (healthy PPRs prior to vehicle application: 1.3 ± 0.03, after vehicle application 1.3 ± 0.03, P = 0.0938, paired t-test; Figure 4-5C. Epileptic PPRs: 1.2 ± 0.07 before vehicle application, 1.3 ± 0.08 after vehicle, P = 0.7529, paired t-test; Figure 4-5D). PPPs were also not significantly different between healthy and epileptic hippocampal slices in the presence of only aCSF (two-way repeated measures ANOVA, variation due to epilepsy F (1, 12) = 0.1103, P = 0.7455; variation due to PPI F (8, 96) = 0.3393, P < 0.0001), nor following the application of vehicle (in healthy hippocampal slices, variation due to vehicle F (1, 5) = 0.0074, P = 0.9347; variation due to paired pulse interval F (8, 40) = 11.53, P < 0.0001; Figure 4-5E. In epileptic hippocampal slices, variation due to vehicle F (1, 5) = 0.5334, P = 0.4980; variation due to paired pulse interval F (8, 40) = 5.263, P = 0.0002; Figure 4-5F).

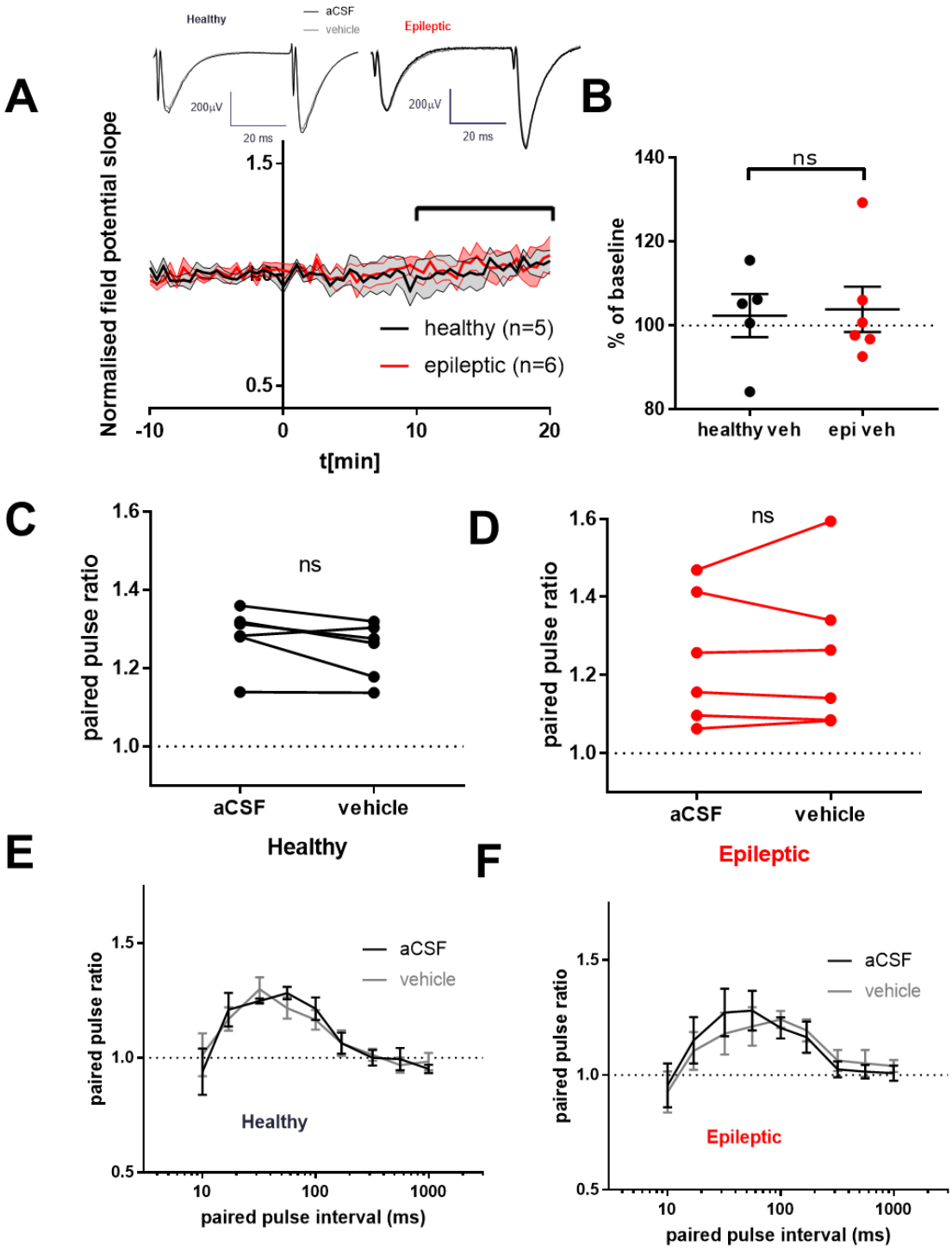

Figure 4-5: No change between healthy and epileptic evoked field potentials upon bath application of vehicle (0.01% DMSO). A: Normalised field potential slopes against time, following initial application of vehicle at t[min]=0 in healthy and epileptic hippocampal slices. Insets show representative traces in healthy and epileptic slices, prior to (black) and after (grey) application of vehicle; traces are means of 10 sweeps. **B:** No significant difference between normalised field potential slopes averaged between 10 – 20 min (as indicated in A) of healthy and epileptic animals following vehicle application (ns: P = 0.8474, unpaired t-test). **C&D:** Mean ratio of 50 ms paired pulses of 10 min baseline and

between 10 – 20 min following vehicle administration is not significantly different in healthy (C) or epileptic (D) hippocampal slices. **E&F:** No change in paired pulse profile before and after vehicle application in healthy (E) or epileptic (F) hippocampal slices.

Application of exogenous adenosine was able to significantly inhibit field potentials in the presence of vehicle up to the highest tested concentrations of adenosine (1 – 500 µM) in healthy and epileptic hippocampal slices, with no significant difference between the two (two-way ANOVA, variation due to adenosine concentration: $F(6, 60) = 157.9$, $P < 0.0001$, variation due to epilepsy $F(1, 10) = 0.71$, $P = 0.4191$). Raw field potential slopes across representative experiments is given for healthy and epileptic slices in Figure 4-6A&B, along with mean wash on and off dynamics for each concentration of adenosine (Figure 4-6C&D). Of note, although all adenosine concentrations were applied for 10 min each to allow a plateau, the highest concentrations of adenosine (300 µM and 500 µM) maintained the inhibition plateau for a significant amount of time following wash-off, before responses began to recover. This may be an effect of high concentrations of adenosine being retained by the tissue, possibly due to the endogenous metabolism mechanisms being overwhelmed by the high concentrations of adenosine. Statistical comparisons were not made between the length of 300 µM and 500 µM post-wash plateaus in healthy and epileptic slices, however, due to the confounding effect of PPPs being run in 300 µM but not in 500 µM. Length of time following wash-off of exogenous adenosine, but before recovery of field potentials, may prove to be an interesting future experiment to assess adenosine retention of adenosine effect and metabolism in chronic epileptic tissue.

Nonlinear regression of adenosine-induced inhibition in healthy and epileptic hippocampal slices are shown below in Figure 4-6E, and fitted parameters are displayed in Table 4-4 below, as well as adjusted P values by Sidak's post-hoc test for multiple comparisons between healthy and epileptic recordings. The inhibition plateau reached between 300 µM to 500 µM was fitted to bottom values by nonlinear regression as 19.3 ± 5.6% of baseline field potential slope in healthy hippocampal slices, and 15.0 ± 5.6% of baseline in epileptic hippocampal slices (adjusted $P = 0.8495$). The fitted "top" value, as all doses were normalised to pre-adenosine LFP baseline response, indicate whether any inhibition was induced by the lowest concentrations of adenosine (1 – 3 µM). In healthy slices, this was 92.0 ± 3.6% of baseline while in epileptic slices, the top value was fitted at 97.5 ± 3.2%; this suggests that low concentrations of adenosine are more effective in inducing inhibition in healthy slices, however this did not reach statistical significance (adjusted $P = 0.0536$). IC_{50} values (49.2 µM in healthy and 52.6 µM in epileptic; $P = 0.9823$) and Hill slopes (-1.7 ± 0.5 in healthy and -1.4 ± 0.3 in epileptic; adjusted $P = 0.7159$) were not different between the two conditions, although Hill slope values are roughly consistent with the literature (Dunwiddie and Diao, 1994) and indicate that overall adenosine response is mediated through cooperativity at multiple sites.

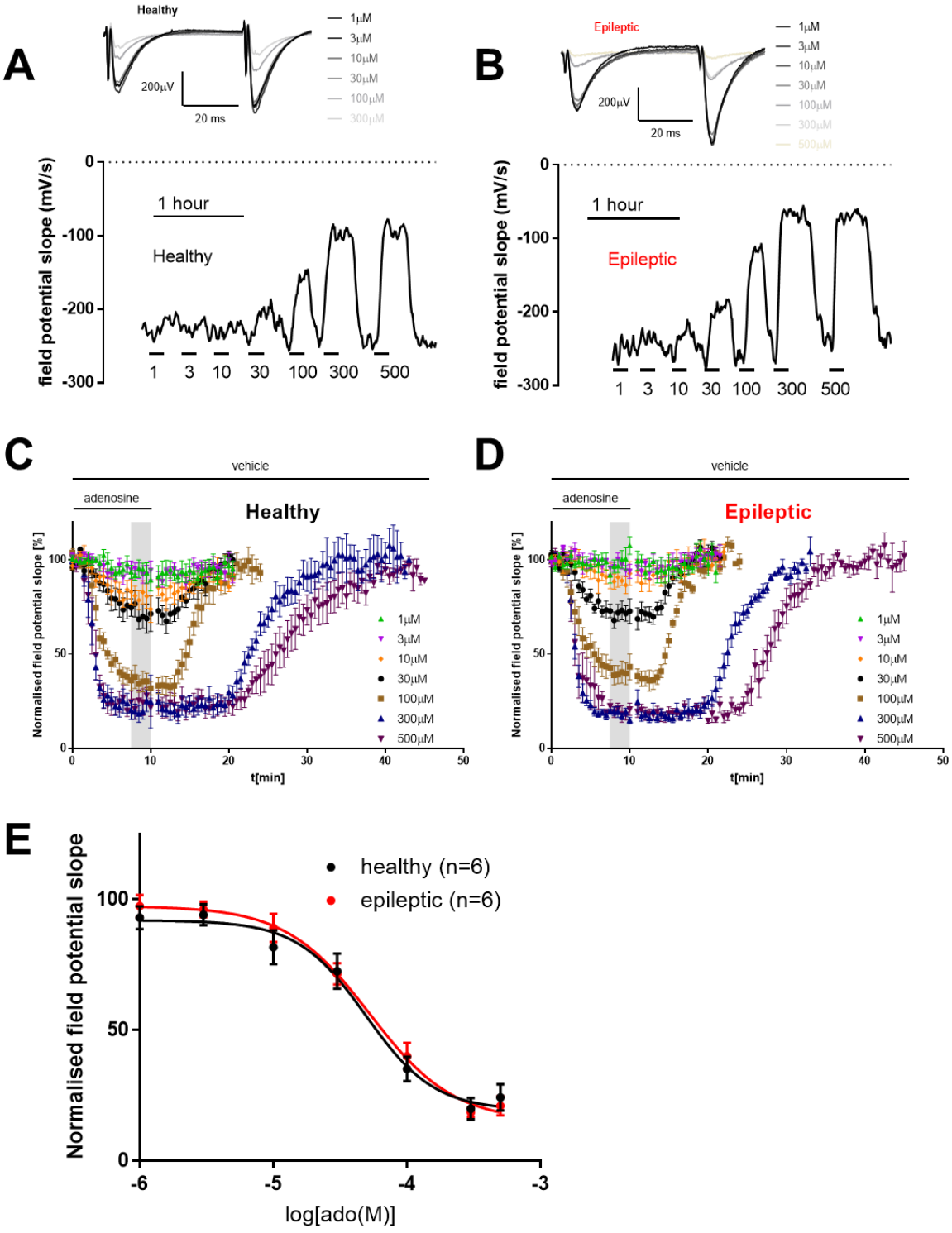

Figure 4-6: No overall difference between healthy and epileptic hippocampal slices in exogenously applied adenosine-induced inhibition of field potentials. A&B: Representative raw field potential slopes in healthy and epileptic tissue, showing the time course of sample experiments and effect of exogenous adenosine application on field potentials. Field potential slopes are smoothed with the 4 neighbours (2 min windows) on either side. Insets show sample field potential traces from healthy and epileptic slices, with increasing doses of adenosine superimposed. Traces are averages of 10 sweeps.

C&D: Mean ± SEM plots of normalised field potential slopes during wash-on and wash-off of exogenous adenosine in healthy and epileptic slices. Shaded grey box indicates points from which average dose responses were calculated. **E:** Concentration-response inhibition curves of normalised field potential slopes in response to exogenously applied adenosine in both healthy and epileptic hippocampal slices (average responses as indicated in C&D). Application of exogenous adenosine significantly inhibited field potentials up to 500 µM but was not significantly different between healthy and epileptic hippocampal slices.

Parameter	Vehicle		P value
± Standard error	Healthy	Epileptic	Healthy vs epileptic
n	**6**	**6**	
Bottom (%)	19.3 ± 5.6	15.0 ± 5.6	0.8495
Top (%)	92.0 ± 3.6	97.5 ± 3.2	0.0536
$LogIC_{50}$	-4.3 ± 0.1	-4.3 ± 0.1	0.9823
IC_{50} (µM)	49.2	52.6	
Hill slope	-1.7 ± 0.5	-1.4 ± 0.3	0.7159

Table 4-4: Summary of adenosine-induced inhibition nonlinear regression parameters in the presence of vehicle: log(adenosine [µM]) vs. response - Variable slope (four parameters). P values displayed are adjusted for multiple comparisons using Sidak's post-hoc test.

The ongoing 50 ms paired pulse stimulations were also assessed during the same analysis window of maximal adenosine-induced inhibition, with the aCSF and vehicle PPRs previously represented in Figure 4-5C&D above, and the mean PPRs of the remaining adenosine concentrations are presented in Figure 4-7A below. There was no significant difference across the range of adenosine concentrations either due to adenosine concentration or epilepsy (two-way repeated measures ANOVA, variation due to adenosine $F(7, 70) = 1.769$, $P = 0.1074$; variation due to epilepsy $F(1, 10) = 0.0572$, $P = 0.8158$). This was an unexpected finding, as adenosine activity on presynaptic A_1R should cause an increase in PPF. Possible reasons for lack of significant change in PPF in the presence of exogenous adenosine are discussed below in section 4.5.1.2.

There was no significant effect of adenosine concentration against vehicle baseline in either healthy or epileptic PPPs (Figure 4-7B&C), although variation due to PPI was still significant in all conditions, as expected. Adjusted P values for each PPI were obtained by family-wise comparisons using Dunnett's test, and identified significant differences from baseline at 300 µM adenosine at 32 ms (adjusted

P = 0.0124) and 100 ms (adjusted P = 0.0475) PPI in healthy hippocampal slices, as well as a significant paired pulse facilitation (PPF) at 10 ms in epileptic hippocampal slices also at 300 µM adenosine (adjusted P = 0.0001).

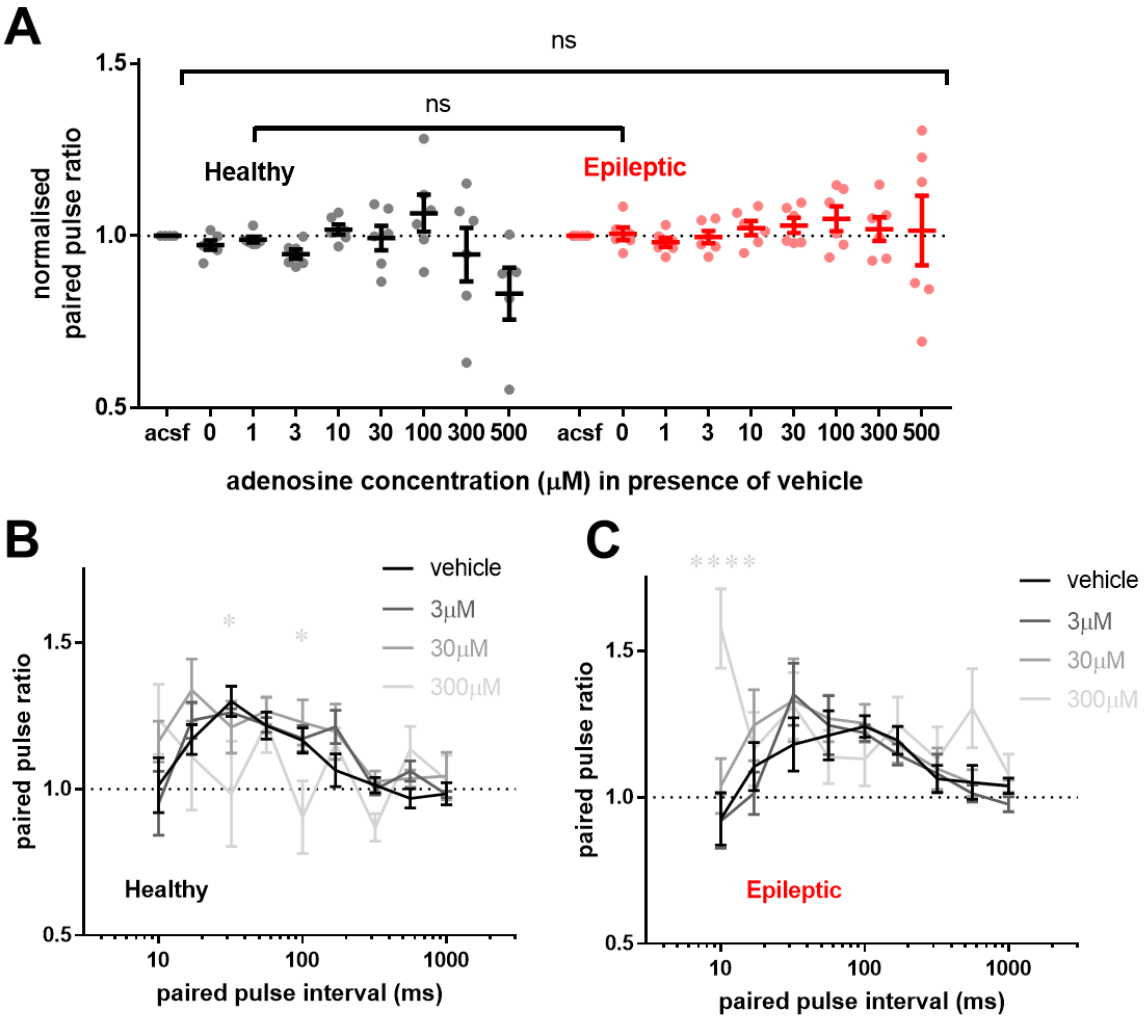

Figure 4-7: No overall difference in PPF due to epilepsy or adenosine concentration. A: Averaged paired pulse ratios, normalised to aCSF (prior to vehicle application), in increasing concentrations of adenosine in healthy and epileptic tissue. **B:** Paired pulse profiles in healthy hippocampal slices in the presence of vehicle plus increasing concentrations of adenosine are largely unaffected, except in 300 µM adenosine at 32 ms (*: adjusted P = 0.0124) and 100 ms (*: adjusted P = 0.0475) PPI against vehicle baseline. **C:** Paired pulse profiles in epileptic hippocampal slices in the presence of vehicle plus increasing adenosine concentrations are not significantly affected by adenosine, except in 300 µM adenosine at 10 ms (****: adjusted P = 0.0001) PPI against vehicle baseline. Adjusted P values from Dunnett's multiple comparisons tests. *: $P \leq 0.05$; ****: $P \leq 0.0001$.

4.4.3. Blockade of A_1R

To assess the contribution of the A_1Rs to the effects of exogenously applied adenosine, and to investigate whether the measured decrease in A_1R expression in epilepsy detected through radioligand binding has a functionally detectable effect, the above experiments were repeated in the presence of the specific A_1R antagonist 8-CPT (1 µM) (Etherington and Frenguelli, 2004) in healthy and epileptic hippocampal slices.

Normalised LFP slopes in both healthy and epileptic hippocampal slices were potentiated following 8-CPT application. Healthy LFPs plateaued after 10 min following 8-CPT application at 37.2 ± 4.21% of baseline. Epileptic LFPs potentiated and plateaued in the same time frame, but reached a mean of 123.5 ± 2.24% of baseline. The difference between healthy and epileptic was significant ($P = 0.0090$, unpaired t-test; Figure 4-8A-B). This could be due to decreased basal adenosine tone in epileptic tissue, but as radioligand binding indicated a decreased expression of A_1R in chronic epilepsy, this decrease in potentiation response may also reflect basal activation of fewer A_1Rs.

Ongoing paired pulse stimulations at 50 ms PPI before and after 8-CPT application were also significantly different in both healthy and epileptic hippocampal slices. In healthy slices, PPR significantly decreased from 1.3 ± 0.08 at baseline to 1.1 ± 0.04 after 8-CPT application ($P = 0.0250$, paired t-test; Figure 4-8C). In epileptic slices, PPR was 1.12 ± 0.03 before 8-CPT application, which significantly decreased to 1.05 ± 0.04 after 8-CPT ($P = 0.0243$, paired t-test; Figure 4-8D).

PPPs were also significantly altered in both healthy and epileptic slices following the application of 8-CPT. For healthy hippocampal slices, variation due to 8-CPT was significant ($F(1, 4) = 9.738$, $P = 0.0355$; variation due to PPI $F(8, 32) = 12.23$, $P < 0.0001$. The interaction was significant $F(8, 32) = 2.6$, $P = 0.0260$). Sidak's multiple comparisons post-hoc test identified a significant decrease in PPRs in the 10 ms interval following 8-CPT application (adjusted $P = 0.0022$, Sidak's multiple comparisons test; Figure 4-8E). In epileptic hippocampal slices, variation due to 8-CPT was also significant ($F(1, 7) = 23.01$, $P = 0.0020$; variation due to PPI $F(8, 56) = 11.22$, $P < 0.0001$. The interaction was not significant). The 17 ms paired pulse interval was significantly different following 8-CPT application (adjusted $P = 0.0495$, Sidak's multiple comparisons test; Figure 4-8E). The difference in interaction significance between healthy and epileptic indicates that in epileptic slices, 8-CPT unilaterally seemed to decrease PPR at all intervals, whereas in healthy slices the effect was isolated to the smaller intervals, of less than 50 – 100 ms. This could suggest a greater involvement of presynaptic A_1R activity in epileptic slices than in healthy, although this would require far greater levels of research to elucidate.

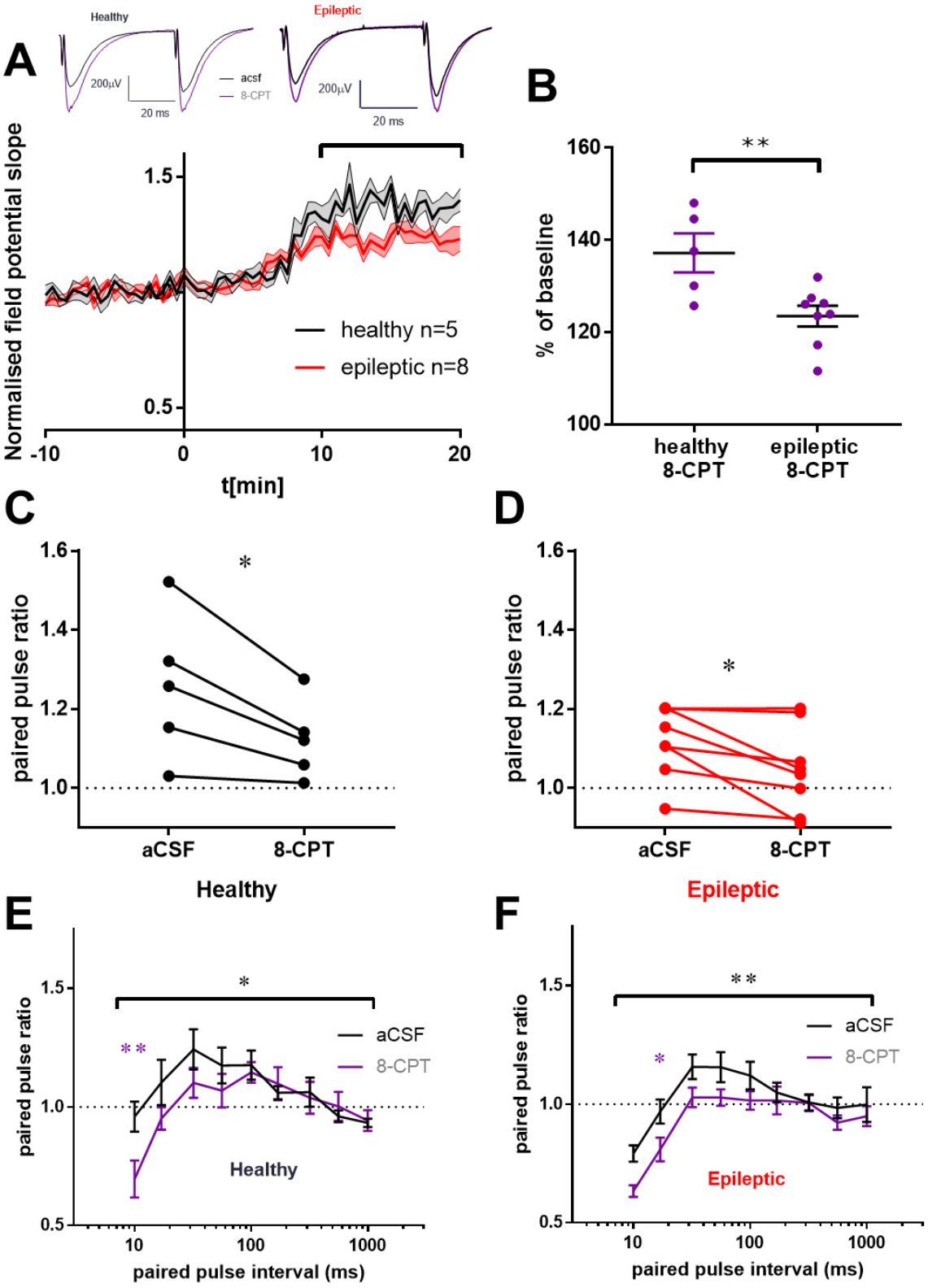

Figure 4-8: Potentiation of field potentials by 1 µM 8-CPT is significantly reduced in epileptic hippocampal slices compared to healthy. A: Normalised field potential slopes against time, showing potentiation in both healthy and epileptic hippocampal slices following initial application of 8-CPT at

t[min]=0. Insets show representative traces, averaged from 10 sweeps, before and after 8-CPT application in healthy and epileptic slices. **B:** Normalised field potential slopes averaged between 10 – 20 min following 8-CPT application are significantly different between healthy and epileptic hippocampal slices (**: P = 0.0090, unpaired t-test). **C&D:** Mean ratio of 50 ms paired pulses in healthy and epileptic slices are significantly decreased following 8-CPT application (*: P = 0.0250, paired t-test). **E&F:** Paired pulse profiles were significantly decreased from baseline in healthy and epileptic hippocampal slices due to application of 8-CPT. *: $P \leq 0.05$; **: $P \leq 0.01$

Presence of 8-CPT was able to significantly prevent field potential inhibition in the across the tested concentrations of applied exogenous adenosine (1 – 500 µM) in healthy and epileptic hippocampal slices, as was to be expected. The effect of washing on and off on exogenous adenosine on the field potential slopes is shown in Figure 4-9A&B below; of note, while no responses were seen up to 100 µM, 300 µM and 500 µM of adenosine were able to start inhibiting field potentials, but on average did not reach inhibitory plateaus within the 10 min adenosine application window. This shows that presence of 8-CPT, the competitive A_1R antagonist, significantly delays the adenosine-induced inhibition at high concentrations. The decision was made to take the average response within the same window as the other concentrations and conditions for consistency, rather than waiting for an inhibitory plateau to be reached, as it was unknown whether the lower concentrations of adenosine, e.g., 100 µM adenosine, which induces inhibition in the presence of vehicle within 10 minutes, may also have been able to reach an inhibitory plateau if left long enough. The delay in onset of inhibition is, however, an interesting aspect of A_1R inhibition, and could be a future experiment in which high concentrations of adenosine were allowed to reach an inhibitory plateau in the presence of 8-CPT; the time dynamics of this could shed some light on the activity of adenosine at A_1Rs in epileptic tissue.

The nonlinear regression parameters are presented in Table 4-5 below; the fitted "top" parameters were 97.1 ± 3.1% of baseline in healthy inhibition curves, and 100.3 ± 1.9% in epileptic inhibition curves; neither of these were significantly different from each other or respective vehicle parameters. As the concentration-response curves did not reach an inhibition plateau, as can be seen in Figure 4-9C&D below, the nonlinear regression parameters (bottom values, $IC_{50}s$, and Hill slopes) were not able to be accurately generated or compared (the extremely large errors are shown in Table 4-5), and were therefore excluded from analysis of regression parameters.

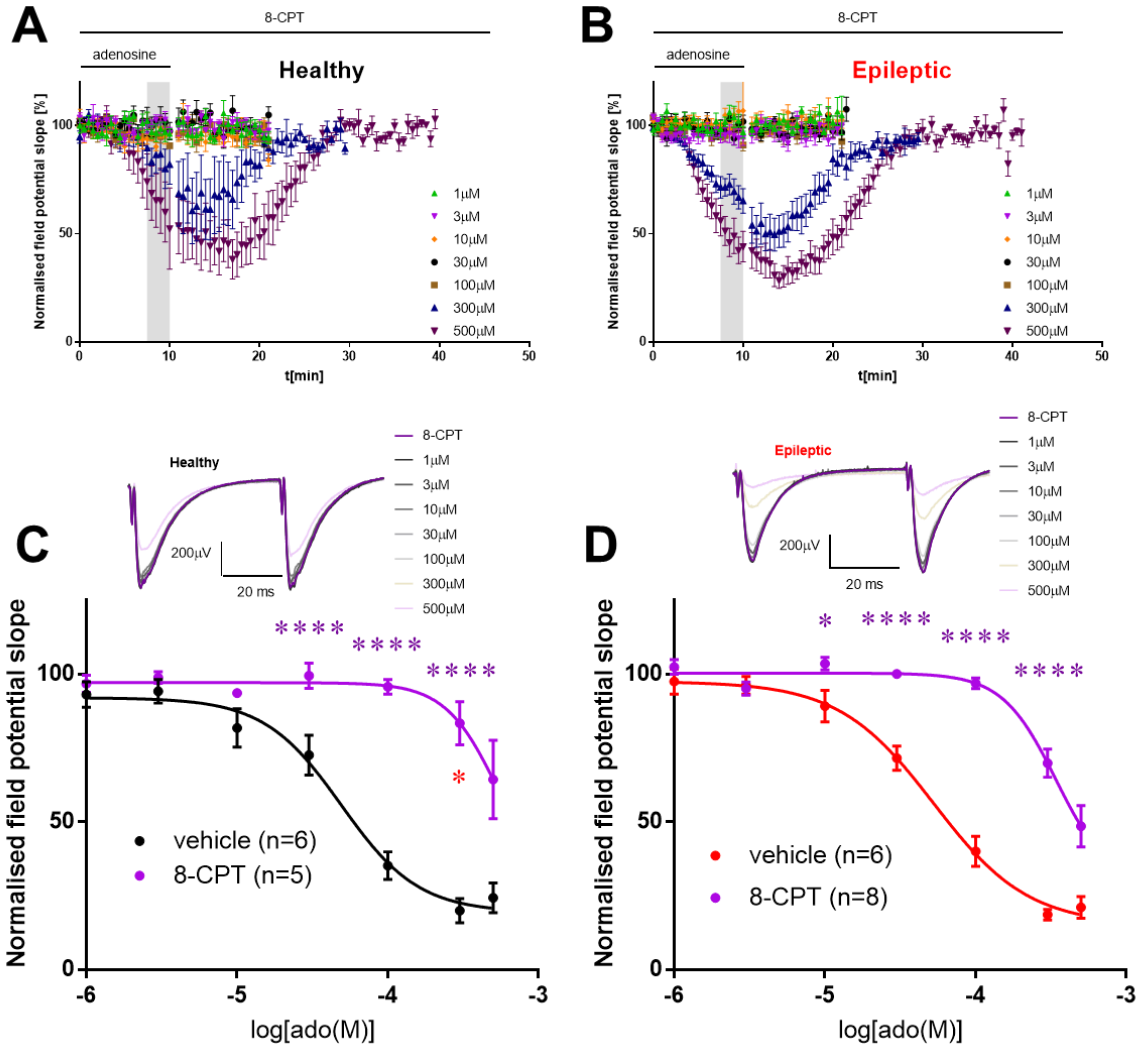

Figure 4-9: 8-CPT prevents adenosine-induced inhibition of field potentials in both healthy and epileptic hippocampal slices. A&B: Mean time course of adenosine wash on and off effect on normalised field potential slopes in healthy and epileptic slices. Shaded grey box indicates points from which average dose responses were calculated. Note that while responses were seen in the 300 µM and 500 µM concentrations, inhibition plateaus were not reached within the protocol-defined window of 10 min exogenous adenosine application. **C&D:** Concentration-response inhibition curves of normalised field potential slopes in response to exogenously applied adenosine in healthy (C) and epileptic (D) hippocampal slices, in the presence of either vehicle (previously shown in Figure 4-7 and presented again here for reference) or 1 µM 8-CPT. Inhibition of A_1R by 8-CPT prevents adenosine-induced field potential inhibition significantly up to 300 µM in both conditions. Sidak's multiple comparisons across the groups within each adenosine concentration found significance between vehicle and 8-CPT in both healthy and epileptic slices against respective vehicle. Additionally, at 300 µM, the healthy and epileptic points were significantly different. Insets show representative field potential traces, averaged over 10 sweeps at each adenosine concentration. ****: adjusted $P < 0.0001$, ***: adjusted $P < 0.001$, **: adjusted $P < 0.01$*: adjusted $P < 0.05$.

Parameter	8-CPT		P value		
± Standard error	Healthy	Epileptic	Healthy vs epileptic	Healthy vs veh	Epileptic vs veh
n	**5**	**8**			
Bottom (%)	23.1 ± 452.9	28.2 ± 33.3	nc	nc	nc
Top (%)	97.1 ± 3.1	100.3 ± 1.9	0.4380	0.0818	0.4191
$LogIC_{50}$	-3.3 ± 2.0	-3.5 ± 0.2	nc	nc	nc
IC_{50} (µM)	549.3	341.3			
Hill slope	-2.4 ± 6.6	-2.4 ± 1.4	nc	nc	nc

Table 4-5: Summary of adenosine-induced inhibition nonlinear regression parameters in the presence of 8-CPT: log(adenosine [µM]) vs. response - Variable slope (four parameters). P values displayed are adjusted for multiple comparisons using Sidak's post-hoc test. nc: not calculated; note that "Bottom" and "IC_{50}" parameters in particular show extreme standard errors and/or fitted values, due to an inhibition plateau not being reached within the applied concentrations of adenosine.

Analysis was able to be performed on responses to the range of adenosine concentrations, using two-way repeated measures ANOVA and post-hoc Sidak's multiple comparison tests. When compared with the adenosine-induced inhibition in vehicle, there was significant difference due to epilepsy and 8-CPT (two-way repeated measures ANOVA, significant variation due to adenosine concentration: $F(6, 126) = 144.5$, $P < 0.0001$) and significant variation due to the consolidated conditions of healthy/epileptic and vehicle/8-CPT ($F(3, 21) = 53.09$, $P < 0.0001$). The interaction was significant ($F(18, 126) = 21.93$, $P < 0.0001$). Sidak's multiple comparisons across the groups within each adenosine concentration found a significant difference in the epileptic inhibition curve between vehicle and 8-CPT from 10 µM adenosine (adjusted $P = 0.0232$ against epileptic vehicle), and in both healthy and epileptic from 30 µM adenosine up to 300 µM (adjusted $P < 0.0001$ against respective vehicle curves). A significant difference was found between the healthy and epileptic hippocampal slices at the highest adenosine concentration included in the analysis (300 µM: healthy 84.7 ± 7.5%; epileptic 69.5 ± 4.7%; adjusted $P = 0.0162$). This indicates that in the presence of 8-CPT, adenosine in epileptic hippocampal slices induces a greater degree of inhibition at the same concentration than in healthy hippocampal slices, suggesting that the 8-CPT-induced rightward shift of the inhibition curves is less in epileptic slices than in healthy. Again, this would require further investigation to confirm, but could also indicate a change in activity/efficacy of A_1Rs in epilepsy, as the same concentration of 8-CPT is less effective in epileptic than healthy tissue.

The ongoing 50 ms paired pulse stimulations were measured during maximal inhibition at each adenosine concentration, with the aCSF and 8-CPT PPRs previously represented in Figure 4-8C&D, and the normalised PPRs of the remaining adenosine concentrations in the presence of 8-CPT are presented in Figure 4-10A. In the presence of 8-CPT, there was a significant difference due to adenosine concentration but not epilepsy (two-way repeated measures ANOVA, variation due to adenosine $F(7, 77) = 6.996$, $P < 0.0001$; variation due to epilepsy $F(1, 11) = 1.355$, $P = 0.2690$). No differences were found between healthy and epileptic at each adenosine concentration from Sidak's family-wise post-hoc comparisons; this could be considered due to the range of PPRs, particularly in epilepsy, and the large number of multiple comparison corrections being made. There does however appear to be a trend that at the higher concentrations of adenosine, epileptic PPR responses show an increase above the pre-8-CPT baseline PPR, whereas in healthy tissue the PPR on average returns to levels seen prior to 8-CPT application. Although there was no overall significant difference between healthy and epileptic recordings, this again is an indication that high concentrations of adenosine may facilitate short-term synaptic plasticity in the epileptic hippocampus.

There was no overall significant effect of adenosine concentration against 8-CPT baseline in healthy PPPs (in healthy slices: two-way repeated measures ANOVA: variation due to adenosine $F(3, 12) = 3.47$, $P = 0.0508$; variation due to PPI $F(8, 32) = 10.77$, $P < 0.0001$. The interaction was not significant $F(24, 96) = 0.9053$, $P = 0.5943$). However, Dunnett's family-wise post-hoc tests found significance from 8-CPT baseline at 300 µM, at the PPIs 10 ms (adjusted $P = 0.0093$), 17 ms (adjusted $P = 0.0055$), and 56 ms (adjusted $P = 0.0239$); Figure 4-10D. This is in alignment with the observations that, at 300 µM, adenosine is able to start to induce inhibition once more and the PPR returns to that seen prior to 8-CPT application. In epileptic slices, the overall variation due to adenosine was significant ($F(3, 21) = 20.16$, $P < 0.0001$; variation due to PPI $F(8, 56) = 12.51$, $P = 0.0032$. The interaction was significant $F(24, 168) = 2.116$, $P = 0.0032$). Additionally, at 300 µM adenosine the PPR was significantly different from baseline at 10 ms (adjusted $P < 0.0001$), 17 ms (adjusted $P < 0.0001$), 32 ms (adjusted $P < 0.0001$), 100 ms (adjusted $P = 0.0151$), 169 ms (adjusted $P = 0.0001$), and 557 ms (adjusted $P = 0.0191$); Figure 4-10E. Again, this indicates a very strong paired pulse potentiation due to 300 µM adenosine which was stronger in epileptic hippocampal slices than healthy.

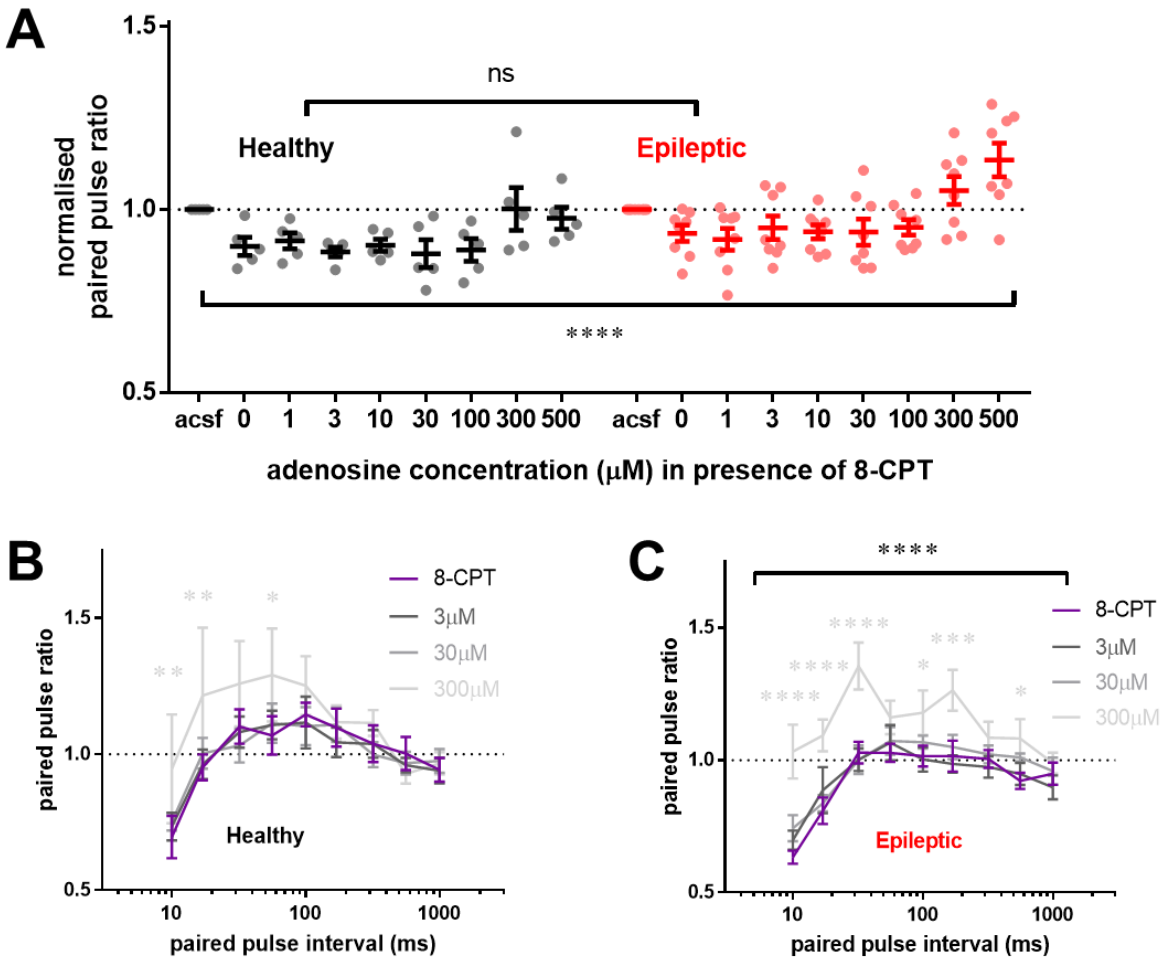

Figure 4-10: Inhibition of PPF by 8-CPT is overcome by high concentrations of adenosine. A: Averaged paired pulse ratios at 50 ms interval, normalised to average PPR in aCSF pre-8-CPT application. No significant difference was found between healthy and epileptic responses across the range of adenosine concentrations; however, it can be seen that epileptic PPRs cover a wider error range than in healthy, and on average the PPF is lower in epileptic slices than healthy, except at the highest adenosine concentrations. **B:** Paired pulse profiles in healthy hippocampal slices in the presence of 8-CPT and increasing concentrations of adenosine are overall not significantly different. At 300 μM, paired pulse ratios at 10 ms, 17 ms and 56 ms interval are significantly different from baseline. **C:** Paired pulse profiles in epileptic hippocampal slices in the presence of 8-CPT are significantly affected by increasing adenosine concentrations. ****: adjusted $P < 0.0001$, ***: adjusted $P < 0.001$, **: adjusted $P < 0.01$*: adjusted $P < 0.05$.

4.4.4. Blockade of $A_{2A}R$

With the function of A_1R assessed in healthy and epileptic hippocampal slices, the contribution of $A_{2A}R$ was next investigated. As $A_{2A}R$ was unable to be detected using radioligand binding and changes were not detected at the transcriptional level, there was no prior evidence within the experiments presented thus far as to any change in $A_{2A}R$ expression level in this particular model. To assess $A_{2A}R$ contribution

to network response to adenosine, the same LFP protocols were run in the presence of specific $A_{2A}R$ antagonist SCH 58261 (100nM) (Rombo et al., 2015).

In healthy hippocampal slices, the initial application of SCH 58261 caused a transient depression in LFPs, reaching a maximal inhibition between 8 – 10 min following bath application of SCH 58261, with a return to baseline in the next 10 min. This transient depression was not observed in epileptic hippocampal slices (mean of LFPs evoked between 8 – 10 min following drug application: healthy 86.6 ± 7.3% of baseline; epileptic 106.9 ± 5.3%; P = 0.0422, unpaired t-test; Figure 4-11A-B). This decrease in LFP would be consistent with blockade of $A_{2A}R$ resulting in isolation of A_1R, however this transient depression of field potential was not seen in single pyramidal cell responses to SCH 58261 wash-on (Rombo et al., 2015), nor in field experiments washing on another $A_{2A}R$ antagonist, ZM 241385 (Etherington and Frenguelli, 2004). This transience suggests a network desensitisation effect, and may be a finding specific to the drug and methodology used in this study (i.e., MEA stimulation, possibly a factor of the smaller distance between stimulation and recording electrodes, or the planar electrode array possibly contributing to light hypoxia at the bottom of the slices).

PPRs of ongoing 50 ms paired pulse stimulations were not significantly altered by SCH 58261 in either healthy or epileptic hippocampal slices at the peak of the transient field potential depression (healthy PPRs before and after SCH 58261 application: 1.2 ± 0.07 and 1.2 ± 0.07 respectively, P = 0.1191, paired t-test; Figure 4-11C. Epileptic PPRs: 1.1 ± 0.02 before SCH 58261 application, 1.1 ± 0.03 after, P = 0.0929, paired t-test; Figure 4-11D).

PPPs were performed in slices after 20 minutes, once field potentials in healthy slices had returned to baseline. In healthy slices, PPPs were not significantly different following the application of SCH 58261 (healthy hippocampal slices: variation due to SCH 58261 F (1, 4) = 2.066, P = 0.2240; variation due to PPI F (8, 32) = 9.307, P < 0.0001. The interaction was not significant F (8, 32) = 1.751, P = 0.1246). The 17 ms interval was significantly different following SCH 58261 application, (adjusted P = 0.0054, Sidak's multiple comparisons test; Figure 4-11E. Although these PPPs were not performed during the peak of the transient inhibition to field potentials, there was no significant difference in PPR for the ongoing 50 ms intervals seen at this time (Figure 4-11C). This does not rule out a change to PPR at different interval lengths during this transient SCH 58261 depression, but does suggest it may be unlikely.

Epileptic hippocampal slices were overall significantly different from aCSF baseline, with the PPF usually observed between 32 – 100 ms reduced to a PPR of around 1 (variation due to SCH 58261 F (1, 6) = 6.341, *: P = 0.0454; variation due to PPI F (8, 48) = 9.267, P < 0.0001. The interaction was not significant. No individual PPI comparisons were significant by Sidak's multiple comparisons;

Figure 4-11F). Although this appears to contradict the lack of significant difference in mean PPR from ongoing 50 ms interval stimulations in epileptic tissue (Figure 4-11D), the significance across all intervals suggests detection of a more subtle effect of SCH 58261 which could be detected at multiple PPIs. As blockade of $A_{2A}R$ would theoretically isolate basal adenosine activity at A_1R, this could suggest that $A_{2A}R$ plays a role in short-term synaptic potentiation in epileptic tissue which it does not in healthy.

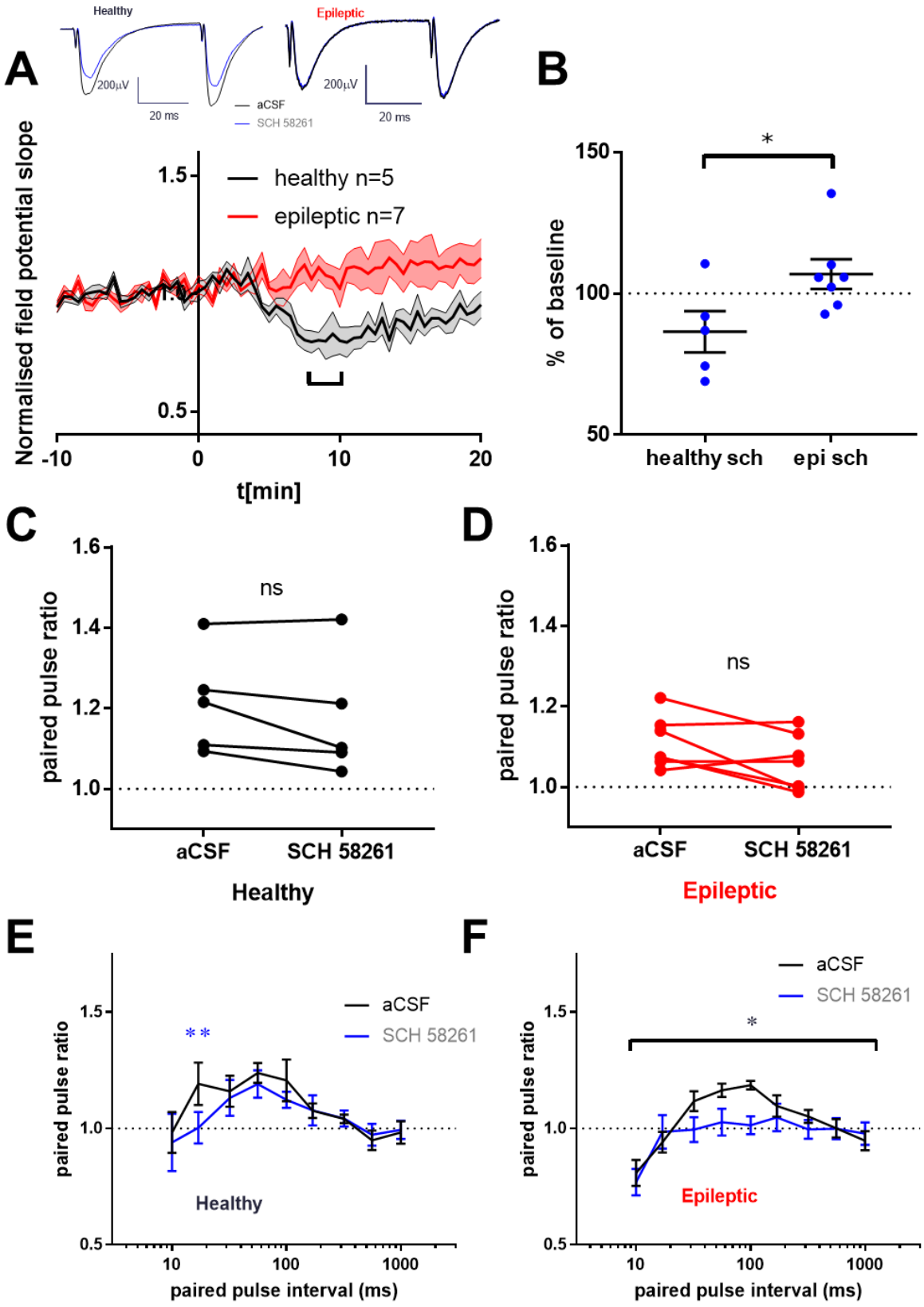

Figure 4-11: Inhibition of $A_{2A}R$ through SCH 58261 (100 nM) has different effects on field potentials in healthy and epileptic hippocampal slices. A: Application of SCH 58261 (at t[min]=0)

transiently reduces slopes of normalised field potentials in healthy hippocampal slices but not in epileptic hippocampal slices. Insets show representative field potential waveforms at the 8 – 10 min peak of effect in healthy slices; baseline traces are averaged from 10 sweeps, SCH 58261 traces are averaged from 5 sweeps.**B:** Normalised field potential slopes averaged between 8 – 10 min following SCH 58261 application are significantly different between healthy and epileptic hippocampal slices. **C&D:** Mean ratio of 50 ms paired pulses of 10 min baseline and between 8 – 10 min following SCH 58261 application (as indicated in A) is not different in either healthy or epileptic slices. **E:** Paired pulse profiles were not altered in healthy hippocampal slices due to application of SCH 58261, except at the 17 ms interval. **F:** Epileptic paired pulse profiles were significantly different following SCH 58261 application, with PPF appearing to be inhibited between 30 ms and 100 ms. Error bars show SEM; ns: not significant; *: $P < 0.05$; **: $P < 0.01$

Application of exogenous adenosine significantly inhibited field potentials in the presence of SCH 58261 across the tested concentrations of adenosine (1 – 500 µM) in healthy and epileptic hippocampal slices, and when compared with the vehicle inhibition levels there was no significant difference due to epilepsy or drug conditions (two-way repeated measures ANOVA, significant variation due to adenosine concentration: $F(6, 120) = 236.6$, $P < 0.0001$) but no overall variation due to the consolidated condition groups of healthy/epileptic and vehicle/SCH 58261 $F(3, 20) = 1.527$, $P = 0.0843$. The interaction was not significant. Figure 4-12C&D). No differences were found at any adenosine concentration with Sidak's post-hoc comparisons.

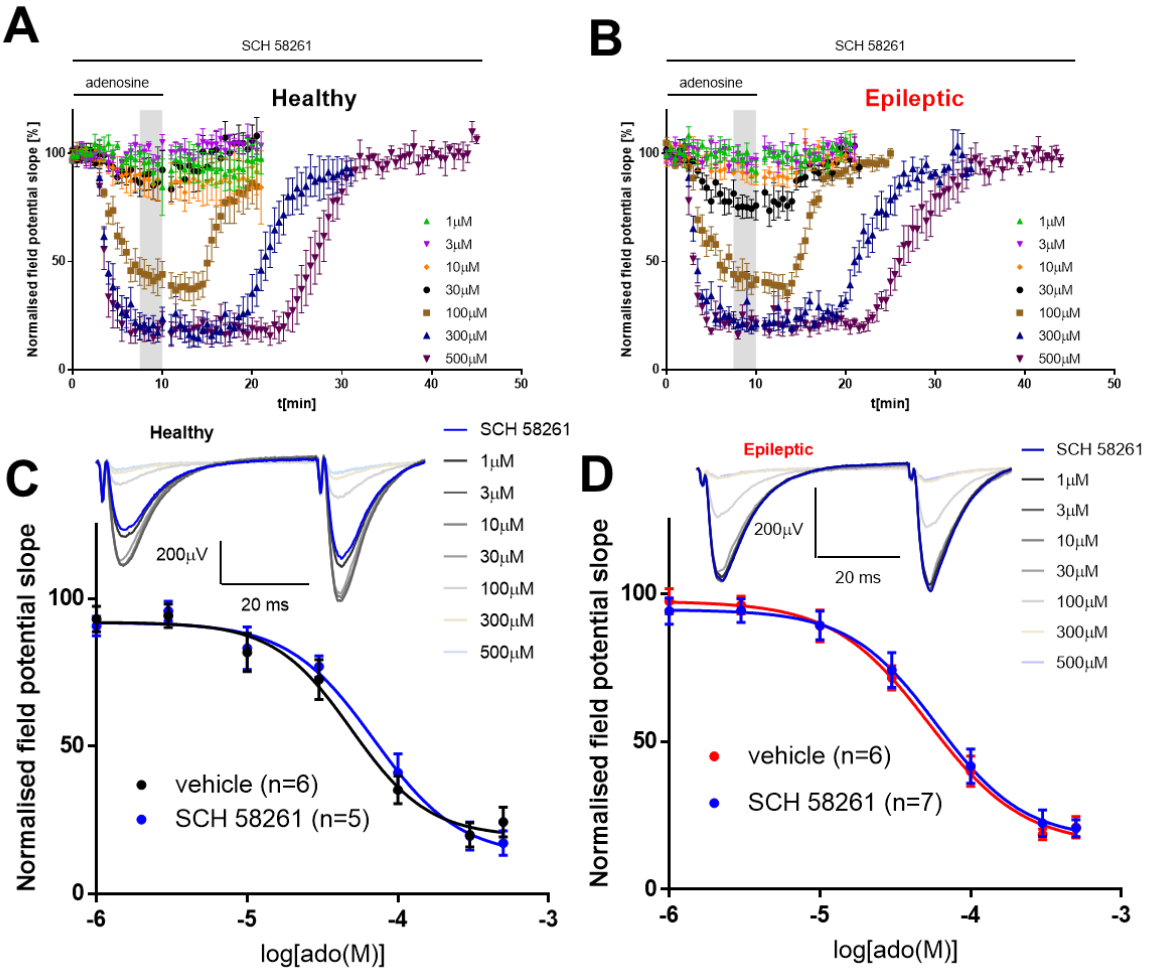

Figure 4-12: Application of SCH 58261 does not significantly change adenosine-induced inhibition in healthy or epileptic hippocampal slices. A&B: Normalised field potentials before and after wash on and off of increasing concentrations of adenosine in the presence of SCH 58261 in healthy (A) and epileptic (B) hippocampal slices. Shaded grey box indicates points from which average dose responses were calculated. **C&D:** Concentration-response inhibition curves of normalised field potential slopes in response to exogenously applied adenosine in healthy (C) and epileptic (D) hippocampal slices, in the presence of either vehicle (previously shown in Figure 4-7, presented again here for reference) or 100 nM SCH 58261. Across both healthy and epileptic hippocampal slices, adenosine significantly inhibited field potentials, and a significant overall effect was found due to SCH 58261 across both healthy and epileptic slices. Insets show representative raw field potential traces, each averaged from 10 sweeps.

Nonlinear regression fitted parameters are displayed in Table 4-6 below, with adjusted P values between healthy and epileptic inhibition parameters as well as against respective vehicle. Top values were 92.0 ± 3.5% in healthy slices and 94.7 ± 3.4 in epileptic slices; although no significant difference was found between vehicle values, it can be noted that while the top values in healthy were comparable to vehicle (92.0 ± 3.6%, as presented in Table 4-4 above), inhibition of $A_{2A}R$ using SCH 58261 appears to

have slightly increased the degree of inhibition induced by low-concentration adenosine inhibition from 97.5 ± 3.2% in vehicle by approximately 3 percentage points; this small increase in inhibition could be consistent with the theory that blockade of $A_{2A}R$ allows greater inhibitory activity of adenosine at low concentrations through A_1R due to a higher potentiating activity of $A_{2A}R$ in epilepsy. However, it should still be emphasised that although this may be consistent with the hypothesis, this increased inhibition was far from statistical significance (adjusted P = 0.4262).

Bottom values generated from nonlinear regression fit the inhibition plateau as 16.8 ± 4.9% of baseline in healthy, and 17.0 ± 6.1% of baseline in epileptic – no significance was found in comparison with each other or vehicle bottom values, (adjusted P > 0.9 for all). The IC_{50} for healthy and epileptic adenosine-induced inhibition was 69.2 µM and 59.5 µM respectively, and the Hill slope was -1.5 in both conditions. No significance was detected between healthy and epileptic, or against respective vehicle inhibition curves.

Parameter	SCH 58261		P value		
± Standard error	Healthy	Epileptic	Healthy vs epileptic	Healthy vs veh	Epileptic vs veh
n	**5**	**7**			
Bottom (%)	12.6 ± 7.1	17.0 ± 6.1	>0.9999	0.901	0.9251
Top (%)	92.0 ± 3.5	94.7 ± 3.4	0.6300	>0.9999	0.4262
$LogIC_{50}$	-4.2 ± 0.1	-4.2 ± 0.1	0.8402	0.2136	0.7785
IC_{50} (µM)	69.2	59.5			
Hill slope	-1.5 ± 0.5	-1.5 ± 0.4	0.9999	0.086	0.9286

Table 4-6: Summary of adenosine-induced inhibition nonlinear regression parameters in the presence of SCH 58261: log(adenosine [µM]) vs. response - Variable slope (four parameters). P values displayed are adjusted for multiple comparisons using Sidak's post-hoc test.

The ongoing 50 ms paired pulse stimulations were measured during maximal inhibition at each adenosine concentration, with the aCSF and SCH 58261 PPRs previously represented in Figure 4-11D&F, and the mean PPRs of the increasing adenosine concentrations in the presence of SCH 58261 are presented in Figure 4-13A below. In SCH 58261, there was a significant difference due to adenosine concentration but not epilepsy (two-way repeated measures ANOVA, variation due to adenosine $F(7, 70) = 2.459$, $P = 0.0258$; variation due to epilepsy $F(1, 10) = 1.367$, $P = 0.2695$). No

differences were found between healthy and epileptic at each adenosine concentration from Sidak's family-wise post-hoc comparisons.

There was no overall significant effect of adenosine concentration against SCH 58261 baseline in healthy PPPs (in healthy slices: two-way repeated measures ANOVA: variation due to adenosine F (3, 12) = 1.856, P = 0.1893; variation due to PPI F (8, 32) = 3.18, P = 0.0091). Dunnett's family-wise post-hoc tests found significance from SCH 58261 baseline at 300 µM adenosine, with the 100 ms interval significantly different from baseline (adjusted P = 0.0285). Figure 4-13D. In epileptic slices, the overall variation was not significant (variation due to adenosine F (3, 18) = 5.408, P = 0.0079; variation due to PPI F (8, 48) = 2.599, P = 0.0191. The interaction was very significant F (24, 144) = 2.629, P = 0.0002). At 300 µM adenosine, the 10 ms PPR was significantly different from the same interval at SCH 58261-only baseline (adjusted P < 0.0001), as were the 100 ms (adjusted P = 0.0136) and 557 ms intervals (adjusted P = 0.0424, Dunnett's multiple comparisons test; Figure 4-13E).

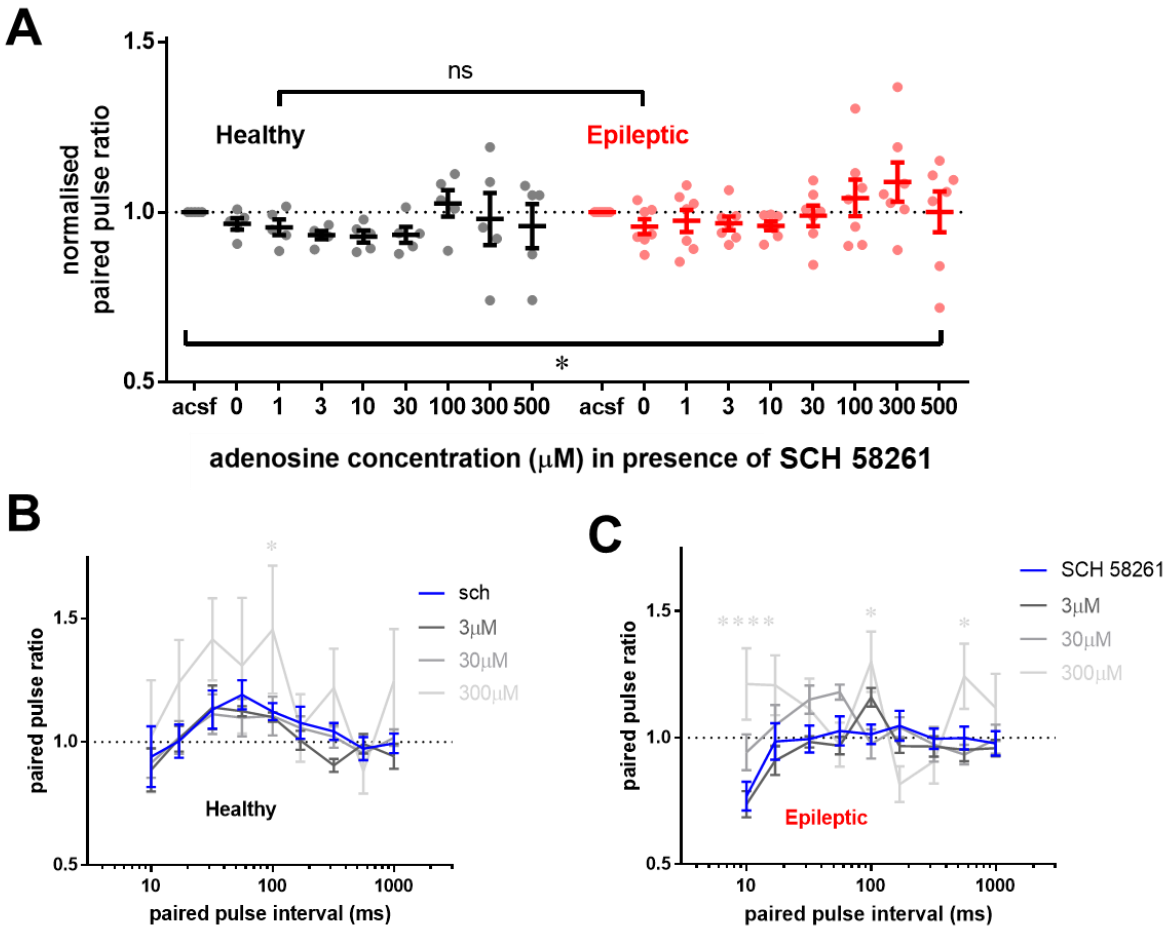

Figure 4-13: Increasing adenosine concentration in the presence of SCH 58261 modified PPF, but no difference between healthy and epileptic tissue. A: Average 50 ms PPR at each adenosine concentration of adenosine in the presence of SCH 58261, normalised to the pre-SCH 58261 baseline

PPR. A significant effect of adenosine was found, but no significant difference between healthy and epileptic responses. **B&C:** Paired pulse profiles in healthy (B) and epileptic (C) hippocampal slices in the presence of SCH 58261 and increasing concentrations of adenosine are overall not significantly different, with some exceptions at 300 µM at some PPIs in both healthy and epileptic. ns: not significant; *: $P < 0.05$; ****: $P < 0.0001$.

4.4.5. Interaction between CBD and network response to exogenously applied adenosine

Having assessed the contribution of A_1Rs and A_{2A}Rs to healthy and epileptic network activity in the presence of exogenous adenosine, CBD was once again tested. In Chapter 3, 10 µM CBD appeared to have a modulatory effect on the network inhibition associated with evoked endogenous adenosine release. This effect could either have been an effect of the high levels of stimulation to the Schaffer collaterals by which adenosine release was induced, or possibly a direct modulatory activity on receptors regardless of previous network activity. To see whether this might be due to an overall change in how adenosine receptors respond to adenosine in epilepsy, the above experiments probing network response to increasing concentrations of adenosine were once again performed, this time in the presence of 10 µM CBD.

To assess any immediate change to basal activity due to CBD, the normalised field potentials and paired pulse properties were assessed in the 10 – 20 min immediately following wash-on of CBD. Normalised LFP slopes in both healthy and epileptic hippocampal slices were unaffected following CBD application (healthy LFPs between 10 – 20 min following CBD application 105.7 ± 3.34% of baseline, epileptic 98.1 ± 2.45%; $P = 0.0843$, unpaired t-test; Figure 4-14A-B). PPRs in the same time frames were also not different in either healthy or epileptic hippocampal slices (healthy PPRs prior to CBD application: 1.2 ± 0.04, after CBD application 1.2 ± 0.04, $P = 0.7057$ paired t-test; Figure 4-14C. Epileptic PPRs: 1.2 ± 0.06 before CBD application, 1.2 ± 0.06 after CBD, $P = 0.5934$, paired t-test; Figure 4-14D). PPPs were also not significantly different following the application of CBD (healthy hippocampal slices, variation due to CBD $F(1, 5) = 0.9849$, $P = 0.3665$; variation due to paired pulse interval $F(8, 40) = 3.014$, $P < 0.0096$; Figure 4-14E. Epileptic hippocampal slices, variation due to CBD $F(1, 7) = 1.187$, $P = 0.3120$; variation due to PPI $F(8, 56) = 3.675$, $P = 0.0017$; Figure 4-14F).

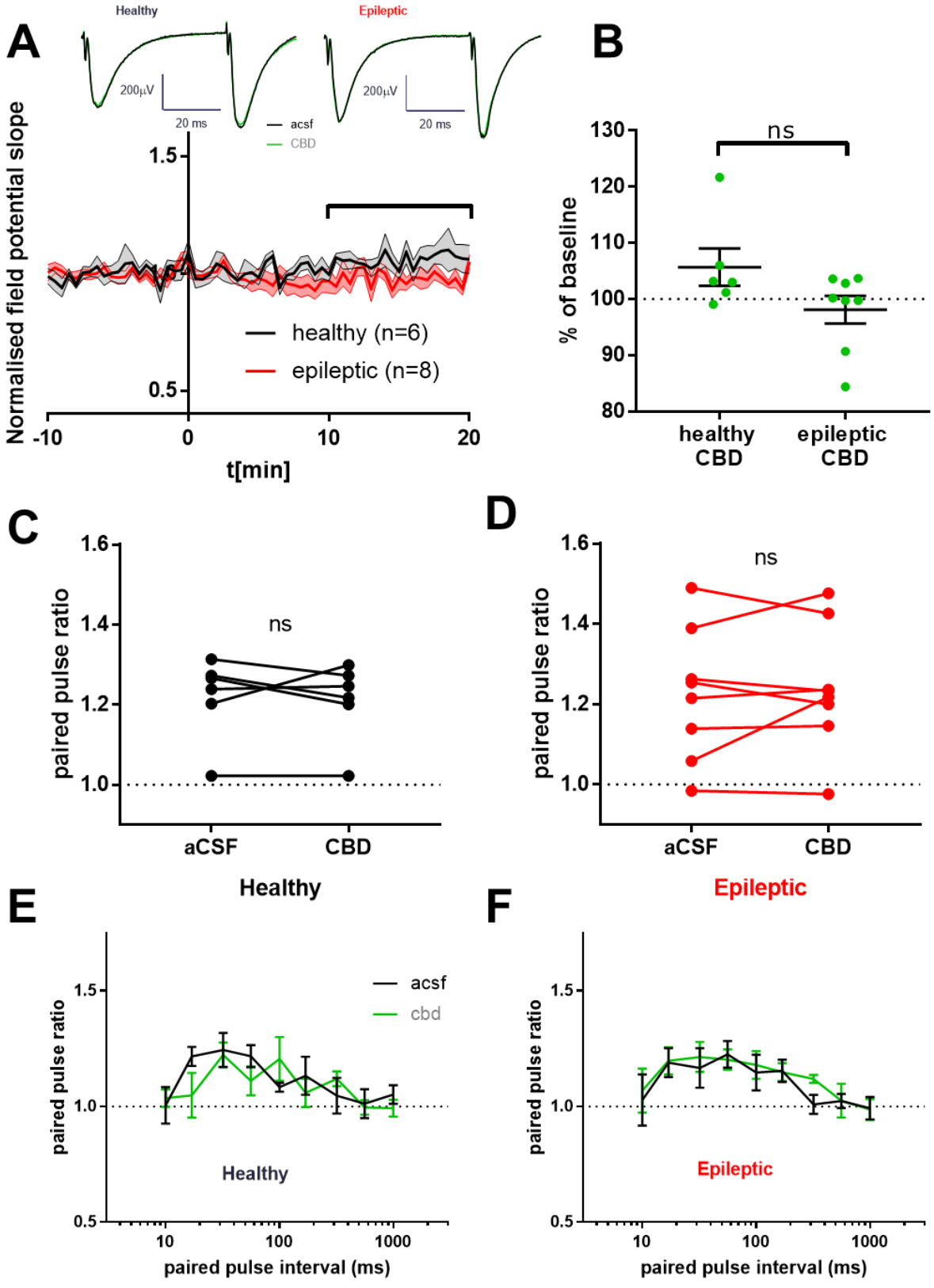

Figure 4-14: No change between healthy and epileptic evoked field potentials upon bath application of 10 μM CBD. A: Normalised field potential slopes against time, following initial

application of CBD at t[min]=0 in healthy and epileptic hippocampal slices. Insets show representative field potential traces before and after CBD application in healthy and epileptic traces. All traces are averaged over 10 sweeps. **B:** No significant difference between normalised field potential slopes mean between 10 – 20 min (as indicated in A) of healthy and epileptic animals following CBD application. **C&D:** Mean paired pulse ratio at 50 ms intervals during 10 min baseline and between 10 – 20 min following CBD application (as indicated in A) is not significantly different in healthy (C) or epileptic (D) hippocampal slices. **E&F:** No change in paired pulse profile before and after CBD application in healthy (E) or epileptic (F) hippocampal slices.

Application of exogenous adenosine was able to significantly inhibit field potentials in the presence of CBD across the tested concentrations of adenosine (1 – 500 µM) in healthy and epileptic hippocampal slices, but when compared with the vehicle inhibition levels there was no significant difference due to the consolidated groups of healthy/epileptic and vehicle/CBD (two-way repeated measures ANOVA, significant variation due to adenosine concentration: $F(6.\ 60) = 157.9$, $P < 0.0001$; no overall variation due to epilepsy or CBD; $F(3, 22) = 1.407$, $P = 0.2675$; Figure 4-15C&D). A two-way ANOVA rather than three-way was used due to unequal dataset sizes preventing the analysis from being run in Graphpad Prism. Sidak's multiple comparisons across the groups within each adenosine concentration found a significant difference in the healthy CBD inhibition curve at the 100 µM adenosine point (adjusted $P = 0.0031$ against healthy vehicle, also $P < 0.05$ against both epileptic vehicle and epileptic CBD), as well as at 300 µM (adjusted $P < 0.05$ against healthy vehicle and epileptic vehicle).

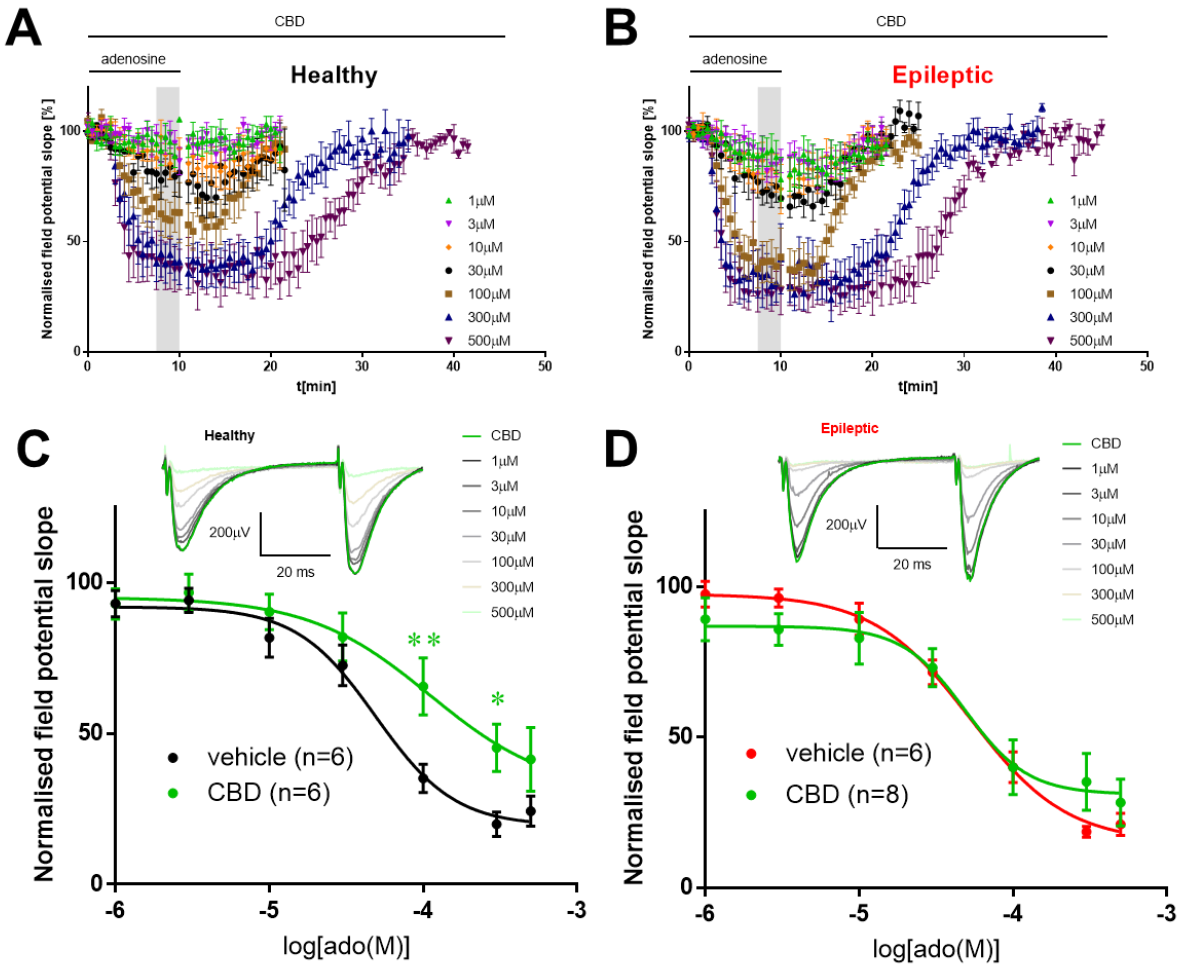

Figure 4-15: CBD decreases field potential response to exogenously applied adenosine in healthy hippocampal slices at high concentrations, and increases adenosine-induced inhibition by lower concentrations of adenosine in epileptic tissue. A&B: Mean normalised field potential response to wash on and off of increasing concentrations of adenosine in healthy and epileptic hippocampal slices. Grey box indicates plateau from which mean adenosine-induced inhibition response was taken for each concentration. **C&D:** Concentration-response inhibition curves of normalised field potential slopes in response to exogenously applied adenosine in healthy (C) and epileptic (D) hippocampal slices, in the presence of either vehicle (previously shown in Figure 4-7, presented again here for reference) or 10 µM CBD. Across both healthy and epileptic hippocampal slices, adenosine significantly inhibited field potentials up to 500 µM. Sidak's multiple comparisons across the groups within each adenosine concentration found a significant difference in the healthy CBD inhibition curve at the 100 µM adenosine point against healthy vehicle, as well as at the 300 µM point against healthy vehicle and epileptic vehicle.

Fitted parameters from nonlinear regression of adenosine-induced inhibition curves are presented in Table 4-7 below. The fitted top value of the inhibition curve at low concentrations of adenosine was 93.6 ± 5.8% of baseline in healthy, and 89.3 ± 4.7% in epileptic tissue; these were not significantly different from each other, but the fitted top value in epileptic tissue in the presence of CBD was

significantly decreased from the same value in vehicle (97.5 ± 3.2% as shown in Table 4-4 above; adjusted P = 0.0012). This indicates that CBD increases the inhibitory potential of lower concentrations of adenosine at in epileptic tissue, but not healthy.

The inhibition plateau reached between 300 µM to 500 µM was fitted to bottom values by nonlinear regression as 22.9 ± 23.3% of baseline field potential slope in healthy hippocampal slices, and 23.3 ± 6.2% of baseline in epileptic hippocampal slices; no difference found between either healthy and epileptic or against respective vehicle; see Table 4-7). However, it can be observed that in healthy slices there is a higher degree of variation than previously at the higher concentrations of adenosine, which may confound statistical analyses. The epileptic bottom value is also nonsignificantly higher than seen in vehicle, with a comparable error, as opposed to the large error seen in healthy tissue.

The IC_{50} value of adenosine in the presence of CBD in healthy tissue was 97.4 µM; this represents a significant increase from adenosine in presence of vehicle only (49.2 µM; P = 0.0017), as well as from the IC_{50} in epileptic tissue in CBD (43.5 µM; P = 0.0054). This seems to suggest that CBD diminishes the ability of high concentrations of adenosine to inhibit field potentials, which is not seen in epileptic hippocampal slices. As can be inferred from Figure 4-16A, the mean inhibition curve of adenosine in CBD may not reach a satisfactory inhibition plateau (also reflected in the bottom parameter fit values for this curve), which again may confound analyses of IC_{50} and Hill slope. However, this possible decrease in the ability of high concentrations of adenosine to induce inhibition in the presence of CBD is an unexpected finding; coupled with the high degree of variation seen within this group of recordings, this would benefit from further investigation to assess the accuracy of this finding.

The Hill slopes of the inhibition curves in the presence of CBD had a greater variability than other interventions (with the exception of 8-CPT); in healthy hippocampal slices, Hill slope was fitted to -1.1 ± 0.7, and in epileptic Hill slope was determined to be -2.0 ± 0.8. However, for the reasons discussed above regarding IC_{50}, the fitted parameter values for healthy inhibition curves in the presence of CBD may benefit from further investigation and/or n numbers due to the high variability; accordingly, there is not quite statistical significance between the two (P = 0.0539). It may be worth noting, however, that this Hill slope (healthy CBD) is the closest of all recorded to unity, suggesting a single binding site, whereas on epileptic slices the Hill slope of -2 suggests a high degree of cooperativity.

Parameter	CBD		P value		
± Standard error	Healthy	Epileptic	Healthy vs epileptic	Healthy vs veh	Epileptic vs veh
n	**5**	**7**			
Bottom	22.9 ± 23.3	23.3 ± 6.2	0.9999	0.8141	0.3111
Top	93.6 ± 5.8	89.3 ± 4.7	0.2129	0.8592	**: 0.0012
$LogIC_{50}$	-4.0 ± 0.3	-4.4 ± 0.1	**: 0.0017	**: 0.0054	0.5705
IC_{50} (µM)	97.4	43.5			
Hill slope	-1.1 ± 0.7	-2.0 ± 0.8	0.0539	0.2721	0.2387

Table 4-7: Summary of adenosine-induced inhibition nonlinear regression parameters in the presence of 8-CPT: log(adenosine [µM]) vs. response - Variable slope (four parameters). P values displayed are adjusted for multiple comparisons using Sidak's post-hoc test.

The ongoing 50 ms paired pulse stimulations were again assessed during maximal adenosine-induced inhibition, with the aCSF and CBD PPRs previously represented in Figure 4-14E&F, and the mean PPRs of the increasing adenosine concentrations in the presence of CBD are presented in Figure 4-16A. There was no significant difference across the range of adenosine concentrations due to either adenosine concentration or epilepsy, with PPRs remaining generally the same as pre-CBD baseline through adenosine concentrations (two-way repeated measures ANOVA, variation due to adenosine $F(7, 84) = 1.186$, $P = 0.3196$; variation due to epilepsy $F(1, 12) = 0.0146$, $P = 0.9058$). However, a small increase can be seen in healthy tissue at high concentrations of adenosine; the high variation in PPR in epileptic tissue makes this difficult to ascertain for epilepsy; additionally, as there was no significant finding of adenosine concentration on PPR in vehicle, it is also difficult to draw conclusions regarding presynaptic activity of CBD based on these data.

There was no significant effect of adenosine concentration against CBD baseline in either healthy or epileptic PPPs (in healthy slices: two-way repeated measures ANOVA: variation due to adenosine $F(3, 15) = 1.856$, $P = 0.1804$; variation due to PPI $F(8, 40) = 5.804$, $P < 0.0001$; Figure 4-16B. In epileptic slices: variation due to adenosine $F(3, 21) = 0.3471$, $P = 0.7916$; variation due to PPI $F(8, 56) = 3.837$, $P = 0.0012$; Figure 4-16C). Adjusted P values for each PPI were obtained by family-wise comparisons using Dunnett's test, and found significant differences from baseline at 300 µM adenosine at 17 ms and 32 ms PPI in healthy hippocampal slices, as well as a significant PPF at 10 ms in epileptic hippocampal slices also at 300 µM adenosine.

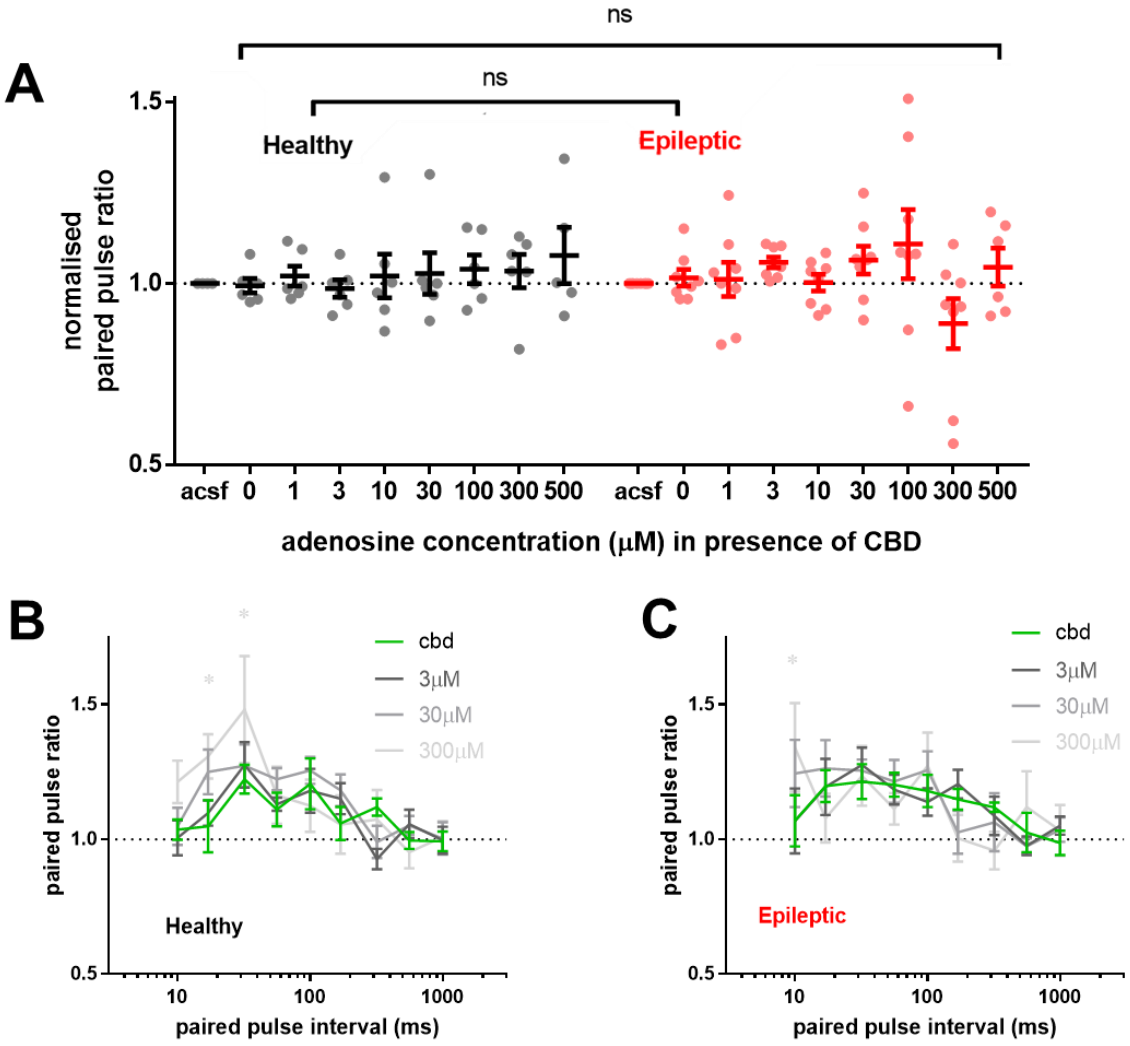

Figure 4-16: CBD does not significantly modulate PPF between healthy and epileptic tissue (or from vehicle). A: Paired pulse ratios at 50 ms intervals in the presence of CBD did not change at increasing concentrations of adenosine. **B:** Paired pulse profiles in healthy hippocampal slices in the presence of CBD and increasing concentrations of adenosine are overall not significantly different. At 300 µM, paired pulse ratios at 17 ms and 32 ms interval are significantly different from baseline**. C:** Paired pulse profiles in epileptic hippocampal slices in the presence of CBD with increasing adenosine concentrations are not significantly affected by adenosine. At 300 µM adenosine, the 10 ms PPR was significantly different to the same interval at CBD-only baseline. *: adjusted $P < 0.05$.

4.5. Discussion

Since it was demonstrated that exogenous adenosine exhibited inhibitory properties on induced ictal events in rodent slices in vitro (Dunwiddie, 1980) and that around 65 µM adenosine can be released from epileptogenic hippocampus following seizures in human patients (During and Spencer, 1992), it has been generally accepted that adenosine release following seizures promotes seizure termination (Dragunow et al., 1985). Previous investigatory efforts into adenosine-based epilepsy therapy have

therefore focused on the augmentation of extracellular adenosine to increase activation of the inhibitory adenosine A_1R. Adenosine augmentation might have therapeutic efficacy in healthy hippocampus, with the abundance of inhibitory adenosine A_1 receptors - and indeed the majority of preclinical studies examining the inhibitory properties of adenosine have focused on acute seizures models in otherwise healthy animals (Boison, 2012a).

In this chapter, the interaction between increased adenosine concentration, adenosine receptors and adenosine in chronic epileptic hippocampus (at least 4 months from the confirmation of SRS) was more closely interrogated. The putative modulatory effect of CBD, a potential finding indicated by results in the previous chapter, was also assessed in healthy and epileptic hippocampal slices in the presence of high concentrations of exogenous adenosine.

4.5.1. Network activity in chronic epilepsy

So as to be able to compare the contribution of the two adenosine receptors under investigation between healthy tissue and the chronic epileptic condition, the overall synaptic connectivity of hippocampal Schaffer collaterals in both conditions were probed. Of note, while input/output curves generated did not show significant difference between field potential properties evoked in healthy and epileptic hippocampal slices, indicating that initial release probability was not changed in epileptic hippocampus, there was a significant decrease in PPF in epileptic tissue. This decrease in PPF is consistent with literature on seizures and epilepsy (Wilson et al., 1998; Pena et al., 2002; Chen et al., 2018).

Paired pulse stimulations are a useful method to investigate presynaptic release mechanisms of neurotransmitters. The PPF or paired pulse depression (PPD) which can occur at different intervals between two pulses can provide information as to the neurotransmitter release and presynaptic calcium (Zucker and Regehr, 2002). In this case, the decrease of PPF at 50 ms in chronic epileptic hippocampus is indicative of a decreased chance of transmitter release in epilepsy, possibly due to pathological presynaptic calcium modulation. If paired pulse stimulations had been used in Chapter 3, we may have been able to gain information on presynaptic release potential during and after high-frequency stimulation.

However, the overall PPRs we obtained from healthy tissue, a mean of 1.3 ± 0.02, is lower than the ratio of 1.5 which has been reported in literature for healthy Schaffer collateral stimulations using multielectrode arrays (Steidl et al., 2006; Chong et al., 2011). The reason for this is unknown, as factors such as age of the rats (~5 – 6 months old), or the possibility of hypoxia due to method of stimulation and recording (slice lying on a flat MEA surface) would either be unlikely to decrease PPF, or be more likely to increase PPF (Tanaka et al., 2001; Arias-Cavieres et al., 2017). Some possible reasons which could require troubleshooting or experimental improvements include decreased detection capacity of the

recording electrodes due to the dead cell layer against the electrodes dampening field response detection; this could be improved through use of a 3D MEA, in which the electrodes "spike" into healthier fibres further into the slice (this technique was used by Steidl et al. (2006) to record the PPF of 1.5). Additionally, Tanaka et al. (2001) observed that the higher the stimulation intensity, the lower the PPF; it could be plausible that in this study, the stimulation intensity required to achieve a response through a dead cell layer may have over-stimulated the fibres and reduced PPR overall.

4.5.1.1. Dysregulation of adenosine receptors in epilepsy

Findings described here have shown a decrease of A_1R protein expression in the hippocampus of chronic epileptic rats, which is consistent with previous studies in the cortex of kindled rats and in human patients (Glass et al., 1996; Rebola et al., 2005). Based upon other seizure and epilepsy studies (Rebola et al., 2005; Barros-Barbosa et al., 2016), a parallel increase in $A_{2A}R$ had been expected but was unable to be shown in epileptic hippocampus here. This was likely due to the low expression of $A_{2A}R$ in hippocampus along with the low volume of protein able to be extracted from isolated rat hippocampus resulting in being unable to detect a specific binding signal from radiolabelled SCH 58261. No transcriptional differences were observed in either A_1R (*Adora1)* or $A_{2A}R$ (*Adora2a*), indicating that the observed decrease in A_1R binding is a most likely a post-translational effect; possibly due to a decrease in membrane-trafficking following transcription. As K_D was not changed between healthy and epileptic hippocampus, this indicates that the affinity has not changed, ruling out the possibility of a conformational change to the membrane-bound A_1R protein decreasing affinity for [^{3}H]-CCPA. The lack of a detectable difference in $A_{2A}R$ mRNA also does not preclude a post-translational effect. Additionally, although no transcriptional difference was seen across any treatment groups, post-translational modifications on either receptor due to chronic CBD treatment also cannot be ruled out.

Electrophysiological comparisons between healthy and epileptic acute hippocampal slices (in the presence of vehicle only) showed no significant difference in their response to exogenously applied adenosine. This contrasts with the observed response to endogenously released adenosine in chapter 3, where epileptic hippocampal networks showed a reduced adenosine potency when compared with healthy. However, in the previous chapter, the sensor-recorded adenosine peaks post-stimulation in control conditions were 0.26 ± 0.04 µM' and 0.37 ± 0.05 µM' for healthy and epileptic hippocampal slices respectively – additionally, the biosensor values include unknown concentrations of adenosine metabolites, indicating that the actual concentration of adenosine in these situations is lower than the micromolar prime measurement suggests. These recorded adenosine concentrations correspond with peak post-stimulation inhibition at 27 ± 3% (healthy) and 25 ± 9% (epileptic) of baseline LFP slope (section 3.6) This degree of inhibition would correspond to approximately the 100 - 300 µM bracket of

exogenously applied adenosine in this chapter, an almost hundred-fold difference between biosensor-recorded endogenous adenosine concentration and bath applied exogenous adenosine. This clearly indicates that the two assays are of vastly different mechanics – the adenosine-releasing stimulation involved 20 Hz stimulation across the CA1, thereby activating a multitude of signalling responses for a transient effect (time to peak generally occurred within 1 min post-stimulation), whereas in this chapter, adenosine application was the only independent variable on the hippocampal networks and was measured once a plateau had been reached. Investigating the effect of blocking A_1R using 8-CPT on basal field potentials showed that network activity was potentiated, both in healthy and epileptic hippocampi but less so in epilepsy. The observed potentiation of healthy hippocampal slices (137.2 ± 4.21% of baseline) is consistent with previously reported LFP potentiation values following A_1R blockade, such as 145 ± 4.0% of baseline in adult WT mouse hippocampal slices following DPCPX application (Diogenes et al., 2014). The same study reported a decreased potentiation in mice overexpressing ADK at 118 ± 4.1% of baseline, comparable to the 123.5 ± 2.24% in epileptic hippocampus seen in this chapter. This similarity suggests that the decreased potentiation could be due to a decrease in basal adenosine tone, from increased uptake of adenosine by astrocytes (the ADK theory of chronic epilepsy (Boison, 2012b)), or it could also be a loss in function of A_1R related to the observed decreased in receptor expression. Alternatively, both theories could be true in conjunction. However, a significant difference in adenosine-induced inhibition was found between healthy and epileptic hippocampal slices at 300 µM, with the epileptic LFPs more potentiated at that concentration of adenosine. As the basal level of endogenous adenosine is likely to have little influence at these exogenous concentrations, this effect is likely to be due to the decrease of A_1R expression in epilepsy.

A decrease in adenosine tone could also potentially underlie the lack of field potential response in epileptic tissue to blockade of $A_{2A}R$ with the antagonist SCH 58261, as there was a clear transient effect in healthy which was not seen in epileptic hippocampus. However, the overall lack of functional effects observed with SCH 58261 application in epilepsy, following initial exposure and with exogenous adenosine, appears to contradict studies that have suggested a gain in function of $A_{2A}R$ in pathology, including epilepsy (Barros-Barbosa et al., 2016). Barros-Barbosa and colleagues describe an increase in $A_{2A}R$ expression in human TLE hippocampus, generally co-localised with astrocytic markers and increasing with astrogliosis. This suggests a primarily astrocytic rather than presynaptic expression of $A_{2A}R$ in epileptic hippocampus, where it has been shown that $A_{2A}R$ activation inhibits synaptic glutamate uptake (Matos et al., 2012a). Rombo et al. (2015) demonstrated how selective expression of $A_{2A}R$ on excitatory glutamatergic-glutamatergic and inhibitory GABAergic-GABAergic synapses, but not detectable on synapses between pyramidal cells and interneurons, allows for a very effective increase of network excitability by activation of $A_{2A}R$ leading to inhibition of interneurons. As these studies describe

effects of $A_{2A}R$ activation, further studies could use $A_{2A}R$ agonism to interrogate the epileptic hippocampal network further, as well as the balance between neuronal and astroglial expression.

4.5.1.2. Paired pulse stimulations and adenosine receptors

In addition to the smaller than expected overall PPR, discussed above in section 4.5.1, the lack of change of PPR in the presence of increasing concentrations of exogenous adenosine was unexpected. With the strong expression of inhibitory A_1Rs on presynaptic terminals, and the clear inhibitory effect of exogenous adenosine on field potentials, the clear expectation would be an increase in PPF. Indeed, any increase in facilitation due to hypoxia is due to endogenous adenosine release acting on A_1R at presynaptic terminals (Tanaka et al., 2001). It is possible that enhanced PPF is particularly seen when adenosine is released endogenously, possibly due to co-localisation of presynaptic ENT1 and presynaptic A_1R; this would mean that any adenosine released from neurons would preferentially activate presynaptic A_1R and thereby increase PPF (Brundege and Dunwiddie, 1996). By applying exogenous adenosine, this may be allowing the preferential activation of postsynaptic A_1R, which has less of a detectable effect on the PPF. This could be assessed through the use of $BaCl_2$, to block postsynaptic potassium currents and isolate presynaptic activity of exogenous adenosine. This could then be compared with a single-cell experiment, such as by Brundege and Dunwiddie (1996), in which a high concentration of adenosine is loaded into a cell by glass electrode. It was noted in this study that, although 5 mM adenosine was loaded intracellularly, only an estimated 1.5 µM of adenosine reached presynaptic receptors and was able to induce strong PPF.

This endogenous-adenosine possibility of PPF can also be seen in the differential responses in presence of adenosine receptor antagonists. Inhibiting A_1R with 8-CPT significantly decreased PPRs when initially applied, indicating that there was a basal activation of presynaptic A_1Rs in both healthy and epileptic slices; similarly to the overall potentiation of field potentials, the effect was less pronounced in epileptic tissue. This smaller decrease in PPF again indicates less basal adenosine acting on presynaptic A_1R, less A_1R expressed on presynaptic terminals for adenosine to have an effect on, or a combination of both factors.

The decrease in PPR across approximately 30 ms to 100 ms following application of SCH 58261 in epileptic tissue is also an indication of some sort of basal endogenous adenosine having a pathological effect in the epileptic hippocampus. With $A_{2A}R$ blocked by SCH 58261, this finding indicates that there was some form of $A_{2A}R$-mediated mechanism of presynaptic release that has developed as a result of epileptogenesis, as the effect was not seen in healthy tissue.

Broadly, paired pulse stimulations in the presence of increasing concentrations of adenosine did not change significantly from the pre-adenosine baseline, in whichever vehicle or drug had been applied.

The higher concentrations of adenosine generally show a greater degree of error and variation; this is due to the strongly inhibited field potentials being much more vulnerable to background noise when measuring field potential slope; a vulnerability which is magnified through the ratio calculation. This overall lack of change due to adenosine may be in line with the previous discussion about exogenous adenosine preferentially activating postsynaptic A_1Rs rather than presynaptic. In the presence of 8-CPT, it appears that 300 – 500 µM of adenosine finally "overcome" the competitive inhibition at A_1Rs and the PPR increases to around baseline or above; this may be an indication that these high concentrations of exogenous adenosine start of have an effect at presynaptic A_1Rs, but the effect is masked by the high levels of background noise.

Additionally, it was observed in the epileptic hippocampus in the presence of only vehicle and 300 µM adenosine that there was a very strong PPF at the 10 ms interval, but this was not seen at any other adenosine concentration or PPI. This could be an indication that in the epileptic hippocampus, high concentrations of adenosine induce potentiation at high-frequency repeated pulses. While 300 µM is a higher concentration of adenosine than is likely to be seen in physiological conditions, previous studies on rats and humans collecting microdialysate during seizures have estimated seizure-associated adenosine release to reach around 60-65 µM (During and Spencer, 1992), which is higher than the 30 µM at which no 10 ms potentiation was seen in this study. Additionally, a 10 ms PPI is equivalent to 100Hz, slower than the 200 – 500 Hz "fast ripples" seen in KA-treated rats and human epilepsy patients (Bragin et al., 1999). It could be possible that high adenosine concentrations might play a part in these fast ripples at stimulation intervals that were not assessed in this chapter. Although adenosine is generally seen as a broad neuroregulatory molecule, it may still play a part in the more rapid ripple-style events in the epileptic hippocampus.

Assessing the PPFs in epileptic hippocampus in the presence of 300 µM adenosine across the different drugs tested is an interesting comparison. Between vehicle, CBD, 8-CPT and SCH 58261, it is only in the presence of CBD that the 10 ms PPF is not highly significantly different from baseline ($P<0.0001$). However, the PPP at 300 µM adenosine in epileptic hippocampus is significantly different from baseline due to the baseline being so strongly depressed, and 300 µM represents the first concentration at which the PPRs recover from the 8-CPT-induced depression. Therefore, as SCH 58261 does not block the very significant PPF at 10 ms PPI, it is possible that this is the same modulation of A_1R by CBD as seen at higher concentrations in Figure 4-16A.

Decrease of PPR in PPPs in the presence of SCH 58261 in epileptic hippocampus is an effect which, unlike the transient decrease in LFPs seen in healthy but not epileptic conditions, cannot be explained by a decrease of the basal adenosine tone. The initial application of SCH 58261 has a similar profile to the decreased PPR profile of 8-CPT application, despite the two receptors having opposing effects.

However, decrease of PPR for both receptor antagonists is consistent with a recent study showing that application of caffeine, a non-specific adenosine receptor antagonist, also decreased PPR is mouse hippocampal slices (Lopes et al., 2019).

4.5.2. CBD modulation of adenosine response

CBD effect on LFPs in the presence of exogenously applied adenosine appears to elicit a different response here than following stimulation-evoked adenosine described in Chapter 3. While the first initial application of CBD appeared to have no effect in either healthy or epileptic hippocampal slices, CBD appeared to decrease the adenosine-induced inhibition of LFP at higher concentrations of adenosine in healthy hippocampus, while increasing adenosine-induced inhibition at lower concentrations of adenosine in epileptic hippocampus.

A significant finding of adenosine response in the presence of CBD is the increased inhibition at lower concentrations of adenosine (the fitted "Top" of the inhibition binding curve). Although all field potentials were normalised to pre-adenosine baseline, meaning that generally the inhibition curves start at 100%, the fitted "Top" values ranging from 92% to 97% indicate a 3% to 8% inhibition of field potentials due to adenosine between 1 – 3 µM. This is significant due to estimations of physiological levels of basal adenosine in human patients sitting around this region (During and Spencer, 1992); the estimated basal hippocampal adenosine from microdialysed human epilepsy patients was 2.33 µM in the non-epileptogenic hippocampus, and 1.8 µM in the epileptogenic hippocampus. This may suggest that at basal adenosine levels, CBD allows for increased inhibition of network activity by adenosine.

The effect of CBD on adenosine potency in healthy tissue at higher concentrations of adenosine was an unexpected finding. While a modulation in potency was not seen following stimulation in chapter 3, this effect of CBD may be one only seen at higher concentrations of adenosine, which the stimulation-evoked release did not reach; or it may be another factor confounded by the global hippocampal stimulation activating many systems and releasing excitatory neurotransmitters which might overcome any putative inhibition of A_1R by CBD. The fact that CBD inhibiting potency of high concentrations of adenosine is not seen in epileptic slices is also interesting, as the epileptic response to 8-CPT has consistently been weaker than seen in healthy tissue, possibly suggesting that this is an effect of CBD negatively modulating A_1Rs at high adenosine concentrations in healthy tissue. Additionally, while this may have implications for the use of CBD-containing products in "healthy" people, it is unlikely that CBD increases the risk of seizures via modulation of high concentrations of adenosine. No potentiation of field potentials is seen at low adenosine concentrations, and the modulatory effect of CBD only starts to be seen at concentrations of adenosine which would likely only be endogenously seen during trauma or seizure. Additionally, it is worth noting that there have been no studies reporting a proconvulsant effect

of CBD in acute or chronic models of seizure or epilepsy (Lupica et al., 2017), meaning that it is unlikely this modulation of adenosine-induced inhibition has any physiological or pathophysiological relevance.

In conjunction with chapter 3, these studies could be interpreted as suggesting that in epileptic hippocampus, CBD might have the following effects:

- decreases overall adenosine release following seizure-like stimulation
- modulates low and post-stimulation concentrations of adenosine towards greater inhibition (increases potency of adenosine at lower concentrations)

Combined, these effects of CBD appear to offer a neuroprotective role through modulation of adenosine signalling and response.

4.5.3. Conclusion

This chapter has presented findings supporting the dysregulation of adenosine receptors in chronic epilepsy. A_1Rs showed a decreased hippocampal expression at the protein level, as well as decreased function in epilepsy. However, A_{2A}R in contrast to existing literature suggesting their overexpression or gain of function in pathology such as epilepsy, this chapter showed no change in transcription, and pharmacological inhibition of A_{2A}R with SCH 58261 in hippocampal slices do not respond to exogenous adenosine as expected. Further studies, perhaps with specific A_{2A}R agonists, may be required to investigate the electrophysiological role of A_{2A}R in the RISE-SRS model of temporal epilepsy.

We have found that CBD may modulate low concentrations of adenosine to increase inhibitive potency in epileptic tissue, which aligns with our findings in Chapter 3. However, this effect seems concentration-dependent, as an overall shift in IC_{50} of adenosine was not seen. Further experiments focusing on low doses of adenosine in epilepsy are warranted, possibly at the individual cellular level to assess effect of CBD and/or receptor inhibitors in greater detail.

5. Results Chapter 3: Characterisation of ENT1 in Epilepsy and Interaction with CBD

5.1. Introduction

5.1.1. ENT1 and seizures

The connection between ENT1 blockade and increased latency to seizure onset has been documented *in vivo* and *in vitro*. In adult zebrafish injected with PTZ, pretreatment with both dipyridamole (5 – 20 mg/kg) and NBTI (5 – 15 mg/kg) increased latency to stage II or stage III seizures by up to 230 s in a dose-dependent manner (Siebel et al., 2015). This has also been shown in a lithium-pilocarpine model of seizures in rats, with NBTI either microinjected directly to bilateral hippocampi or through systemic i.p. injection prior to first pilocarpine dose. In both direct and systemic NBTI pretreatment, latency to reach Racine scale 4 was delayed around 40 min (Xu et al., 2015). Additionally, in acute brain slices, NBTI applied with aCSF to spiking CA1 pyramidal neurons significantly decreases number of action potentials (Xu et al., 2015).

These studies indicate that ENT1 plays a role in seizure formation, potentially at the single-cell level.

5.1.2. CBD inhibition of ENT1

Uptake assays showing CBD inhibition of adenosine uptake in neural cells have previously been performed in cultured microglia (Carrier et al., 2006; Liou et al., 2008) and rat striata (Pandolfo et al., 2011). In cultured EOC-20 microglia, CBD inhibited 0.5µCi tritiated adenosine uptake (1 min incubation) with an IC_{50} of 124nM, and was also found to be a competitive inhibitor with tritiated NBTI, a high-affinity ENT1 inhibitor (Carrier et al., 2006). Similarly, in microglial cells cultured from newborn rat retinas, 0.5 µM CBD inhibited [2-^{3}H]-adenosine uptake competitively with 0.02 – 0.5 µM NBTI (Liou et al., 2008). In rat striata, synaptosomes were obtained from 6-8 week Wistar rats and incubated with 22nM tritiated adenosine for 5 min. In these conditions, CBD inhibited adenosine uptake with an IC_{50} of 3.5 µM (Pandolfo et al., 2011).

Here, we assessed the ability of CBD, CBDV, and their metabolites 7-OH-CBD, 7-COOH-CBD, 7-OH-CBD and 7-COOH-CBDV for inhibiting adenosine uptake in synaptosomes obtained from rat cortex. Cortical synaptosomes were chosen for their relevance in generalised seizures, and to provide an overview of neuronal ENT1 in brain tissue separate from specific regions with specialised cellular and molecular set-up.

5.1.3. ENT1 expression between healthy and epileptic tissue

Changes in expression of ENT1 due to seizures or epilepsy has also been reported. In lithium-pilocarpine rats, ENT1 expression was shown to increase following seizures. This was shown both by Western

blotting, with ENT1 expression peaking at 24 hours following pilocarpine seizure, as well as immunohistochemistry and immunofluorescence. In these studies, ENT1 was shown to have a primarily neuronal immunoreactivity, with some co-localisation with GFAP (Xu et al., 2015; Zhang et al., 2018). Additionally, neocortical tissue removed from treatment-resistant TLE patients undergoing resection surgery displayed a strong increase in ENT1 expression compared to non-epileptic trauma brain tissue (Xu et al., 2015).

5.1.4. Chapter Aims

Following observation of a CBD-induced decrease of activity-evoked adenosine release in *in vitro* hippocampal slices, we assessed whether this effect of CBD could be due to inhibition of ENT1, and whether any difference observed between healthy and epileptic adenosine release dynamics could be due to differential expression of ENT1.

5.2. Methods and Data Analysis

5.2.1. Reuptake assay (RenaSci)

A synaptosome uptake assay was commissioned by GW Pharmaceuticals at the CRO RenaSci (Nottingham, UK; Appendix 8.3) as part of this project. The intention of the study was to assess the ability of CBD and its metabolites 7-OH-CBD and 7-COOH-CBD, as well as CBDV and corresponding metabolites, of inhibiting uptake of tritiated adenosine against a known inhibitor (dipyridamole). All experiments and procedures were performed solely by RenaSci employees with no contribution from Reading.

Preparation of synaptosomes for this study is presented in Appendix 8.3, section 8.3.2. Raw adenosine uptake data were provided by RenaSci following study completion. In summary, 4 independent experiments were run using each cannabinoid and metabolites or reference compound, with 4 different sets of 'concentration ranges' allowing for 18 concentrations between 1 nM - 100 µM to be assessed across all the compounds, but with only 10 concentrations used per experiment. Total binding and non-specific binding DPM values for each experiment were provided by RenaSci, which were then analysed by this candidate as described below.

Each assay included a 'total binding' (disintegrations per minute) DPM value with no uptake inhibition compound, as well as a non-specific binding DPM value in the presence of 50 µM dipyridamole providing transporter saturation. For each experiment, uptake inhibition curves were normalised using GraphPad Prism, with binding value set as 100% uptake and non-specific binding set as 0%. With all experiments normalised, the full range of drug concentrations could be integrated, allowing for a full analysis of the complete dataset. The 'log(inhibitor) vs. normalised response – variable slope' nonlinear

regression analysis of GraphPad Prism was used on integrated data to calculate best-fit values for $logIC_{50}$ and Hill slope for each compound. The standard error of $logIC_{50}$ values were used to compare $logIC_{50}$ values in a one-way ANOVA across all compounds; $logIC_{50}$ was used for statistical comparison due to the asymmetrical design of the doses used.

K_i (inhibition constant) values were calculated using the affinity constant (K_m) of 1 µM (Bender et al., 1980) using the Cheng-Prusoff equation for each concentration of ligand [L]:

$$Ki = \frac{IC50}{1 + [L]/Km}$$

5.2.2. Molecular biology experiments

5.2.2.1. Western blotting

Full protein quantification and Western Blotting protocol is described in section 2.3.3. In brief, healthy 'test' hippocampi were used to validate antibody blotting linearity, with protein extracted and assessed for concentration values identically to experimental samples. A range of protein concentrations, determined through comparison with known protein concentration standards of BSA, were used (10 µg – 81.2 µg (max protein possible) per well) to assess the linear detection range for the ENT1 antibody (Proteintech, Europe). As 50 µg protein per well was feasible with our lysate concentrations, was within the linear detection range of our antibody visualisation assay, and provided a reasonable signal intensity, this concentration was chosen for experimental conditions.

Dilution factors of primary and secondary antibodies are described in Table 2-16.

Each experimental group contained 5 isolated hippocampal samples (biological replicates), and each sample was run independently on between 2-5 separate 10% acrylamide gels (technical replicates). Relative band densities for technical replicates were meaned, and biological replicates were averaged for each experimental group on both observed bands. Each gel contained a PrecisionPlus Protein ladder, and a single epileptic hippocampus lysate was used as a gel control on each gel. Once optical density had been obtained from each gel band following horseradish peroxidase (HRP) chemiluminescence probing, density values were normalised to the gel control for each gel, then normalised values for ENT1 were expressed as a ratio with the corresponding GAPDH band (Marques et al., 2013).

5.2.2.2. RT-qPCR determination of gene expression

Gene expression analysis was carried out by RT-qPCR as described in section 2.3.2, using the following primer sets: ENT1 (*Slc29a1*) forward TGAAGCAGCACCACTACCTG, reverse GCCTCAGCCGGTTTGACTT; GAPDH (*Gapdh*) forward GAAGCTCATTTCCTGGTATGACAA, reverse ATGTAGGCCATGAGGTCCAC.

The gene expression ratio of ENT1 was calculated using the Pfaffl equation (Pfaffl, 2001), using an amplification factor calculated for each primer set to compare ΔC_T values of each sample against a control sample (equations detailed in section 2.3.2.4).

5.2.2.3. Statistical testing

For both Western blot and RT-qPCR data, one-way ANOVA was performed as opposed to two-way ANOVA. This was due to no tissue being available in a 'Healthy, CBD-treated' group and therefore incomplete data for two-way ANOVA comparisons. For RT-qPCR data, positive control values based on expression levels in commercial whole-brain RNA samples (Takara, Clontech) are shown only as a qualitative validation of primer and assay success and were not included in comparative statistics.

5.3. CBD Inhibits [3H]-Adenosine Uptake in Rat Brain Synaptosomes

Cannabinoid test compounds, as well as reference compound dipyridamole, were found to inhibit adenosine uptake in synaptosomes in a dose-dependent manner (Figure 5-1). Dipyridamole demonstrated the highest potency for inhibiting [3H]-adenosine uptake, with a calculated Ki value of 299nM (Table 5-1). CBD and 7-OH-CBD were approximately 3-fold less potent than dipyridamole, with Ki values of 1.29 µM and 1.10 µM respectively. CBDV displayed a weaker potency at a Ki of 2.79 µM, with 7-OH-CBDV at 5.45 µM. 7-COOH-CBD and 7-COOH-CBDV showed very weak inhibition activity, with Ki values at 12.35 µM and 11.39 µM, respectively.

A one-way ANOVA showed that logIC_{50} values of the compounds were overall significantly different ($F(6, 20) = 512.8$, $P<0.0001$). Post-hoc analyses using Tukey's multiple comparisons tests found significance between all compounds ($P<0.0001$), except between CBD and 7-OH-CBD ($P=0.5966$) and between 7-COOH-CBD and 7-COOH-CBDV ($P=0.9579$).

Compound	IC_{50} (µM)	Ki (µM)
CBD	**1.32**	**1.29**
7-OH-CBD	**1.13**	**1.10**
7-COOH-CBD	**11.68**	**11.39**
CBDV	**2.86**	**2.79**
7-OH-CBDV	**5.59**	**5.45**
7-COOH-CBDV	**12.65**	**12.35**
DIPY	**0.306**	**0.299**

Table 5-1: IC_{50} and Ki values calculated from rodent synaptosome uptake data.

Hill slope analyses were carried out to estimate single-target activity, by close approximation to unity, and are represented in Figure 5-1D. Dipyridamole was the furthest from unity (-0.742, 95% CI -0.912 to -0.6115), with cannabinoid compounds generally closer to unity (Table 5-2).

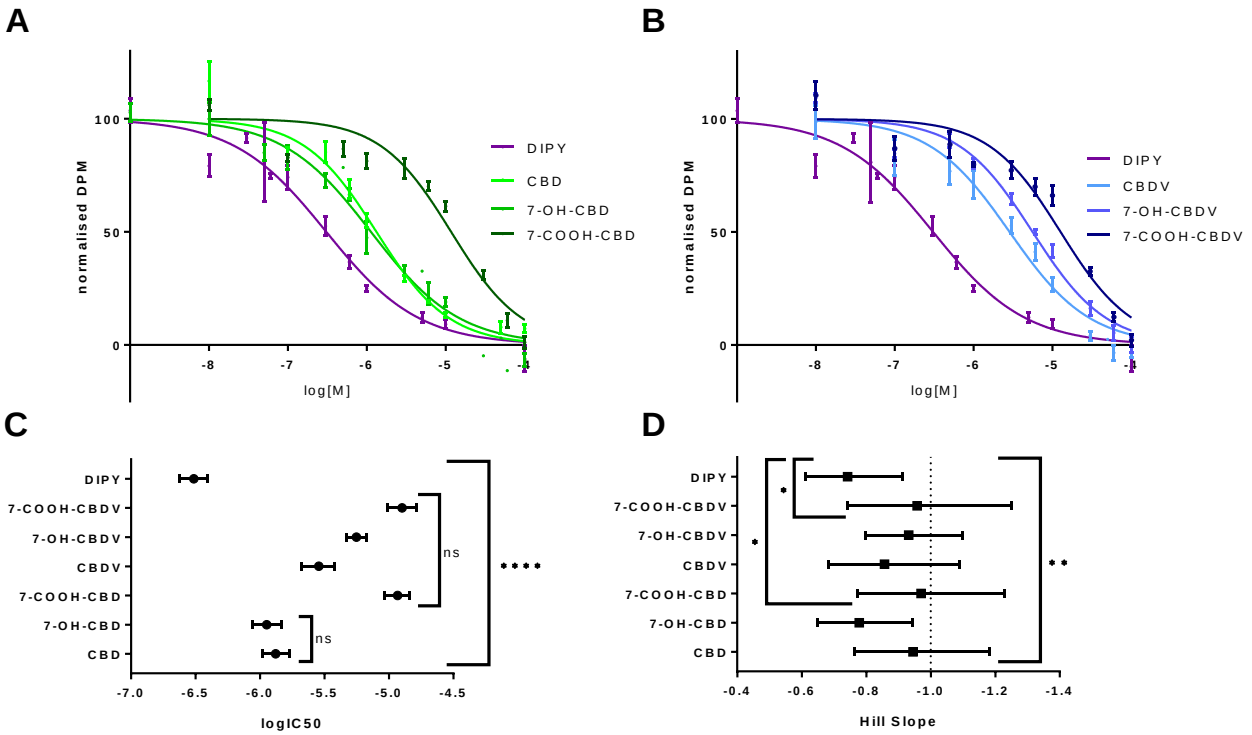

Figure 5-1: Inhibition of [3H]-adenosine uptake into rat synaptosomes by cannabinoid compounds and reference inhibitor dipyridamole. A&B: normalised dpm of synaptosome uptake experiments for dipyridamole against CBD metabolite compounds (A) and CBDV metabolite compounds (B). All compounds n=4 except CBD n=3, error bars show SEM for each dose concentration. **C:** LogIC_{50} values for each compound from nonlinear regression with 95% confidence limits. P<0.0001. **D:** Hill Slope mean values for each compound, with 95% confidence limits. **: P=0.0067 (Ordinary one-way ANOVA, Tukey's multiple comparison's post-hoc tests, *: P<0.05). **NB Experimental data shown in this figure was collected from procedures performed by the CRO RenaSci (Appendix 8.3.2). Data analysis was performed following receipt of raw data from the CRO.**

Compound	Hill slope	95% CI
CBD	**-0.945**	-1.183 to -0.7645
7-OH-CBD	**-0.778**	-0.9429 to -0.6495
7-COOH-CBD	**-0.970**	-1.23 to -0.7721
CBDV	**-0.857**	-1.088 to -0.6828
7-OH-CBDV	**-0.932**	-1.099 to -0.7973
7-COOH-CBDV	**-0.958**	-1.25 to -0.7436
DIPY	**-0.742**	-0.912 to -0.6115

Table 5-2: Hill slope and 95% CI values for all compounds in inhibiting synaptosome uptake.

5.4. Hippocampal ENT1 Gene and protein Expression Levels Are Unaltered in Epilepsy

To assess if the observed changes in adenosine release dynamics were due to changes in ENT1 expression, we used isolated rat hippocampi taken from the same experimental groups used in functional acute slice electrophysiology, with additional age-matched chronic treatment groups.

5.4.1. ENT1 protein expression

Western blotting using a specific anti-ENT1 antibody detected two clear bands – one at the predicted 50kD size, and a higher band at ~73kD (Figure 5-2A&B). Antibody manufacturer guidance had shown mouse brain lysate showing a single band at 62 kD (Proteintech, 2017), but the reason for our observed higher and lower bands in rat brain lysate is unknown (see Discussion below in section 5.5.2).

Antibody signal linearity was validated through a series dilution of protein per well using control hippocampal tissue (Figure 5-2A). A linear regression analysis including a Runs test found for the 73 kD band an R^2 value of 0.978, with the Runs test reporting no deviation from linearity ($P>0.9999$). For the 50kD band, linear regression $R^2 = 0.957$ with no deviation from linearity ($P=0.8000$). (Figure 5-2B&C). Mean density values in the 73 kD band were 1.04 ± 0.09 in healthy, 1.07 ± 0.09 in epileptic hippocampi, 0.93 ± 0.08 in the healthy vehicle-treated group, 0.94 ± 0.11 for epileptic vehicle-treated, and 0.99 ± 0.13 in the epileptic CBD-treated group. A one-way ANOVA found no difference across any groups, $F(4, 20) = 0.3689$, $P=0.8279$. Similarly, in the 50 kD band, no difference was found ($F(4, 20) = 0.5597$, $P = 0.6945$. Healthy: 1.21 ± 0.11; Epileptic: 1.13 ± 1.22; Healthy vehicle: 0.93 ± 0.03; Epileptic vehicle: 1.11 ± 0.12; Epileptic treated: 1.09 ± 0.13).

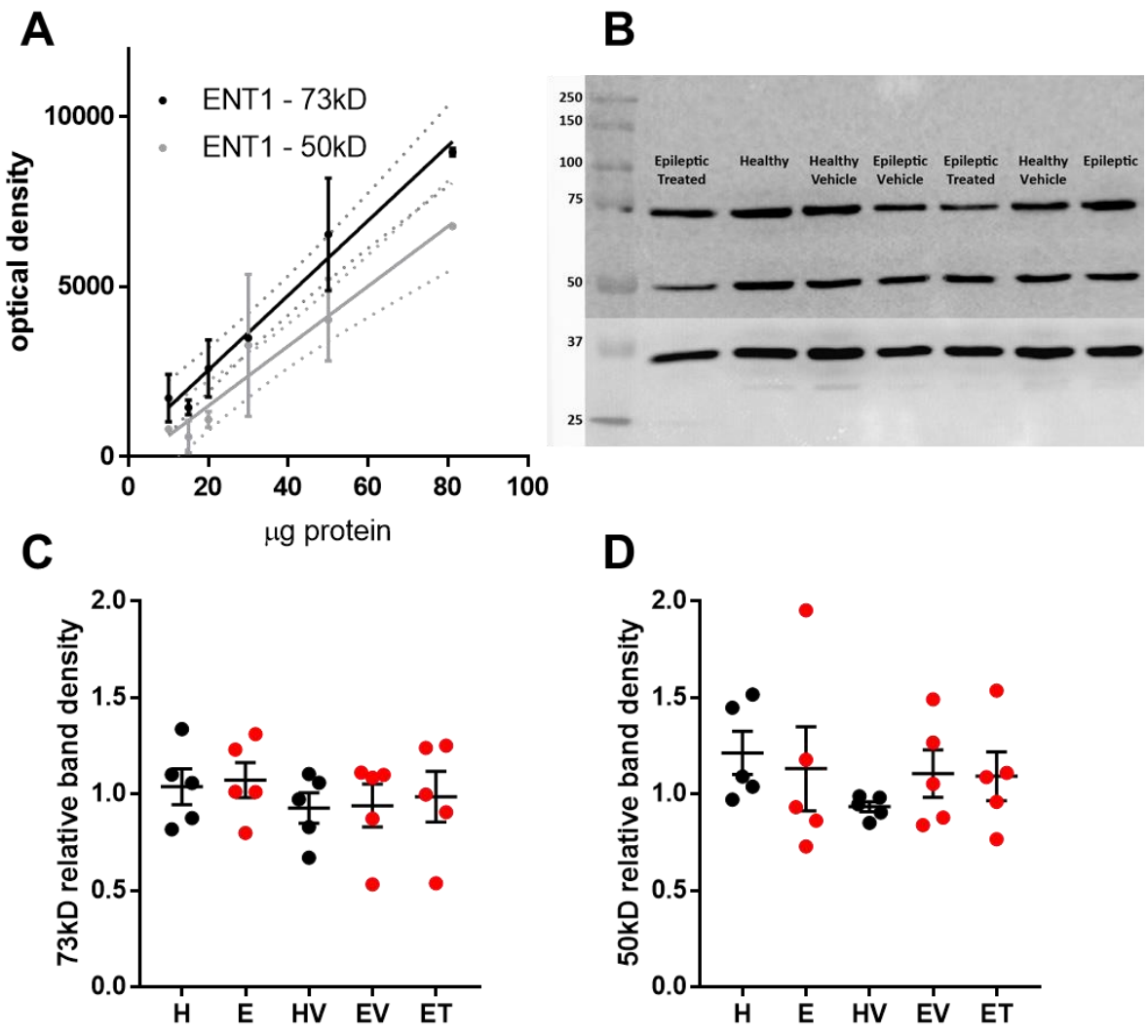

Figure 5-2: Western blot quantification of ENT1 expression showed no significant difference across experimental groups. A: Optical band densities from specific anti-ENT1 antibody blotting showing a linear increase of density data with increasing protein concentration per well. N=1-4 technical replicates per concentration, dotted lines show 95% confidence intervals. **B:** Representative gel bands for all experimental groups at 50 µg protein per well. Top 2 bands bound to anti-ENT1 antibodies; bottom band corresponded to GAPDH. **C&D:** Normalised relative band density for the two observed bands for ENT1. No difference by one-way ANOVA was found for either band. H = Healthy, no treatment; E = Epileptic, no treatment; HV = Healthy, vehicle-treated, EV = Epileptic, vehicle-treated; ET = Epileptic, CBD-treated. Error bars show mean ± SEM.

5.4.2. ENT1 gene expression

Following RT-qPCR, gene expression values were analysed for ENT1 across experimental groups as well as commercial positive control whole-brain RNA. Product specificity of the designed primers was shown through agarose gel electrophoresis of end products of positive and negative controls (Figure 5-3A), demonstrating single product amplification of primer sets as well as lack of amplification in no sample water controls. Using primer efficiencies determined from serial dilution of cDNA (Figure 5-3B), gene expression ratios were calculated for each of the experimental groups relative to a single healthy control sample. No significance differences in expression were observed across groups, determined by one-way ANOVA, $F(4, 18) = 0.3577$, $P = 0.8354$. Positive control whole-brain RNA gave a value of 13.6-fold difference compared with experimental control, with experimental group ratios as follows: Healthy 1.27 ± 0.16, Epileptic 1.13 ± 0.07, Healthy vehicle 1.26 ± 0.28, Epileptic vehicle 1.13 ± 0.12, Epileptic treated 1.35 ± 0.15.

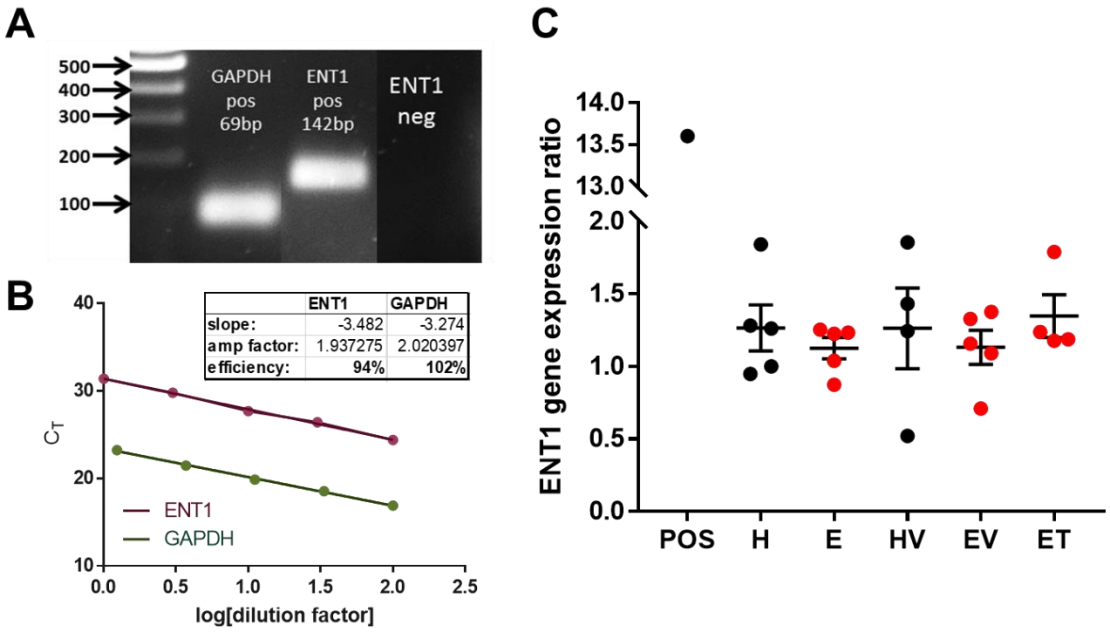

Figure 5-3: Gene expression of ENT1 measured by RT-qPCR showed no significant difference across experimental groups. A: Representative end-product bands following RT-qPCR separated via a 1.5% agarose gel electrophoresis. Positive control (pos) end products show single-band specificity corresponding to the expected amplicon product sizes. Negative control (neg) sample shows no amplification (water/no template control reactions). **B:** Calculation of primer efficiency via q-PCR of a cDNA serial dilution series. Inset: Efficiency calculations using slope from linear regression. **C:** Relative expression of ENT1 in isolated hippocampi from experimental groups (H = Healthy, no treatment; E = Epileptic, no treatment; HV = Healthy, vehicle-treated, EV = Epileptic, vehicle-treated; ET = Epileptic, CBD-treated) with total whole-brain RNA (positive control, POS) shown for reference. No significant difference in expression was found across the experimental groups. Error bars show SEM.

5.5. Discussion

5.5.1. Cannabinoid inhibition at ENT1 and antiseizure implications

CBD inhibition of ENT1 has been proposed to mediate its underlying anticonvulsant mechanism of action since its activity at the transporter was first shown (Carrier et al., 2006). The synaptosome study data described here confirmed the role of CBD on inhibiting adenosine flux through cell membranes, both neuronal and glial. Although previous work in this thesis has been hippocampal, there is no evidence of a change in isoforms within the CNS of rat ENT1; additionally, due to the widespread nature of seizures, cortical ENT1 has just as much relevance of seizures and epilepsy as hippocampal ENT1. As this study was to assess functionality of CBD (and CBDV, and their metabolites) rather than expression, use of cortical synaptosomes allows for the greater chance of synaptosome concentration and assay success. The fact that CBD and its metabolites have a greater affinity for ENT1 than CBDV has interesting implications for the clinical antiseizure efficacy of CBD, for which there is greater evidence than CBDV. If indeed CBD is more effective than CBDV at reducing seizures, this overall finding may be an indication that ENT1 inhibition has some role to play. Future experiments could include comparisons of

The calculated IC_{50} of 1.32 µM in this study for CBD is comparable to the previously reported rat *ex vivo* synaptosome IC_{50} in striata of 3.50 µM, under reasonably similar conditions except our study's longer incubation time of 10 min compared to previous study's 5 min (Pandolfo et al., 2011).

These IC_{50} concentrations are physiologically relevant in rat brain, with pharmacokinetic studies previously showing, following an oral or intraperitoneal administration of 120 mg/kg CBD, a C_{max} in the brain of 5.2 – 12.6 µg/mL, corresponding to ~14.9 - 40 µM, with putative half-life between 222 – 663 min (Deiana et al., 2012). CBDV (60 mg/kg) in the same study displayed a C_{max} in the brain of 6.3 µg/mL (22 µM) following oral administration with a half-life of 232 min, and following intraperitoneal administration 3.9 µg/mL (13.6 µM) with a 383 min half-life.

Section 5.3 has also shown some action of cannabinoid metabolites, with 7-OH-CBD having a similar affinity profile to CBD itself, while 7-COOH-CBD displayed a decreased affinity. This has potential implications for CBD metabolism, as 7-COOH-CBD has been previously described as being the most abundant metabolite in humans (Ujváry and Hanuš, 2016) and would therefore display a much decreased potential therapeutic efficacy through acting at inhibiting adenosine uptake.

Previous theories of CBD inhibition of adenosine uptake required astrocytic ENT1 blockade, preventing ADK-mediated clearance of extracellular adenosine, localisation studies in rat brains have previously shown a strong neuronal expression as well as GFAP cross-reactivity (Xu et al., 2015; Zhang et al.,

2018). This would indicate that, while CBD activity at astroglial ENT1 is still likely, the inhibitory effect of CBD at neuronal ENT1 must be substantial when considering therapeutic effect.

It is also worth noting, while ENT1 blockade with NBTI or dipyridamole appears to show anticonvulsant efficacy in *in vivo* models of seizures, these studies primarily report a significant effect of ENT1 blockade through increasing latency to seizures (Siebel et al., 2015; Xu et al., 2015). Neither the zebrafish nor rat study report a significant overall decrease in seizure intensity, except a decreased severity at certain time points following convulsant injection, which is accounted for by an increased latency. This profile of PTZ/pilocarpine does not match the well-documented effect of CBD/CBDV in these seizure models, in which cannabinoid administration generally decreases seizure severity, mortality, and incidence in a dose-dependent manner, but with no effect on seizure onset latency (Jones et al., 2010; Hill et al., 2012). This would suggest that CBD and indeed CBDV blockade of ENT1 does not solely contribute to the overall acute anticonvulsant effect. Additionally, the precise mechanism through which specific ENT1 blockade increases seizure latency or decreases *in vitro* pyramidal cell spiking is still unknown (Xu et al., 2015), as there would appear to exist a balance between astroglial prevention of adenosine uptake, or neuronal prevention of adenosine release (Lovatt et al., 2012).

The other consideration, in addition to acute anticonvulsant effect of CBD, is the demonstrated long-term benefit of CBD in chronic epilepsy (Patra et al., 2019). While CBD activity at ENT1 might not underlie acute seizure initiation following administration of a convulsant drug, it is perhaps still long-term activity at astroglial ENT1 preventing the astrogliosis-induced increased ADK-driven extracellular adenosine uptake which creates a longer-term neuroprotection. Additionally, with adenosine metabolism implicated in epigenetic mechanisms of epileptogenesis (Williams-Karnesky et al., 2013), prevention of neuronal efflux of adenosine could increase neuronal intracellular adenosine concentration for a significant effect of balancing the DNA methylation pathway at a critical seizure time.

5.5.2. Detected hippocampal ENT1 expression does not change between healthy and epileptic animals

Gene and protein expression analyses of ENT1 revealed no significant difference between healthy and epileptic animals. These data do not correspond with similar studies in the literature, which have generally found an increase in ENT1 expression following seizures. However, in the majority of these studies, Western blotting or immunostaining was carried out in dissected tissue from rats either 24 hours following seizure (Xu et al., 2015), at which point the study also showed hippocampal ENT1 expression was at its peak expression. By 72 hours and 1 week following seizure, ENT1 expression had fallen from the 24-hour peak, although was still significantly higher than control. It is unknown whether this transient increase of ENT1 expression consistently occurs during seizure, or what further epileptogenic

processes may have taken place in the 16 weeks following pilocarpine induction in the chronic epileptic rats used in our study.

An increase in ENT1 is however shown in temporal neocortical tissue resected from human TLE patients (Xu et al., 2015). This difference with our findings may be due to the difference in temporal neocortex rather than hippocampus, or potentially due to these patients having been preselected based on having extremely pharmacoresistant epilepsy. All patients used in this particular study had been shown to be resistant to maximal doses of three or more AEDs, a pharmacoresistance which has not been proven in the RISE-SRS model of chronic rat epilepsy used in this thesis.

Our finding of two bands from ENT1 antibodies may also confound this study. The calculated weight of the ENT1 protein is 50 kDa, however the manufacturer lists a heavier observed weight of ~62 kDa in mouse Western blots (Proteintech, 2017), suggesting that the heavier weight is likely due to post-transcription glycosylation. Other studies using the same antibody in rat tissue do not provide information on band weights and number of bands seen from the antibody, making it difficult to ascertain the expectedness of our results (Tanaka et al., 2011; Kretschmar et al., 2016; Alarcon et al., 2017). However, the methods reported by other papers are in alignment with the ones used in this thesis. It should be noted, however, that although the manufacturer does not report an observed band weight which aligns with the calculated protein size, the fact that our Western blots resulted in a band at the exact predicted size, as well as at a heavier weight (likely due to glycosylation), is a favourable indication that the antibody detection is specific for ENT1, and an indication that in rat hippocampus ENT1 can be detected both pre- and post-glycosylation. A possible method of confirming that the isolated protein bands are in fact ENT1 could involve isolating the particular band weight, inserting the proteins into synthetic phospholipid "bubbles" and allowing to properly fold into its native state on the membrane bilayer, and assessing passage of adenosine or any other nucleoside (Iwamoto and Oiki, 2015).

Although our RT-qPCR or Western blotting assays do not appear to show any changes in ENT1 transcription or expression, this does not preclude functional alterations since lack of transcriptional expression does not preclude potential differences in posttranscriptional modifications, and homogenised protein data do not allow for detection of changes in cytosolic/surface membrane ratio. Similarly, complete hippocampal tissue homogenisation does not account for any putative change in cell-specific expression – for instance, astrogliosis in chronic epilepsy could account for an increase in ENT1 expression, which we do not see. This could suggest that the pathological astrogliosis in epilepsy causing astrocyte proliferation does not also cause upregulation of ENT1, or perhaps if astrocytic ENT1 is upregulated there is a counterbalance of decreased neuronal ENT1, although there is currently no evidence to support either theory. Compartmental localisation of ENT1 could be assessed in future using

immunostaining, although a very rigorous and controlled methodology would need to be used to compare ENT1 localisation between healthy and epileptic tissue.

6. General Discussion and Conclusions

6.1. Potential Interactions Between CBD and the Adenosine Signalling System

The initial hypothesis regarding the underlying mechanism by which CBD confers antiepileptic efficacy was based on the concept that CBD-mediated inhibition of ENT1 prevents the reuptake of synaptic adenosine during seizures, thereby increasing activation of inhibitory A_1Rs. While chapter 5 shows that CBD, as well as CBDV and their metabolites, are effective in inhibiting adenosine passage through membranes, the previous studies in this thesis suggest that this proposed mechanism of CBD's therapeutic efficacy is an incomplete story. Table 6-1 summarises the major effects of CBD on the adenosine signalling system described in this thesis, along with a putative mechanism of action for that effect.

CBD observations	**healthy**		**epileptic**		**putative activity on:**	
	CTL	CBD	CTL	CBD	ENT1	adenosine receptors
basal adenosine	-	-	-	-		
stimulation-released adenosine	-	-	-	↓	•	
post-stimulation adenosine potency	-	-	↓	↑		•
exogenous adenosine logIC_{50}	-	↑	-	-	?	?
network inhibition at low concentrations of exogenous adenosine	-	-	↓	↑		•
adenosine uptake in synaptosomes	n/a	↓	n/a	n/a	•	

Table 6-1: A summary of the activity of CBD shown within this thesis. Hyphenated entry indicates no significant difference from healthy control; n/a indicates assays not performed.

Firstly, experiments described in Chapter 3 showed that in the absence of network activity, CBD or CBDV alone had no detectable effect measurable by biosensors upon the basal tone of adenosine in either healthy or epileptic hippocampal slices. This is possibly due to there being very low concentrations of adenosine present in a quiescent hippocampus, as suggested previously (Thompson et al., 1992; Diez et al., 2017). However, following multielectrode stimulation across the hippocampal CA1 region, adenosine release could be detected. This evoked adenosine release was decreased by CBD in epileptic, but not healthy slices. While this finding contradicts the initial theory described above, it is in agreement with previous studies that have inhibited ENT1 in hippocampal slices and reduced stimulated adenosine release (Lovatt et al., 2012; Wall and Dale, 2013; Diez et al., 2017). It has been suggested that

stimulation-evoked adenosine release has a primarily neuronal source, due to the intracellular dephosphorylation of ATP to adenosine resulting in a concentration gradient of adenosine and synaptic "release" through neuronal ENT1 (Lovatt et al., 2012). Extracellular adenosine is then primarily metabolised by the astrocyte-bound enzyme ADK, again via ENT1. Putative (although unconfirmed) blockade by CBD would appear to inhibit the peak neuronal release of adenosine, but regression decay constant τ did not find a significant change in the dynamics of adenosine reuptake. This would suggest, for an unknown reason, that CBD would be preferentially inhibiting neuronal ENT1. Chapter 5 describes an unchanged overall gene and protein expression of ENT1 in the hippocampus between healthy and epileptic, as well as following chronic CBD treatment. However, any loss of function or an expression shift in different cell types or cellular compartments cannot be detected – for instance an increase in glial ENT1 expression with a concurrent decrease in neuronal ENT1 in epilepsy may underlie the disease-dependent action of CBD. This could be further clarified by co-localisation imaging studies, visualising ENT1 with neuronal and glial markers in healthy and epileptic hippocampus and quantifying if chronic epilepsy has caused a shift in cellular expression of ENT1.

As described in section 5.5.1, blockade of ENT1 *in vivo* using NBTI/dipyridamole generally only increases the latency of emergent seizure activity, rather than decreasing seizure intensity (Siebel et al., 2015; Xu et al., 2015), which does not match the therapeutic profile of CBD (Jones et al., 2010; Jones et al., 2012). Together with the *in vitro* studies showing that ENT1 inhibition during high neuronal activity increases synaptic activity (Lovatt et al., 2012; Diez et al., 2017), this indicates that the protective effect of CBD in seizure is unlikely to be due to inhibition of ENT1 leading to prolonged activation of A_1R from inhibition of adenosine reuptake.

However, another possibility for CBD activity is through indirect modulation of ENT1, rather than direct inhibition. Bicket et al. (2016) reported a novel method of ENT1, via receptor-stimulated Ca^{2+}-dependent calmodulin binding. This suggests that increased intracellular Ca^{2+} through receptor activation increases the flux of ENT1, increasing purine uptake. With a known increase of intracellular Ca^{2+} in the pilocarpine model of chronic epilepsy (Raza et al., 2001), this suggests that an epileptogenic pathology of ENT1 function may involve increased flux of adenosine through cell membranes. There may even be a compartmental effect to the calcium-dependent modulation of ENT1 flux, as neuronal and astroglial ENT1 control the source and sink of extracellular adenosine; if there was a differential calcium signal between neurons and astrocytes, the dynamics of the adenosine cycle could be unbalanced; e.g., increased calcium in astrocytes leading to a more rapid clearing of adenosine than the efflux from neurons. As CBD has been shown to have a homeostatic effect on intracellular calcium levels (Ryan et al., 2009), this suggests that CBD may have a balancing role in the dynamics of regulation of ENT1 flux. This could be assessed in future experiments by assessing adenosine uptake, similar to the synaptosome

study in section 5.3, with healthy and epileptic tissue, with different incubation times to assess if there is indeed a change in adenosine uptake dynamic.

Other possible mechanisms within the adenosine signalling system through which CBD might have a therapeutic benefit in epilepsy have been less researched in literature. Previous CBD studies and those examining adenosine receptors, as described in section 1.4, have generally concluded that the anti-inflammatory or antiarrhythmic effects of CBD were due to reuptake inhibition via ENT1.

Chapters 3 and 4 investigated the CA1 network response to adenosine, following stimulation-evoked adenosine release or with exogenously applied adenosine, as well as the behaviour of the adenosine receptors in healthy and epileptic states (to be discussed further below). Following stimulation-evoked adenosine release, CBD had no effect on adenosine potency in healthy hippocampus, while its effect on potency in epileptic hippocampus appeared to return it to healthy baseline. Following exogenous adenosine application, however, CBD modulates and decreases the potency of high concentrations of adenosine in healthy hippocampus, while potentiating the inhibition induced by low adenosine concentrations in epileptic tissue. This could potentially be due to the post-stimulation state of hippocampal networks overcoming the modulatory effect of CBD at A_1Rs in healthy tissue, for instance other inhibitory mechanisms following heightened neuronal activity.

Further in-depth studies are required to assess whether CBD has a modulatory effect at A_1Rs, which could potentially involve allosteric modulation. Alternatively, biased agonism studies have shown that specific A_1R agonists are capable of activating differential downstream G-protein or β-arrestin-associated intracellular pathways, resulting in activation of alternate downstream intracellular pathways than usual (Baltos et al., 2016; Vecchio et al., 2018). This has never before been investigated in conjunction with epileptic pathology or with CBD, and could explain some of the differential effects of CBD on adenosine signalling between healthy and epileptic hippocampus. These could be relevant for the strong PPF seen at 10 ms PPI in the presence of 300 µM adenosine in epileptic hippocampal slices, which might be indicative of adenosine-related presynaptic facilitation at high-frequency activity (Bragin et al., 1999). This strong facilitation compared with higher intervals is decreased by CBD but not by A_{2A}R antagonism, suggesting that it could be due to isolated A_1R activation and meliorated by CBD.

Another, longer-term possibility of CBD antiepileptic efficacy could lie within DNA methylation (Williams-Karnesky et al., 2013). Blockade of ENT1 during seizure allows a build-up of high intracellular concentrations of neuronal adenosine, which may have an effect on the DNMT enzymes and reduce DNA methylation. With hypermethylated DNA found in human TLE hippocampus (Kobow et al., 2009; Boison, 2016b), this increase of intracellular adenosine could possibly have longer-term

effects independently from extracellular activation of adenosine receptors. This could contribute to the benefits of chronic CBD treatment in decreasing seizures, seen both in preclinical studies of TLE (Patra et al., 2019) as well as clinical studies in other epilepsies (Devinsky et al., 2017; Devinsky et al., 2018; Thiele et al., 2018).

6.2. Adenosine Receptors Dysfunction in Chronic Epilepsy

Chapter 4 explored the function of individual adenosine receptor subtypes in chronic epilepsy as compared to healthy hippocampus.

Protein expression and function of A_1R, as consistent with literature (Glass et al., 1996; Rebola et al., 2005), is decreased in epileptic hippocampus, as demonstrated through binding data and evoked field potentials.

Clarifying the role of $A_{2A}R$, on the other hand, proved to be challenging. It is likely that the methods used in this study may not have been precise or robust enough to detect the levels of $A_{2A}R$-based change that we were seeking. Previous literature had described an upregulation of $A_{2A}R$ in epilepsy in rat models of seizure and in human hippocampus (Rebola et al., 2005; Barros-Barbosa et al., 2016), suggesting increased excitability of neuronal networks in response to adenosine. Unfortunately no signal was able to be detected using either radioligand binding or Western blotting for the receptor; possibly a larger pool of tissue would have been required, as it is known $A_{2A}R$ is expressed in very low levels in the hippocampus. Similarly, while very little was able to be confirmed from evoked field potentials, methods scrutinising the single cell, e.g., patch clamping, may be able to shed more light. Several studies have emphasised the subtle but dynamic role of the $A_{2A}R$, with widespread influence through astrocytes or interneurons (Matos et al., 2012b; Rombo et al., 2015). A closer look at these systems, for instance through interneuron patch clamping similar to experiments performed by Rombo et al., could clarify whether the A_{2A} receptor has a widespread potentiation effect which is more pronounced in epilepsy.

6.3. Conclusion and Outlook

While subtle interactions between CBD and the adenosine signalling system can be shown in some assays, a definitive answer regarding whether the system underlies this effect cannot be concluded from the studies described in this thesis. The mechanism of action is far more likely to be a multifaceted combination of different systems working cohesively to reduce pathological processes causing seizures. However, this thesis has found a dysregulation of adenosine signalling in chronic epilepsy, which would be of interest to future investigation. Further exploratory work could be carried out as to the function and expression of ENT1 in epileptic pathology, in particular assessing the localisation among neurons/astrocytes/synapses, the disease-dependent activity of CBD, and whether CBD acts upon the

calcium-dependent flux of ENT1. Additionally, the activity of adenosine receptors could also be further characterised in epilepsy, particularly with regards to downstream intracellular signalling, and potentially whether CBD may have an allosteric interaction with A_1R.

7. References

Abcam. (2017). "Anti-Adenosine A1 Receptor antibody (ab82477), Product Information." 2020, from https://www.abcam.com/adenosine-a1-receptor-antibody-ab82477.html.

Alarcon, S., Garrido, W., Vega, G., Cappelli, C., Suarez, R., Oyarzun, C., Quezada, C. and San Martin, R. (2017). Deficient insulin-mediated upregulation of the equilibrative nucleoside transporter 2 contributes to chronically increased adenosine in diabetic glomerulopathy. *Sci Rep* **7**(1): 9439.

Alcami, P., Franconville, R., Llano, I. and Marty, A. (2012). Measuring the firing rate of high-resistance neurons with cell-attached recording. *J Neurosci* **32**(9): 3118-3130.

Amada, N., Yamasaki, Y., Williams, C. M. and Whalley, B. J. (2013). Cannabidivarin (CBDV) suppresses pentylenetetrazole (PTZ)-induced increases in epilepsy-related gene expression. *PeerJ* **1**: e214.

Anschel, D. J., Ortega, E. L., Kraus, A. C. and Fisher, R. S. (2004). Focally injected adenosine prevents seizures in the rat. *Exp Neurol* **190**(2): 544-547.

Arias-Cavieres, A., Adasme, T., Sanchez, G., Munoz, P. and Hidalgo, C. (2017). Aging impairs hippocampal- dependent recognition memory and LTP and prevents the associated RyR up-regulation. *Front Aging Neurosci* **9**: 111.

Arzimanoglou, A., French, J., Blume, W. T., Cross, J. H., Ernst, J. P., Feucht, M., Genton, P., Guerrini, R., Kluger, G., Pellock, J. M., Perucca, E. and Wheless, J. W. (2009). Lennox-Gastaut syndrome: a consensus approach on diagnosis, assessment, management, and trial methodology. *Lancet Neurol* **8**(1): 82-93.

Avanzini, G., Depaulis, A., Tassinari, A. and de Curtis, M. (2013). Do seizures and epileptic activity worsen epilepsy and deteriorate cognitive function? *Epilepsia* **54 Suppl 8**: 14-21.

Baltos, J. A., Gregory, K. J., White, P. J., Sexton, P. M., Christopoulos, A. and May, L. T. (2016). Quantification of adenosine A(1) receptor biased agonism: Implications for drug discovery. *Biochem Pharmacol* **99**: 101-112.

Barros-Barbosa, A. R., Ferreirinha, F., Oliveira, A., Mendes, M., Lobo, M. G., Santos, A., Rangel, R., Pelletier, J., Sevigny, J., Cordeiro, J. M. and Correia-de-Sa, P. (2016). Adenosine A2A receptor and ecto-5'-nucleotidase/CD73 are upregulated in hippocampal astrocytes of human patients with mesial temporal lobe epilepsy (MTLE). *Purinergic Signal* **12**(4): 719-734.

Basheer, R., Strecker, R. E., Thakkar, M. M. and McCarley, R. W. (2004). Adenosine and sleep-wake regulation. *Prog Neurobiol* **73**(6): 379-396.

Bazelot, M., Bocchio, M., Kasugai, Y., Fischer, D., Dodson, P. D., Ferraguti, F. and Capogna, M. (2015). Hippocampal theta input to the amygdala shapes feedforward inhibition to gate heterosynaptic plasticity. *Neuron* **87**(6): 1290-1303.

Beltramini, G. C., Cendes, F. and Yasuda, C. L. (2015). The effects of antiepileptic drugs on cognitive functional magnetic resonance imaging. *Quant Imaging Med Surg* **5**(2): 238-246.

Belzung, C. and Lemoine, M. (2011). Criteria of validity for animal models of psychiatric disorders: focus on anxiety disorders and depression. *Biol Mood Anxiety Disord* **1**(1): 9.

Ben-Ari, Y., Crepel, V. and Represa, A. (2008). Seizures beget seizures in temporal lobe epilepsies: the boomerang effects of newly formed aberrant kainatergic synapses. *Epilepsy Curr* **8**(3): 68-72.

Bender, A. S., Wu, P. H. and Phillis, J. W. (1980). The characterization of [3H] adenosine uptake into rat cerebral cortical synaptosomes. *J Neurochem* **35**(3): 629-640.

Berg, A. T., Berkovic, S. F., Brodie, M. J., Buchhalter, J., Cross, J. H., van Emde Boas, W., Engel, J., French, J., Glauser, T. A., Mathern, G. W., Moshe, S. L., Nordli, D., Plouin, P. and Scheffer, I. E. (2010). Revised terminology and concepts for organization of seizures and epilepsies: report of the ILAE Commission on Classification and Terminology, 2005-2009. *Epilepsia* **51**(4): 676-685.

Bicket, A., Mehrabi, P., Naydenova, Z., Wong, V., Donaldson, L., Stagljar, I. and Coe, I. R. (2016). Novel regulation of equlibrative nucleoside transporter 1 (ENT1) by receptor-stimulated Ca2+-dependent calmodulin binding. *Am J Physiol Cell Physiol* **310**(10): C808-820.

Blume, W. T., Luders, H. O., Mizrahi, E., Tassinari, C., van Emde Boas, W. and Engel, J., Jr. (2001). Glossary of descriptive terminology for ictal semiology: report of the ILAE task force on classification and terminology. *Epilepsia* **42**(9): 1212-1218.

Boison, D. (2010). Adenosine dysfunction and adenosine kinase in epileptogenesis. *Open Neurosci J* **4**: 93-101.

Boison, D. (2012a). Adenosine augmentation therapy. Jasper's Basic Mechanisms of the Epilepsies. Noebels, J. L., Avoli, M., Rogawski, M. A., Olsen, R. W. and Delgado-Escueta, A. V. Bethesda (MD).

Boison, D. (2012b). Adenosine dysfunction in epilepsy. *Glia* **60**(8): 1234-1243.

Boison, D. (2013a). Adenosine kinase: exploitation for therapeutic gain. *Pharmacol Rev* **65**(3): 906-943.

Boison, D. (2013b). Role of adenosine in status epilepticus: a potential new target? *Epilepsia* **54 Suppl 6**: 20-22.

Boison, D. (2016a). Adenosinergic signaling in epilepsy. *Neuropharmacology* **104**: 131-139.

Boison, D. (2016b). The biochemistry and epigenetics of epilepsy: focus on adenosine and glycine. *Front Mol Neurosci* **9**: 26.

Boison, D., Sandau, U. S., Ruskin, D. N., Kawamura, M., Jr. and Masino, S. A. (2013). Homeostatic control of brain function - new approaches to understand epileptogenesis. *Front Cell Neurosci* **7**: 109.

Bolsterli, B. K., Schmitt, B., Bast, T., Critelli, H., Heinzle, J., Jenni, O. G. and Huber, R. (2011). Impaired slow wave sleep downscaling in encephalopathy with status epilepticus during sleep (ESES). *Clin Neurophysiol* **122**(9): 1779-1787.

Booth, C. A., Brown, J. T. and Randall, A. D. (2014). Neurophysiological modification of CA1 pyramidal neurons in a transgenic mouse expressing a truncated form of disrupted-in-schizophrenia 1. *Eur J Neurosci* **39**(7): 1074-1090.

Bragin, A., Engel, J., Jr., Wilson, C. L., Fried, I. and Mathern, G. W. (1999). Hippocampal and entorhinal cortex high-frequency oscillations (100--500 Hz) in human epileptic brain and in kainic acid--treated rats with chronic seizures. *Epilepsia* **40**(2): 127-137.

Brown, P. (2018). "CDER, Non-Clinical Reviews." from https://www.accessdata.fda.gov/drugsatfda_docs/nda/2018/210365Orig1s000PharmR.pdf.

Brundege, J. M. and Dunwiddie, T. V. (1996). Modulation of excitatory synaptic transmission by adenosine released from single hippocampal pyramidal neurons. *J Neurosci* **16**(18): 5603-5612.

Carrier, E. J., Auchampach, J. A. and Hillard, C. J. (2006). Inhibition of an equilibrative nucleoside transporter by cannabidiol: a mechanism of cannabinoid immunosuppression. *Proc Natl Acad Sci U S A* **103**(20): 7895-7900.

Cavalheiro, E. A., Leite, J. P., Bortolotto, Z. A., Turski, W. A., Ikonomidou, C. and Turski, L. (1991). Long-term effects of pilocarpine in rats: structural damage of the brain triggers kindling and spontaneous recurrent seizures. *Epilepsia* **32**(6): 778-782.

Chen, J. F., Huang, Z., Ma, J., Zhu, J., Moratalla, R., Standaert, D., Moskowitz, M. A., Fink, J. S. and Schwarzschild, M. A. (1999). A(2A) adenosine receptor deficiency attenuates brain injury induced by transient focal ischemia in mice. *J Neurosci* **19**(21): 9192-9200.

Chen, J. F., Xu, K., Petzer, J. P., Staal, R., Xu, Y. H., Beilstein, M., Sonsalla, P. K., Castagnoli, K., Castagnoli, N., Jr. and Schwarzschild, M. A. (2001). Neuroprotection by caffeine and A(2A) adenosine receptor inactivation in a model of Parkinson's disease. *J Neurosci* **21**(10): RC143.

Chen, Y. H., Kuo, T. T., Yi-Kung Huang, E., Hoffer, B. J., Chou, Y. C., Chiang, Y. H., Ma, H. I. and Miller, J. P. (2018). Profound deficits in hippocampal synaptic plasticity after traumatic brain injury and seizure is ameliorated by prophylactic levetiracetam. *Oncotarget* **9**(14): 11515-11527.

Cherian, A. and Thomas, S. V. (2009). Status epilepticus. *Ann Indian Acad Neurol* **12**(3): 140-153.

Chong, S. A., Benilova, I., Shaban, H., De Strooper, B., Devijver, H., Moechars, D., Eberle, W., Bartic, C., Van Leuven, F. and Callewaert, G. (2011). Synaptic dysfunction in hippocampus

of transgenic mouse models of Alzheimer's disease: a multi-electrode array study. *Neurobiol Dis* **44**(3): 284-291.

Cunha, J. M., Carlini, E. A., Pereira, A. E., Ramos, O. L., Pimentel, C., Gagliardi, R., Sanvito, W. L., Lander, N. and Mechoulam, R. (1980). Chronic administration of cannabidiol to healthy volunteers and epileptic patients. *Pharmacology* **21**(3): 175-185.

Cunha, R. A. (2005). Neuroprotection by adenosine in the brain: From A(1) receptor activation to A (2A) receptor blockade. *Purinergic Signal* **1**(2): 111-134.

Curia, G., Longo, D., Biagini, G., Jones, R. S. and Avoli, M. (2008). The pilocarpine model of temporal lobe epilepsy. *J Neurosci Methods* **172**(2): 143-157.

D'Alimonte, I., D'Auro, M., Citraro, R., Biagioni, F., Jiang, S., Nargi, E., Buccella, S., Di Iorio, P., Giuliani, P., Ballerini, P., Caciagli, F., Russo, E., De Sarro, G. and Ciccarelli, R. (2009). Altered distribution and function of A2A adenosine receptors in the brain of WAG/Rij rats with genetic absence epilepsy, before and after appearance of the disease. *Eur J Neurosci* **30**(6): 1023-1035.

Dale, N. (1998). Delayed production of adenosine underlies temporal modulation of swimming in frog embryo. *J Physiol* **511 (Pt 1)**: 265-272.

Dale, N., Pearson, T. and Frenguelli, B. G. (2000). Direct measurement of adenosine release during hypoxia in the CA1 region of the rat hippocampal slice. *J Physiol* **526 Pt 1**: 143-155.

Deiana, S., Watanabe, A., Yamasaki, Y., Amada, N., Arthur, M., Fleming, S., Woodcock, H., Dorward, P., Pigliacampo, B., Close, S., Platt, B. and Riedel, G. (2012). Plasma and brain pharmacokinetic profile of cannabidiol (CBD), cannabidivarine (CBDV), Delta(9)-tetrahydrocannabivarin (THCV) and cannabigerol (CBG) in rats and mice following oral and intraperitoneal administration and CBD action on obsessive-compulsive behaviour. *Psychopharmacology (Berl)* **219**(3): 859-873.

Devinsky, O., Cilio, M. R., Cross, H., Fernandez-Ruiz, J., French, J., Hill, C., Katz, R., Di Marzo, V., Jutras-Aswad, D., Notcutt, W. G., Martinez-Orgado, J., Robson, P. J., Rohrback, B. G., Thiele, E., Whalley, B. and Friedman, D. (2014). Cannabidiol: pharmacology and potential therapeutic role in epilepsy and other neuropsychiatric disorders. *Epilepsia* **55**(6): 791-802.

Devinsky, O., Cross, J. H., Laux, L., Marsh, E., Miller, I., Nabbout, R., Scheffer, I. E., Thiele, E. A., Wright, S. and Cannabidiol in Dravet Syndrome Study, G. (2017). Trial of cannabidiol for drug-resistant seizures in the Dravet Syndrome. *N Engl J Med* **376**(21): 2011-2020.

Devinsky, O., Marsh, E., Friedman, D., Thiele, E., Laux, L., Sullivan, J., Miller, I., Flamini, R., Wilfong, A., Filloux, F., Wong, M., Tilton, N., Bruno, P., Bluvstein, J., Hedlund, J., Kamens, R., Maclean, J., Nangia, S., Singhal, N. S., Wilson, C. A., Patel, A. and Cilio, M. R. (2016). Cannabidiol in patients with treatment-resistant epilepsy: an open-label interventional trial. *Lancet Neurol* **15**(3): 270-278.

Devinsky, O., Patel, A. D., Cross, J. H., Villanueva, V., Wirrell, E. C., Privitera, M., Greenwood, S. M., Roberts, C., Checketts, D., VanLandingham, K. E., Zuberi, S. M. and Group,

G. S. (2018). Effect of cannabidiol on drop seizures in the Lennox-Gastaut Syndrome. *N Engl J Med* **378**(20): 1888-1897.

Di Angelantonio, S., Bertollini, C., Piccinin, S., Rosito, M., Trettel, F., Pagani, F., Limatola, C. and Ragozzino, D. (2015). Basal adenosine modulates the functional properties of AMPA receptors in mouse hippocampal neurons through the activation of A1R A2AR and A3R. *Front Cell Neurosci* **9**: 409.

Diez, R., Richardson, M. J. E. and Wall, M. J. (2017). Reducing extracellular ca(2+) induces adenosine release via equilibrative nucleoside transporters to provide negative feedback control of activity in the hippocampus. *Front Neural Circuits* **11**: 75.

Diogenes, M. J., Neves-Tome, R., Fucile, S., Martinello, K., Scianni, M., Theofilas, P., Lopatar, J., Ribeiro, J. A., Maggi, L., Frenguelli, B. G., Limatola, C., Boison, D. and Sebastiao, A. M. (2014). Homeostatic control of synaptic activity by endogenous adenosine is mediated by adenosine kinase. *Cereb Cortex* **24**(1): 67-80.

Dixon, A. K., Gubitz, A. K., Sirinathsinghji, D. J., Richardson, P. J. and Freeman, T. C. (1996). Tissue distribution of adenosine receptor mRNAs in the rat. *Br J Pharmacol* **118**(6): 1461-1468.

Dona, F., Conceicao, I. M., Ulrich, H., Ribeiro, E. B., Freitas, T. A., Nencioni, A. L. and da Silva Fernandes, M. J. (2016). Variations of ATP and its metabolites in the hippocampus of rats subjected to pilocarpine-induced temporal lobe epilepsy. *Purinergic Signal* **12**(2): 295-302.

Dragunow, M., Goddard, G. V. and Laverty, R. (1985). Is adenosine an endogenous anticonvulsant? *Epilepsia* **26**(5): 480-487.

Dravet, C. and Oguni, H. (2013). Dravet syndrome (severe myoclonic epilepsy in infancy). *Handb Clin Neurol* **111**: 627-633.

DrugBank. (2020). "DrugBank online database, version 5.1.7, released 2020-07-02." from https://www.drugbank.ca/.

Dulla, C. G., Dobelis, P., Pearson, T., Frenguelli, B. G., Staley, K. J. and Masino, S. A. (2005). Adenosine and ATP link PCO2 to cortical excitability via pH. *Neuron* **48**(6): 1011-1023.

Dunwiddie, T. V. (1980). Endogenously released adenosine regulates excitability in the in vitro hippocampus. *Epilepsia* **21**(5): 541-548.

Dunwiddie, T. V. and Diao, L. (1994). Extracellular adenosine concentrations in hippocampal brain slices and the tonic inhibitory modulation of evoked excitatory responses. *J Pharmacol Exp Ther* **268**(2): 537-545.

During, M. J. and Spencer, D. D. (1992). Adenosine: a potential mediator of seizure arrest and postictal refractoriness. *Ann Neurol* **32**(5): 618-624.

El-Hassar, L., Esclapez, M. and Bernard, C. (2007). Hyperexcitability of the CA1 hippocampal region during epileptogenesis. *Epilepsia* **48 Suppl 5**: 131-139.

El Yacoubi, M., Ledent, C., Parmentier, M., Costentin, J. and Vaugeois, J. M. (2009). Adenosine A2A receptor deficient mice are partially resistant to limbic seizures. *Naunyn Schmiedebergs Arch Pharmacol* **380**(3): 223-232.

Elsohly, M. A. and Slade, D. (2005). Chemical constituents of marijuana: the complex mixture of natural cannabinoids. *Life Sci* **78**(5): 539-548.

Eltzschig, H. K. (2009). Adenosine: an old drug newly discovered. *Anesthesiology* **111**(4): 904-915.

Engel, J. (2013). Diagnostic evaluation. Seizures and Epilepsy, OUP USA**:** 407.

Etherington, L. A. and Frenguelli, B. G. (2004). Endogenous adenosine modulates epileptiform activity in rat hippocampus in a receptor subtype-dependent manner. *Eur J Neurosci* **19**(9): 2539-2550.

Etherington, L. A., Patterson, G. E., Meechan, L., Boison, D., Irving, A. J., Dale, N. and Frenguelli, B. G. (2009). Astrocytic adenosine kinase regulates basal synaptic adenosine levels and seizure activity but not activity-dependent adenosine release in the hippocampus. *Neuropharmacology* **56**(2): 429-437.

Fedele, D. E., Li, T., Lan, J. Q., Fredholm, B. B. and Boison, D. (2006). Adenosine A1 receptors are crucial in keeping an epileptic focus localized. *Exp Neurol* **200**(1): 184-190.

Ferré, S., Lluís, C., Justinova, Z., Quiroz, C., Orru, M., Navarro, G., Canela, E. I., Franco, R. and Goldberg, S. R. (2010). Adenosine-cannabinoid receptor interactions. Implications for striatal function. *Br J Pharmacol* **160**(3): 443-453.

Fisher, R. S., Acevedo, C., Arzimanoglou, A., Bogacz, A., Cross, J. H., Elger, C. E., Engel, J., Jr., Forsgren, L., French, J. A., Glynn, M., Hesdorffer, D. C., Lee, B. I., Mathern, G. W., Moshe, S. L., Perucca, E., Scheffer, I. E., Tomson, T., Watanabe, M. and Wiebe, S. (2014). ILAE official report: a practical clinical definition of epilepsy. *Epilepsia* **55**(4): 475-482.

Fisher, R. S., Cross, J. H., French, J. A., Higurashi, N., Hirsch, E., Jansen, F. E., Lagae, L., Moshe, S. L., Peltola, J., Roulet Perez, E., Scheffer, I. E. and Zuberi, S. M. (2017). Operational classification of seizure types by the International League Against Epilepsy: Position Paper of the ILAE Commission for Classification and Terminology. *Epilepsia* **58**(4): 522-530.

Fisher, R. S. and Engel, J. J., Jr. (2010). Definition of the postictal state: when does it start and end? *Epilepsy Behav* **19**(2): 100-104.

Fisher, R. S., van Emde Boas, W., Blume, W., Elger, C., Genton, P., Lee, P. and Engel, J., Jr. (2005). Epileptic seizures and epilepsy: definitions proposed by the International League Against Epilepsy (ILAE) and the International Bureau for Epilepsy (IBE). *Epilepsia* **46**(4): 470-472.

Franklin, P. H., Zhang, G., Tripp, E. D. and Murray, T. F. (1989). Adenosine A1 receptor activation mediates suppression of (-) bicuculline methiodide-induced seizures in rat prepiriform cortex. *J Pharmacol Exp Ther* **251**(3): 1229-1236.

Fredholm, B. B., Ap, I. J., Jacobson, K. A., Klotz, K. N. and Linden, J. (2001). International Union of Pharmacology. XXV. Nomenclature and classification of adenosine receptors. *Pharmacol Rev* **53**(4): 527-552.

Frenguelli, B. G. and Wall, M. J. (2016). Combined electrophysiological and biosensor approaches to study purinergic regulation of epileptiform activity in cortical tissue. *J Neurosci Methods* **260**: 202-214.

Frenguelli, B. G., Wigmore, G., Llaudet, E. and Dale, N. (2007). Temporal and mechanistic dissociation of ATP and adenosine release during ischaemia in the mammalian hippocampus. *J Neurochem* **101**(5): 1400-1413.

Geiger, J. D. and Nagy, J. I. (1986). Distribution of adenosine deaminase activity in rat brain and spinal cord. *J Neurosci* **6**(9): 2707-2714.

Glass, M., Faull, R. L., Bullock, J. Y., Jansen, K., Mee, E. W., Walker, E. B., Synek, B. J. and Dragunow, M. (1996). Loss of A1 adenosine receptors in human temporal lobe epilepsy. *Brain Res* **710**(1-2): 56-68.

Glien, M., Brandt, C., Potschka, H., Voigt, H., Ebert, U. and Loscher, W. (2001). Repeated low-dose treatment of rats with pilocarpine: low mortality but high proportion of rats developing epilepsy. *Epilepsy Res* **46**(2): 111-119.

Gonca, E. and Darici, F. (2015). The effect of cannabidiol on ischemia/reperfusion-induced ventricular arrhythmias: the role of adenosine A1 receptors. *J Cardiovasc Pharmacol Ther* **20**(1): 76-83.

Gouder, N., Fritschy, J. M. and Boison, D. (2003). Seizure suppression by adenosine A1 receptor activation in a mouse model of pharmacoresistant epilepsy. *Epilepsia* **44**(7): 877-885.

Gouder, N., Scheurer, L., Fritschy, J. M. and Boison, D. (2004). Overexpression of adenosine kinase in epileptic hippocampus contributes to epileptogenesis. *J Neurosci* **24**(3): 692-701.

Gowers, W. R. (1881). Epilepsy and other chronic convulsive disorders. *London: Churchill* **223**.

Guttinger, M., Fedele, D., Koch, P., Padrun, V., Pralong, W. F., Brustle, O. and Boison, D. (2005). Suppression of kindled seizures by paracrine adenosine release from stem cell-derived brain implants. *Epilepsia* **46**(8): 1162-1169.

GWPharma (2019). GW Pharmaceuticals plc Reports Financial Results and Operational Progress for the Second Quarter Ended June 30, 2019. London, UK, GW Pharmaceuticals: Press Release.

Hamil, N. E., Cock, H. R. and Walker, M. C. (2012). Acute down-regulation of adenosine A(1) receptor activity in status epilepticus. *Epilepsia* **53**(1): 177-188.

Hammond, C. (2015). Cellular and Molecular Neurophysiology, Elsevier.

Hauser, W. A., Annegers, J. F. and Rocca, W. A. (1996). Descriptive epidemiology of epilepsy: contributions of population-based studies from Rochester, Minnesota. *Mayo Clin Proc* **71**(6): 576-586.

Heng, K., Haney, M. M. and Buckmaster, P. S. (2013). High-dose rapamycin blocks mossy fiber sprouting but not seizures in a mouse model of temporal lobe epilepsy. *Epilepsia* **54**(9): 1535-1541.

Hill, A. J., Jones, N. A., Smith, I., Hill, C. L., Williams, C. M., Stephens, G. J. and Whalley, B. J. (2014). Voltage-gated sodium (NaV) channel blockade by plant cannabinoids does not confer anticonvulsant effects per se. *Neurosci Lett* **566**: 269-274.

Hill, A. J., Mercier, M. S., Hill, T. D., Glyn, S. E., Jones, N. A., Yamasaki, Y., Futamura, T., Duncan, M., Stott, C. G., Stephens, G. J., Williams, C. M. and Whalley, B. J. (2012). Cannabidivarin is anticonvulsant in mouse and rat. *Br J Pharmacol* **167**(8): 1629-1642.

Hill, T. D., Cascio, M. G., Romano, B., Duncan, M., Pertwee, R. G., Williams, C. M., Whalley, B. J. and Hill, A. J. (2013). Cannabidivarin-rich cannabis extracts are anticonvulsant in mouse and rat via a CB1 receptor-independent mechanism. *Br J Pharmacol* **170**(3): 679-692.

Howlett, A. C., Barth, F., Bonner, T. I., Cabral, G., Casellas, P., Devane, W. A., Felder, C. C., Herkenham, M., Mackie, K., Martin, B. R., Mechoulam, R. and Pertwee, R. G. (2002). International Union of Pharmacology. XXVII. Classification of cannabinoid receptors. *Pharmacol Rev* **54**(2): 161-202.

Huber, A., Guttinger, M., Mohler, H. and Boison, D. (2002). Seizure suppression by adenosine A(2A) receptor activation in a rat model of audiogenic brainstem epilepsy. *Neurosci Lett* **329**(3): 289-292.

Huber, A., Padrun, V., Deglon, N., Aebischer, P., Mohler, H. and Boison, D. (2001). Grafts of adenosine-releasing cells suppress seizures in kindling epilepsy. *Proc Natl Acad Sci U S A* **98**(13): 7611-7616.

Huberfeld, G., Blauwblomme, T. and Miles, R. (2015). Hippocampus and epilepsy: Findings from human tissues. *Rev Neurol (Paris)* **171**(3): 236-251.

Hughes, V., Richardson, M. J. E. and Wall, M. J. (2018). Acute ethanol exposure has bidirectional actions on the endogenous neuromodulator adenosine in rat hippocampus. *Br J Pharmacol* **175**(9): 1471-1485.

Hussain, S. A., Zhou, R., Jacobson, C., Weng, J., Cheng, E., Lay, J., Hung, P., Lerner, J. T. and Sankar, R. (2015). Perceived efficacy of cannabidiol-enriched cannabis extracts for treatment of pediatric epilepsy: A potential role for infantile spasms and Lennox-Gastaut syndrome. *Epilepsy Behav* **47**: 138-141.

Ibeas Bih, C., Chen, T., Nunn, A. V., Bazelot, M., Dallas, M. and Whalley, B. J. (2015). Molecular targets of cannabidiol in neurological disorders. *Neurotherapeutics* **12**(4): 699-730.

Incorpora, G. (2009). Dravet syndrome. *Ital J Pediatr* **35**(1): 27.

Iwamoto, M. and Oiki, S. (2015). Contact bubble bilayers with flush drainage. *Sci Rep* **5**: 9110.

Jefferys, J. G. (2003). Models and mechanisms of experimental epilepsies. *Epilepsia* **44 Suppl 12**: 44-50.

Jenssen, S., Gracely, E. J. and Sperling, M. R. (2006). How long do most seizures last? A systematic comparison of seizures recorded in the epilepsy monitoring unit. *Epilepsia* **47**(9): 1499-1503.

Jones, N. A., Glyn, S. E., Akiyama, S., Hill, T. D., Hill, A. J., Weston, S. E., Burnett, M. D., Yamasaki, Y., Stephens, G. J., Whalley, B. J. and Williams, C. M. (2012). Cannabidiol exerts anti-convulsant effects in animal models of temporal lobe and partial seizures. *Seizure* **21**(5): 344-352.

Jones, N. A., Hill, A. J., Smith, I., Bevan, S. A., Williams, C. M., Whalley, B. J. and Stephens, G. J. (2010). Cannabidiol displays antiepileptiform and antiseizure properties in vitro and in vivo. *J Pharmacol Exp Ther* **332**(2): 569-577.

Karanian, D. A., Brown, Q. B., Makriyannis, A., Kosten, T. A. and Bahr, B. A. (2005). Dual modulation of endocannabinoid transport and fatty acid amide hydrolase protects against excitotoxicity. *J Neurosci* **25**(34): 7813-7820.

Karler, R., Cely, W. and Turkanis, S. A. (1973). The anticonvulsant activity of cannabidiol and cannabinol. *Life Sciences* **13**(11): 1527-1531.

Klaft, Z. J., Hollnagel, J. O., Salar, S., Caliskan, G., Schulz, S. B., Schneider, U. C., Horn, P., Koch, A., Holtkamp, M., Gabriel, S., Gerevich, Z. and Heinemann, U. (2016). Adenosine A1 receptor-mediated suppression of carbamazepine-resistant seizure-like events in human neocortical slices. *Epilepsia* **57**(5): 746-756.

Kobow, K., Jeske, I., Hildebrandt, M., Hauke, J., Hahnen, E., Buslei, R., Buchfelder, M., Weigel, D., Stefan, H., Kasper, B., Pauli, E. and Blumcke, I. (2009). Increased reelin promoter methylation is associated with granule cell dispersion in human temporal lobe epilepsy. *J Neuropathol Exp Neurol* **68**(4): 356-364.

Kochanek, P. M., Vagni, V. A., Janesko, K. L., Washington, C. B., Crumrine, P. K., Garman, R. H., Jenkins, L. W., Clark, R. S., Homanics, G. E., Dixon, C. E., Schnermann, J. and Jackson, E. K. (2006). Adenosine A1 receptor knockout mice develop lethal status epilepticus after experimental traumatic brain injury. *J Cereb Blood Flow Metab* **26**(4): 565-575.

Kretschmar, C., Oyarzun, C., Villablanca, C., Jaramillo, C., Alarcon, S., Perez, G., Diaz-Encarnacion, M. M., Pastor-Anglada, M., Garrido, W., Quezada, C. and San Martin, R. (2016). Reduced Adenosine Uptake and Its Contribution to Signaling that Mediates Profibrotic Activation in Renal Tubular Epithelial Cells: Implication in Diabetic Nephropathy. *PLoS One* **11**(1): e0147430.

Kuruba, R., Hattiangady, B. and Shetty, A. K. (2009). Hippocampal neurogenesis and neural stem cells in temporal lobe epilepsy. *Epilepsy Behav* **14 Suppl 1**: 65-73.

Kwan, P. and Brodie, M. J. (2000). Early identification of refractory epilepsy. *N Engl J Med* **342**(5): 314-319.

Lado, F. A. and Moshe, S. L. (2008). How do seizures stop? *Epilepsia* **49**(10): 1651-1664.

Lakatos, R. K., Dobolyi, A., Todorov, M. I., Kekesi, K. A., Juhasz, G., Aleksza, M. and Kovacs, Z. (2016). Guanosine may increase absence epileptic activity by means of A2A adenosine receptors in Wistar Albino Glaxo Rijswijk rats. *Brain Res Bull* **124**: 172-181.

Laprairie, R. B., Bagher, A. M., Kelly, M. E. and Denovan-Wright, E. M. (2015). Cannabidiol is a negative allosteric modulator of the cannabinoid CB1 receptor. *Br J Pharmacol* **172**(20): 4790-4805.

Latini, S. and Pedata, F. (2001). Adenosine in the central nervous system: release mechanisms and extracellular concentrations. *J Neurochem* **79**(3): 463-484.

Layland, J., Carrick, D., Lee, M., Oldroyd, K. and Berry, C. (2014). Adenosine: physiology, pharmacology, and clinical applications. *JACC Cardiovasc Interv* **7**(6): 581-591.

Lee, S. K. (2014). Old versus new: Why do we need new antiepileptic drugs? *J Epilepsy Res* **4**(2): 39-44.

Li, T., Lan, J. Q. and Boison, D. (2008). Uncoupling of astrogliosis from epileptogenesis in adenosine kinase (ADK) transgenic mice. *Neuron Glia Biol* **4**(2): 91-99.

Li, T., Quan Lan, J., Fredholm, B. B., Simon, R. P. and Boison, D. (2007a). Adenosine dysfunction in astrogliosis: cause for seizure generation? *Neuron Glia Biol* **3**(4): 353-366.

Li, T., Ren, G., Kaplan, D. L. and Boison, D. (2009). Human mesenchymal stem cell grafts engineered to release adenosine reduce chronic seizures in a mouse model of CA3-selective epileptogenesis. *Epilepsy Res* **84**(2-3): 238-241.

Li, T., Steinbeck, J. A., Lusardi, T., Koch, P., Lan, J. Q., Wilz, A., Segschneider, M., Simon, R. P., Brustle, O. and Boison, D. (2007b). Suppression of kindling epileptogenesis by adenosine releasing stem cell-derived brain implants. *Brain* **130**(Pt 5): 1276-1288.

Liou, G. I., Auchampach, J. A., Hillard, C. J., Zhu, G., Yousufzai, B., Mian, S., Khan, S. and Khalifa, Y. (2008). Mediation of cannabidiol anti-inflammation in the retina by equilibrative nucleoside transporter and A2A adenosine receptor. *Invest Ophthalmol Vis Sci* **49**(12): 5526-5531.

Llaudet, E., Botting, N. P., Crayston, J. A. and Dale, N. (2003). A three-enzyme microelectrode sensor for detecting purine release from central nervous system. *Biosens Bioelectron* **18**(1): 43-52.

Lopes, J. P., Pliássova, A. and Cunha, R. A. (2019). The physiological effects of caffeine on synaptic transmission and plasticity in the mouse hippocampus selectively depend on adenosine A. *Biochem Pharmacol* **166**: 313-321.

Loscher, W. (2011). Critical review of current animal models of seizures and epilepsy used in the discovery and development of new antiepileptic drugs. *Seizure* **20**(5): 359-368.

Lovatt, D., Xu, Q., Liu, W., Takano, T., Smith, N. A., Schnermann, J., Tieu, K. and Nedergaard, M. (2012). Neuronal adenosine release, and not astrocytic ATP release, mediates feedback inhibition of excitatory activity. *Proc Natl Acad Sci U S A* **109**(16): 6265-6270.

Luan, G., Wang, X., Gao, Q., Guan, Y., Wang, J., Deng, J., Zhai, F., Chen, Y. and Li, T. (2017). Upregulation of Neuronal Adenosine A1 Receptor in Human Rasmussen Encephalitis. *J Neuropathol Exp Neurol* **76**(8): 720-731.

Lupica, C. R., Hu, Y., Devinsky, O. and Hoffman, A. F. (2017). Cannabinoids as hippocampal network administrators. *Neuropharmacology* **124**: 25-37.

Maa, E. and Figi, P. (2014). The case for medical marijuana in epilepsy. *Epilepsia* **55**(6): 783-786.

Maitre, M., Chesielski, L., Lehmann, A., Kempf, E. and Mandel, P. (1974). Protective effect of adenosine and nicotinamide against audiogenic seizure. *Biochem Pharmacol* **23**(20): 2807-2816.

Manford, M., Hart, Y. M., Sander, J. W. and Shorvon, S. D. (1992). National General Practice Study of Epilepsy (NGPSE): partial seizure patterns in a general population. *Neurology* **42**(10): 1911-1917.

Mańko, M., Bienvenu, T. C., Dalezios, Y. and Capogna, M. (2012). Neurogliaform cells of amygdala: a source of slow phasic inhibition in the basolateral complex. *J Physiol* **590**(22): 5611-5627.

Mao, K., You, C., Lei, D. and Zhang, H. (2015). High dosage of cannabidiol (CBD) alleviates pentylenetetrazole-induced epilepsy in rats by exerting an anticonvulsive effect. *Int J Clin Exp Med* **8**(6): 8820-8827.

Marques, T. E., de Mendonca, L. R., Pereira, M. G., de Andrade, T. G., Garcia-Cairasco, N., Paco-Larson, M. L. and Gitai, D. L. (2013). Validation of suitable reference genes for expression studies in different pilocarpine-induced models of mesial temporal lobe epilepsy. *PLoS One* **8**(8): e71892.

Marsicano, G., Goodenough, S., Monory, K., Hermann, H., Eder, M., Cannich, A., Azad, S. C., Cascio, M. G., Gutierrez, S. O., van der Stelt, M., Lopez-Rodriguez, M. L., Casanova, E., Schutz, G., Zieglgansberger, W., Di Marzo, V., Behl, C. and Lutz, B. (2003). CB1 cannabinoid receptors and on-demand defense against excitotoxicity. *Science* **302**(5642): 84-88.

Matos, M., Augusto, E., Machado, N. J., dos Santos-Rodrigues, A., Cunha, R. A. and Agostinho, P. (2012a). Astrocytic adenosine A2A receptors control the amyloid-beta peptide-induced decrease of glutamate uptake. *J Alzheimers Dis* **31**(3): 555-567.

Matos, M., Augusto, E., Santos-Rodrigues, A. D., Schwarzschild, M. A., Chen, J. F., Cunha, R. A. and Agostinho, P. (2012b). Adenosine A2A receptors modulate glutamate uptake in cultured astrocytes and gliosomes. *Glia* **60**(5): 702-716.

Matsuda, L. A., Lolait, S. J., Brownstein, M. J., Young, A. C. and Bonner, T. I. (1990). Structure of a cannabinoid receptor and functional expression of the cloned cDNA. *Nature* **346**(6284): 561-564.

Mecha, M., Feliu, A., Inigo, P. M., Mestre, L., Carrillo-Salinas, F. J. and Guaza, C. (2013). Cannabidiol provides long-lasting protection against the deleterious effects of inflammation in a viral model of multiple sclerosis: a role for A2A receptors. *Neurobiol Dis* **59**: 141-150.

Mijangos-Moreno, S., Poot-Ake, A., Arankowsky-Sandoval, G. and Murillo-Rodriguez, E. (2014). Intrahypothalamic injection of cannabidiol increases the extracellular levels of adenosine in nucleus accumbens in rats. *Neurosci Res* **84**: 60-63.

Millipore. (2017). "Anti-Adenosine Receptor A2a Antibody, clone 7F6-G5-A2, Product Information." 2020, from https://www.merckmillipore.com/GB/en/product/Anti-Adenosine-Receptor-A2a-Antibody-clone-7F6-G5-A2,MM_NF-05-717.

Modebadze, T., Morgan, N. H., Peres, I. A., Hadid, R. D., Amada, N., Hill, C., Williams, C., Stanford, I. M., Morris, C. M., Jones, R. S., Whalley, B. J. and Woodhall, G. L. (2016). A low mortality, high morbidity reduced intensity status epilepticus (RISE) model of epilepsy and epileptogenesis in the rat. *PLoS One* **11**(2): e0147265.

Moreno, E., Canet, J., Gracia, E., Lluis, C., Mallol, J., Canela, E. I., Cortes, A. and Casado, V. (2018). Molecular Evidence of Adenosine Deaminase Linking Adenosine A2A Receptor and CD26 Proteins. *Front Pharmacol* **9**: 106.

Nazario, L. R., Antonioli, R., Jr., Capiotti, K. M., Hallak, J. E., Zuardi, A. W., Crippa, J. A., Bonan, C. D. and da Silva, R. S. (2015). Caffeine protects against memory loss induced by high and non-anxiolytic dose of cannabidiol in adult zebrafish (Danio rerio). *Pharmacol Biochem Behav* **135**: 210-216.

Nguyen, M. D. and Venton, B. J. (2015). Fast-scan cyclic voltammetry for the characterization of rapid adenosine release. *Comput Struct Biotechnol J* **13**: 47-54.

Olah, A., Toth, B. I., Borbiro, I., Sugawara, K., Szollosi, A. G., Czifra, G., Pal, B., Ambrus, L., Kloepper, J., Camera, E., Ludovici, M., Picardo, M., Voets, T., Zouboulis, C. C., Paus, R. and Biro, T. (2014). Cannabidiol exerts sebostatic and antiinflammatory effects on human sebocytes. *J Clin Invest* **124**(9): 3713-3724.

Oviedo, A., Glowa, J. and Herkenham, M. (1993). Chronic cannabinoid administration alters cannabinoid receptor binding in rat brain: a quantitative autoradiographic study. *Brain Res* **616**(1-2): 293-302.

Pak, M. A., Haas, H. L., Decking, U. K. and Schrader, J. (1994). Inhibition of adenosine kinase increases endogenous adenosine and depresses neuronal activity in hippocampal slices. *Neuropharmacology* **33**(9): 1049-1053.

Pandolfo, P., Silveirinha, V., dos Santos-Rodrigues, A., Venance, L., Ledent, C., Takahashi, R. N., Cunha, R. A. and Kofalvi, A. (2011). Cannabinoids inhibit the synaptic uptake of adenosine and dopamine in the rat and mouse striatum. *Eur J Pharmacol* **655**(1-3): 38-45.

Pascual, O., Casper, K. B., Kubera, C., Zhang, J., Revilla-Sanchez, R., Sul, J. Y., Takano, H., Moss, S. J., McCarthy, K. and Haydon, P. G. (2005). Astrocytic purinergic signaling coordinates synaptic networks. *Science* **310**(5745): 113-116.

Patel, R. R., Barbosa, C., Brustovetsky, T., Brustovetsky, N. and Cummins, T. R. (2016). Aberrant epilepsy-associated mutant Nav1.6 sodium channel activity can be targeted with cannabidiol. *Brain* **139**(Pt 8): 2164-2181.

Patra, P. H., Barker-Haliski, M., White, H. S., Whalley, B. J., Glyn, S., Sandhu, H., Jones, N., Bazelot, M., Williams, C. M. and McNeish, A. J. (2019). Cannabidiol reduces seizures and associated behavioral comorbidities in a range of animal seizure and epilepsy models. *Epilepsia* **60**(2): 303-314.

Pelkey, K. A., Chittajallu, R., Craig, M. T., Tricoire, L., Wester, J. C. and McBain, C. J. (2017). Hippocampal GABAergic inhibitory interneurons. *Physiol Rev* **97**(4): 1619-1747.

Pena, F., Bargas, J. and Tapia, R. (2002). Paired pulse facilitation is turned into paired pulse depression in hippocampal slices after epilepsy induced by 4-aminopyridine in vivo. *Neuropharmacology* **42**(6): 807-812.

Pertwee, R. G. (2008). The diverse CB1 and CB2 receptor pharmacology of three plant cannabinoids: delta9-tetrahydrocannabinol, cannabidiol and delta9-tetrahydrocannabivarin. *Br J Pharmacol* **153**(2): 199-215.

Perucca, P., Carter, J., Vahle, V. and Gilliam, F. G. (2009). Adverse antiepileptic drug effects: toward a clinically and neurobiologically relevant taxonomy. *Neurology* **72**(14): 1223-1229.

Perucca, P. and Gilliam, F. G. (2012). Adverse effects of antiepileptic drugs. *Lancet Neurol* **11**(9): 792-802.

Pfaffl, M. W. (2001). A new mathematical model for relative quantification in real-time RT-PCR. *Nucleic Acids Res* **29**(9): e45.

Pinar, C., Fontaine, C. J., Trivino-Paredes, J., Lottenberg, C. P., Gil-Mohapel, J. and Christie, B. R. (2017). Revisiting the flip side: Long-term depression of synaptic efficacy in the hippocampus. *Neurosci Biobehav Rev* **80**: 394-413.

Porter, B. E. and Jacobson, C. (2013). Report of a parent survey of cannabidiol-enriched cannabis use in pediatric treatment-resistant epilepsy. *Epilepsy Behav* **29**(3): 574-577.

Proteintech. (2017). "11337-1-AP, ENT1 Polyclonal antibody, Product Information." 2020, from https://www.ptglab.com/Products/ENT1-Antibody-11337-1-AP.htm.

PsyPost. (2017). "Problematic alcohol use linked to reduced hippocampal volume." 2020, from https://www.psypost.org/2017/12/problematic-alcohol-use-linked-reduced-hippocampal-volume-50354.

Radwan, M. M., Elsohly, M. A., Slade, D., Ahmed, S. A., Khan, I. A. and Ross, S. A. (2009). Biologically active cannabinoids from high-potency Cannabis sativa. *J Nat Prod* **72**(5): 906-911.

Raza, M., Pal, S., Rafiq, A. and DeLorenzo, R. J. (2001). Long-term alteration of calcium homeostatic mechanisms in the pilocarpine model of temporal lobe epilepsy. *Brain Res* **903**(1-2): 1-12.

Rebola, N., Porciuncula, L. O., Lopes, L. V., Oliveira, C. R., Soares-da-Silva, P. and Cunha, R. A. (2005). Long-term effect of convulsive behavior on the density of adenosine A1 and A 2A receptors in the rat cerebral cortex. *Epilepsia* **46 Suppl 5**: 159-165.

Ribeiro, A., Ferraz-de-Paula, V., Pinheiro, M. L., Vitoretti, L. B., Mariano-Souza, D. P., Quinteiro-Filho, W. M., Akamine, A. T., Almeida, V. I., Quevedo, J., Dal-Pizzol, F., Hallak, J. E., Zuardi, A. W., Crippa, J. A. and Palermo-Neto, J. (2012). Cannabidiol, a non-psychotropic plant-derived cannabinoid, decreases inflammation in a murine model of acute lung injury: role for the adenosine A(2A) receptor. *Eur J Pharmacol* **678**(1-3): 78-85.

Robson, P. (2011). Abuse potential and psychoactive effects of δ-9-tetrahydrocannabinol and cannabidiol oromucosal spray (Sativex), a new cannabinoid medicine. *Expert Opin Drug Saf* **10**(5): 675-685.

Rombo, D. M., Newton, K., Nissen, W., Badurek, S., Horn, J. M., Minichiello, L., Jefferys, J. G., Sebastiao, A. M. and Lamsa, K. P. (2015). Synaptic mechanisms of adenosine A2A receptor-mediated hyperexcitability in the hippocampus. *Hippocampus* **25**(5): 566-580.

Rosenberg, E. C., Tsien, R. W., Whalley, B. J. and Devinsky, O. (2015). Cannabinoids and epilepsy. *Neurotherapeutics* **12**(4): 747-768.

Rosim, F. E., Persike, D. S., Nehlig, A., Amorim, R. P., de Oliveira, D. M. and Fernandes, M. J. (2011). Differential neuroprotection by A(1) receptor activation and A(2A) receptor inhibition following pilocarpine-induced status epilepticus. *Epilepsy Behav* **22**(2): 207-213.

Ryan, D., Drysdale, A. J., Lafourcade, C., Pertwee, R. G. and Platt, B. (2009). Cannabidiol targets mitochondria to regulate intracellular Ca2+ levels. *J Neurosci* **29**(7): 2053-2063.

SarissaBiomedical. (2015). "sarissaprobe® Adenosine / ADO." 2015, from http://www.sarissa-biomedical.com/products/sarissaprobes/adenosine.aspx.

Scheffer, I. E., Berkovic, S., Capovilla, G., Connolly, M. B., French, J., Guilhoto, L., Hirsch, E., Jain, S., Mathern, G. W., Moshe, S. L., Nordli, D. R., Perucca, E., Tomson, T., Wiebe, S., Zhang, Y. H. and Zuberi, S. M. (2017). ILAE classification of the epilepsies: Position paper of the ILAE Commission for Classification and Terminology. *Epilepsia* **58**(4): 512-521.

Schiavon, A. P., Soares, L. M., Bonato, J. M., Milani, H., Guimaraes, F. S. and Weffort de Oliveira, R. M. (2014). Protective effects of cannabidiol against hippocampal cell death and cognitive impairment induced by bilateral common carotid artery occlusion in mice. *Neurotox Res* **26**(4): 307-316.

Schutte, R. J., Schutte, S. S., Algara, J., Barragan, E. V., Gilligan, J., Staber, C., Savva, Y. A., Smith, M. A., Reenan, R. and O'Dowd, D. K. (2014). Knock-in model of Dravet syndrome reveals a constitutive and conditional reduction in sodium current. *J Neurophysiol* **112**(4): 903-912.

Schwartzkroin, P. A. (1994). Role of the hippocampus in epilepsy. *Hippocampus* **4**(3): 239-242.

Sebastiao, A. M. and Ribeiro, J. A. (2009). Triggering neurotrophic factor actions through adenosine A2A receptor activation: implications for neuroprotection. *Br J Pharmacol* **158**(1): 15-22.

Semah, F., Picot, M. C., Adam, C., Broglin, D., Arzimanoglou, A., Bazin, B., Cavalcanti, D. and Baulac, M. (1998). Is the underlying cause of epilepsy a major prognostic factor for recurrence? *Neurology* **51**(5): 1256-1262.

Sheth, S., Brito, R., Mukherjea, D., Rybak, L. P. and Ramkumar, V. (2014). Adenosine receptors: expression, function and regulation. *Int J Mol Sci* **15**(2): 2024-2052.

Shinohara, M., Saitoh, M., Nishizawa, D., Ikeda, K., Hirose, S., Takanashi, J., Takita, J., Kikuchi, K., Kubota, M., Yamanaka, G., Shiihara, T., Kumakura, A., Kikuchi, M., Toyoshima, M., Goto, T., Yamanouchi, H. and Mizuguchi, M. (2013). ADORA2A polymorphism predisposes children to encephalopathy with febrile status epilepticus. *Neurology* **80**(17): 1571-1576.

Shirazi-zand, Z., Ahmad-Molaei, L., Motamedi, F. and Naderi, N. (2013). The role of potassium BK channels in anticonvulsant effect of cannabidiol in pentylenetetrazole and maximal electroshock models of seizure in mice. *Epilepsy Behav* **28**(1): 1-7.

Siebel, A. M., Menezes, F. P., Capiotti, K. M., Kist, L. W., da Costa Schaefer, I., Frantz, J. Z., Bogo, M. R., Da Silva, R. S. and Bonan, C. D. (2015). Role of adenosine signaling on pentylenetetrazole-induced seizures in zebrafish. *Zebrafish* **12**(2): 127-136.

Sims, R. E., Wu, H. H. and Dale, N. (2013). Sleep-wake sensitive mechanisms of adenosine release in the basal forebrain of rodents: an in vitro study. *PLoS One* **8**(1): e53814.

Sosnowski, M., Stevens, C. W. and Yaksh, T. L. (1989). Assessment of the role of A1/A2 adenosine receptors mediating the purine antinociception, motor and autonomic function in the rat spinal cord. *J Pharmacol Exp Ther* **250**(3): 915-922.

Spooner, C. G., Berkovic, S. F., Mitchell, L. A., Wrennall, J. A. and Harvey, A. S. (2006). New-onset temporal lobe epilepsy in children: lesion on MRI predicts poor seizure outcome. *Neurology* **67**(12): 2147-2153.

Steidl, E. M., Neveu, E., Bertrand, D. and Buisson, B. (2006). The adult rat hippocampal slice revisited with multi-electrode arrays. *Brain Res* **1096**(1): 70-84.

Studer, F. E., Fedele, D. E., Marowsky, A., Schwerdel, C., Wernli, K., Vogt, K., Fritschy, J. M. and Boison, D. (2006). Shift of adenosine kinase expression from neurons to astrocytes during postnatal development suggests dual functionality of the enzyme. *Neuroscience* **142**(1): 125-137.

Szybala, C., Pritchard, E. M., Lusardi, T. A., Li, T., Wilz, A., Kaplan, D. L. and Boison, D. (2009). Antiepileptic effects of silk-polymer based adenosine release in kindled rats. *Exp Neurol* **219**(1): 126-135.

Tanaka, A., Nishida, K., Okuda, H., Nishiura, T., Higashi, Y., Fujimoto, S. and Nagasawa, K. (2011). Peroxynitrite treatment reduces adenosine uptake via the equilibrative nucleoside transporter in rat astrocytes. *Neurosci Lett* **498**(1): 52-56.

Tanaka, E., Yasumoto, S., Hattori, G., Niiyama, S., Matsuyama, S. and Higashi, H. (2001). Mechanisms underlying the depression of evoked fast EPSCs following in vitro ischemia in rat hippocampal CA1 neurons. *J Neurophysiol* **86**(3): 1095-1103.

Tellez-Zenteno, J. F. and Hernandez-Ronquillo, L. (2012). A review of the epidemiology of temporal lobe epilepsy. *Epilepsy Res Treat* **2012**: 630853.

Thiele, E. A., Marsh, E. D., French, J. A., Mazurkiewicz-Beldzinska, M., Benbadis, S. R., Joshi, C., Lyons, P. D., Taylor, A., Roberts, C., Sommerville, K. and Group, G. S. (2018). Cannabidiol in patients with seizures associated with Lennox-Gastaut syndrome (GWPCARE4): a randomised, double-blind, placebo-controlled phase 3 trial. *Lancet* **391**(10125): 1085-1096.

Thom, M. (2014). Review: Hippocampal sclerosis in epilepsy: a neuropathology review. *Neuropathol Appl Neurobiol* **40**(5): 520-543.

Thomas, A., Baillie, G. L., Phillips, A. M., Razdan, R. K., Ross, R. A. and Pertwee, R. G. (2007). Cannabidiol displays unexpectedly high potency as an antagonist of CB1 and CB2 receptor agonists in vitro. *Br J Pharmacol* **150**(5): 613-623.

Thomas, B. F., Gilliam, A. F., Burch, D. F., Roche, M. J. and Seltzman, H. H. (1998). Comparative receptor binding analyses of cannabinoid agonists and antagonists. *J Pharmacol Exp Ther* **285**(1): 285-292.

Thompson, S. M., Haas, H. L. and Gahwiler, B. H. (1992). Comparison of the actions of adenosine at pre- and postsynaptic receptors in the rat hippocampus in vitro. *J Physiol* **451**: 347-363.

Tononi, G. and Cirelli, C. (2006). Sleep function and synaptic homeostasis. *Sleep Med Rev* **10**(1): 49-62.

Trinka, E., Cock, H., Hesdorffer, D., Rossetti, A. O., Scheffer, I. E., Shinnar, S., Shorvon, S. and Lowenstein, D. H. (2015). A definition and classification of status epilepticus--Report of the ILAE Task Force on Classification of Status Epilepticus. *Epilepsia* **56**(10): 1515-1523.

Ujváry, I. and Hanuš, L. (2016). Human metabolites of cannabidiol: A review on their formation, biological activity, and relevance in therapy. *Cannabis Cannabinoid Res* **1**(1): 90-101.

Van Gompel, J. J., Bower, M. R., Worrell, G. A., Stead, M., Chang, S. Y., Goerss, S. J., Kim, I., Bennet, K. E., Meyer, F. B., Marsh, W. R., Blaha, C. D. and Lee, K. H. (2014). Increased cortical extracellular adenosine correlates with seizure termination. *Epilepsia* **55**(2): 233-244.

Vecchio, E. A., Baltos, J. A., Nguyen, A. T. N., Christopoulos, A., White, P. J. and May, L. T. (2018). New paradigms in adenosine receptor pharmacology: allostery, oligomerization and biased agonism. *Br J Pharmacol* **175**(21): 4036-4046.

Vollner, L., Bieniek, D. and Korte, F. (1969). [Hashish. XX. Cannabidivarin, a new hashish constituent]. *Tetrahedron Lett*(3): 145-147.

W. H. O., W. H. O. (2015, May 2015). "Epilepsy Fact sheet N°999 May 2015." Retrieved October, 2015, from http://www.who.int/mediacentre/factsheets/fs999/en/.

Wall, M. J. and Dale, N. (2013). Neuronal transporter and astrocytic ATP exocytosis underlie activity-dependent adenosine release in the hippocampus. *J Physiol* **591**(Pt 16): 3853-3871.

Wall, M. J. and Richardson, M. J. (2015). Localized adenosine signaling provides fine-tuned negative feedback over a wide dynamic range of neocortical network activities. *J Neurophysiol* **113**(3): 871-882.

Wallace, M. J., Wiley, J. L., Martin, B. R. and DeLorenzo, R. J. (2001). Assessment of the role of CB1 receptors in cannabinoid anticonvulsant effects. *Eur J Pharmacol* **428**(1): 51-57.

Williams-Karnesky, R. L., Sandau, U. S., Lusardi, T. A., Lytle, N. K., Farrell, J. M., Pritchard, E. M., Kaplan, D. L. and Boison, D. (2013). Epigenetic changes induced by adenosine augmentation therapy prevent epileptogenesis. *J Clin Invest* **123**(8): 3552-3563.

Wilson, C. L., Khan, S. U., Engel, J., Jr., Isokawa, M., Babb, T. L. and Behnke, E. J. (1998). Paired pulse suppression and facilitation in human epileptogenic hippocampal formation. *Epilepsy Res* **31**(3): 211-230.

Wilz, A., Pritchard, E. M., Li, T., Lan, J. Q., Kaplan, D. L. and Boison, D. (2008). Silk polymer-based adenosine release: therapeutic potential for epilepsy. *Biomaterials* **29**(26): 3609-3616.

Xu, Z., Xu, P., Chen, Y., Liu, J., Zhang, Y., Lv, Y., Luo, J., Fang, M., Zhang, J., Wang, J., Wang, K., Wang, X. and Chen, G. (2015). ENT1 inhibition attenuates epileptic seizure severity via regulation of glutamatergic neurotransmission. *Neuromolecular Med* **17**(1): 1-11.

Zeraati, M., Mirnajafi-Zadeh, J., Fathollahi, Y., Namvar, S. and Rezvani, M. E. (2006). Adenosine A1 and A2A receptors of hippocampal CA1 region have opposite effects on piriform cortex kindled seizures in rats. *Seizure* **15**(1): 41-48.

Zhang, G., Franklin, P. H. and Murray, T. F. (1994). Activation of adenosine A1 receptors underlies anticonvulsant effect of CGS21680. *Eur J Pharmacol* **255**(1-3): 239-243.

Zhang, Y. N., Dong, H. T., Yang, F. B., Wang, Z. Q., Ma, Z. H., Ma, S. Z., Ma, X. D. and Duan, L. (2018). Nrf2-ARE signaling pathway regulates the expressions of A1R and ENT1 in the brain of epileptic rats. *Eur Rev Med Pharmacol Sci* **22**(20): 6896-6904.

Zimmermann, H. and Braun, N. (1996). Extracellular metabolism of nucleotides in the nervous system. *J Auton Pharmacol* **16**(6): 397-400.

Zucker, R. S. and Regehr, W. G. (2002). Short-term synaptic plasticity. *Annu Rev Physiol* **64**: 355-405.

Zuker, M. (2003). Mfold web server for nucleic acid folding and hybridization prediction. *Nucleic Acids Res* **31**(13): 3406-3415.

8. Appendices

Appendix 8.1. Producing, Maintaining, and Testing the RISE-SRS Model, and Compliance with ASPA Regulations

Home Office Animals Scientific Procedures Act (ASPA) Licensing personal licence (Modules 1-4) was obtained on 10-Dec-2015.

All procedures described in section 2.1 were performed in accordance with ASPA 1986, under project licence 70/7672.

This candidate was heavily involved in the induction and maintenance of the RISE-SRS model used in this thesis. During this project, this candidate took part in 26 inductions of the model, including formulating and injecting drugs and rat welfare during and after induction procedures. Additionally, this candidate led and was primary coordinator of 12 of these inductions, including managing the research team who took part during induction day and for the welfare and PSBB tests in the subsequent 13 weeks.

This appendix contains the following documents, showing the procedures for inducting and maintaining the welfare of RISE-SRS rats:

- By-induction summary of rats induced and mortality rate (Table 8-1)
- Written logistical protocol, showing management of research team on induction days (Figure 8-1)
- Welfare tracking sheets (printouts used for each induction)
    - Injection welfare sheets, used during the 2 days of induction (Figure 8-2)
    - Long-term welfare sheets, used twice a week from induction through entire maintenance of rats in Bioresource Unit (Figure 8-3)
- Example scoring sheet for PSBB, maintained as shared online spreadsheet (Figure 8-4)

Table 8-1: By-induction summary of RISE-SRS rats induced during this project, and reasons for mortality.

Induction #	#rats	died during induction	Reason for Schedule 1 termination		
			during induction (not met criteria and/or welfare reasons)	welfare reasons >1 week after induction	not confirmed epileptic after 13 weeks
48	10				3
49	12				3
50	10				4
51	12	1[a]	1		3
52	12		1		3
53	12		2		
54	5				1
55	5				
56	10				2
57*	10		3		2
58*	12				
59*	12				1
60*	12		1		1
61*	10				2
62**	6				2
63**	10				2
64**	10		3		2
65**	12				4
66**	8				4
67**	8		8[b]		
68**	8			1[c]	
69**	5				1
70**	5				
71**	12				1
72**	8				
73**	10				3
Total	**246**	**1**	**19**	**1**	**44**

* this candidate contributed to coordinating and leading these inductions, including performing s.c. and i.m. injections

** this candidate was the primary coordinator of these inductions, including performing s.c. and i.m. injections

a rat died following SE termination with STOP

b protocol violation – due to a lab error, on day 2 of the induction, MSP/pilocarpine injections were delayed by ~90 min and none of the rats developed SE after 3 injections of pilocarpine

c rat was terminated 6 weeks following induction for welfare reasons

Figure 8-1: Guidelines for the research team taking part in RISE-SRS induction days, written and circulated by this candidate.

The LiCl injection will always be on a Tuesday and the chronic pilocarpine induction will be on Wednesday.

- The number of animals ordered for each induction will be determined by the number of participants.
  - 3 people: 5 rats
  - 4 people: 7 rats
  - 5 people: 10 rats
  - 6+ people: 12 rats
- We always need a minimum of 3 people for each induction.
- Animals (STA02 50-74g) will be ordered on Tuesday (at 1 pm) the week before the induction, from Harlan Envigo to arrive on the Friday.
- Two people are needed for the LiCl injection on Tuesday: One person will prepare and weigh the animals and should arrive at 8am at the BRU. The other person will make the drug and must arrive at Hopkins at 7:45. In any case, the LiCl injections should start on Tuesday at 8:30am and wrapped up before 9am.
- On the day of the induction:
  - At least two people are needed to prepare the drugs. Both should arrive at Hopkins at 7:45am. At 8:10, one of these people should bring the drugs which are ready (but at the very least, the MSP (1mg/kg), the pilo (25mg/kg), and the saline for the xylazine) to the BRU. A third person is needed to set up B10 and weigh the animals at 8:00. MSP injections should start at the 24hr mark following LiCl.
  - The rest of the group can join between 9:30-10:00. The bulk of people will be required while we expect the animals to be seizing and requiring injections – generally until ~13:00. After this it's only necessary for a couple of people to wrap up for recovery and clean-up – depending on how long it takes for all rats to wake up following induction, induction is likely to end ~16:00-17:00.
- The day after the induction is VERY IMPORTANT: the welfare should be done at 9:00, as there's only until 36 hours after the STOP solution to schedule 1 in case an animal is not doing well. Also, it can be difficult to feed or inject some of them, so the earlier we start monitoring the animal the more time we have to make any important decisions.
- We think it would be best if at least one of the people who do the next day welfare checks was present during most of the induction day on Wednesday, just so they know if there are particular rats that we need to be keeping a closer eye on.

Figure 8-2: Injection welfare sheet templates for both days of induction. Printouts were used for the inductions led by this candidate. These updated sheets were a streamlined and more efficient method of taking records than welfare sheets previously used by the research team, which consisted of 2 rats per sheet of paper. Note that Part 2 of Day 2 allows for rats to be listed in order of xylazine injection, clarifying the process of order and time of STOP injections for rats.

Day 1

		LiCl		
Animal ID	weight	dose	time	notes (vocalising, jumping, running)

Day 2
part 1

		MSP		pilo 25mpk (30min interval)			pilo 50mpk (30min int)			pilo 75mpk (30min int)			xylazine time
animal ID	weight	dose	time	dose	time	notes	dose	time	notes	dose	time	notes	--> part 2

notes: MC (mouth clonus), WDS (wet dog shakes), HLS (hind limb scratching), UL (unilateral, tally), BL (bilateral, tally), BLF (bilateral falling, administer xylazine)

Day 2
part 2

animal ID	xylazine dose	xylazine time	STOP (1hr int) dose	STOP (1hr int) time	STOP 2? (half dose, 30min int) dose	STOP 2? (half dose, 30min int) time	STOP 3? (half dose, 30min int) dose	STOP 3? (half dose, 30min int) time	2mL saline/5% glucose inj time	accepts glu?	final weight

Figure 8-3: Long-term welfare sheets used twice-weekly throughout RISE-SRS rats post-induction lifetimes.

Animal ID:

Date	Weight (g)	Eyes (√/X)	Lesions (Y/N)	Body Condition Score	Grimace Scale					Severity level ok? (Y/N)	Notes	Researcher initials
					Eyes	Nose	Cheeks	Ears	Whiskers			

Figure 8-4: Example scoring sheet for PSBB (maintained as shared online spreadsheet) PSBB scores shown for induction 72; note that all 8 rats were confirmed epileptic through PSBB by week 10 post-induction.

Touch task

Animal ID	Wk3 Tue 26th Sept	Wk3 Fri 29th Sept	wk4 Tue 3rd Oct	wk4 Fri 6th Oct	wk5 Tue 10th Oct	Wk5 Fri 13th Oct	wk6 tue 17th Oct	wk6 fri 20th Oct	wk7 tue 24th oCT	wk7 fri 27th Oct	wk8 tue 31st Oct	wk8 fri 3rd Nov	wk9 Tue 7th Nov
1	1	3	2	3	3	6	4	5	3	2	1	2	6
2	1	3	2	2	2								
3	1	4	1	2	3	1	6	1	6	1	1	1	2
4	1	3	2	3	6	6	2						
5	1	2	6	2	5								
6	2	1	6	2	3	1	1	3	5	2	6	2	2
7	2	6	5	2									
8	2	2	5	5									

Pick-up task

Animal ID	Wk3 Tue 26th Sept	Wk3 Fri 29th Sept	wk4 Tue 3rd Oct	wk4 Fri 6th Oct	wk5 Tue 10th Oct	Wk5 Fri 13th Oct	wk6 tue 17th Oct	wk6 fri 20th Oct	wk7 tue 24th oCT	wk7 fri 27th Oct	wk8 tue 31st Oct	wk8 fri 3rd Nov	wk9 Tue 7th Nov
1	5	5	1	5	5	5	1	5	5	5	5	5	5
2	1	5	5	5	5								
3	5	5	5	5	5	5	1	5	1	1	5	1	5
4	1	5	1	5	5	5	5						
5	5	5	5	5	5								
6	5	1	5	5	5	5	5	5	1	5	5	5	5
7	5	5	5	5									
8	5	5	5	5									

SR S criterion touch x pick-up	Animal ID	wk4		wk5		wk6		wk7		wk8		wk9	
	1	5	15	2	15	15	30	4	25	15	10	5	10	30
	2	1	15	10	10	10	0	0	0	0	0	0	1	0
	3	5	20	5	10	15	5	6	5	6	1	5	1	10
	4	1	15	2	15	30	30	10	0	0	0	0	0	0
	5	5	10	30	10	25	0	0	0	0	0	0	0	0
	6	10	1	30	10	15	5	5	15	5	10	30	10	10
	7	10	30	25	10	0	0	0	0	0	0	0	0	0
	8	10	10	25	25	0	0	0	0	0	0	0	0	0

wk9 Fri 10th Nov	wk10 Tue 14th Nov	wk10 Fri 17th Nov	wk11 Tue 21st Nov	wk11 Fri 24th Nov	wk12 Tue 28th Nov	wk12 Fri 1st Dec	wk13 tues 5th dec	wk 13 fri 8th dec
6	3							
6	2	3						

wk9 Fri 10th Nov	wk10 Tue 14th Nov	wk10 Fri 17th Nov	wk11 Tue 21st Nov	wk11 Fri 24th Nov	wk12 Tue 28th Nov	wk12 Fri 1st Dec	wk13 tues 5th dec	wk 13 fri 8th dec
5	5							
5	5	4						

wk10			wk11			wk12			wk13		
30	15	0	0	0	0	0	0	0	0	0	0
0	0	0	0	0	0	0	0	0	0	0	0
30	10	12	0	0	0	0	0	0	0	0	0
0	0	0	0	0	0	0	0	0	0	0	0
0	0	0	0	0	0	0	0	0	0	0	0
0	0	0	0	0	0	0	0	0	0	0	0
0	0	0	0	0	0	0	0	0	0	0	0
0	0	0	0	0	0	0	0	0	0	0	0

Appendix 8.2. Summary of Experiments That Were Piloted but Not Formally Analysed

This appendix presents summaries of experiments performed during this thesis, but not formally analysed or presented in the thesis due to methodological or logistical constraints.

8.2.1. DPCPX electrophysiology

Prior to the study design in Chapter 4, whereupon A_1Rs were blocked using the competitive inhibitor 8-CPT, some pilot studies were attempted using DPCPX, another A_1R-inhibitor used in literature. The goal was to assess whether this could be used to detect changes in adenosine concentration and/or A_1Rs in chronic epilepsy using a protocol similar to that used by Diogenes et al. (2014), in which DPCPX application was shown to induce at least 150% potentiation from baseline field potentials in adult WT mice.

Initially, DPCPX was purchased from Sigma (UK) and aliquoted in DMSO. No potentiation response was seen on LFPs evoked and detected by MEAs when applied to healthy hippocampal slices at the 50 nM used by Diogenes et al. (2014), nor at increased concentrations of 100 nM or 200 nM (data not shown). A new batch of DPCPX was then purchased from Tocris (UK), which when applied to hippocampal slices was able to show the expected potentiation at 100 nM (Figure 8-5A).

However, the potentiation of basal field potentials did not match the time dynamics shown in the original paper, even with increased flow rate for bath perfusion; DPCPX was shown by Diogenes et al. (2014), to reach a plateau after about 20 min, whereas our experiments with DPCPX (n = 6) showed a wide variation in time to start potentiating, time to reach a plateau, and degree of potentiation; normalised slope at plateau ranged from 0.8 to 2.6, with a mean ± SEM of 1.5 ± 0.3.

Due to the wide variation and inconsistency in efficacy dynamics, DPCPX was not chosen to take forward into full experiments assessing function of A_1R in epileptic hippocampal slices; 8-CPT was chosen to use for experiments shown in Chapter 4. However, as the stimulation experiments in Chapter 3 were ongoing, 2 stimulations were performed in the presence of DPCPX prior to the decision not to use the drug. Field potential slopes following adenosine-releasing stimulations are presented in Figure 8-5B; no correlations were able to be performed for these stimulations, as the sensor recordings were discarded due to failing screening with 5-HT following removal from slice. For the 2 slices in which DPCPX recordings were taken, there appeared to be some post-stimulation inhibition, but to a lesser degree and faster recovery than control; statistical analyses were not performed due to lack of n numbers.

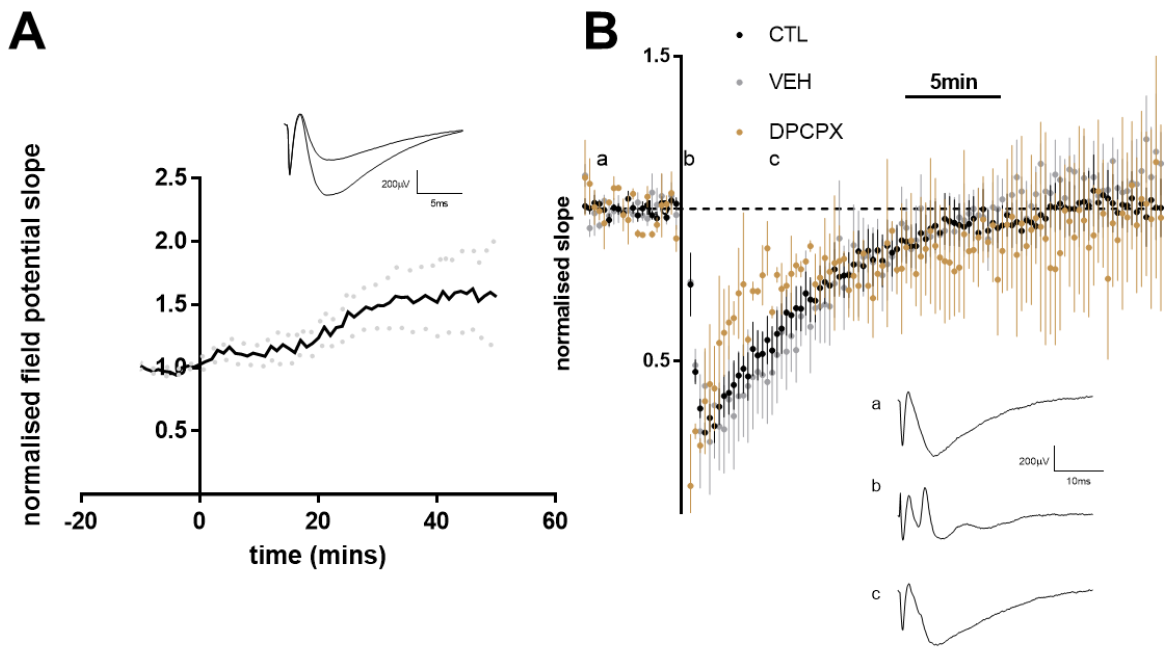

Figure 8-5: Piloted field potential experiments using A_1R inhibitor DPCPX on healthy hippocampal slices. A: Application of 100 nM DPCPX potentiated some field potential recordings on healthy slices (n = 6). A variety of potentiation and dynamics were seen, and not all experiments reached a plateau at consistent times following application. Mean data shown in figure seems to suggest an immediate slight potentiation, followed by some slices showing a larger potentiation after 20 min of application. Inset shows representative field traces, averaged over 10 sweeps, before and after DPCPX application. **B:** Field potential traces following adenosine-releasing stimulation train (as described in section 3.6). Control and vehicle traces were previously presented in the body of the thesis; pilot experiments in the presence of DPCPX (following incubation ~1 hour) are presented here (n = 2). Insets show representative field potential traces (averaged over 4 sweeps) at baseline (a), immediately post-stimulation (b), and approximately 5 min post-stimulation (c).

A full set of adenosine-release stimulations in the presence of an A_1R antagonist would have helped to demonstrate a causative effect of adenosine; that post-stimulation field potential inhibition, which correlated with the concurrent adenosine release detected by biosensors, was in fact due in part to A_1R activation by the released adenosine. This would of course be an experiment which could be done in the presence of 8-CPT or another A_1R inhibitor, to potentially show if the epilepsy-based change in correlation between adenosine concentration and field potential inhibition could be due to A_1R dysfunction in epilepsy.

8.2.2. Adenosine receptor Western blots

As part of Chapter 4, several attempts were made to refine and validate a Western blotting protocol to detect A_1R and $A_{2A}R$ in healthy and epileptic hippocampal tissue.

Refinements included the following:

- Changing the tissue lysis buffer and protocols
- Using different protease inhibitor cocktails while lysing tissue based upon reported inhibitors used in literature for isolating membrane-bound receptors
- Using spin cycles to isolate cell membranes rather than using whole tissue homogenate
- Changing temperature and length of time at which lysates were denatured
- Changing type and concentrations of gels used (including trialling pre-bought gels)
- Changing membranes from PVDF to nitrocellulose
- Adjusting methods/intensities/times for running gels and membrane transfers
- Changing concentration/incubation time and method of primary antibodies
- Changing components of block and wash buffers, number and length of membrane washes, and method of chemiluminescence detection

While the well-validated anti-GAPDH control antibody was able to produce clean blots with clear, clean bands (as shown in Figure 8-6C), and anti-ENT1 antibodies, while producing two bands, where otherwise clean and consistent, the antibodies for the two receptors were consistently messy and unspecific, with multiple bands being detected at different weights and an inconsistent pattern of detection.

Anti-A_1R antibodies were purchased from Abcam (Rabbit polyclonal IgG) (Abcam, 2017). Manufacturer's guidance indicated that a band can be detected using Western blotting at the predicted weight of 36 kDa, with additional bands reported at118 kDa and 18 kDa of unknown identity. As shown in Figure 8-6A, however, despite multiple refinements of the lysing and blotting protocol, multiple, streaky bands would be detected throughout the molecular weights. A light band at 36 kDa was occasionally detected, and consistent double bands were detected just under 50 kDa, which was not reported by the manufacturer's guidance or the literature. It was noted that the representative image on the manufacturer's website use cell lysates rather than tissue lysates, and multiple pale bands can also be seen in addition to the ones reported.

Anti-$A_{2A}R$ antibodies (Mouse monoclonal IgG2a) were purchased from Millipore (2017), with guidance stating that the predicted weight of 42 kDa could be detected, although no representative images were available on the website. This antibody was the most difficult to refine a protocol for, with very faint

bands initially being detected and therefore a lot of background signal when attempting to resolve the image; this was likely due to the low expected signal of $A_{2A}R$ in hippocampal tissue. With higher concentrations of antibody used, strong bands could be detected both higher and lower than the predicted weight, with only very light bands occasionally detected around the expected location of 42 kDa. Additionally, this antibody would sometimes create a large signal at the higher weights of the protein ladder (Figure 8-6B).

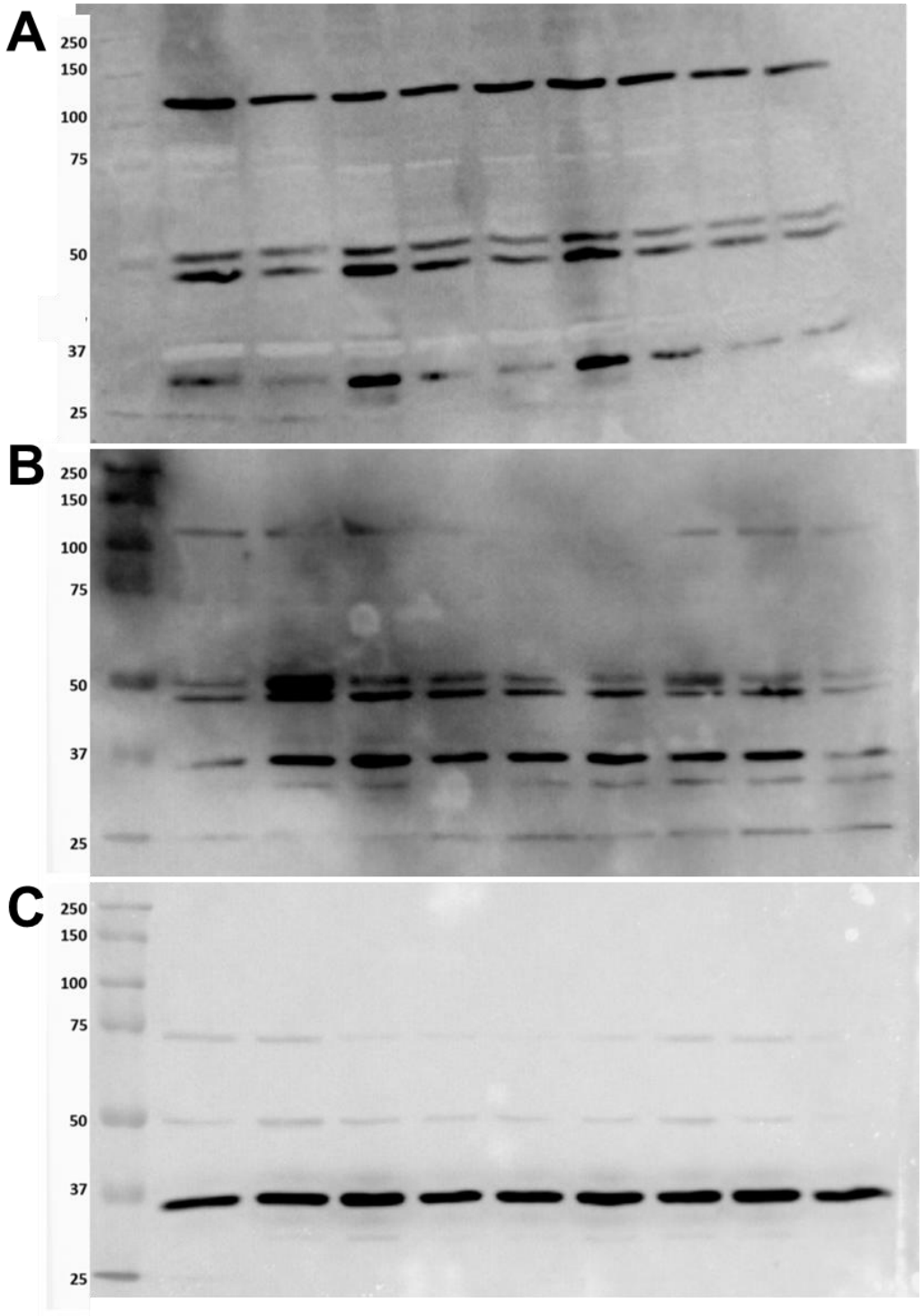

Figure 8-6: Attempts to validate antibodies against A_1R and $A_{2A}R$ in lysed hippocampal tissue. A&B: Representative blots using antibodies against A_1R and $A_{2A}R$, respectively. Note the high degree of background signal and streaky blots; only faint bands could occasionally be detected at the predicted weights, while multiple other bands could be shown, indicating lack of specificity of the antibodies in hippocampal lysate. **C:** Representative blot of the loading control GAPDH, showing that clean, single-band blots were able to be obtained using the Western blotting protocol employed.

It is likely that, as complicated membrane-bound G-protein coupled receptors, purifying and isolating these proteins for blotting was a difficult endeavour. Ideally, a positive control would have involved using a cell line specifically expressing these receptors to allow for the verification of whether the antibodies were binding to the correct proteins; however these were not able to be obtained. As the specificity of these two antibodies was not able to be confirmed from multiple attempts at refining the blotting protocol, the decision was made that the lack of specificity would not create accurate and/or reliable data. Therefore, protein expression data was instead probed using the radioligand binding technique, as presented in section 4.3.2.

Appendix 8.3. Methods of Studies Performed by Contract Research Organisations

This appendix details the methodological studies presented in this thesis which were contracted to external CROs.

8.3.1. Radioligand saturation binding

Bilateral hippocampi were dissected from 10 healthy and 10 epileptic age-matched rats (as per section 2.3.1) at the University of Reading, and couriered on dry ice to the CRO Eurofins (Eurofins Cerep SA, Le Bois L'évêque, BP 30001, F- 86600 Celle-L'Evescault, France). The radioligand saturation binding study was performed at the CRO using the tissue provided, and results are presented in section 4.3.2.

Membrane isolation

Isolated healthy and epileptic hippocampi were sent to Eurofins (France), a Contract Research Organisation, to carry out membrane isolation preparation and radioligand saturation binding for A_1R, using [^{3}H]-CCPA, a radiolabelled specific A_1R agonist, and $A_{2A}R$ using [^{3}H]-SCH 58261, a specific $A_{2A}R$ antagonist. Membranes were prepared by pooling all healthy hippocampi, and all epileptic hippocampi together. Preparation of membranes was carried out following Eurofins Cerep's standard protocol, and protein concentration in each preparation determined through a Bradford assay.

Assay optimisation for [3H] CCPA and [3H]-SCH 58261

Assay condition optimisation assessed the optimum amount of protein per well as 90 µg for [^{3}H]-CCPA binding, as well as incubation time and temperature as 180 min at 22°C. No specific signal was found on isolated hippocampal membranes using [^{3}H]-SCH 58261, up to 180 µg of protein per well.

Radioligand saturation

Samples were incubated in the optimal conditions identified for [^{3}H]-CCPA in increasing concentrations of [^{3}H]-CCPA (0 – 7.73nM, Perkin Elmer, CUST82830000MC) in incubation buffer (Table 8-2). Non-specific binding of [^{3}H]-CCPA concentrations was measured using 10 µM CPA, a saturating concentration of a specific A_1R agonist.

Glass fibre filters (GF/B, Packard) were pretreated using 0.3% polyethylenimine (PEI), a cationic polymer, to minimise free ligand binding to filters by neutralising the negative charge of the glass fibre filter and prevent background binding signal. Following incubation, membranes were rapidly filtered under vacuum through these pretreated filters to remove free unbound ligand. Filters were then rinsed with ice-cold 50 mM Tris-HCl using a 96-sample cell harvester (Unifilter, Packard), then dried. Once dry, MicroScint-O scintillation cocktail was added to filters and counted for radioactivity in a scintillation counter (Topcount, Packard). All samples were run in duplicate and an average taken, before

non-specific signal was subtracted from total signal at each concentration of specific [^{3}H]-CCPA binding to hippocampal membranes.

Component	concentration
Tris-HCl pH 7.4	50 mM
MgCl2	5 mM
EDTA	1 mM
ADA	2 Ul/mL
Leupeptin	1 mg/mL
Pepstatin	1uM
Trypsin inhibitor	10 µg/mL

Table 8-2: Incubation buffer for radioligand binding.

Specific binding in counts per minute (cpm) was converted to fmol/mg of bound ligand based on 0.09 mg protein per well and the conversion factor of 68 cpm/fmol.

8.3.2. Cortical synaptosome uptake of [3H]-adenosine

The following study was performed at the CRO RenaSci (RenaSci Ltd, BioCity, Pennyfoot Street, Nottingham, NG1 1GF, United Kingdom). The results are presented in section 5.3.

Cortical tissue collection

Male adult Sprague-Dawley rats (250-300 g) were obtained from Charles River (Margate, UK) and group-housed in temperature and humidity controlled conditions on a standard 12 hr light/dark cycle. Rats were provided with food and drink *ad libitum* at all times and habituated for at least 5 days following arrival prior to experimental use. For collection of cortical tissue, rats were humanely killed by cervical dislocation and whole brains removed. The cortex was rapidly dissected after peeling back olfactory tubercles, weighed, then stored in 0.32 M sucrose on ice.

Preparation of synaptosomes

Cortices were homogenised in ice-cold 0.32 M sucrose (1:40 w/v) using 12 strokes at 800 rpm at 0.5 mm clearance. Lysates were centrifuged at 1500 RCF for 10 min at 4°C to remove nuclei and cell debris, then the supernatant was recentrifuged at 18000 RCF for 10 min at 4°C for a pellet containing sheared synaptosomal membranes. Crude synaptosome pellets were resuspended in Krebs physiological buffer (Table 8-3), carboxygenated for 10 min to reach pH 7.4, and preincubated for 15 min at 37°C in a shaking water bath.

Krebs Physiological buffer	mM
NaCl	120.8
$NaHCO_3$	15.5
KCl	5.9
$CaCl_2$	2.5
$MgCl_2$•6H2O	1.2
NaH_2PO_4•$2H_2O$	1.2
glucose	11.5

Table 8-3: Krebs physiological buffer used at RenaSci for synaptosome suspension.

Synaptosomal uptake assays

Assay tubes were prepared according to Table 8-4, with freshly prepared tritiated adenosine being the final component added to tubes to initiate uptake. Non-specific binding was determined through presence of 50 µM dipyridamole. Tubes were vortexed and then incubated for 10 min at 37°C, before uptake was terminated by being filtered under vacuum through Skatron 11731 filters, which were pretreated with 0.5% PEI. Rapidly, filters were washed using ice-cold saline, then filters were read for radioactivity in the presence of 1 mL scintillation cocktail (Packard MV Gold scintillator).

	volume added (µL)	final concentration
Krebs buffer	275	-
drug solution (varied concentrations)	50	1 nM - 100 µM
crude synaptosomes	150	2.4 mg/mL (of initial wet tissue)
[^{3}H]-adenosine	25	25 nM
Total	**500**	

Table 8-4: Components of individual tubes for synaptosome uptake assays.

Drugs and Reagents

Cannabinoids were dissolved in diethylene glycol (DEG) to 1 mM stock and diluted in Krebs buffer. For reference experiments, dipyridamole was dissolved to 1 mM stock in deionised water and 10 µl/ml glacial acetic, and diluted in Krebs buffer. For non-specific binding, dipyridamole was dissolved to 1 mM stock in DEG and further diluted for use in DEG.

Drug	Batch #	Company
Pure CBD	6066919	GW Pharmaceuticals
Pure CBDV	CBDV270116	GW Pharmaceuticals
7-OH CBD	NCT/1281/05	GW Pharmaceuticals
7-OH CBDV	NCT/1283/02	GW Pharmaceuticals
[^{3}H]-adenosine	ART 1812/170210	American Radiolabeled Chemicals, Inc, USA
dipyridamole	0691/03	Tocris, UK

Table 8-5: Batch numbers and origin of drugs used in synaptosome uptake assays.